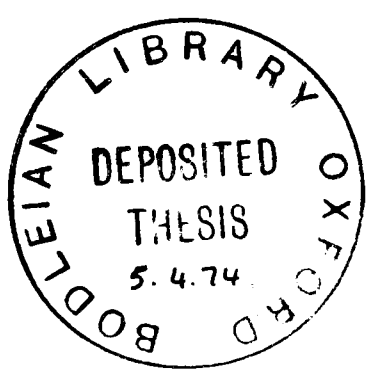
ON THE THEORY OF DISORDERED MAGNETS

I.D. Saville

A thesis submitted for the degree of Doctor of Philosophy at the University of Oxford



Magdalen College, Oxford

September 1973

ACKNOWLEDGEMENTS

I wish to thank my supervisor, Dr. R.J. Elliott, for his advice and encouragement during the past three years: my thanks also go to Dr. Brooks Harris, Dr. Holcomb and Dr. Nickel for many helpful discussion.

I also acknowledge the award of the Don Scholarship by St. Andrews University during this period.

ABSTRACT

This thesis consists of three discrete parts. The first is concerned with the study of the ferromagnetic phase transition in the Ising spin $\frac{1}{2}$ model, with random substitutional impurities. Series in the impurity concentration for the susceptibility are extended by one or two terms for the cubic, square and face-centred cubic lattices, using a set of rules which cuts the number of clusters to be considered. Closed analytic form for all terms in the series are obtained. An eight term series for the tetragonal zircon lattice is also developed. Phase boundaries and critical indices are obtained by use of ratio methods and Padé approximants. Comparison of the results, particularly for the critical index, with recent high temperature series work is made, and the single pole assumption usually made for the divergence of the susceptibility is critically examined. High temperature series for the dilute Ising model with a transverse field are also generated for the tetragonal zircon (7 terms) and face-centred cubic lattices (6 terms): the results for the former are compared with recent experimental work, and some general conclusions are drawn from the latter series about the shape of the phase surface in concentration, temperature and transverse field. Some features of the behaviour of the critical index are also examined.

In the second part the description of the two-magnon Raman scattering profile in dilute antiferromagnets is attempted by calculation of the first few moments. Using the Néel state as an approximation, the zeroth, first, second and third moments are calculated at zero temperature: the zeroth and second moments are also evaluated in the infinite temperature limit. As the profile at low temperatures is thought to consist of two peaks, various attempts are made to construct moments that will describe solely the two-magnon peak. Reasonable agreement with experiment at low and high temperatures is found, and some comparison with low temperature experiments on dilute MnF_2 is made. Temperature and concentration dependent forms for the zeroth, first and second moments are also derived, using the constant coupling approximation to provide a consistent treatment of thermal averages of one and two spins, and comparison with experiment on pure NiF_2 is made.

The third part is concerned with the location of the phase transition in more random systems: a CPA-like treatment for the Fourier transformed spin correlation function is developed and applied to the cubic Ising spin $\frac{1}{2}$ model with next neighbour interactions randomly removed, with some degree of success. A more random model due to Handrich is also considered, and the transition temperature is found to rise as fluctuations in the inter-

action increase, if the average interaction is held constant. Comparison with a constant coupling theory due to Handrich which predicts the reverse is made.

CONTENTS

		Page
PART 1.	Series Expansions for the Susceptibility in Dilute Ising Magnets	
Chapter 1.	Introduction to Exact Series Expansions for the Susceptibility	
1.1	Introduction	1
1.2	Series for the Susceptibility in p	3
1.3	High Temperature Series	5
Chapter 2.	Derivation of Series for the Susceptibility	
2.1	Series in the Impurity Concentration	7
2.2	Cluster Susceptibilities	8
2.3	Cluster Occurrences	11
2.4	Equivalence of Series	12
Chapter 3.	Techniques and Results of Series Analysis	
3.1	Hypotheses of analysis	19
3.2	Ratio Tests	19
3.3	Padé Approximants	25
3.4	Conclusions	32
Chapter 4.	High Temperature Series for the Dilute Transverse Ising Model	
4.1	Introduction	39
4.2	Derivation of Series	45
4.3	Calculation of Diagrams	50
4.4	Calculation of Occurrences	53
4.5	Analysis of the Series	55
Appendix 1.	Cluster Susceptibilities	
	Occurrences of Seven and Eight Point Clusters	
	Simple Cubic Susceptibility p-series	65
	FCC lattice Susceptibility p-series	66
	Quadratic lattice Susceptibility p-series	67
	Tetragonal Zircon Susceptibility p-series	68

Page

Appendix 2. Face-centred Cubic, Quadratic and Tetragonal Zircon Lattices 69

Appendix 3. Confluent Singularity Analysis 74

Appendix 4. Diagram values for $.05 \leq G\beta \leq 1.25$

References for Part 1 82

PART 2. Moments Calculation for Two-Magnon Raman Scattering in Dilute Heisenberg Antiferromagnets

Chapter 1. Introduction to Two-Magnon Raman Scattering

1.1 Introduction 84

1.2 Theoretical Approaches 89

Chapter 2. Calculation of Moments in the Zero and Infinite Temperature Limits

2.1 Calculation of Commutators 94

2.2 Zero Temperature Intensity 94

2.3 Zero Temperature First Moment 98

2.4 Transverse and Longitudinal Moments 100

2.5 Second Moment 104

2.6 Third Moment 107

2.7 Infinite Temperature Limit 108

2.8 Analysis of Results 110

Chapter 3. Finite Temperature Moments

3.1 Constant Coupling Model 118

3.2 Intensity 125

3.3 First Moment 130

3.4 Second Moment 138

3.5 Results for Finite Temperature Moments 148

Appendix. Occurrences of Lattice Diagrams 156

References for Part 2 159

PART 3. More Random Systems

Chapter 1.

1.1 Introduction 161

Page

1.2 Development of a CPA-type approximation 162

1.3 The dilute bond problems 168

1.4 More Random Models 170

References for Part 3 175

LIST OF FIGURES

PART 1

		Opposite page
Figure 1.	The sequence u_n vs. $\frac{1}{n}$ for the Simple Cubic Lattice	20
Figure 2.	The sequence u_n vs. Temperature for the Simple Cubic Lattice	21
Figure 3.	The sequence v_n vs. $\frac{1}{n}$ for the Simple Cubic Lattice	22
Figure 4.	The sequence w_n vs. $\frac{1}{n}$ for the Simple Cubic Lattice	22
Figure 5.	Phase Boundary for the Simple Cubic Lattice by Ratio Methods	23
Figure 6.	The sequence v_n vs. Temperature for the Simple Cubic Lattice	23
Figure 7.	The sequence w_n vs. Temperature for the Simple Cubic Lattice	23
Figure 8.	Critical Index vs. Temperature for the Simple Cubic Lattice by Ratio Methods from the 7 term p-series	24
Figure 9.	Critical Index vs. Temperature for the Simple Cubic Lattice by Ratio Methods from the 6 term p-series	24
Figure 10.	Phase Boundary for the Simple Cubic Lattice by method 4 from series in p,t and $(\frac{1}{2}\beta J)$	25
Figure 11.	Critical Index vs. Temperature for the Simple Cubic Lattice by method 4 from series in p,t and $(\frac{1}{2}\beta J)$	25
Figure 13.	Phase Boundary for the Simple Cubic Lattice by Padé Approximant	26
Figure 14.	Critical Exponent vs. Temperature for the Simple Cubic Lattice by Padé Approximant	26
Figure 15.	Phase Boundary for the Simple Cubic Lattice: comparison of Ratio Methods and Padé Approximants	27

		Opposite page
Figure 16.	The sequence u_n vs. $\frac{1}{n}$ for the FCC lattice from the 11 term t-series of Rapaport (1972(a))	31
Figure A.	The structure of $DyVO_4$	42
Figure B.	Phase Boundary for TZ lattice: comparison of results from series in p and $(\frac{1}{2}\beta J)$	56
Figure C.	Phase Boundary for $(Dy,Y)VO_4$: comparison of experiment, series results, molecular field results and constant coupling results	57
Figure D.	Critical Temperature vs. Critical Field for fixed concentration for the FCC lattice	58
Figure E.	Critical Temperature vs. Critical Concentration for constant Field for the FCC lattice	59
Figure F.	Critical Field vs. Critical Concentration for fixed Temperature for the FCC lattice	59
Figure G.	Critical Index vs. Temperature at Constant Field for the FCC lattice	60
Figure H.	Critical Index vs. Temperature at fixed Concentration for the FCC lattice	62
Figure 17.	The sequence u_n vs. $\frac{1}{n}$ for the FCC lattice	App. 2
Figure 18.	The sequence v_n vs. $\frac{1}{n}$ for the FCC lattice	App. 2
Figure 19.	Phase Boundary for the FCC lattice by Ratio Methods	App. 2
Figure 20.	Critical Index vs. Temperature for the FCC lattice by Ratio Methods	App. 2
Figure 21.	The sequence u_n vs. $\frac{1}{n}$ for the Qaudratic Lattice	App. 2
Figure 22.	The sequence w_n vs. $\frac{1}{n}$ for the Quadratic Lattice	App. 2
Figure 23.	Phase Boundary for the Quadratic Lattice by Ratio Methods	App. 2

		Opposite page
Figure 24.	Critical Index vs. Temperature for the Quadratic Lattice by Ratio Methods	App. 2
Figure 25.	The sequence u_n vs. $\frac{1}{n}$ for the Tetragonal Zircon Lattice	App. 2
Figure 26.	The sequence w_n vs. $\frac{1}{n}$ for the Tetragonal Zircon Lattice	App. 2
Figure 27.	Phase Boundary for the Tetragonal Zircon Lattice by Ratio Methods	App. 2
Figure 28.	Critical Index vs. Temperature for the Tetragonal Zircon Lattice by Ratio Methods	App. 2
PART 2.		
Figure 1.	Spin Quantities in the Pair Model for spin 1	122
Figure 2.	Peak Position and First Moment in $(Mn,Zn)F_2$ at zero temperature	110
Figure 3a.	Second Moment about the Mean vs. Concentration for S=5/2 at zero temperature	111
Figure 3b.	Third Moment about the Mean vs. Concentration for S=5/2 at zero temperature	112
Figure 4.	Relative Intensity vs. Temperature in Pure NiF_2	148
Figure 5.	First Moment in NiF_2: Theory and Experiment	150
Figure 6.	Predicted Total Intensity for NiF_2 vs. Temperature for a Range of Concentrations	151
Figure 7.	Predicted First Moment for NiF_2 vs. Temperature for a Range of Concentrations	152
Figure 8.	Predicted Transverse Second Moment about the mean for NiF_2 for a Range of Concentrations	153
PART 3.		
Figure 1.	Phase Boundary for the Dilute Bond Problem	168
Figure 2.	Phase Boundary for the Spin Glass model of Handrich	170

PART 1

Series Expansions for the Susceptibility in Dilute Ising Magnets

CHAPTER ONE

INTRODUCTION TO EXACT SERIES FOR THE SUSCEPTIBILITY

§1.1 The Ising model of a magnet has been much studied in the last twenty years, and its critical properties are now thought to be fairly well understood, partly due to exact analytical results, and partly due to the use of exact series expansions. Comprehensive reviews of this work have been made by Domb (1960), Fisher (1967) and Kadanoff et al (1967), and a recent book by Stanley (1971) offers a good introduction. In particular, series expansions have helped in the formulation of new theories of critical behaviour not only by the accuracy with which critical parameters are estimated, but by the insights their methods of derivation give into the mechanisms underlying the transition.

However, the model most studied is that of a pure magnet, with, consequently, translational invariance: markedly different critical behaviour may be expected when some alteration of the model destroys this invariance. Several such alterations have been attempted: the Syozi model is an Ising system with magnetic impurities on the lattice bonds (Syozi and Miyazima, 1966; Essam and Garelick, 1967), and exhibits exponent renormalisation. McCoy and others have studied a square Ising system in which next neighbour interactions between spins in different rows

are constant, while that between spins in different columns is the same for any spins in these columns, but is a random variable for different pairs of columns (McCoy and Wu, 1968; McCoy, 1970). These systems seem rather artificial, but are mathematically tractable (the latter is exactly soluble): their critical behaviour exhibits marked differences from that of the ideal Ising model.

Simpler (and more physical) possibilities are to replace magnetic atoms by fixed (or mobile) non-magnetic impurities at random, or to replace magnetic bonds by non-magnetic ones, which again may be fixed or mobile. The bond problem again seems reasonably tractable to analytic methods (e.g. Rapaport, 1972(a)), whereas the site problem, the most physical, has so far only been successfully studied by exact series expansions. This section is concerned with the study of the fixed or "quenched" site transition by exact expansion of the longitudinal susceptibility in p, the concentration of magnetic atoms, or some appropriate high temperature variable.

The Hamiltonian used is

$$H = -2J \sum_{\langle ij \rangle} S_i^z S_j^z - \mu H \sum_i S_i^z \qquad - 1.1$$

where the sum is over all next neighbour pairs of magnetic atoms (i,j), and the atom i has spin magnetic moment μS_i^z. For computational convenience only the case of spin $\frac{1}{2}$ is considered.

§1.2 Series for the susceptibility in p

A series in p for the reduced susceptibility

$$\chi^R = \frac{4\chi(T)}{N\mu^2\beta p}$$

may be derived by adding together the susceptibilities of small isolated clusters, multiplied by the probability of their occurrence on the lattice

$$\chi^R = \sum_{n=o}^{\infty} a_{n+1} p^n : \qquad a_n = a_n(T) \qquad - 1.2$$

Such a method was first used by Behringer (1957), who expanded the cluster susceptibilities in powers of $\beta(= \frac{1}{kT})$: accordingly his results were invalid at low temperature. Later, independent, work by Elliott and Heap (1962) and Rushbrooke and Morgan (1961) resulted in four, and in some cases, five term series for various lattices, with the coefficients a_n as closed analytic functions of T: the Heisenberg spin $\frac{1}{2}$ model was also studied. In a subsequent paper, Heap (1963) produced the first six terms of the series 1.2 for several lattices. Such series may be analysed at various temperatures to give a phase boundary, or curve $T_c(p)/J$ against p, where $T_c(p)$ is the critical temperature at concentration p,

if the asymptotic assumption

$$\chi^R = \frac{A}{(p_c - p)^{\gamma(T)}} \quad \text{as } p \to p_c^+(T) \qquad - 1.3$$

is made. Such an assumption was well verified by the series available at that time, and consistent estimates of the phase boundary could be made from it by several techniques.

It may be demonstrated that the percolation concentration of magnetic atoms p_c^s below which there is no magnetic phase is independent of the model, and is a topological feature of the lattice (Elliott, Heap, Morgan and Rushbrooke, 1960). For Ising or Heisenberg models, and any value of spin, the divergence of the susceptibility at zero temperature is easily shown to depend on the divergence of the series

$$\chi = \sum_{n=1}^{\infty} n^2 N_n p^n \qquad - 1.4$$

where there are N_n isolated clusters of n atoms in the lattice. This quantity is just the mean cluster size: the number of magnetic atoms connected to any given magnetic atom: and is a property purely of the lattice. Long series for the mean cluster size, of the type 1.4, have been derived for many lattices, and the value p_c^s which makes the mean cluster size diverge estimated from assumption 1.3 with great consistency (Domb and Sykes, 1961(a); Sykes and Essam, 1964). The whole field of

percolation theory has been recently reviewed by Shante and Kirkpatrick (1971) and Essam (1972). At zero temperature, then, co-operative behaviour can only exist if the mean cluster size is infinite: each magnetic atom is on average connected to all the other magnetic atoms by $\mathcal{T}$ interactions. A crude estimate of $p_c^{\ s}$ may be made by assuming that each magnetic atom has on average two magnetic neighbours, so that $p_c^{\ s} \sim \frac{2}{z}$.

The behaviour of $\gamma(T)$ is of some interest, and estimates of this may also be made. Mean cluster size series appear to support the view that $\gamma(T=0) = \frac{27}{16}$ ($\frac{19}{8}$ in two dimensions) for any lattice, and it would be useful to know how $\gamma(T)$ changes as the temperature is increased, and whether this universal behaviour continues.

Accordingly extra terms are added to the p-series of Heap, and the resulting series analysed in some detail for four different lattices in Chapters 2 and 3. Recent work by Rapaport (1972(b)) has extended the series for the face -centred cubic lattice to seven terms at selected values of T (analytic forms for $a_n(T)$ are not obtained), and his results are also discussed in Chapter 3.

§1.3 High temperature series

Series of the form

$$\chi^R = \sum_{n=0}^{\infty} b_{n+1}(p)x^n$$

may also be derived, where $x = (\frac{1}{2}\beta J)$, by straightforward expansion of the exponential appearing in the partition function, and double differentiation with respect to H. Such series were developed for the pure substance and the Heisenberg model in 1955, by Rushbrooke and Wood, and later extended to the dilute Ising model of arbitrary spin (Morgan and Rushbrooke, 1961). However, $t = \tanh(\frac{1}{2}\beta J)$ is a more natural high temperature variable for the Ising spin $\frac{1}{2}$ model, and extremely long series (up to 14 terms) have been derived for pure lattices in terms of this variable (Domb and Sykes, 1961(b); Moore, Jasnow and Wortis, 1969) by use of a counting theorem. These long series again support an assumption of the type

$$\chi \sim \frac{A}{(t_c - t)^{\gamma(p)}} \qquad t \to t_c(p)$$

when $p = 1$, and extremely consistent values of $t_c(1)$ and $\gamma(p=1)$ are obtained.

However, the counting theorem is not applicable to the dilute lattice, and t-series are usually derived via the weak cluster theorem in this case, (Rushbrooke et al, 1972; Rapaport, 1972(a)). Rapaport obtains the first ten terms of this series for the face-centred cubic lattice at various values of p. The results of his work are discussed in the following chapters, and more details of the derivation of high temperature series given.

CHAPTER TWO

DERIVATION OF SERIES FOR THE SUSCEPTIBILITY

§2.1 The Hamiltonian used is the following:

$$H = -2J \sum_{<ij>} S_i^z S_j^z - \mu H' \sum_i S_i^z \qquad - 2.1$$

for the case of nearest neighbour interactions only, and spin $\frac{1}{2}$. Each pair of magnetic atoms $<ij>$ is counted once in the sum. Each site on the lattice may be occupied with probability p by a magnetic atom: the remaining N(1-p) sites are occupied by 'quenched' impurities - quenched in the sense that the impurities are frozen randomly into the lattice, and are not in thermal equilibrium with it. Accordingly, the thermodynamics of each configuration of atoms is first determined, and then averaging over all possible configurations performed (Brout, 1959).

The susceptibility of the lattice is written as:

$$\chi(T) = \sum_{n,\alpha} N_{n,\alpha} \, \phi_{n,\alpha}(T) \qquad - 2.2$$

where $\phi_{n,\alpha}(T)$ is the susceptibility of an isolated cluster of n magnetic atoms: one in which each atom has at least one next neighbour belonging to the cluster and no magnetic neighbours which do not. The suffix α distinguishes clusters which are connected differently, and $N_{n,\alpha}$ is the probability of finding such a cluster on the lattice.

Since

$$N_{n,\alpha} = Np^n \sum_{m_i} (1-p)^{m_i} O_{n,\alpha}^{m_i} \qquad - 2.3$$

where m_i is the number of impurity atoms required to isolate a cluster of type α and a particular topology, and $O_{n,\alpha}^{m_i}$ is the occurrence of such a topology on the lattice, the sum for $\chi(T)$ can be rewritten as a power series in p in the form:

$$\chi^R(T) = \frac{4\chi(T)}{N\mu^2\beta p} = \sum_{n=0}^{\infty} a_{n+1}(T)p^n \qquad - 2.4$$

where $\beta = \frac{1}{kT}$ and μS^z is the spin magnetic moment. In order to obtain N terms in the series for $\chi^R(T)$ it is necessary to calculate the cluster susceptibilities $\phi_{n,\alpha}$ and occurrences $N_{n,\alpha}$ for all isolated clusters of N points or less which are allowed on the lattice of interest.

§2.2 Cluster Susceptibilities

In the Ising problem the cluster eigenfunctions are just the products of spin functions for the individual atoms of the cluster.

Now $\phi_{n,\alpha} = \frac{1}{\beta}\frac{d^2}{dH'^2}\ln Z\big|_{H'=0}$

where $Z = \mathrm{Tr}\{\exp(-\beta H)\}$.

Since the two parts of the Hamiltonian commute, this can be written as

$$\phi_{n,\alpha} = \beta\mu^2\,\mathrm{Tr}\{(\Sigma_i S_i^z)^2 \exp(-2\beta J \sum_{\langle ij\rangle} S_i^z S_j^z)\}/\mathrm{Tr}\{\exp-2\beta J \sum_{\langle ij\rangle} S_i^z S_j^z)\} \qquad -2.5$$

where the sums are restricted to sites lying on the magnetic cluster. It is now straightforward, if tedious, to calculate the traces required to find $\phi_{n,\alpha}$ as a ratio of polynomials in $x = \exp(-\beta J)$, at least for small clusters.

We calculate the dimensionless $\chi_{n,a} = \phi_{n,a}/\beta\mu^2$. In Appendix 1 the results of this are tabulated for all the clusters required to obtain a five-term series for the face-centred cubic (FCC) lattice, and seven-term series for the simple cubic (SC) lattice, the plane square (Q) lattice and the tetragonal zircon (TZ) lattice. The five-point cluster susceptibilities for the FCC lattice and the seven-point cluster susceptibilities have not been previously published. In addition, the susceptibilities of eight-point clusters required for the SC, Q, and TZ lattices which contain at least one closed loop of magnetic atoms are presented, in a slightly different form, the variable $t = \tanh(\beta J/2)$ being employed.

Several checks have been employed to test the accuracy of these expressions.

At zero temperature we expect that

$$\chi_{n,a} = n^2S^2 = \tfrac{1}{4}n^2$$

since the ground state of the cluster has all the spins aligned, and also that at infinite temperature

$$\chi_{n,a} = nS^2 = \tfrac{1}{4}n.$$

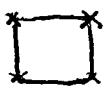
A more rigorous check is imposed by transforming the $\chi_{n,a}$, ratios of polynomials in x, to ratios of polynomials in t, by $x = \frac{1-t}{1+t}$. Again $\chi(t=1) = \frac{1}{4}n^2$, and $\chi(t=0) = \frac{1}{4}n$: further as the coefficient of each power of t in $\chi_{n,a}(t)$ has contributions from every power of x in $\chi_{n,a}(x)$, it is found

that reasonable forms for $\chi_{n\alpha}(t)$ can only be obtained from correct expressions for the $\chi_{n\alpha}(x)$.

These "reasonable" forms may now be compared with those derivable from the formula:

$$\chi_{n\alpha}(t) = n + 2\left(\sum_{g^2} t^{n(g^2)}\right)/\left(1 + \sum_{g^o} t^{n(g^o)}\right) \qquad - 2.6$$

which is a particularisation to the case of a finite cluster of the high temperature expansion in t first developed by Oguchi (Oguchi, 1951; Domb, 1960). Here g^2 is any single line graph - including separated graphs - with two odd vertices that may be embedded on the cluster (n,α) and g^o is any such graph with no odd vertices: $n(g)$ is the number of bonds on graph g. It is worth noticing that such embedding is "weak", in the sense that no lines may be introduced into graphs by the lattice itself: for example, consider the isolated cluster (4c).



- 4c

The three-line graph *x–x–x belonging to the set $\{g^2\}$ may be embedded on this graph weakly in four ways, despite each such embedding leaving its ends on next neighbour sites. If the embedding were strong, each embedding would introduce a new line: no embedding which made sites not explicitly nearest neighbours to be so would be allowed.

The application of formula 2.6 to clusters of seven or eight atoms becomes rather difficult to perform with

confidence as a method of producing $\chi_{n\alpha}(t)$: however it is useful in checking the forms produced by the more mechanical approach adopted in this work.

§2.3 Cluster Occurrences

Even for the simple lattices studied, the calculation of the $O_{n,\alpha}^{m_i}$ for each cluster rapidly becomes impossibly tedious. It is worth noting that to obtain an extra term for the FCC lattice, 15 new clusters had to be determined: in order to obtain the next term, a further 58 clusters would be required. Two simplifications are, however, possible. One is that to obtain the Nth term of the series it is not necessary to have full information about the occurrences of N-pt clusters: equation 2.3 shows that only the sum over all possible m_i of $O_{n,\alpha}^{m_i}$ for the cluster is needed. The other, which will be discussed more fully in Section 2.4, is that for the Nth term only the self-avoiding walk cluster of (N-1) steps and N-pt clusters with loops are required. With eight-point clusters on a square lattice (the case where this is used) the result is of value not so much in cutting the number of clusters to be determined (from 51 to 37) as in removing those clusters whose occurrences are most difficult to determine - and most likely to lead to error.

Checks on the occurrences are rather few: some of them have been previously tabulated (Muse, D.Phil. thesis,

Rushbrooke and Morgan, 1961; Domb, 1960), but most have been worked out by hand and checked by repeating the calculations. We do know, however, that at zero temperature each $\chi_{n\alpha} \to \frac{1}{4}n^2$: accordingly the expressions for a_n for the various series tabulated at the end of this section should reduce to the mean cluster size coefficients derived by Sykes and Essam (1964), which are also tabulated on the FCC, SC, and Q lattices.

Also, since in the infinite temperature limit all the spins are essentially independent,

$$\lim_{T\to\infty} \chi^R(T) = 1.$$

Each $a_n(t)$ should be zero when T is infinite if $n > 1$.

The expressions found for the various $a_n(t)$ do satisfy these checks, which are necessary but not sufficient for correctness. A more rigorous check is found by exploiting the essential identity of series in p,t and $(\frac{1}{2}\beta J)$ for $\chi^R(T)$, and this investigation will lead us to the simplification referred to earlier.

§2.4 Equivalence of Series

The series of type 2.4 may be rewritten to permit comparison with the series in t derived for the FCC lattice by Rushbrooke et al (1972) or the series in $(\frac{1}{2}\beta J)$ derived for FCC, SC, and Q lattices by Morgan and Rushbrooke (1961). Since all these series are derived by "exact" methods it

is expected that the same coefficient of $p^n t^m$ or $p^n(\frac{1}{2}\beta J)^m$ should be found from p and t or p and $(\frac{1}{2}\beta J)$ series if known to sufficiently high order. Since a series in t for the SC and Q lattices can be easily deduced from the $(\frac{1}{2}\beta J)$ series of Morgan and Rushbrooke, discussion will centre on comparison of the p and t series - see table 1.

Table 1. Simple Cubic Lattice

$$\chi = \sum_{n=0}^{\infty} a_{n+1} p^n = \sum_{n=0}^{\infty} b_{n+1} t^n$$

a_1	1	b_1	1
a_2	$6t$	b_2	$6p$
a_3	$30t^2$	b_3	$30p^2$
a_4	$150t^3 - \frac{24t^5}{1+t^4}[1+t+t^2]$	b_4	$150p^3$
a_5	$726t^4 - \frac{192t^6}{1+t^4}[1+t+t^2]$	b_5	$726p^4$
a_6	$3534t^5 + \frac{24t^6}{1+t^4}[24-17t-32t^2 -53t^3] - \frac{48t^7}{1+t^6}[1+t+t^2+t^3+t^4] - \frac{36t^6}{1+2t^4+t^6}[16+34t+30t^2+14t^3 +10t^4]$	b_6	$3534p^5-24p^3$
a_7	$16926t^6 + 0t^7 .....$	b_7	$16926p^6-192p^4-24p^3$

The need for coefficients of particular powersof t obtained from a given a_n to agree with coefficients in the b_n imposes quite a strong check both on the cluster susceptibilities as functions of t and on the occurrences of these clusters: in particular, for $n > 1$, the coefficient of t^{n-1} in a_n must be the number of (n-1) step self avoiding walks which may be weakly embedded on the lattice, and the coefficient of t^n must be zero. It is also noteworthy that no a_n contains powers of t less than t^{n-1}: this is equivalent to saying that no b_n can contain powers of p greater than p^{n-1}. The origin of these empirical 'rules' is found in the Oguchi t-expansion applied to the dilute magnet.

The Hamiltonian 2.1 is rewritten in terms of new spin variables σ_i which may take values ± 1 only.

$$H = -\tfrac{1}{2}J \sum_{<ij>} \sigma_i\sigma_j - \tfrac{1}{2}\mu H \sum_i \sigma_i \qquad - 2.7$$

The partition function z is now given by

$$z = \mathrm{Tr}(e^{-\beta H}) = \sum_{\sigma_i=\pm 1} \exp[\tfrac{1}{2}\beta J \sum_{<ij>} \sigma_i\sigma_j + \tfrac{1}{2}\beta\mu H \sum_i \sigma_i] \qquad - 2.8$$

Using the identities:

$$\sum_{\sigma_i=\pm 1} \exp(\tfrac{1}{2}\beta J \sum_{<ij>} \sigma_i\sigma_j) = \sum_{\pm 1}[\prod_{<ij>} (\cosh\tfrac{\beta J}{2} + \sigma_i\sigma_j \sinh\tfrac{1}{2}\beta J)] \qquad 2.9$$

$$\text{and } \sum_{\sigma_i=\pm 1} \exp(\tfrac{1}{2}\beta\mu H \Sigma\sigma_i) = \sum_{\pm 1}[\prod_i (\cosh\tfrac{1}{2}\beta\mu H + \sigma_i \sinh\tfrac{1}{2}\beta\mu H)] \qquad - 2.10$$

and, noting that the two parts of the Hamiltonian commute, obtain

$$Z = \sum_{\pm 1}[\prod_{<ij>} (\cosh\tfrac{1}{2}\beta J + \sigma_i\sigma_j \sinh\tfrac{1}{2}\beta J) \prod_i (\cosh\tfrac{1}{2}\beta\mu H + \sigma_i \sinh\tfrac{1}{2}\beta\mu H)] \qquad - 2.11$$

The susceptibility may now be obtained from

$$\chi = \frac{1}{\beta} \frac{d^2}{dH^2} \ln Z \Big|_{H=0}$$

as a series in $\tanh(\frac{1}{2}\beta J)$, the coefficients of which are cumulant averages, or, more clearly, from

$$\chi = \beta\mu^2 \sum_{p,q} \mathrm{Tr}(S_p^z S_q^z) \qquad - 2.12$$

where the trace is for the case of zero field. The expression for Z reduces to:

$$Z = \cosh[\frac{\beta J}{2}]^N \sum_{\pm 1} (\prod_{<ij>} (1 + \sigma_i \sigma_j t)) \qquad - 2.13$$

where there are N sites on the lattice, and χ can be written as:

$$\chi = \tfrac{1}{4}\beta\mu^2 \{ \sum_{\pm 1} [\sum_{p,q} \sigma_p \sigma_q \prod_{<ij>} (1+\sigma_i \sigma_j t)] \} (\cosh \frac{\beta J}{2})^N / Z \qquad - 2.14$$

$$= \frac{p\beta\mu^2}{4} \sum_{n=o}^{\infty} b_{n+1} t^n \qquad - 2.15$$

Since $\sum_{\pm 1} \sigma_i = 0$, $\sum_{\pm 1} \sigma_i^2 = 2$ and $\sum_{\pm 1} 1 = 2$, only terms in the product in 2.13 which contain an even number of σ_i for each site will contribute to Z. If we represent the term $\sigma_i \sigma_j t$ by a line joining sites i and j, such terms will correspond to graphs with no repeated lines, and an even number of lines meeting at each site: graphs made up only of loops.

The top line of 2.14 will only allow graphs which have two 'odd' sites, and all the others even. In either class, the graphs may be "separated" or multi-component. The determination of χ as a series in t is now a matter

of counting the weak embeddings of all such graphs with up to the desired number of lines.

In the pure lattice, counting theorems have been developed (Sykes, 1961; Nagle and Temperley, 1968) to simplify this task, and series of 14 terms have been found for a number of lattices (Domb and Sykes, 1961(b); Moore et al, 1969). No such simplification exists for the dilute lattice, where the approach used is to employ the weak cluster expansion to obtain numerical values for the coefficients of t^n for a variety of values of p (Rushbrooke et al, 1972; Rapaport, 1972(a)).

In the expansion 2.15, p^N is associated with an (N+1) site graph: for this graph to contribute to numerator or denominator it must have at least N lines. Accordingly, p^N can only be associated with t^N or higher. The (N+1) site graph with fewest lines is the N-step self-avoiding walk: the coefficient of $p^N t^N$ in 2.15 is therefore the number S_N of N-step self-avoiding walks which can be weakly embedded on the lattice. It can also be shown that the subtraction following expansion of the denominator of 2.14 will lead to no contribution from graphs of (N+1) sites and (N+1) lines (Rapaport, 1972(a)): the coefficient of $p^N t^{N+1}$ is therefore zero in 2.15.

These results are not of much value in expansion 2.15, where the expansion parameter is t, and the coefficients are functions of p, but they lead to substantial simplifi-

cations in the p-series 2.4, where the coefficient of p^N, a_{N+1}, is a function of t.

$$a_{N+1}(t) = S_N t^N + O t^{N+1} \ldots\ldots \text{higher powers} \qquad - 2.16$$

The cluster susceptibilities are given by

$$\chi_{n\alpha} = n + 2(\sum_{g^2} t^{n(g^2)})/(1 + \sum_{g^o} t^{n(g^o)}),$$

and it is readily seen that in clusters with no loops $\chi_{n\alpha}$ is a finite polynomial in t, the highest power of t being the number of steps in the longest self-avoiding walk that can be performed on the cluster. In clusters with no loops, but with branches, this is less than t^N. Accordingly we expect all such clusters to cancel out when $a_{N+1}(t)$ is formed.

There is a contribution t^N from the one branchless, loopless cluster - the straight chain, or self avoiding walk, and also from any clusters with loops. These add to give a total coefficient of t^N which is S_N - the number of <u>weakly</u> embedded self avoiding walks. Higher powers of t can come only from looped clusters, and it is expected that there should be no t^{N+1} term.

Table 1 shows how this works for the simple cubic lattice, and similar checks have been made for the FCC series and the first seven terms of the Q series.

A prescription may now be given to simplify the derivation of new p-series, or further terms in existing series.

To obtain $a_{N+1}(t)$

1. Count the occurrence of the N-step simple chain cluster. Multiply by $2t^N$.
2. Calculate the susceptibilities and occurrences of all clusters with loops of not more than (N+1) sites, and transform to the t-representation.
3. Rewrite the susceptibilities as the ratio of polynomials in t, starting with t^{N+1} in the numerator, and discarding powers of t less than t^N,

   e.g. for a_4 $\quad 4c \quad 4 + 2\,\dfrac{4t + 4t^2 + 4t^3}{1 + t^4}$

   $$\rightarrow (4 + 8t + 8t^2 + 8t^3) - \frac{8t^5+8t^6+8t^7}{1 + t^4}$$

   Keep $\quad 0t^4 - \dfrac{8t^5 + 8t^6 + 8t^7}{1 + t^4}$

4. Gather terms in p^{N+1}.
5. Check that the coefficient of t^N is S_N, of t^{N+1} is 0, and that $a_{N+1}(t=1)$ agrees with the mean cluster size series.

This procedure was used to derive an eighth term for the Q lattice, and an eight term series for the TZ series: an analytic form would have been impossibly tedious to produce otherwise. The occurrences of seven and eight point clusters required in this work are tabulated in Appendix I.

CHAPTER THREE

TECHNIQUES AND RESULTS OF SERIES ANALYSIS

§3.1 It has been seen that the series for χ^R derived for the dilute magnet reduce to the mean cluster size p-series at zero temperature, and to the t-series of Domb and Sykes when $p = 1$. It is natural therefore to extend the assumptions and methods that worked well in those cases - at least in so far as each new term in the series confirmed the results drawn from previous terms - to the dilute finite temperature magnet.

Accordingly the simple assumptions:

$$\chi^R \sim \frac{A_1}{(p_c(t)-p)^{\gamma_1(T)}} \text{ as } p \to p_c(t)^+ \text{ (for the p-series)} - 3.1$$

$$\text{and } \chi^R \sim \frac{A_2}{(t_c(p)-t)^{\gamma_2(p)}} \text{ as } t \to t_c(p) \text{ (for the t-series)} - 3.2$$

are made, and various analyses made to see if these seem justified and to determine the phase boundary and behaviour of the critical exponent γ. The series derived are rather short; ratio methods and Padé analysis may be expected to be most appropriate (Hunter and Baker, 1973).

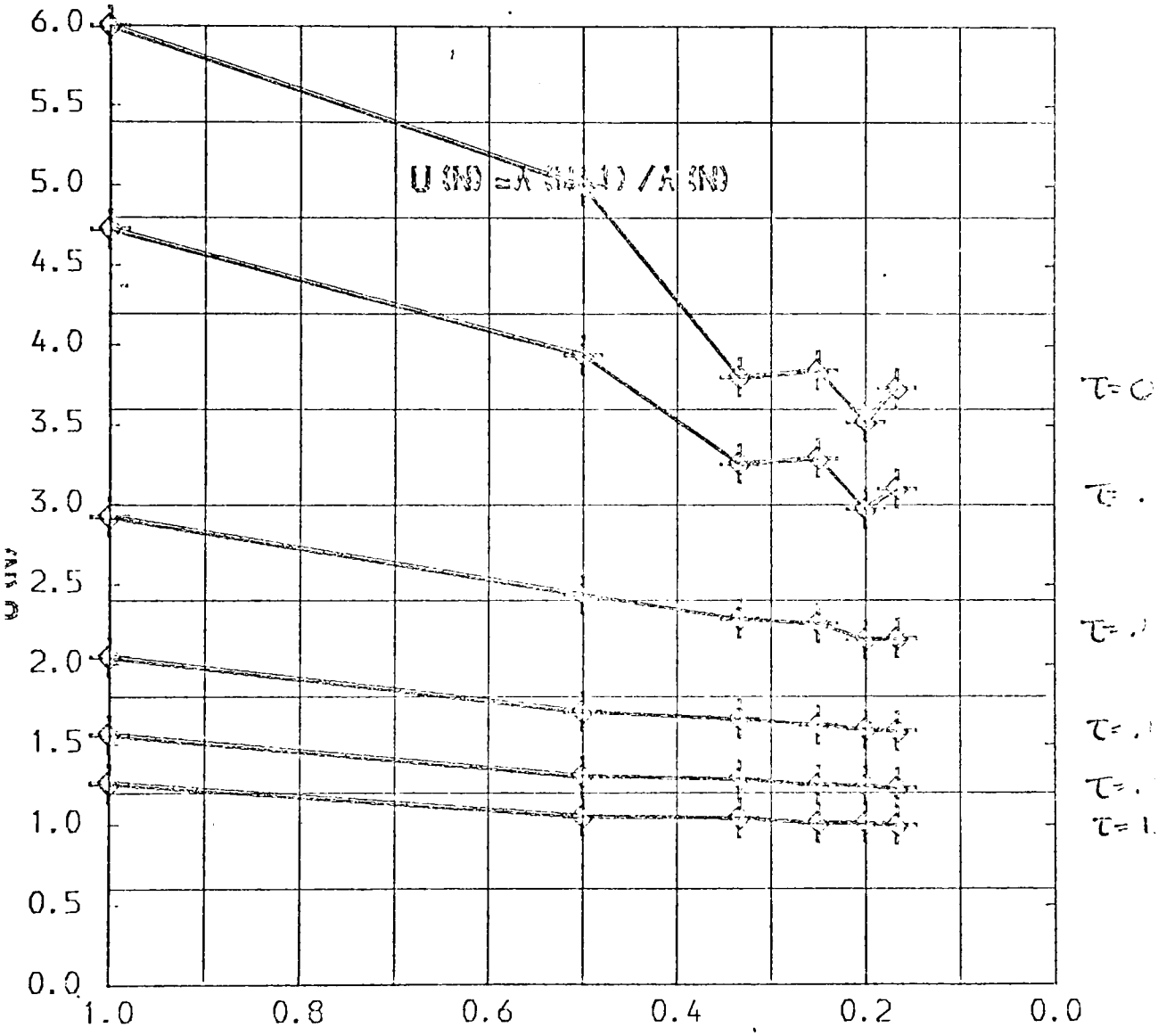
§3.2 Ratio tests

Such tests only determine the singularity closest to the origin: however, as long as all the terms of the series studied are positive, the singularity is on the positive

Figure 1. The Sequence $\{U_N\}$ vs $\frac{1}{N}$ at various temperatures.

SC lattice, 7 term p-series.

$\tau = T / T_c(1)$



real axis, and should be the physical one.

Consider the series

$$f(x) = \sum_{n=o}^{\infty} a_{n+1} x^n \qquad - 3.3$$

and assume $f(x) \sim \frac{A}{(x_c - x)^\gamma}$ as $x \to x_c$

$$= \frac{A}{x_c^\gamma}[1 + \gamma\frac{x}{x_c} \ldots \frac{\gamma \ldots (\gamma+n-1)}{n!}(\frac{x}{x_c})^n \cdots]$$

So as $x \to x_c$, $a_{n+1} \sim \frac{A}{x_c^\gamma} \frac{\gamma..(\gamma+n-1)}{n!} \frac{1}{x_c^n}$ $\qquad n>1$

by this hypothesis.

If u_n is now defined as

$$u_n = a_{n+1}/a_n$$

then $u_n \sim \frac{\gamma+n-1}{n} \frac{1}{x_c} = (1 + \frac{\gamma-1}{n})x_c \qquad - 3.4$

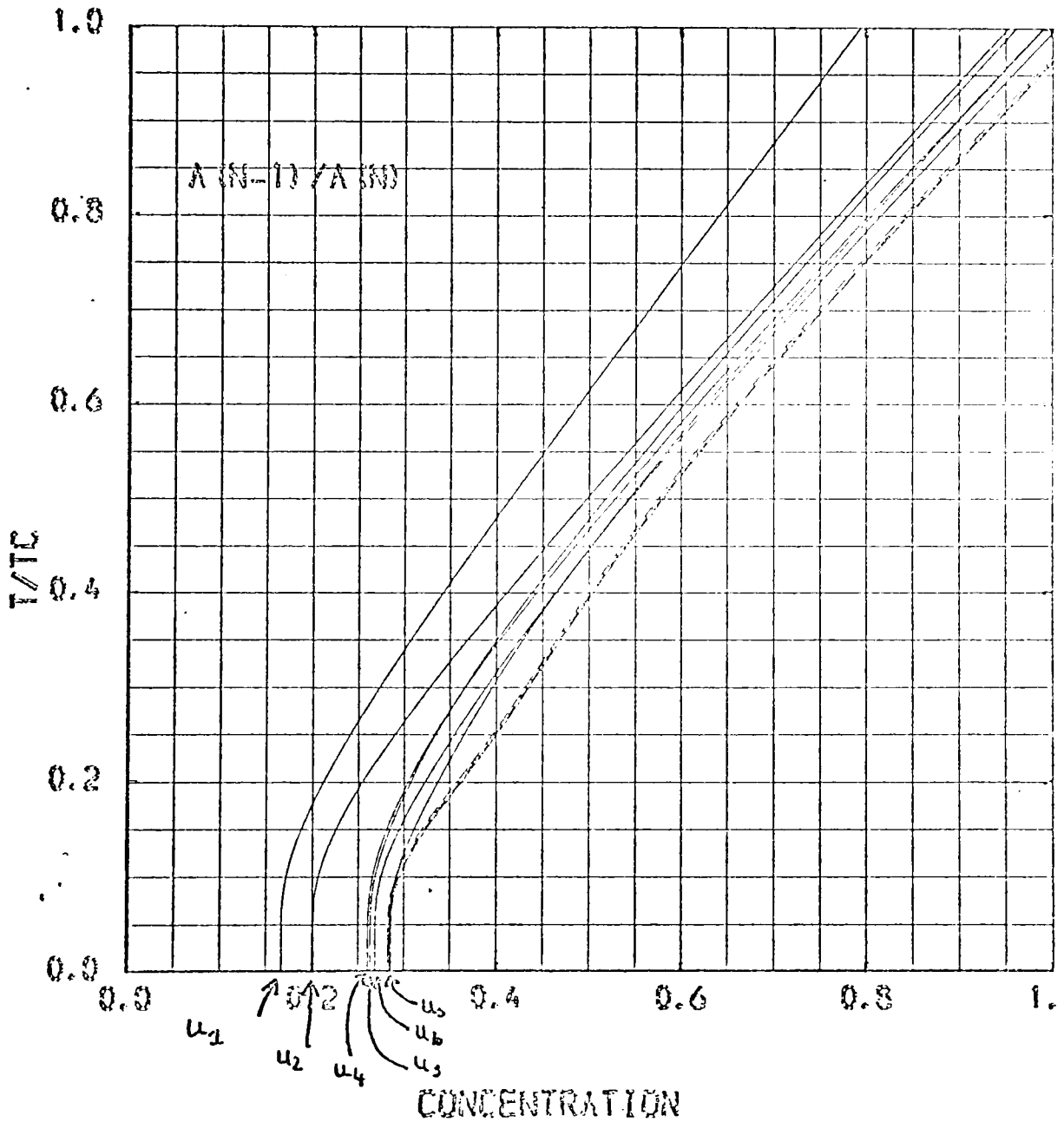
The limit of the sequence u_n as $n \to \infty$ gives the critical value of x, x_c, and the slope of the sequence plotted against $\frac{1}{n}$ then yields an estimate of γ which is 'biassed' in the sense that it depends on the estimate x_c.

Such a sequence is formed for the seven term p-series for the simple cubic lattice, and is plotted against $\frac{1}{n}$ in Fig. 1 for various temperatures. It is noticeable that the sequence alternates regularly, particularly at low temperatures, so that extrapolation and gradient estimation are difficult. This is due essentially to the even coordination number of the lattice. The most

Figure 2 The sequence $\{u_n\}$ vs. Temperature

Simple cubic lattice: 7 term p series.

The bold line is the linear extrapolation of u_4 and u_6



obvious way to circumvent this is to extrapolate linearly u_N and u_{N-2}: Fig. 2 shows the sequence of curves $\{u_n\}$ for n = 1,6 and the extrapolate from u_4, u_6 (bold line) plotted over a range of temperatures.

With more terms in the series it might be worth refining this procedure either by calculating the two straight lines which form an envelope for the sequence in Fig. 1 at a given temperature, or by using the sequence of estimates:

$$\mu_n(\varepsilon) = \tfrac{1}{2}[(n+\varepsilon)u_n - (n+\varepsilon-2)u_{n-2}]$$

where ε is an arbitrary small shift chosen to smooth out the effects of higher order terms neglected in 3.4 (Fisher, 1967).

The sequences

$$v_n = (a_{n+1}/a_1)^{1/n}$$

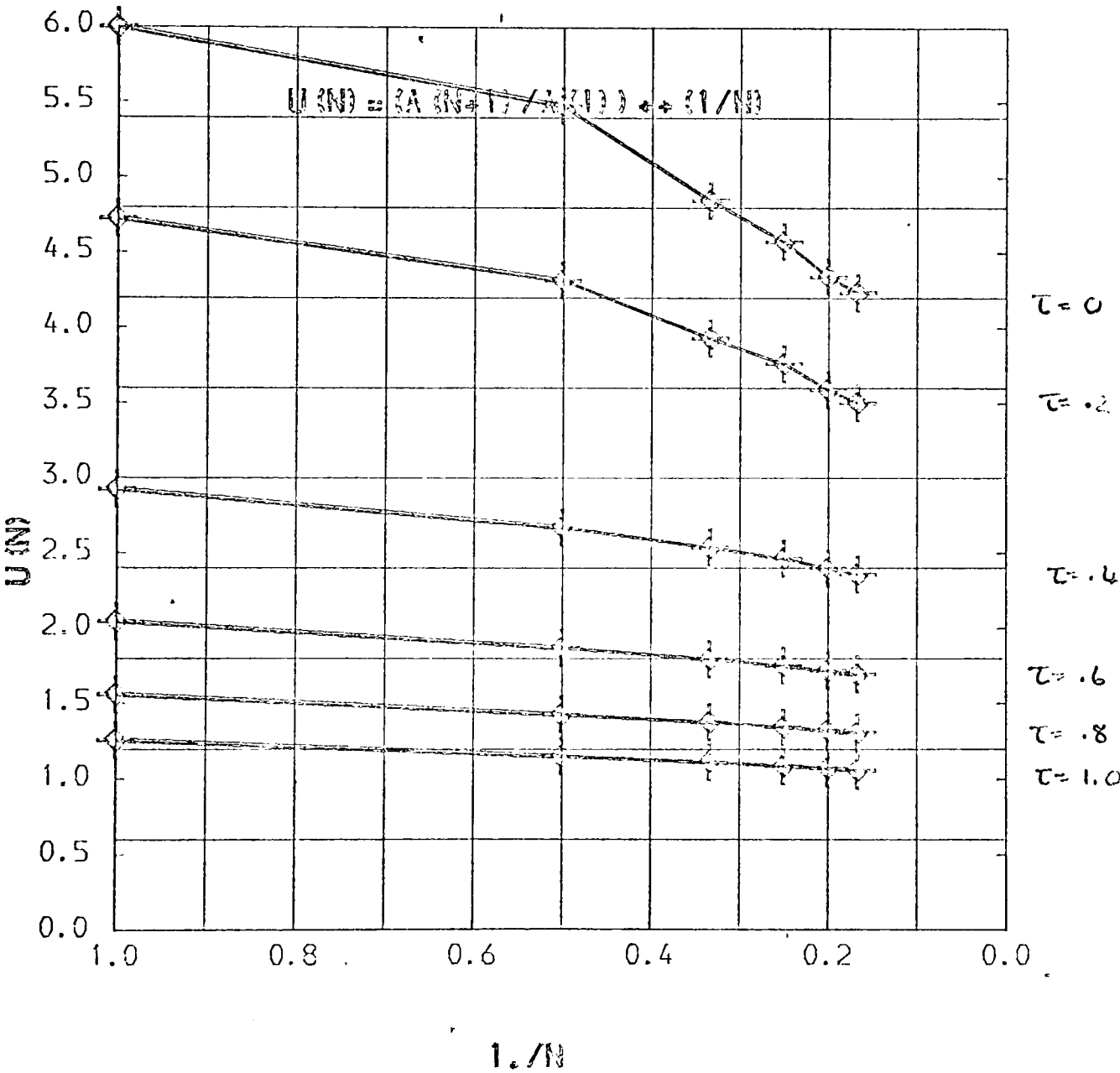
and $$w_n = (a_{n+2}/a_n)^{1/2}$$

may also be formed, and have the same limiting behaviour as $\{u_n\}$. Figs. 3,4 show that there is little evidence of oscillation when these sequences are plotted against $\frac{1}{n}$. Linear extrapolation of the last two, or last and last-but-two of either sequence may now be performed: in addition, polynomial interpolation could be performed by Neville table, though the series are thought too short and oscillatory to make this worthwhile. In the face of such a profusion of results, it is plainly difficult to

Figure 3 The Sequence $\{v_n\}$ vs $\frac{1}{n}$.

7 term p-series : SC lattice

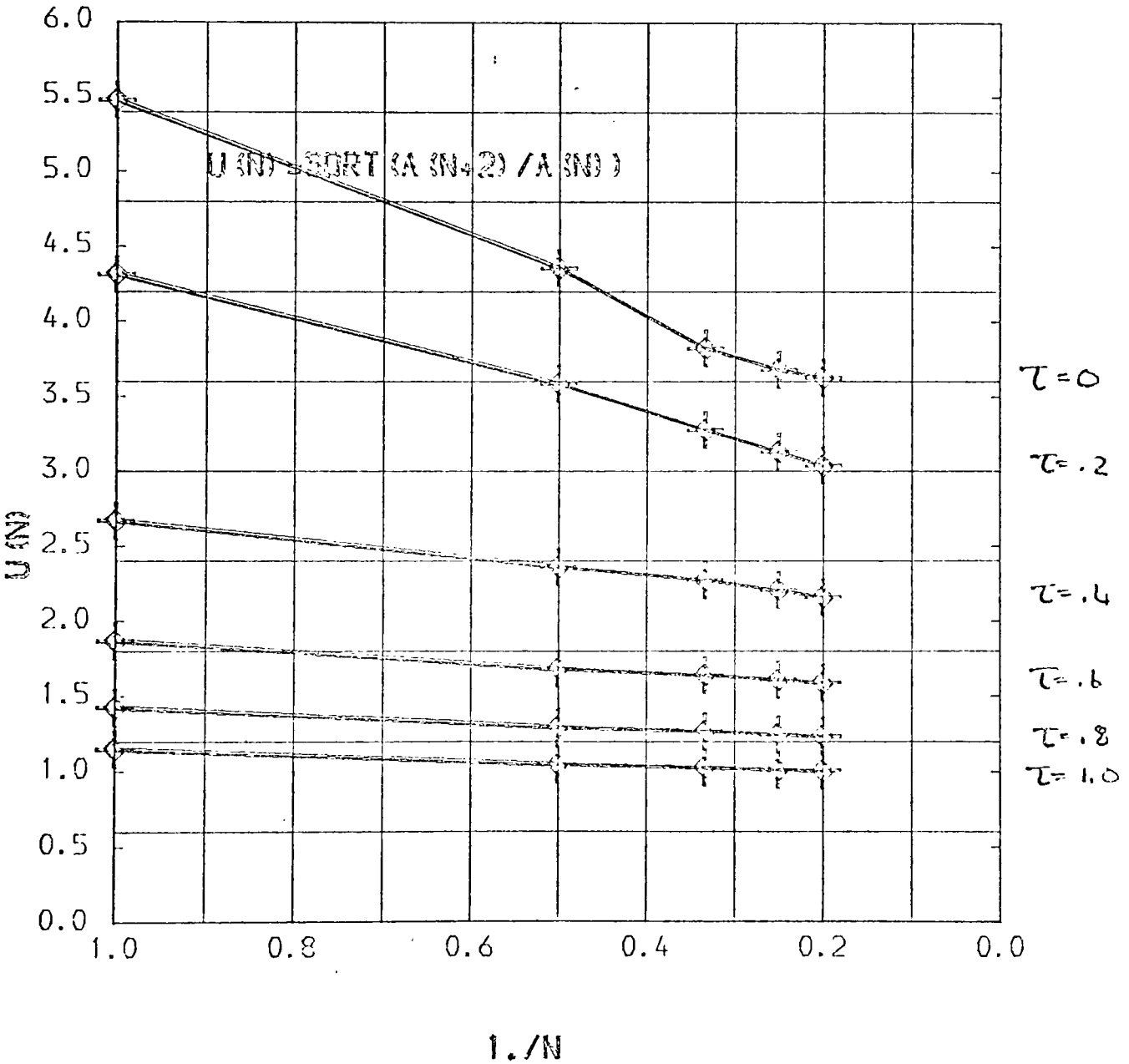
$\tau = T / T_c(1)$.



The Sequence $\{w_n\}_{n=0}^{\infty} = \frac{1}{n}$.

Figure 4 SC lattice, 7 term p-series

$\tau = T / T_c(1)$



select a 'best' method, as there is no intrinsic guide as to which is most reliable. In any case, all the methods used give much the same phase boundary when used on the 7 term p-series for the SC lattice (Fig. 5: methods 2,4,6).

TABLE 2 N = 6: simple cubic lattice

Method No.	Extrapolation of	kT_c/J	p_c^s	$\gamma_1(p=1)$	$\gamma_1(T=0)$
1	u_N, u_{N-1}	2.177	.209	1.42	-.322
2	u_N, u_{N-2}	2.263	.285	1.18	1.38
3	v_N, v_{N-1}	2.329	.271	1.38	1.88
4	v_N, v_{N-2}	2.346	.282	1.34	2.15
5	w_N, w_{N-1}	2.283	.293	1.15	1.31
6	w_N, w_{N-2}	2.267	.300	1.18	1.44
	'Accepted'	2.255*	$.307\pm.01$†	1.25*	$\frac{27}{16}=1.6875\pm .05$†
7	P.A's [4,2]	-	.577	-	26.49
8	" [3,3]	2.268	.285	1.19	1.07
9	" [2,4]	2.268	.321	1.19	1.70

* Domb and Sykes, 1961(b): accurate to the number of places given at least.

† Sykes and Essam, 1964:

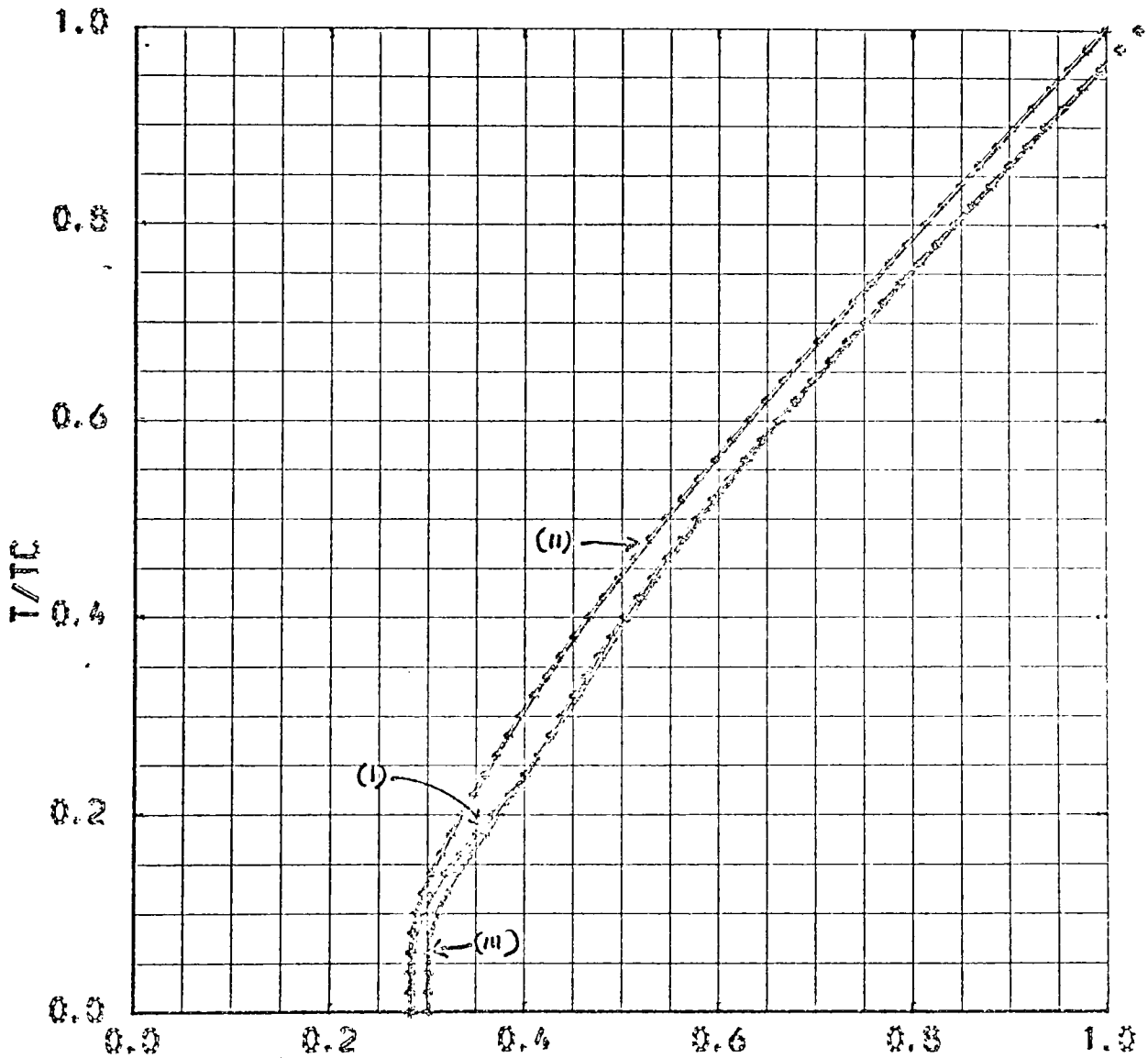
NOTE: Method 1 gives wild values at T=0 due to the oscillation of $\{u_n\}$ vs. $\frac{1}{n}$.

Figure 5. Phase Boundary for the Simple cubic lattice: 7 term p series.

(I) Linear extrapolation of U_n, U_{n-2}

(II) " " U_n, S_{n-2}

(III) " " W_n, W_{n-2}



The Sequence $\{v_n\}$ vs. Temperature

Figure 6

— member of sequence $\{v_n\}$

— extrapolate of v_6, v_7

Simple cubic lattice:
7 term p-series

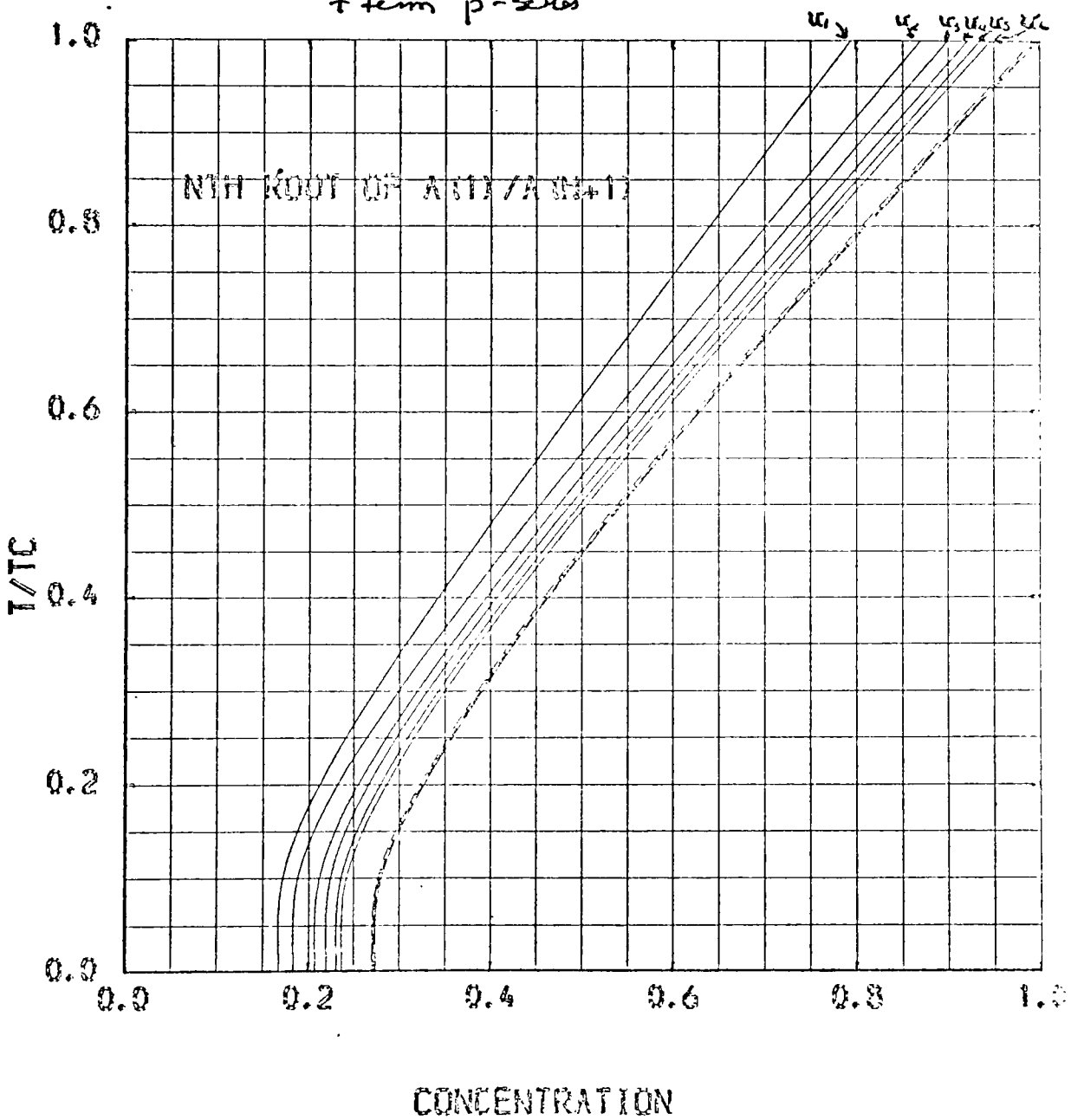
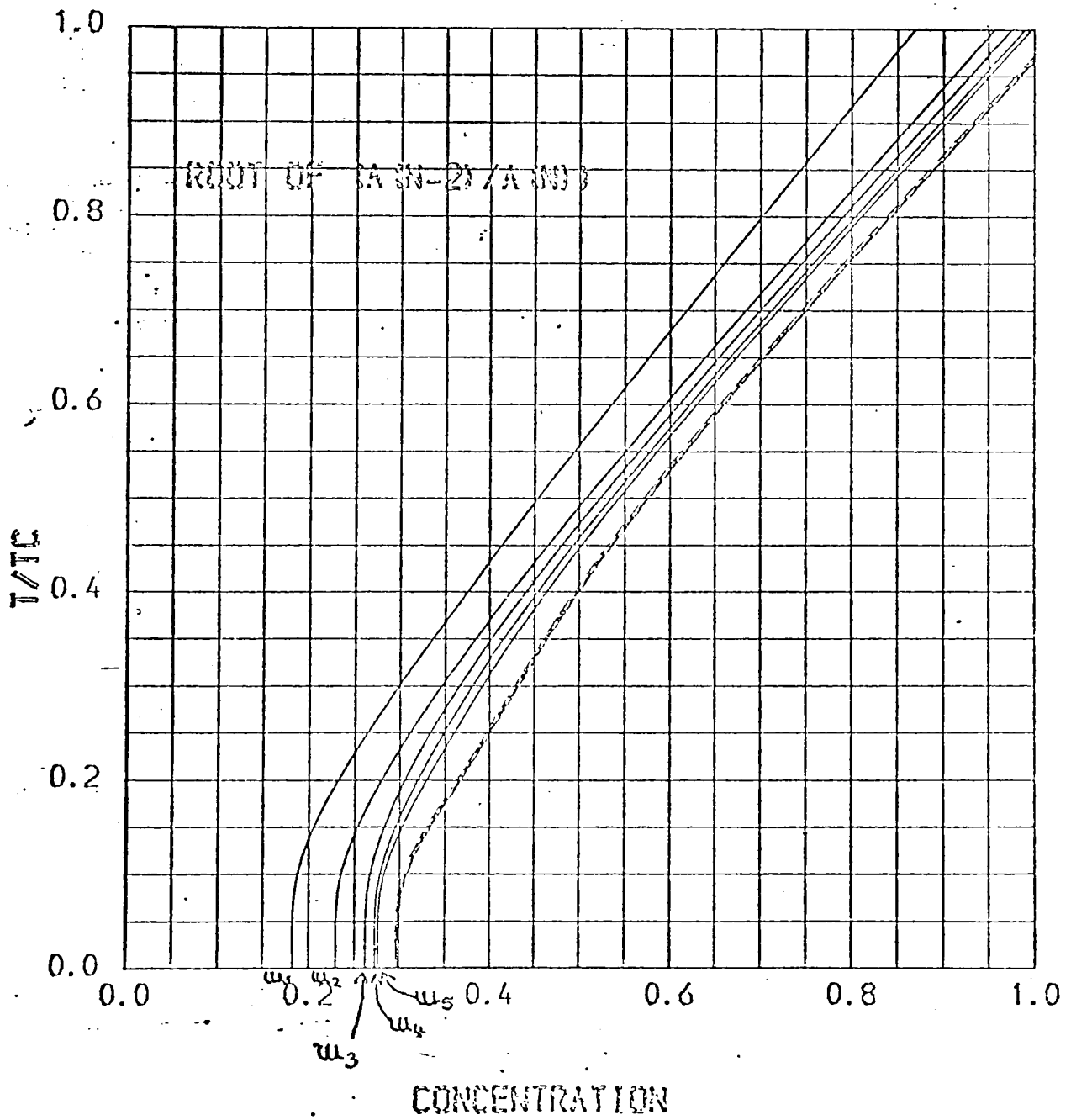


Figure 7 The sequence $\{w_n\}$ vs Temperature

Simple cubic lattice: 7 term p. series

The bold line is the linear extrapolate of w_3 and w_4



It is noteworthy that for this lattice (and the FCC and Q) linear extrapolation of (w_N, w_{N-2}) gives best agreement with the "accepted" values for p_c^s and $kT_c(1)/J$: Heap also found this with shorter series for several lattices. Accordingly this method is used to estimate the percolation concentration and $kT_c(1)/J$ for the TZ lattice, obtaining:

$$p_c^s = .47$$
$$kT_c(1)/J = 1.33$$

These values are reasonably well supported by experiment (see Chapter Four). Phase boundaries derived by methods 2,4 and 6 are plotted together for the FCC, Q' and TZ lattices in Appendix 2.

Of more interest, perhaps, than attempts to refine the calculation of the phase boundary by such means is the question of whether the terms added to the series in this work uphold the simple assumption 3.1. Fig. 2 appears to indicate so: the fresh curve u_6 confirms the trend indicated by the previous u_n. Figs. 6 and 7 show that the sequences $\{v_n\}$ and $\{w_n\}$ also behave thus. Similar results are found for other lattices.

The results that such methods give from the simple hypothesis 3.1 for the critical index γ are much less straightforward. Fig. 8 indicates the biassed estimates for $\gamma_0(\mathcal{T})$ resulting from methods 2,4 and 6. There is little agreement between the curves, and the only general

Figure 8. Critical Index vs Temperature
by methods 2, 4 and 6
SC lattice: 7 term p-series

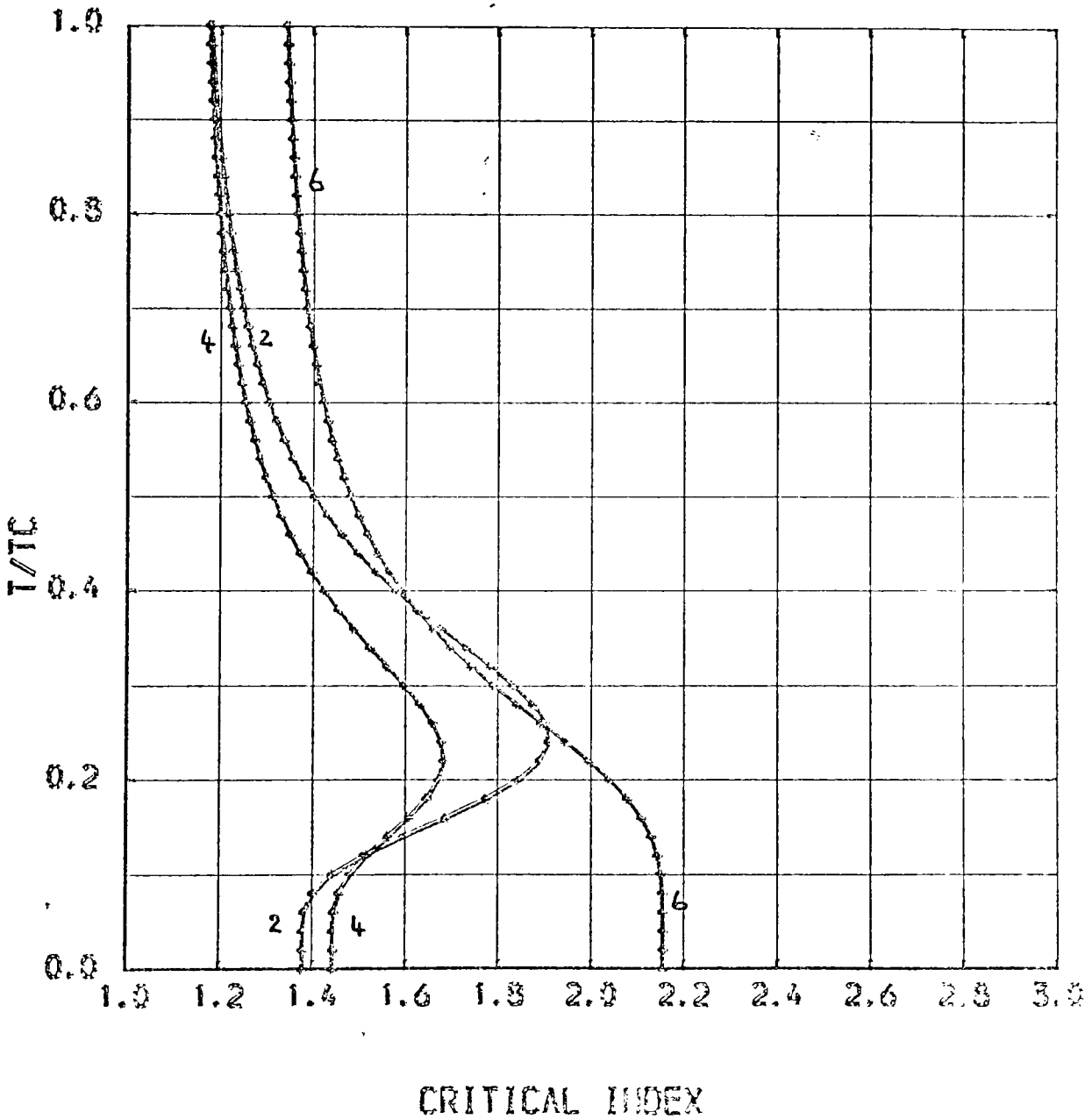


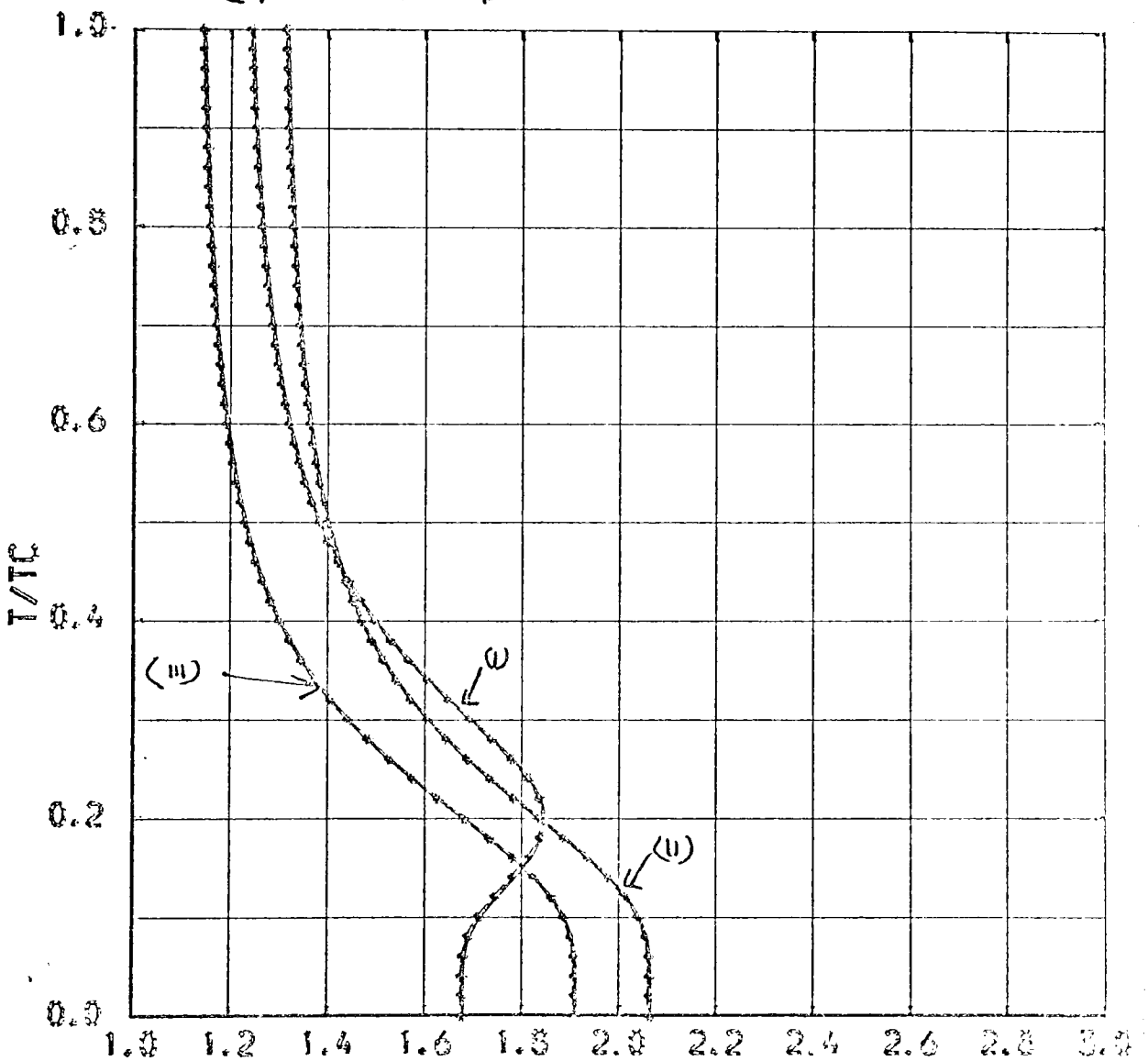
Fig 9 Critical index vs temperature

Simple cubic lattice: 6 term p-series

(I) Method 2

(II) Method 4

(III) Method 6

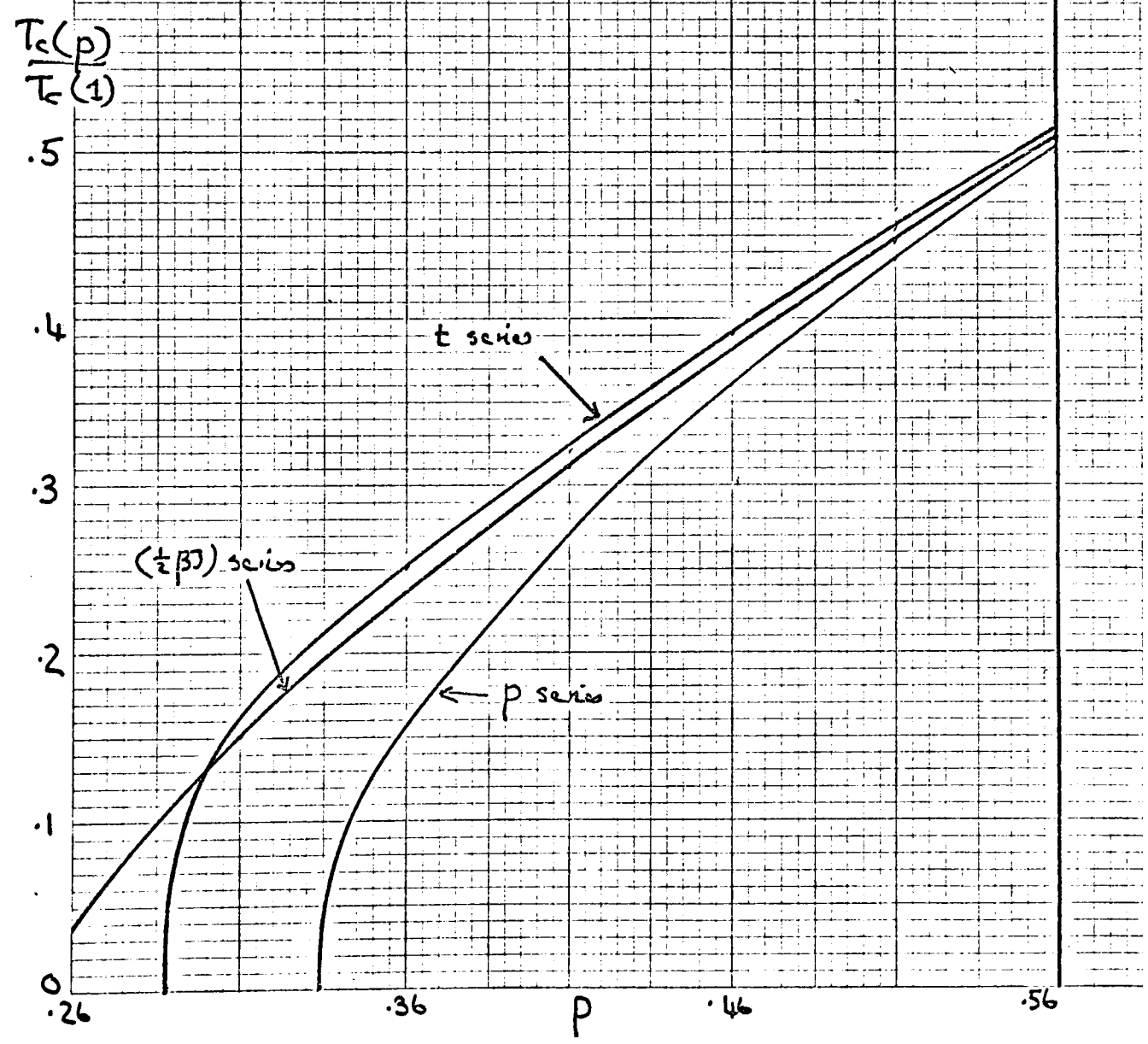


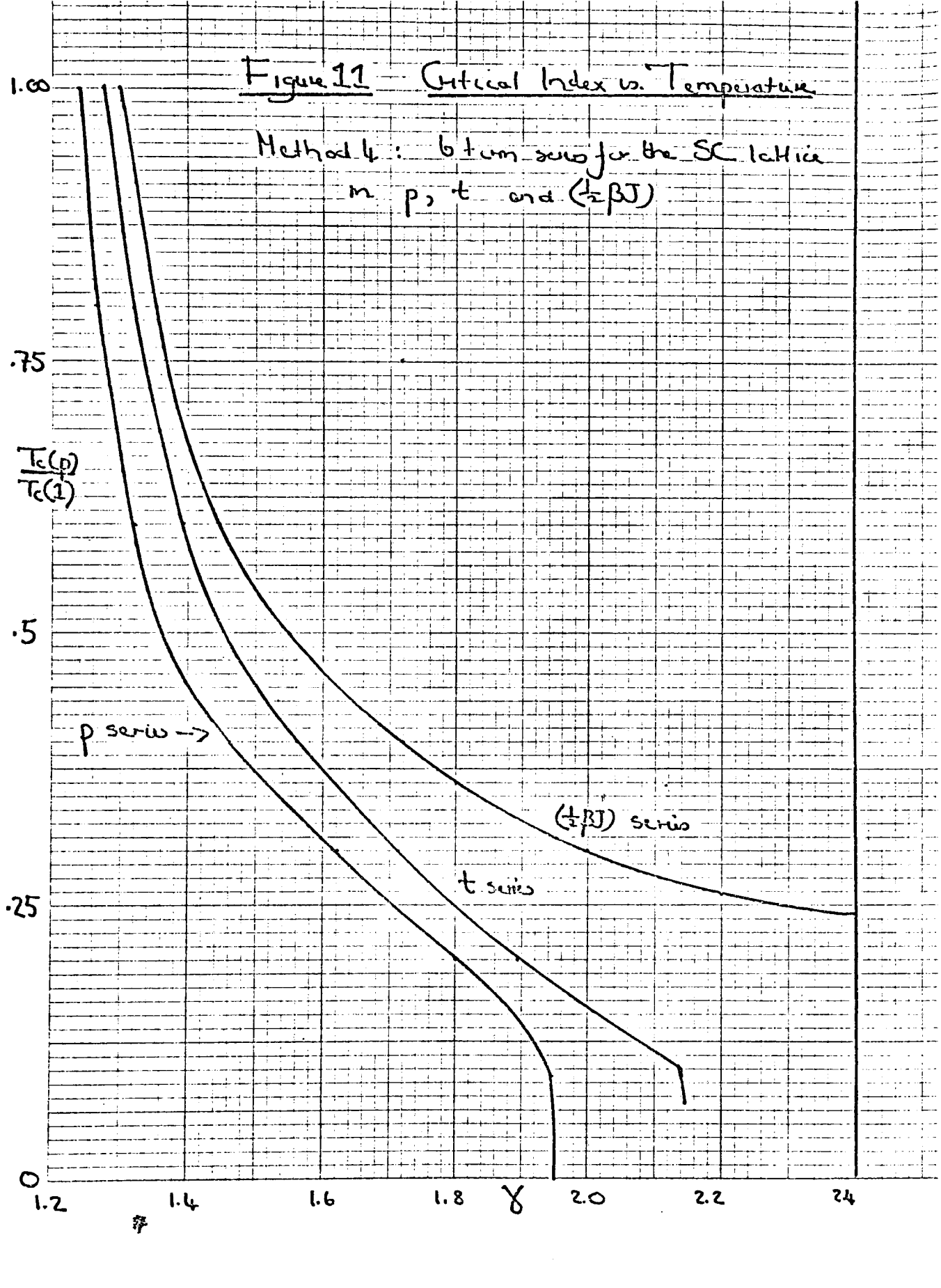
behaviour one can find is that $\gamma_1(T=0)$ has about the right value and decreases to about the right value at p = 1: further, γ_1 seems to increase initially at low temperatures, and then decrease rapidly till $T_c(1)$ is reached. It also appears to be a feature of the method that the γ_1-estimate gets less reliable as more terms are found, in so far as the γ_1 curves are further apart and the right-hand bend is more obvious: this is doubly surprising, as the phase boundary estimate from extra terms is thought to improve, and the γ_1-estimate depends on the phase boundary estimate. (Compare Fig. 9, using six terms only for SC lattice, with Fig. 8).

Similar behaviour can be found in the analysis of the t and $(\frac{1}{2}\beta J)$ series: this is performed here for six-term series, using method 4, and comparison made with a p-series of similar length for the same cubic lattice. (Similar behaviour has been found - to a more pronounced degree - in the longer high temperature series of Rushbrooke et al (1972) and Rapaport (1972(a)).). Fig. 10 shows the phase boundary produced in this manner from the three series: analysis of the $(\frac{1}{2}\beta J)$ series ceases to be possible at low p, as some terms become negative. At high p and T the curves are almost identical: at lower p, most reliance can be placed on the p-series results. Fig. 11 indicates the behaviour of $\gamma_1(p)$ and $\gamma_1(T)$, deduced from the three series. $\gamma_1(T)$ appears to have reasonable

Figure 10 — Phase Boundary for SC lattice

Method 4: 6 term series in p, t and $(\frac{1}{2}\beta J)$




Figure 11 – Critical Index vs. Temperature
Method 4: bt-um series for the SC lattice
m p, t and (½βJ)
1.00
.75
.5
.25
0
$\frac{T_c(p)}{T_c(1)}$
p series →
(½βJ) series
t series
1.2
1.4
1.6
1.8
γ
2.0
2.2
2.4

behaviour (but see the change brought about by another term in Fig. 8); whereas $\gamma_2(p)$ deduced from the $(\frac{1}{2}\beta J)$ and t series becomes large at low temperatures. Addition of further terms leads to $\gamma_2(p)$ becoming very large at about $p = .6$ for the $\frac{1}{2}\beta J$ series (8 terms, FCC lattice; Rushbrooke et al) and the t-series (11 terms, FCC lattice; Rapaport). Although no analytic relationship between $\gamma_2(p)$ and $\gamma_1(T)$ exists, it is suggestive that the analysis should indicate large values of both around $p = .5$. Further discussion of this will follow in Section 3.

Plots similar to Fig. 8 for the FCC, Q and TZ lattices are reproduced in Appendix II. Again analysis consequent on assumption 3.1 has failed to find a consistent behaviour for $\gamma_1(T)$. Notes on particular features of the series will also be found in Appendix II.

§3.3 Padé Approximant Analysis

This method consists in approximating the first N terms of the series by the ratio of two polynomials, the numerator of order P, the denominator of order D, correct to order x^{N-1}.

$$f(x) = \sum_{n=o}^{N-1} a_{n+1}x^n = \frac{A_1+A_2x \ldots .A_{p+1}x^p}{1+B_1x+B_2x^2 \ldots B_Dx^D} \qquad - 3.5$$

The result is the Padé approximant (P.A.) called [P,D], and equating the first P+D+1 = N coefficients of x in 3.5 leads to a set of simultaneous equations for the A_i

Figure 13 Simple cubic lattice : 7 term p series
Phase boundary by Dade' Approximant

(I) [2,4]
(II) [3,3] (III) [4,2]
Note: [4,2] fails below $T/T_c(1) = .45$

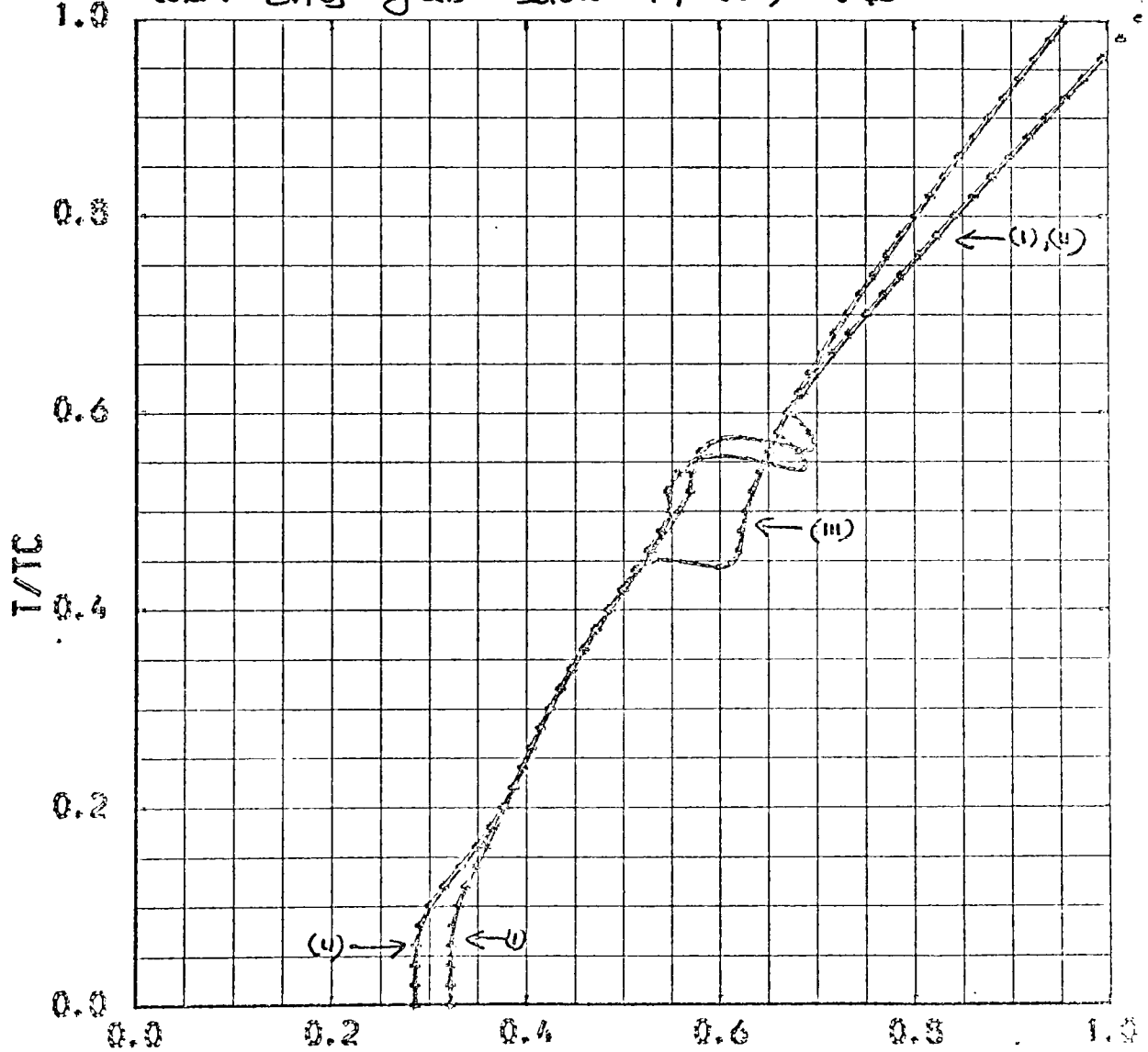
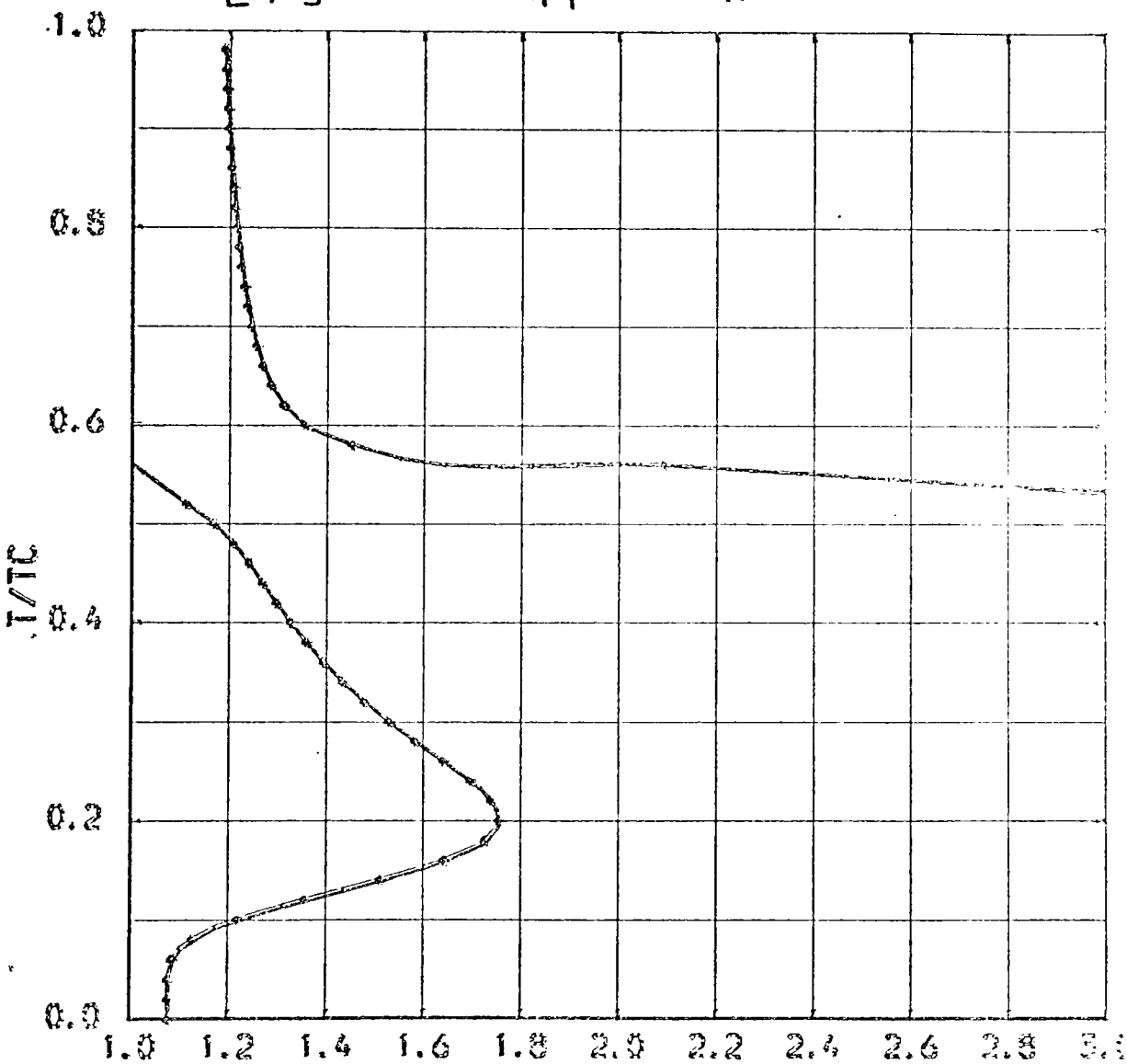


Fig 14 Critical exponent vs Temperature

Simple cubic lattice: 7 term p-series

[3,3] Padé Approximant



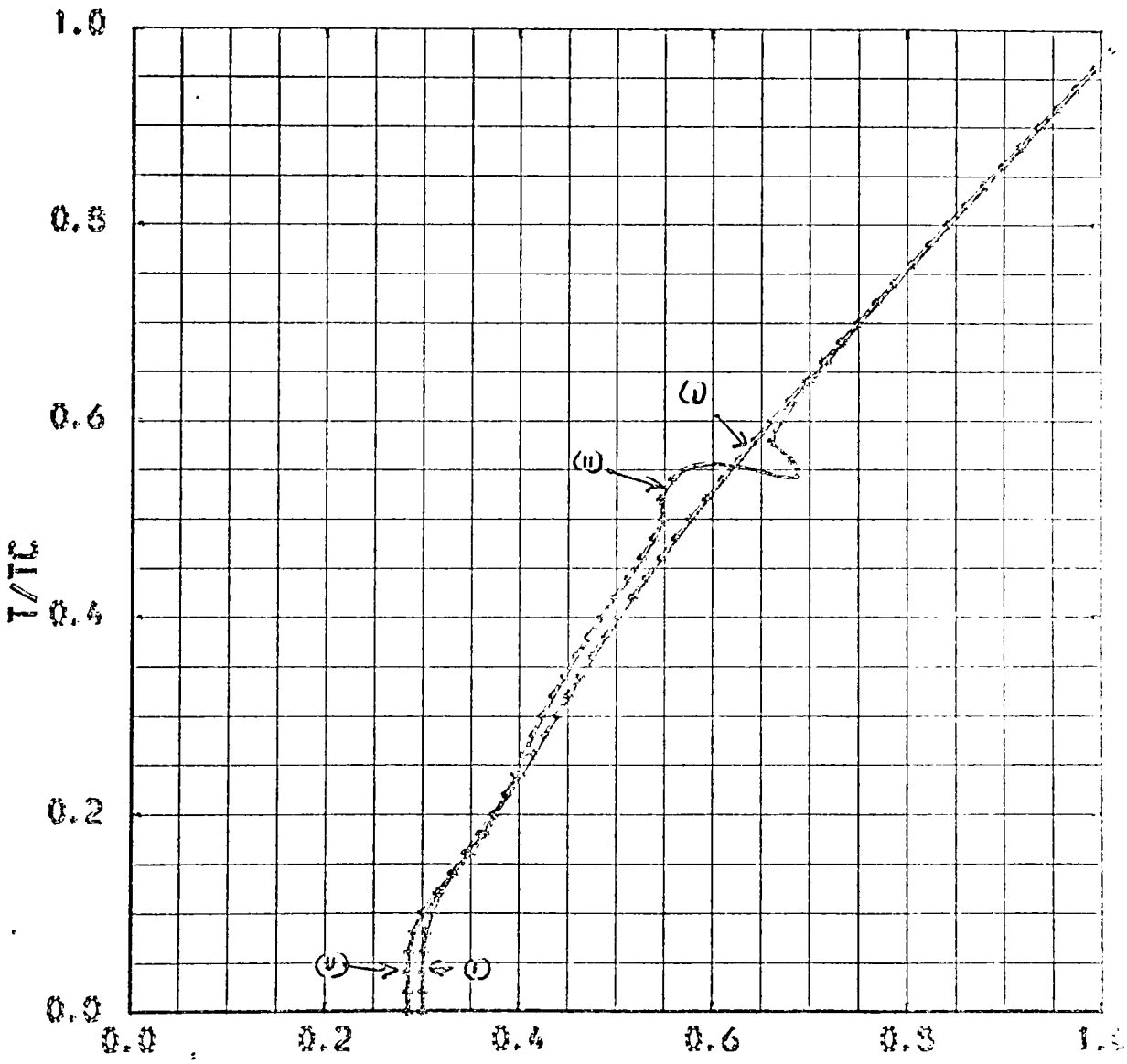
and B_i. This P.A. can represent D separate simple poles: accordingly this sort of analysis is useful when it is thought that there are other singularities near the physical one, and it is usual to convert all poles to simple ones by using $F(x) = \frac{d}{dx} \ln f(x)$. - 3.6

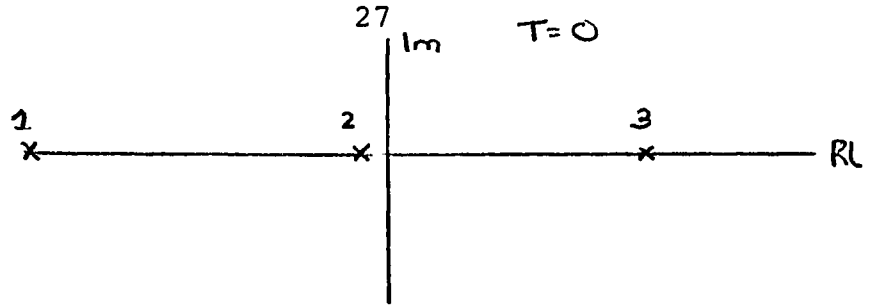
This procedure was first applied to the t-series derived by Domb and Sykes for the susceptibility by Baker (1961), and has since become a standard tool for workers in the field of series expansions. The convergence properties of P.A.'s are not well understood (Hunter and Baker, 1973): however, it is conjectured that under most circumstances the diagonal ($P=D$) P.A.'s do converge to $F(x)$, and it is usually found that the near-diagonal P.A.'s converge reasonably well also.

Again using the 7 term p-series for the SC lattice as an example, the [2,4], [3,3] and [4,2] P.A.'s are formed: Figs. 13, 14 show the phase boundaries and critical exponent curves that result from the 'physical' poles and the corresponding residues. The results for the phase boundary are in reasonable agreement with each other and with the results of ratio methods (Fig. 15: [3,3] P.A. and method 6). Similar broad agreement between methods is found for the other three series studied.

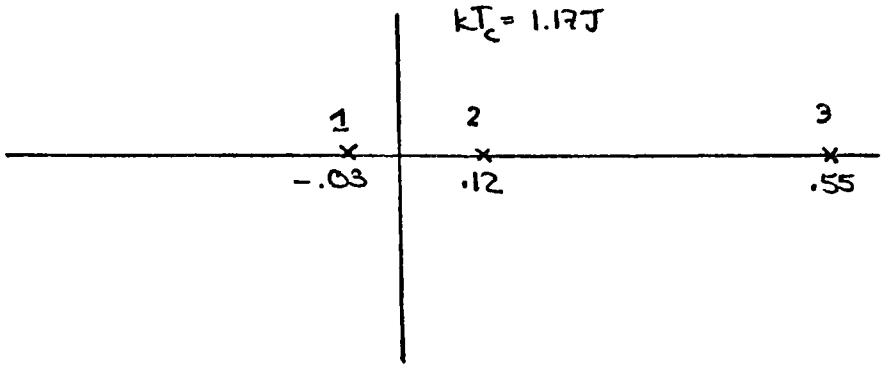
The 'kinks' apparent in Fig. 13 at about $p \approx .6$ result from the following behaviour: (we use [3,3] as an example).

Figure 1.5 Simple cubic 7 term p-series
Phase Boundary by 1) Method 6
2) [3,3] P.A.

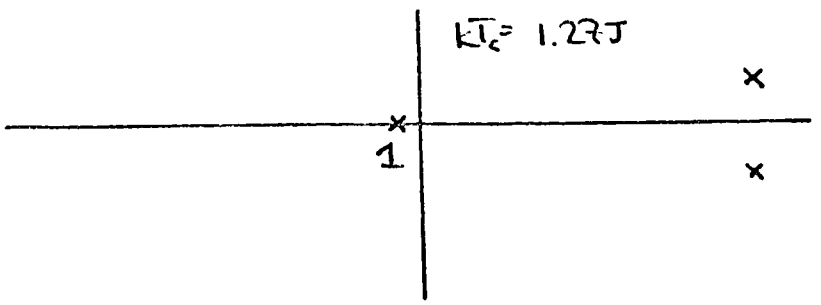




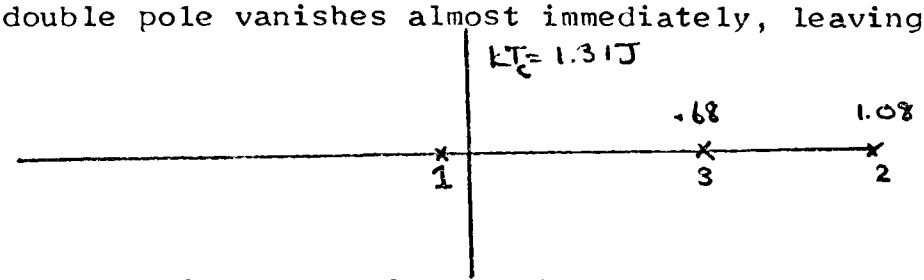
At T=0 all 3 poles are on the real axis: as the temperature is raised, all 3, remaining on the real axis, become larger, pole 1 moving faster than pole 2, initially.



At about half of $T_c(1)$, pole 2 moves rapidly along the real axis towards pole 3 - and meets it, creating a pair of complex poles at .56 ± .125i.

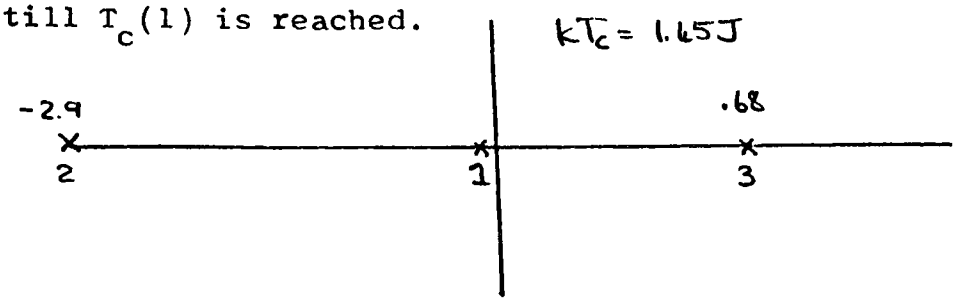


The double pole vanishes almost immediately, leaving:



and shortly after the pole map changes again to the situation

shown where there are two negative real poles, and all three move slowly leftward: this continues uneventfully till $T_c(1)$ is reached.



The poles in [2,4] behave similarly: the double pole is reached at $kT_c = 1.31J$. Naturally the double poles produce large discontinuities in $\gamma(p)$ at the appropriate points (Fig. 14): the eccentricities of the curve fit are the results of attempted polynomial interpolation through data points represented as blobs.

Such behaviour is perhaps merely due to the shortness of the series, and the low order of the P.A.'s used, and it has only been discussed in so much detail as it seems to be a feature of both p and t expansions, even at quite high order. In view of the unsatisfactory behaviour of $\gamma(p)$ estimates (and of the t-series at low p - this will be discussed later) it seems worthwhile to investigate anything that may give a clue as to what new hypothesis should replace 3.1 or to what has gone wrong with the series at this order.

Table 3 summarises the occurrence of double poles as far as this can be done for the Ising ($\frac{1}{2}$) model in 3D.

Table 3

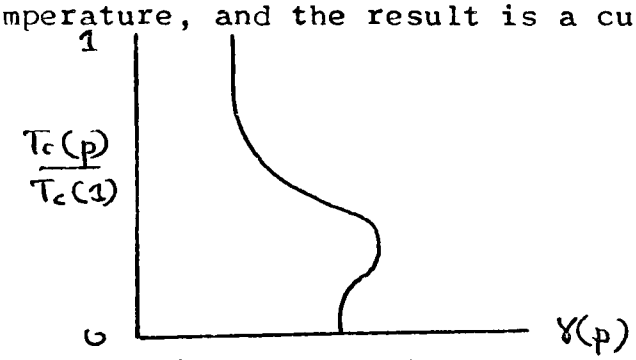
Lattice	Type of series	P.A.	Location of double pole $\frac{T_c(\frac{1}{p})}{T_c(1)}$
SC	p	[3,3]	.56
		[2,4]	.58
	t	[2,2]	$\sim$ .6 (Oguchi, 1969)
FCC	$(\frac{1}{2}\beta J)$	[2,2]	Between .5 and .6 (Rushbrooke, 1972)
		[2,3]	
		[3,2]	
	t	[3,3]	Between .5 and .6 (Rushbrooke, 1972)
		[3,4]	
BCC	t	[3,3]	$\sim$.55 (Rushbrooke, 1972
		[3,4]	
		[4,3]	
FCC	t	[4,4]	.55 $\sim$ .6 (Rapaport, 1972(a))
		[4,5]	
		[5,4]	
TZ	p	[3,4]	.47
		[4,3]	

It would be interesting to analyse the long series (up to t^9 and p^6) obtained by Rapaport for the FCC lattice to see where the double poles occur: however, his method does not yield an analytic form for either series, and neither series is tabulated at appropriate points. The double poles are not present at p = .7 but have appeared at p = .5. It is also worthy of remark that the high temperature series in all cases yield no results after the onset of the double pole (although ratio methods

continue to seem reasonable for a little as p is decreased): no real physical pole appears consistently in the P.A.'s. In the p-series, of course, quite a reasonable consistent physical pole does reappear.

Two-dimensional lattices seem to present a different sort of picture: the Q lattice p-series [4,3] P.A. never has a reasonable physical pole below about $T_c(p)/T_c(1) = .5$, and the [3,4] P.A. always has one, with no nearby poles. Rushbrooke et al find that the 8-term t-series for the plane triangular (P.T) lattice has no P.A.'s with physical poles below about $T_c(p)/T_c(1) = .8$.

One may conjecture, then, that all series for the Ising ($\frac{1}{2}$) susceptibility for 3D lattices of between 5 and 10 terms exhibit a double pole at about $T_c(p)/T_c(1) = .55$. (Series of less than 5 term are too short to allow such behaviour: 10 terms are the most that have been derived). In all cases, this pole is associated with a sharp rise in γ. When p-series are studied, the double pole disappears at lower temperature, and the result is a curve of the type

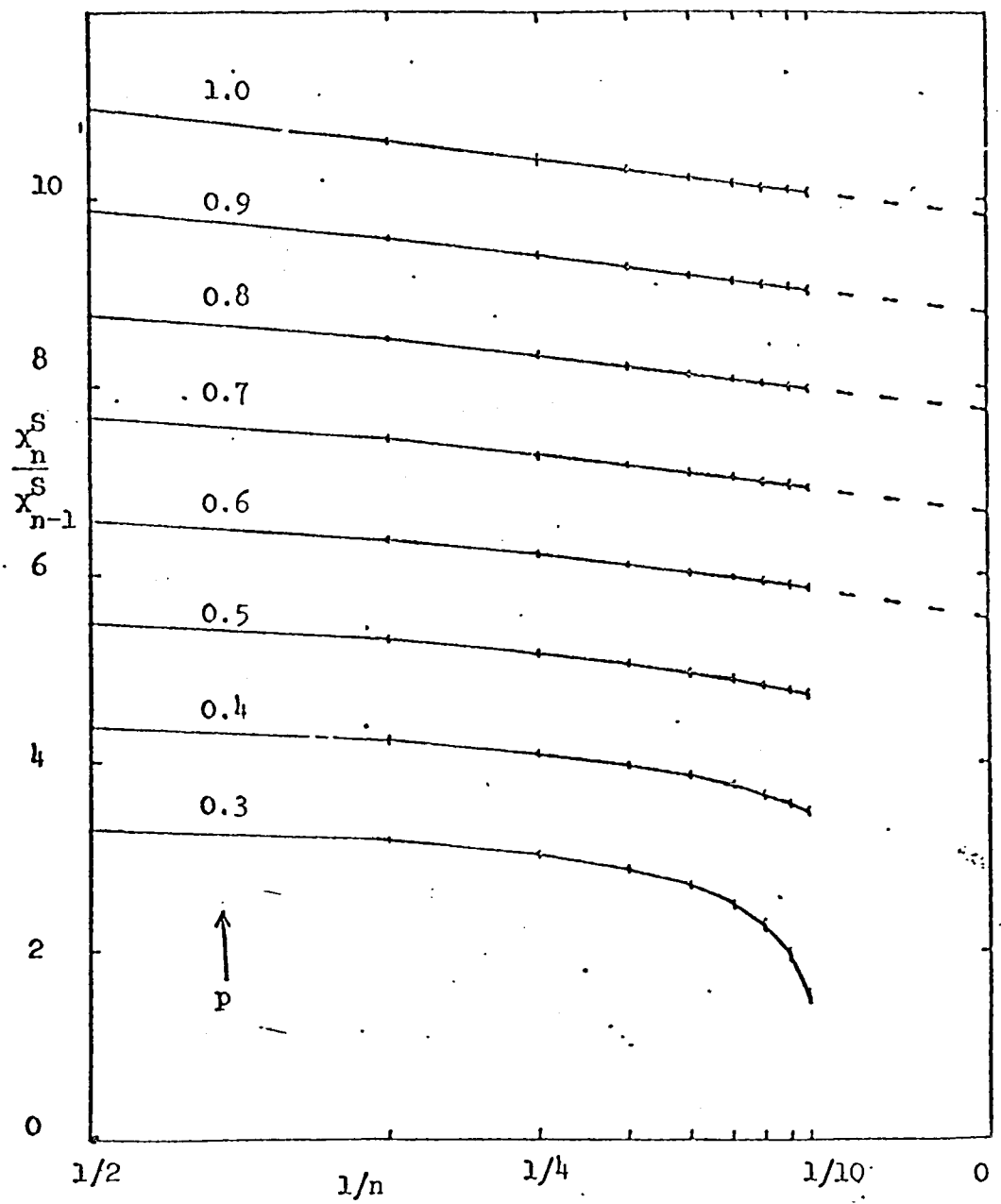


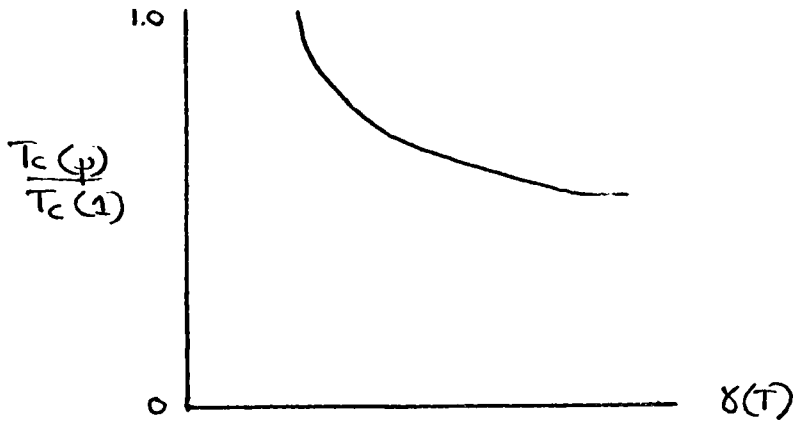
In the case of t-series, no consistent real poles reappear, and one finds:

Figure 16 The sequence $\{i_n\}$ is $\frac{1}{n}$

Taken from Rapaport (1972(a))

Face-centred cubic lattice: 11 term t-series





If one accepts the conjecture, the next question is whether such behaviour is spurious, due only to irregularities in the low order terms available, so that extension of the series would produce results that verify the hypotheses 3.1 and 3.2. One feels that the series are already sufficiently long to indicate that this is not so. The alternative is some more complicated assumption to replace 3.1 and 3.2, which will reduce to them at the correct limits, and which will allow for the type of behaviour discussed. In view of the intimate connection between p and t series, and the feeling that there should be at least some correspondence between $\gamma(p)$ and $\gamma(T)$, such an assumption should be a general one for the asymptotic form of χ in terms of t and p.

Further evidence of the breakdown of 3.2 is seen when we consider the plot of $\{u_n\}$ against $\frac{1}{n}$ (Fig. 16) for the 10-term t-series of Rapaport for a variety of values of p. The sequence appears linear as p is decreased until p = .5: after this, the curvature in late u_n becomes more pronounced, and extrapolation is clearly impossible. Such behaviour

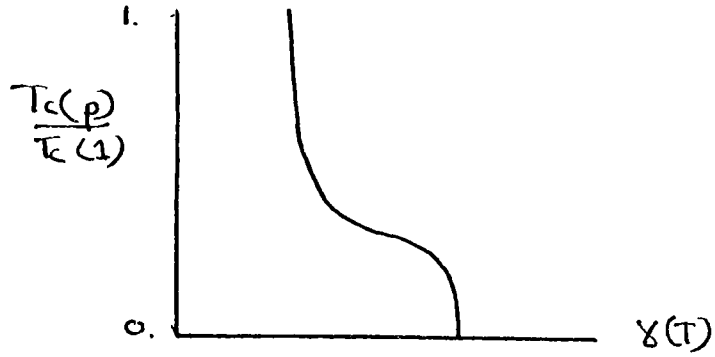
was not apparent to earlier workers, who had much shorter series to consider.

The plot raises a number of disturbing questions. Firstly, would extension of the t-series to yet higher order lead to curvature at higher values of p (and presumably double poles at higher p), so that 3.2 would not be supportable even in a nearly pure substance. Secondly, would the derivation of longer p-series lead to similar behaviour, so that the present evidence, which appears to favour 3.1, except around $T_c/p)/T_c(1) = .55$ where the double pole occurs, would be nullified? At the moment the furthest developed p-series available is the seven-term series for the FCC lattice by Rapaport: this series shows no evidence of curvature, and tends to confirm the estimates of Figs. 5 and 8. Then, the t-series of similar length does not exhibit any curvature either. Another possibility is that such curvature is a transient effect, and the derivation of later terms for the t-series will verify the trend of the first six or seven.

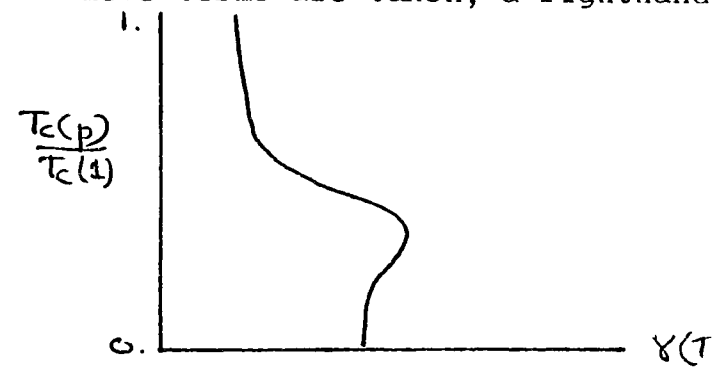
§3.4. The main conclusion that is forced upon one is that the hypotheses 3.1 and 3.2 are probably not adequate to describe the asymptotic behaviour of χ: in the case that $t \to t_c(p)$, 3.2 is not adequate below $p \sim .55$, and possibly even above that: in the case that $p \to p_c(T)$, 3.1 is not adequate about $T_c(p)/T_c(1) \sim .55$, but may well be reasonable elsewhere.

It seems that a reasonable approximation to the phase boundary may be drawn by use of the ratio method (or P.A.'s , except at the double pole) using the p-series; such phase boundaries are also reproduced well down to about $p = .55$ from high temperature series, and estimates which agree well with p-series results can be found to some way below this (particularly from t-series) if less than the full number of terms available are used. The last result is extremely surprising, and means either that the reasonable-seeming phase boundaries resulting from p-series are wrong, or that the first half dozen or so terms in a t-series are a better guide to its asymptotic behaviour than some later terms. It is hard to see how the phase-boundary can be far out: its ends are fixed, and an argument due to Elliott (1963) suggests that it approaches p_c^s vertically. Both molecular field theory and series expansion results $T_c(1)$ indicate that $\frac{dT_c(p)}{dp} \sim 1$ near $p = 1$. The shape of phase boundary shown in Fig. 5 is the simplest consistent with these requirements.

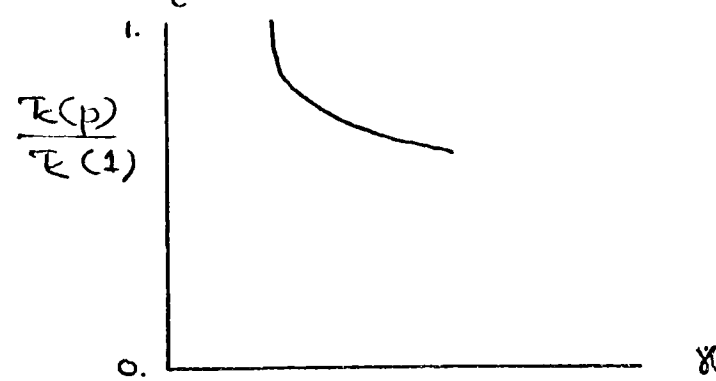
The critical exponent situation is more confused: now we have $\gamma_2(p)$ and $\gamma_1(T)$, with no reason why these should be equal - or indeed why either should equal the γ obtained from a series in $(\frac{1}{2}\beta J)$. In general it seems that 'short' series in p yield a γ_1 curve of the following type from ratio or P.A. analysis:



where at $T = 0$, γ_1 is more or less the percolation problem γ_1 of 1.6875 (2.375 in 2D). At $T_c(1)$, a γ_1 is obtained which is close to the $\gamma_2(p=1)$ value usually accepted, 1.25 (1.75 in 2D). If more terms are taken, a righthand bulge develops:



The "limits" $\gamma_1(T=0)$ and $\gamma_2(p=1)$ are still more or less obeyed. The $\gamma_2(p)$ curve obtained from t-series (and $\gamma'(p)$ from $(\frac{1}{2}\beta J)$ series) always seems to agree fairly closely with this behaviour near $T_c(1)$, and increases rapidly about $p \approx .55$



This encourages one to believe that at least at high

temperatures (low impurity concentrations) all the critical indices are the same: as more impurities are introduced, the double pole appears and u_n plotted vs $\frac{1}{n}$ bends, and consequently γ_2 increases sharply. Once this stage has passed, as it appears to do below $p \sim .4$ for p-series, a behaviour for $\gamma_1(T)$ can again be deduced from p-series, but not for $\gamma_2(p)$ from high temperature series.

Such general results are not compatible with simple assumptions of the type 3.1 and 3.2 for the asymptotic form of χ: the question for the future is whether longer series will expose these results as due to some irregularities in short series, or whether a new and more general assumption can be made that allows for a universal γ until the onset of double poles at about $p = .55$, and for the correct low temperature limiting behaviour. A belief in the first possibility will, of course, enable one to always claim that the series is not long enough: it appears that new hypotheses for χ must be made.

Oguchi (1969) has suggested that as the [2,2] Padé indicates that $\gamma(p) \sim 1.75$ when $p = .6$, the infinite cluster - which determines the behaviour of χ - is in some sense two-dimensional at this point. The fact that $\gamma(p) \to \infty$ at lower p at first sight appears to support this, as the susceptibility of the Ising model has an essential singularity at $T = 0$. However, Rushbrooke et al (1972) point out that

$$\chi^R(1D) = \frac{1 + t}{1 - t}$$

for the pure chain - and this would give $\gamma = 1$ at zero temperature.

Another possibility is that the transition is not sharp in p away from T = 0 (or in t except when p = 1). For example, χ^R could have the form

$$\chi^R = \frac{A}{((p-p_c(T))^2+\Delta^2)^{\bar{\gamma}/2}} \qquad \text{as } p \to p_c(T)$$

and similarly in terms of t. The result of such a form would be that an analysis by P.A.'s would show a series of confluent singularities of increasing strength at $p_c(T)$: a ratio analysis might be expected to show higher and higher estimates for $\gamma(T)$ as more and more terms were used: this is precisely what Fig. 16 indicates for the long t- series of Rapaport. An analysis was carried out to see if such confluent singularities could be found at low p in Rapaport's t-series, and is reported in Appendix III. The results suggest that there are confluent singularities at low p, but do not permit the confident adoption of any simple form for χ that includes a width. The series in p are too short to allow such analysis.

It has also been suggested that the behaviour of $\gamma(p)$ may be due to exponent renormalisation, as in the Syozi model. This can be dismissed on several grounds (Rushbrooke et al, 1972): not least because series analysis

of the Syozi model yields quite a different behaviour for $\gamma(p)$ renormalisation.

It should not be too surprising that 3.1 and 3.2 are inadequate. Griffiths (1969) has shown that the magnetisation M is non-analytic in field H when H = 0 for a range of temperatures right up to $T_c(1)$ which suggests that χ may be non-analytic in other places than on the sharp phase-boundary suggested. Work by McCoy and others (1972) indicates also that χ may be infinite above T_c, where T_c is the temperature when M vanishes. This is a very different sort of random model, but again suggests that some new hypothesis is required to yield reliable information from exact series for the Ising spin$\frac{1}{2}$ susceptibility in a dilute magnet.

The results of this work are, then, far from satisfactory: it seems clear that high temperature series, at the order currently obtained, do not support a simple hypothesis of the type 3.2. Attempts to explain this in physical terms have so far failed, although several results indicate that there may well be a physical behaviour more complex than that allowed by the hypothesis.

Further numerical work on the series available seems to indicate that there is a complex pair of poles for all three dimensional susceptibility series, in p, t or $\frac{1}{2}\beta J$, at about p = .55 associated with the critical index becoming large: above that pair, all methods seem to give

the same critical index and phase boundary, but below it, high temperature series yield extremely unreliable results, whereas p-series behave well once the limited region of the pair's existence is passed. It is not yet clear whether the derivation of longer p-series would lead to their breakdown over more than this isolated region: the available evidence seems to indicate not.

It is also an open question whether the derivation of longer high temperature series would not lead to confirmation of the simple critical index hypothesis that works so well for the pure lattice, the latter half of the present series being in some way spurious, and the results obtained from the first few terms (which agree well with p-series results at lower temperatures) being shown to be more representative of the asymptotic behaviour. The author's opinion is that the series already obtained and the evidence for confluent singularities presented, indicate that this is not so: some new, more general hypothesis is needed to replace 3.1 and 3.2 which will allow the behaviour described for both p-series and high temperature series. It further seems that such a hypothesis is unlikely to be deduced from development of existing series expansions, and must come from further exact work on more tractable disordered models.

CHAPTER FOUR

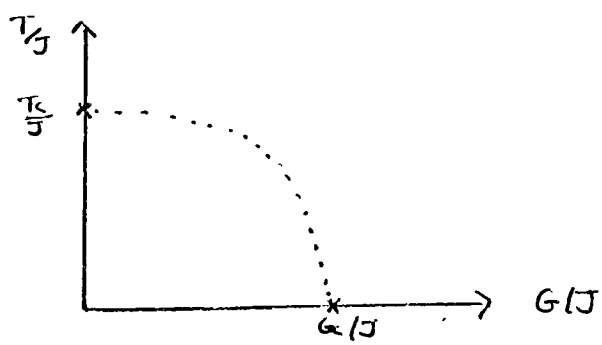
HIGH TEMPERATURE SERIES FOR THE DILUTE TRANSVERSE ISING MAGNET

§ 4.1

This chapter is concerned with the study of the second order phase transition in the Ising spin-$\frac{1}{2}$ model with a transverse field G added: the Hamiltonian used is

$$H = -2J \sum_{<ij>} S_i^z S_j^z - \mu H \sum_i S_i^z - 2G \sum_i S_i^x .$$

At all temperatures T there is some order in the x direction, represented by the order parameter $\langle S_i^x \rangle$ being greater than zero, but the ordering in the z direction due to the spin interaction disappears as T or G is raised. A phase boundary may be drawn for the pure magnet in terms of T/J and G/J.



Several well-tried methods permit the estimation of T_c/J: it is of interest to extend them to find the phase boundary and G_c/J, the critical field which allows no ordering in the z direction even at zero temperature. If p, the concentration of magnetic atoms, is allowed to

fall from 1, a family of such curves may be drawn, and phase boundaries of $T_c(p)/J$ vs. p for varying values of G/J will also result.

This model has been studied by molecular field methods in the pure case (De Gennes, 1963): extension to the dilute case is trivial, and T_c is found analytically in terms of J, G and p. A constant coupling model, following the methods of Kasteleijn and Van Kranendonk (1956 a,b) has been developed for the pure model (Sandercock et al, 1972) and recently extended to the dilute case by Young: the results of this work are shown in §4.5. At zero temperature, a perturbation expansion technique has yielded consistent estimates of $G_c(1)/J$ (Pfeuty and Elliott, 1971) as well as estimates of the order parameter and spin correlation function above and below the transition temperature. However, attempts to extend this work to the dilute lattice have not proved successful.

In the case of zero transverse field, series expansions of the type discussed in earlier chapters yield better results for the location of the transition than molecular field theory or constant coupling approximations: a high temperature expansion for the case of transverse field has therefore been developed by Wood (Wood, 1969; Elliott and Wood, 1971) and is extended to the case of dilute systems and found to higher order in this work. Such a method has the additional advantage that the behaviour

of the critical index as G and p are varied may also be discussed.

A six-term series for the FCC lattice and a seven-term series for the TZ lattice are derived: experience indicates that the former will provide more reliable results in general. However, the results of earlier chapters will lead us to treat the estimates at anything approaching low temperature with some suspicion. An additional motivation for this work has been the recent production of experimental results for the phase transition in a dilute crystal believed to be well described by the Hamiltonian given.

This Hamiltonian is thought to be a good model for several systems, one of the most studied being the hydrogen bonded ferroelectric KH_2PO_4 (De Gennes, 1963). That of particular interest here is the rare earth compound $DyVO_4$, where the crystal field produces essentially an electronic energy level scheme with two low lying singlet states. The Dy^{3+} ions may be randomly replaced by Y^{3+} ions, with little disturbance to the crystal structure, and the second order structural phase transition studied in crystals with different values of p. Recent accurate work by Harley, Perry and Smith has resulted in a curve of $T_c(p)$ against p for this system. A short discussion of the system $DyVO_4$ follows: further details may be found in Sandercock et al (1972), Elliott et al (1972), and references contained in

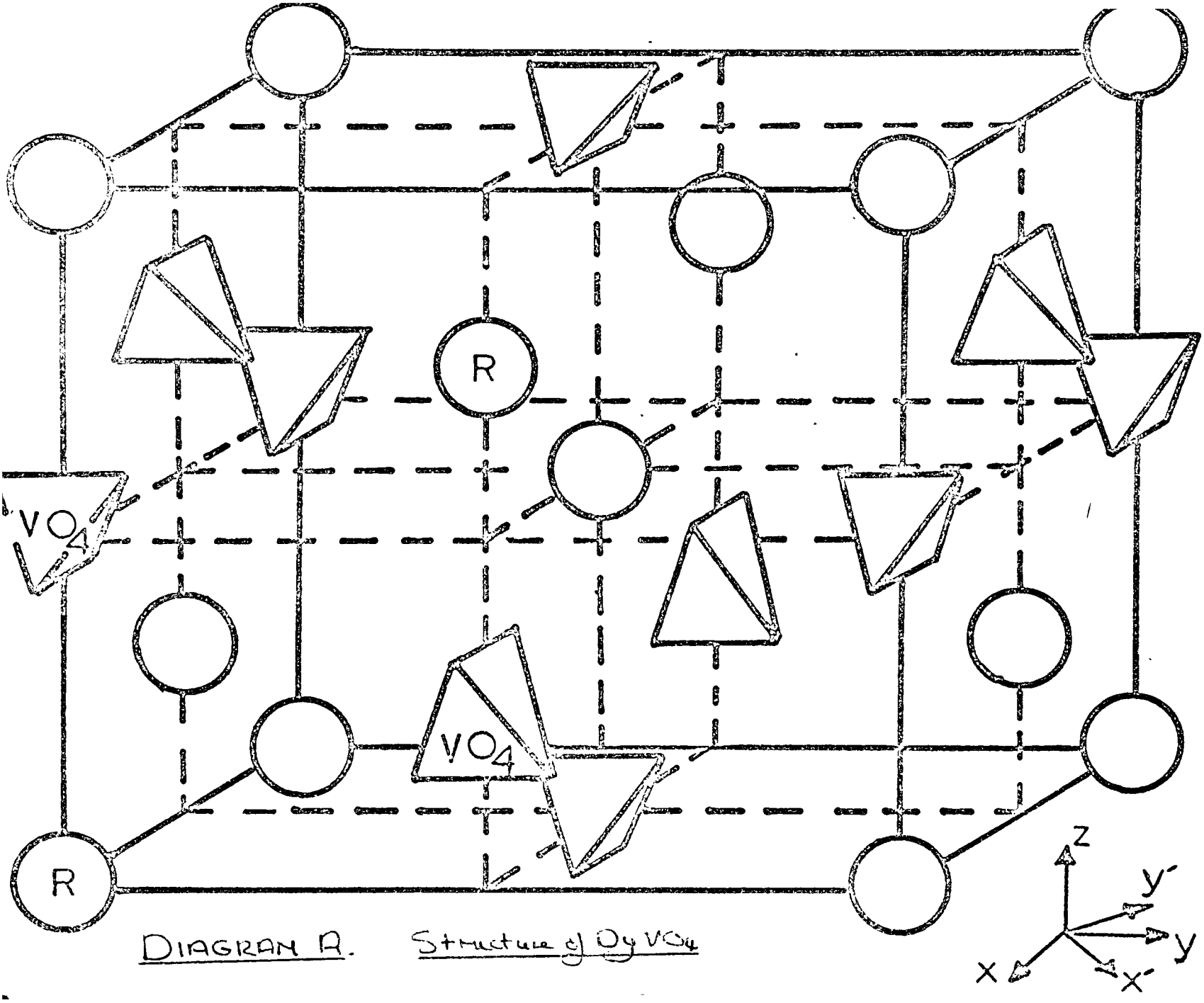


DIAGRAM A. Structure of $DyVO_4$

those papers.

$DyVO_4$ has the structure shown in Fig. A above the transition temperature, T_D: the Dy^{3+} ions lie on the sites of a tetragonal zircon lattice. The crystal field is such as to favour large magnetic quadrupole moments in the basal plane. Above T_D, these have no particular direction: below T_D they are oriented in preferred directions, at 45^o to each other, and the principal axes in the basal plane are no longer equivalent. The resulting macroscopic strain (of B_{1g} symmetry) corresponds to a compression along the y-axis and an equal elongation along the x-axis: $(e_{xx}-e_{yy})$ has been measured as .17%, well below T_D (Sayetat et al, 1971). The structural phase transition is driven by a Jahn-Teller interaction between the lattice phonons and the low lying Dy^{3+} energy levels, producing an effective quadrupolar interaction. At temperatures higher than T_D, the greater entropy of the degenerate system gives the undistorted crystal a lower free energy than the distorted crystal.

Above T_D, the low lying levels of the Dy^{3+} ion are essentially two nearly degenerate Kramers doublets, and this degeneracy is lifted below T_D. Accordingly, if the Kramers degeneracy is neglected, the system has two levels and may be described in terms of spin $\frac{1}{2}$ operators. The model Hamiltonian used for $DyVO_4$ is

$$H = \sum_{j,\underline{k}} \{(\hbar\omega_j(k)[c_j^+(\underline{k})c_j^-(\underline{k})+\tfrac{1}{2}] + \mathcal{G}_j(\underline{k})[c_j(\underline{k}) + c_j^+(-\underline{k})]\sigma^z(\underline{k})\}$$
$$+\tfrac{1}{2}Nc_oV_oe^e - \eta e\sqrt{N}\,\sigma^z(0) - \varepsilon\sqrt{N}\,\sigma^x(0).$$

The first term is the unperturbed phonon Hamiltonian, summed over all branches and wavevectors: the second describes the spin-phonon interaction, where the pseudo-spin operator is used for the two lowest electronic levels of Dy^{3+}. The third and fourth terms arise from the static strain e below T_D, which is coupled to the $\underline{k}=0$ pseudo-spin component. The crystal contains N unit cells of volume V_o, and c_o is the elastic constant corresponding to the B_{1g} mode: η and $\mathcal{G}_j(\underline{k})$ are coupling constants. The last term describes the splitting due to the crystal field ε. In the case of zero crystal field, transformation to a displaced phonon representation (Elliott et al, 1972) completely decouples spin and phonon operators: when $\varepsilon>0$, as here, some residual coupling remains, but is thought to be unimportant for $DyVO_4$. Accordingly the form

$$H = -\varepsilon\sum_i \sigma_i^x - \tfrac{1}{2}\sum_{<ij>} J_{ij}\sigma_i^z\sigma_j^z - \eta e\sum_i \sigma_i^z + \tfrac{1}{2}NV_oc_oe^2$$

may be obtained, if spin and strain terms only are considered. If the interaction J_{ij} is split into a next-neighbour and a long range part, it may be shown that the long range part is almost cancelled by the strain coupling term. (Sandercock et al, 1972). The last term produces only a constant energy shift, and so may be ignored. The remaining Hamiltonian

$$H = -\varepsilon\sum_i \sigma_i^x - J\sum_{<ij>} \sigma_i^z \sigma_j^z$$

is thought to be a reasonable approximation for $DyVO_4$. In other rare earth vanadates, notably $TbVO_4$, the effective coupling is not short range, and molecular field theory works well. The lack of success of molecular field theory for $DyVO_4$ is due to this, and the constant coupling theory and series expansion methods may be expected to do better.

Such a system offers several ways of measuring T_D. Brillouin scattering may be used to locate the softening of the B_{1g} mode as the corresponding elastic constant becomes zero. (Sandercock et al, 1972). Alternatively electronic Raman scattering may be used to find the Raman line below T_D corresponding to transitions between the lowest two levels of the Dy^{3+} ion: this should become very low in energy at and above T_D. Further, the degenerate E_g phonon modes are split due to anharmonic interaction with electronic states below T_D, and such splittings also become zero at T_D (Elliott et al, 1972). Other techniques also exist, but Raman movements on the E_g mode splittings in dilute crystals have been recently used by Harley, Perry and Smith of the Clarendon Laboratory to give an accurate curve for the phase boundary $T_c(p)$ vs. p. This curve is reproduced in §4.5, and compared with the results of series expansions and constant coupling theory. The results of

the experimental work have not yet been published.

§4.2 Derivation of Series

Again the Ising Hamiltonian

$$\mathcal{H} = -2J \sum_{<ij>} S_i^z S_j^z - \mu H \sum_i S_i^z - 2G \sum_i S_i^x \qquad - 4.1$$

is used, with a transverse field 2G added. It is convenient to transform to:

$$\mathcal{H} = \overbrace{-\tfrac{1}{2}J \sum_{<ij>} \sigma_i^x \sigma_j^x}^{H_J} \overbrace{- \tfrac{1}{2}\mu H \sum_i \sigma_i^x}^{H_F} \overbrace{- G \sum_i \sigma_i^x}^{H_O} \qquad - 4.2$$

by interchange of x and z, and replacing the spin $\frac{1}{2}$ S-operators by the Pauli spin operators. A high temperature expansion in $\frac{1}{2}\beta J$ is now developed for this model, following the method of Wood (Wood, 1969; Elliott and Wood, 1971), which employs a Matsubara-type perturbation expansion within the framework of the high temperature expansion developed by Rushbrooke and Wood (1958). The method is extended to the case of a lattice with random quenched impurities.

The Hamiltonian is split into two parts:

$$\mathcal{H} = A + B$$

and the operator $S(\beta)$ defined by:

$$\exp(-\beta\mathcal{H}) = \exp(-A\beta)S(\beta) \qquad - 4.3$$

Now, on differentiating with respect to β,

$$-\mathcal{H}\exp(-\mathcal{H}\beta) = -A\exp(-A\beta)S(\beta) + \exp(-A\beta)\frac{d}{d\beta}S(\beta) \qquad - 4.4$$

Premultiply by $\exp(A\beta)$ and a little rearrangement gives:

$$\frac{d}{d\beta}S(\beta) = -\exp(A\beta)B\exp(-A\beta)S(\beta)$$

$$= -B(\beta)S(\beta) \qquad - 4.5$$

From 4.3, $S(0) = 1$: so integration of 4.5 yields:

$$S(\beta) = 1 - \int_0^\beta B(\tau)S(\tau)d\tau \qquad - 4.6$$

If 4.6 is iterated, a series solution for $S(\beta)$ is obtained:

$$S(\beta) = 1 - \int_0^\beta B(\tau)d\tau + \ldots(-1)^n \int_0^\beta d\tau_1 \ldots \int_0^{\tau_{n-1}} d\tau_n (B(\tau)\ldots B(\tau_n)+\ldots \qquad - 4.7$$

In general B and A do not commute: if they do, the unsurprising result $S(\beta) = e^{-\beta B}$ is obtained. Substitution of 4.7 into 4.3 offers a straightforward series solution for the partition function,

$$z = Tr\{e^{-\beta\mathcal{H}}\} \qquad - 4.8$$

and has been used by many authors to obtain such solutions (e.g. Matsubara, 1955; Bloch and De Dominicis,1958).

A is now chosen to be H_o, and B to be H_J H_F: the following expansion for z is obtained.

$$z = Tr\{e^{-H_o\beta}(1+\sum_{n=1}^{\infty}(-1)^n\int_0^\beta d\tau_1\int_0^{\tau_{n-1}} d\tau_n\ (H_J(\tau_1)+H_F(\tau_1))\ldots + (H_J(\tau_n)+H_F(\tau_n))]\ldots\} \qquad - 4.9$$

which can be rewritten formally as a double series in $(\frac{1}{2}\beta J)$ and $(\frac{1}{2}\mu\beta H)$.

$$z = \sum_{n=0}^{\infty}\sum_{r=0}^{\infty} \mu_n{}^r (G\beta)(\tfrac{1}{2}J\beta)^r(\tfrac{1}{2}\mu H\beta)^{n-r} \qquad - 4.10$$

The corresponding expansion for lnz has coefficients which are the cumulants corresponding to the moments $\mu_n{}^r$. Since

$$\chi(T) = \frac{1}{\beta}\left(\frac{d^2}{dH^2} \ln z\right)\Big|_{H=0} \qquad - 4.11$$

only terms quadratic in H in 4.10 will contribute to the expansion for lnz and hence for $\chi(T)$, which is now a single series in $(\frac{1}{2}\beta J)$. The reduced susceptibility

$$\chi^R = \frac{4\chi(T)}{N\mu^2\beta}$$

is used , so that

$$\chi^R = \frac{1}{N}\frac{4}{\mu^2\beta^2}\frac{d^2}{dH^2} \ln z\Big|_{H=0}$$

The first two moments in 4.10 with n-r=2 are:

$$\mu_2{}^o = \mathrm{Tr}\{e^{-\beta H_o}\int_o^\beta d\tau_1 \int_o^\tau d\tau_2 \; H_F(\tau_1)H_F(\tau_2)\} \qquad - 4.12$$

and $\mu_3{}^1 = \mathrm{Tr}\{e^{-\beta H_o}\int_o^\beta d\tau_1 \int_o^{\tau_1} d\tau_2 \int_o^{\tau_2} d\tau_3 [H_J(\tau_1)H_F(\tau_2)H_F(\tau_3)$

$$+ H_F(\tau_1)H_J(\tau_2)H_F(\tau_3) + H_F(\tau_1)H_F(\tau_2)H_J(\tau_3)]\} \qquad - 4.13$$

In the Pauli representation,

$$\sigma^x{}_i = \sigma_i{}^+ + \sigma_i{}^-$$

where $\sigma_i{}^+$ and $\sigma_i{}^-$ are spin creation and destruction operators respectively. $H_J(\tau)$ therefore can be written:

$$H_J(\tau) = -\tfrac{1}{2}J \sum_{<ij>}[\sigma_i{}^+(\tau)\sigma_j{}^-(\tau) + \sigma_i{}^+(\tau)\sigma_j{}^+(\tau) + \sigma_i{}^-(\tau)\sigma_j{}^-(\tau) + \sigma_i{}^-(\tau)\sigma_j{}^+(\tau)] \qquad - 4.14$$

and $H_F(\tau)$ as

$$H_F(\tau) = -\tfrac{1}{2}\mu H \sum_i[\sigma_i{}^+(\tau) + \sigma_i{}^-(\tau)] \qquad - 4.15$$

where $\sigma_i{}^+(\tau) = \exp(H_o\tau)\sigma_i{}^+ \exp(-H_o\tau)$

$$= \exp(-G\sigma_i{}^z\tau)\sigma_i{}^+ \exp(G\sigma_i{}^z\tau)$$

$$= \sigma_i^+ \exp(-2G\tau) \qquad - 4.16$$

as may be verified by expanding out the exponentials and commuting the operator σ_i^+ through. Similarly,

$$\sigma_i^-(\tau) = \sigma_i^- \exp(+2G\tau) \qquad - 4.17$$

If these expressions are substituted into 4.12 and 4.13, the moments are seen to consist of the trace of products of spin creation and destruction operators, multiplied by an integral over exponential function of the τ's. It is found convenient to represent the traces diagrammatically as follows. Each H_J is represented by a full line joining sites i and j, with an arrow leaving site i or j to represent a creation operator, and one entering to represent a destruction operator. With each H_F a dotted line is associated, one end being attached to site i, carrying an arrow to represent σ_i^+ or σ_i^- as above, the other being "free".

The following terms are obtained in μ_2^o:

$$\mu_2^o = \tfrac{1}{4}\mu^2 H^2 [\mathrm{Tr}\{\exp(-\beta H_o) \sum_{i,j} \sigma_i^+ \sigma_j^+\} \int_o^\beta d\tau_2 \int_o^{\tau_2} d\tau_1$$
$$\exp(-2G\tau_2)\exp(-2G\tau_1) + \mathrm{Tr}\{\exp(-\beta H_o) \sum_{i,j} \sigma_i^- \sigma_j^+\}$$
$$\int_o^\beta d\tau_2 \int_o^{\tau_2} d\tau_1 \exp(+2G\tau_2)\exp(-2G\tau_1) \ldots\ldots] \qquad - 4.18$$

and the first two traces in μ_2^o are represented by





when i and j are equal. The trace of any product of creation and destruction operators will be zero unless there are an equal number of creation and destruction operators on each site: this restricts the class of diagrams to those with an even number of lines at each vertex, and an equal number of arrows pointing to and away from each vertex. Accordingly, the only diagram contributing to μ_2^o is:



and this is associated with the following two integrals and traces:

$$\int_o^\beta d\tau_2 \int_o^{\tau_2} d\tau_1 \, e^{2G\tau_2} e^{-2G\tau_1} : Tr\{e^{-\beta H_o} \sigma_i^- \sigma_i^+\}$$

$$\int_o^\beta d\tau_2 \int_o^{\tau_2} d\tau_1 \, e^{-2G\tau_2} e^{2G\tau_1} : Tr\{e^{-\beta H_o} \sigma_i^+ \sigma_i^-\}$$

The latter may be obtained from the former by permuting the τ labels on the exponentials. In general it is found that all permutations of τ labels and their corresponding lines (i.e. paired or single operators) in the trace are generated for each such diagram. Accordingly, to obtain the moment μ_{n+2}^n, the following procedure is carried out.

(1) All diagrams with n full lines, 2 dotted lines, even vertices only, and equal numbers of arrows pointing in and out of each vertex are drawn.

(2) The (n+2)! traces of operators corresponding to all permutations of each such diagrams are calculated.

(3) The (n+2)! multiple integrals corresponding to each such diagram are calculated.

(4) The occurrence of such a diagram on the lattice is calculated, and the diagrams added up to give μ^n_{n+2}.

§4.3 Calculation of Diagrams

It is convenient from now on to work in terms of 'bare' diagrams - diagrams with the arrows left off. The bare diagrams required to obtain seven terms of the series for the TZ lattice are tabulated in Table 4.1: it is seen that there are ten one-component diagrams required for the sixth term - the seventh requires another twenty eight. The bare diagrams required for the FCC lattice are tabulated in Table 4.2. A theorem due to Wood (1969) cuts the number to be calculated considerably by relating any n-full-line diagram with a vertex carrying one full and one dotted line to an (n-1)-full-line diagram. Suppose the full line joins vertex 2 to a vertex 1 which carries only a dotted line: the full line may be removed, and the dotted line added to vertex 2 if the resulting diagram is multiplied by $\tanh(G\beta)/G\beta$ if vertex 2 has no other dotted line, or twice that if it does. For example:

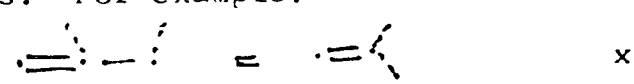


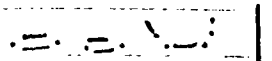
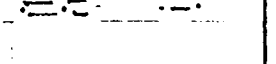
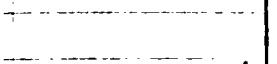
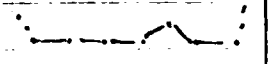
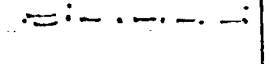
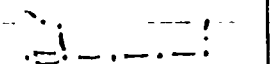
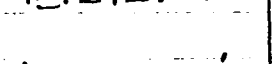
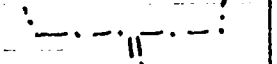
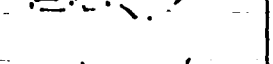
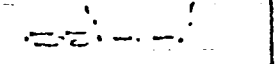


Table 4.1 Diagrams required for TE lattice

	Name	Occurrence
	1A	Np
	2A	$2Np^2$
	3A	$6Np^3$
	IIIA	$4Np^2$
	3C	$-4Np^2$
	4A	$18Np^4$
	4B	$12Np^3$
	IVA	$2Np^2$
	4D	$-12Np^3-2Np^2$
	5A	$54Np^5$
	5B	$12Np^4$
	5C	$12Np^3$
	5D	$-48Np^4-12Np^3$
	5E	$36Np^4$
	5F	$-24Np^3-6Np^2$
	5G	$+24Np^3+6Np^2$
	VA	$6Np^2$
	5I	$-4Np^2$

	Name	Occurrence
	VC	$12Np^3$
	VD	$6Np^3$
	5N	$-6Np^3-12Np^3$
	6A	$162p^6N$
	6B	$108p^5N$
	6C	$72p^5N$
	VIB	$18p^4N$
	6E	$36p^4N$
	6F	$12p^4N$
	6G	$36p^4N$
	6T	$18p^4N$
	VIC	$12p^3N$
	6I	$12p^3N$
	VIA	$2p^2N$
	6M	$-180p^5N$ $-54p^4N$
	6N	$-\frac{96}{}p^4N$ $-24p^3N$
	6O	$-12Np^3$ $-2Np$

Table 6.1 continued

	6P	$78Np^4 + 36Np^3 + 2Np^2$
	6Q	$-12Np^3 - 2Np^2$
	6R	$-48Np^4 - 12Np^3$
	7A	$674\,Np^7$
	7B	$324\,Np^6$
	7C	$216\,Np^6$
	7D	$108\,Np^6$
	VII M	$18Np^6$
	7E	$36Np^5$
	7F	$108\,Np^5$
	7G	$36Np^5$
	7H	$6Np^5$
	VII L	$54Np^5$
	7J	$72Np^5$
	7K	$108Np^5$
	7L	$108\,Np^5$

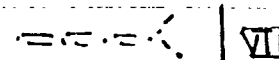
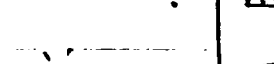
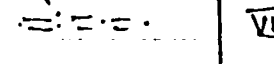
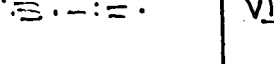
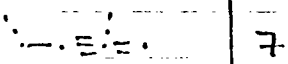
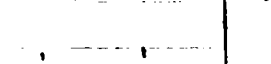
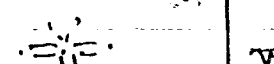
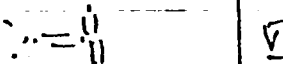
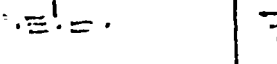
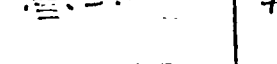
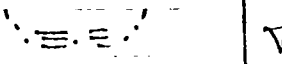
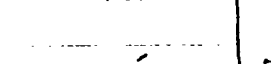
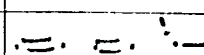
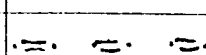
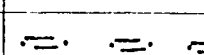
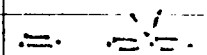
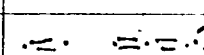
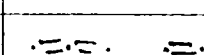
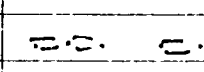
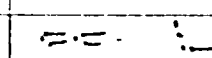
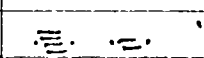
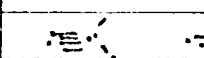
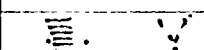
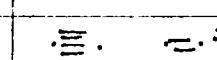
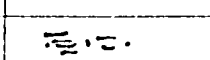
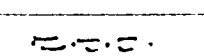
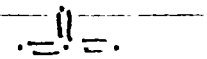
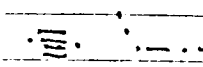
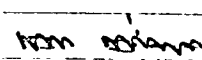
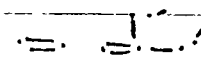
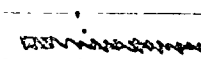
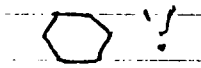
	VII J	$36\,Np^4$
	VII K	$36Np^4$
	VII I	$36\,Np^4$
	7P	$36Np^4$
	7Q	$36\,Np^4$
	VII H	$4\,Np^4$
	VII G	$12\,Np^4$
	7T	$24\,Np^4$
	7U	$12Np^4$
	VII F	$6\,Np^3$
	VII B	$12Np^3$
	VII D	$12Np^3$
	VII C	$12Np^2$
	7Z	$12Np^2$
	VII A	$4Np^2$
	7AA	$(-64p^6 - 216p^5)$
	7BB	$(-360p^5 - 108p^4)N$

Table 4.1 continued

	7CC	$(-96p^4 - 24p^3)N$
	7DD	$(384p^5 + 204p^4 + 24p^3)N$
	7EE	$(-96p^4 - 36p^3 - 4p^2)N$
	7FF	$(+144p^4 + 60p^3 + 4p^2)N$
	7GG	$-48p^4N - 12p^3N$
	7HH	$-96p^4N - 24p^3N$
	7II	$-96p^4N - 24p^3N$
	7JJ	$+192p^4N + 36p^3N$
	7KK	$(-176p^5 - 60p^4 - 12p^3)N$
	7LL	$(48p^3 + 8p^2)N$
	7MM	$(+24p^3 - 4p^2)N$
	7NN	$-4p^2N$
	7OO	$(-24p^3 - 4p^2)N$
	7PP	$-36p^3N$
	7QQ	$-72p^4N$
	7RR	$-16p^4N$

	7SS	$(-48p^4 - 12p^3)N$
	7TT	
	7UU	$(-120p^5 - 36p^4)N$
	7VV	
	7WW	$-12Np^4$

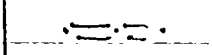
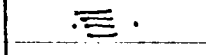
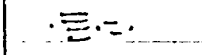
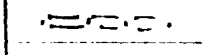
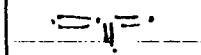
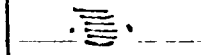
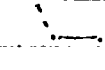
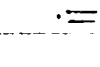
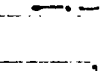
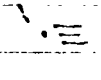
	III D
	III B
	VII N
	VII Y
	VII X
	VII XX
	VII Z

Table 4.2. Diagrams for FCC lattice

	1A	Np
	2A	$6Np^2$
	3A	$66Np^3$
	IIIA	$12Np^2$
	3C	$-12Np^2$
	4A	$702Np^4$
	4B	$132Np^3$
	IVA	$6Np^2$
	VT	$24Np^3$
	4D	$-132Np^3 - 6Np^2$
	4E	$-24Np^3$
	5A	$7350p^5N$
	5B	$660p^4N$
	5E	$1404Np^4$
	5C	$132Np^3$
	5D	$-204Np^4 - 132Np^3 - 24Np^3$
	5J	$+240Np^4$

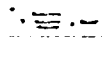
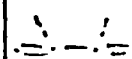
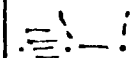
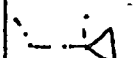
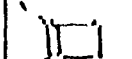
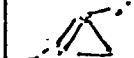
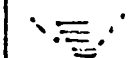
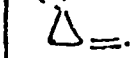
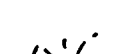
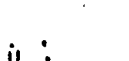
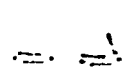
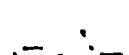
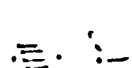
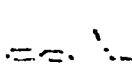
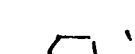
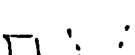
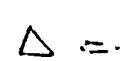
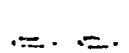
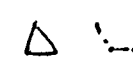
	VT	$24Np^3$
	VB	$132Np^4$
	VC	$132Np^3$
	VD	$66Np^3$
	VA	$12Np^2$
	5F	$-264Np^3 - 12Np^2$
	5G	$+264Np^3 + 12Np^4$
	5N	$-918Np^3$
	5I	$-12Np^2$
	5K	$-132Np^4$
	5L	$-240Np^4 - 24Np^3$
	6A	$76266Np^4$
	6B	$16700Np^5$
	6C	$13560Np^4$
	6G	$1404Np^4$
	6T	$702Np^4$
	6E	$1404Np^4$

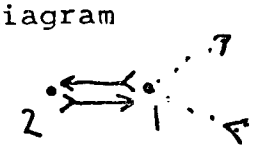
Table 4.2 continued

	6F	$660Np^4$
	VIB	$702Np^4$
	VIC	$132Np^3$
	6I	$132Np^3$
	6D	$1248Np^3$
	6H	$1080Np^3$
	6J	$2496Np^3$
	VID	$132Np^4$
	6K	$480Np^4$
	VIF	$36Np^4$
	VIE	$24Np^3$
	VIA	$6Np^2$
	VIS	$24Np^3$
	VIT	$48Np^3$
	VIG	$840Np^5$
	VIH	$240Np^4$
	VII	$480Np^4$

	VII	$240Np^4$
	6M	$-2826Np^5$ $-2718Np^4$
	6N	$-4428Np^4-$ $-312Np^3$
	6O	$-132Np^3$ $-6Np^2$
	6Q	$-132Np^3$ $-6Np^2$
	6R	$-2064Np^4$ $-156Np^3$
	6U	$-840Np^4$
	6V	$-1248Np^5$ $-132Np^4$
	6W	$-72Np^3$ $-720Np^4$
	6X	$-48Np^3$ $-480Np$
	6Y	$+120Np^3$ $+1200Np^4$
	6Z	$-72Np^3$
	6P	$-3426Np^4$ $-560Np^3$ $-6Np^2$
	6AZ	$-720Np^4$
	6AX	$-3576Np^5$ $-552Np^4$ $-24Np^3$

The result is that only three diagrams have to be evaluated in sixth order, and twelve one-component diagrams in seventh order: these irreducible diagrams have Latin numerals in Table 4.1. It is also possible to find analytic forms fairly easily for diagrams which only have two lines at each vertex: however, Table 4.1 shows that few of those required are in this category.

The problem of steps (2) and (3), that of evaluating the terms represented by irreducible diagrams, is essentially a computing one. Firstly, the bare diagram of interest is decorated with arrows in all possible ways: in seventh order there are frequently 20 or 30 such decorations. The vertices of a particular decorated diagram are labelled 1, 2...n, and the lines of the diagram represented by bracketed pairs of these integers as follows: an arrow on the line pointing towards the vertex labelled i contributes -i, away from it, +i. So the decorated diagram



is represented by

$$\binom{+1}{0}\binom{-1}{0}\binom{+1}{-2}\binom{-1}{+2} \qquad - 4.19$$

Steps (2) and (3) now require that the traces and integrals corresponding to each permutation of the brackets be performed.

Some permutations can be discarded as having zero

trace: they are those which contain two creation operators or two destruction operators on the same site, unseparated by a conjugate operator on that site. Accordingly, the permutation 4.19 has finite trace, but

has no trace. $(^{+\ 1}_{\ 0})(^{+\ 1}_{-\ 2})(^{-\ 1}_{\ 0})(^{-\ 1}_{+\ 2})$
Also the trace required is that of $e^{-\beta H_o}$ multiplied into a product of spin creation and destruction operators. If $\exp(-\beta H_o)$ is written as

$$\exp(-\beta H_o) = \cosh^N(\beta G)_i \prod_{i=1}^{n}(1 + \sigma_i^z \tanh\beta G) \qquad - 4.20$$

then, since

$$\sigma_i^z \sigma_i^{\pm} = \pm \sigma_i^{\pm}$$

the effect of it on the trace is to introduce a factor $(1 \pm \tanh\beta G)$ for each site in the diagram, the plus sign being taken if the first operator on that site in the trace is a spin creation operator. The factor $\cosh^N\beta G$ is lost when lnz is differentiated. Accordingly the trace corresponding to a particular permutation is just a product of $(1 \pm \tanh \beta G)$ factors, divided by 2^n to normalise the trace, as the trace of a product of spin creation or annihilation operators is either zero or unity.

The integrals required for each permutation are harder to compute: however, a subroutine finds the integral symbolically for each permutation, and then evaluates it, multiplied by the trace above, at required values of $G\beta$.

Multicomponent diagrams are calculated in essentially the same way: the contribution of such a diagram is the product of the contributions of its constituent diagrams. The irreducible diagrams without dotted lines which are needed for this work are tabulated with their Latin identifiers at the end of Table 4.1.

Such procedures, in particular the integration, take a great deal of computer time: diagram 7L, for example, may be decorated in 27 ways, and each of these has 4480 non-zero permutations, each involving an 8-fold integral. Each decoration of 7L takes about 9 minutes of CDC 7600 time to calculate: it seems unlikely, therefore, that the series will be extended past seventh order, as each new order involves several magnitudes more calculation. The new diagrams required for the eighth term have their values tabulated in Appendix IV, for a range of values of $G\beta$: the others may be reproduced quite rapidly on a large computer.

§4.4 Calculation of Occurrences

The introduction of cumulants, when the transition from z to lnz is made, has the effect of making all contributions from multi-component diagrams which is of order N^2 or higher cancel. This is, in any case, easily checked by writing out the moments μ^n_{n+2}, and transforming to cumulants. The occurrences on the lattice may now be counted quite easily, remembering that weak embeddings

of the diagrams are those of interest. The extension to the dilute case is made simply for the one-component diagrams, by multiplying by p^{n_s}, where there are n_s vertices in the diagram.

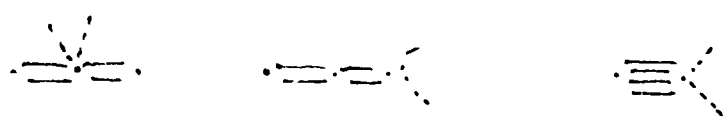
The multicomponent diagrams are slightly more complicated: consider the diagram



The occurrence of this one on a pure TZ lattice is

$$8N^2 - 12N - 12N - 4N \qquad - 4.21$$

where the second, third and fourth terms allow for the overlaps:



not allowed for in $8N^2$.

If the lattice is dilute, it seems logical to replace 4.21 by $8N^2p^4 - 12Np^3 - 12Np^3 - 4Np^2$: this procedure, used by Rushbrooke and Morgan (1961), has been proved to be correct by Wojtowicz (1963).

The resulting occurrences are tabulated in Table 4.1 for the TZ lattice, only the parts proportional to N being kept, and in Table 4.2 for the FCC lattice.

§4.5 Analysis of the Series

The series derived are rather short: experience indicates that ratio methods, and in particular methods 4 and 6 of §3, which use only odd or even terms in the series, are likely to give the most consistent estimates. Accordingly, the rather large task of examining the Padé approximants to each series at each of several thousand combinations of values of $G\beta$ and p is not attempted.

The series for the TZ lattice is examined first, as experimental results for the phase boundary are available for mixed crystals of (Dy, Y)VO_4, which have this structure (see §4.1). In $DyVO_4$, the ratio G/J is thought to be 1.31 (Sandercock et al, 1972), and the results of methods 4 and 6 for the critical temperature, kT_c/J, are shown below for this value. The results on the right are for the six term series, which is known for a wide range of $G\beta$, and those on the left come from the seven term series, derived for $0.5 \leq G\beta \leq 1.25$.

	Method 4	Method 6	Method 4'	Method 6'
p=1.0	2.65	2.58	2.69	2.63
p=.9	2.31	2.24	2.34	2.27
p=.8	1.96	1.89	2.00	1.90
p=.7	1.6	1.51	1.66	1.51
p=.6	1.21	1.08	1.25	1.09

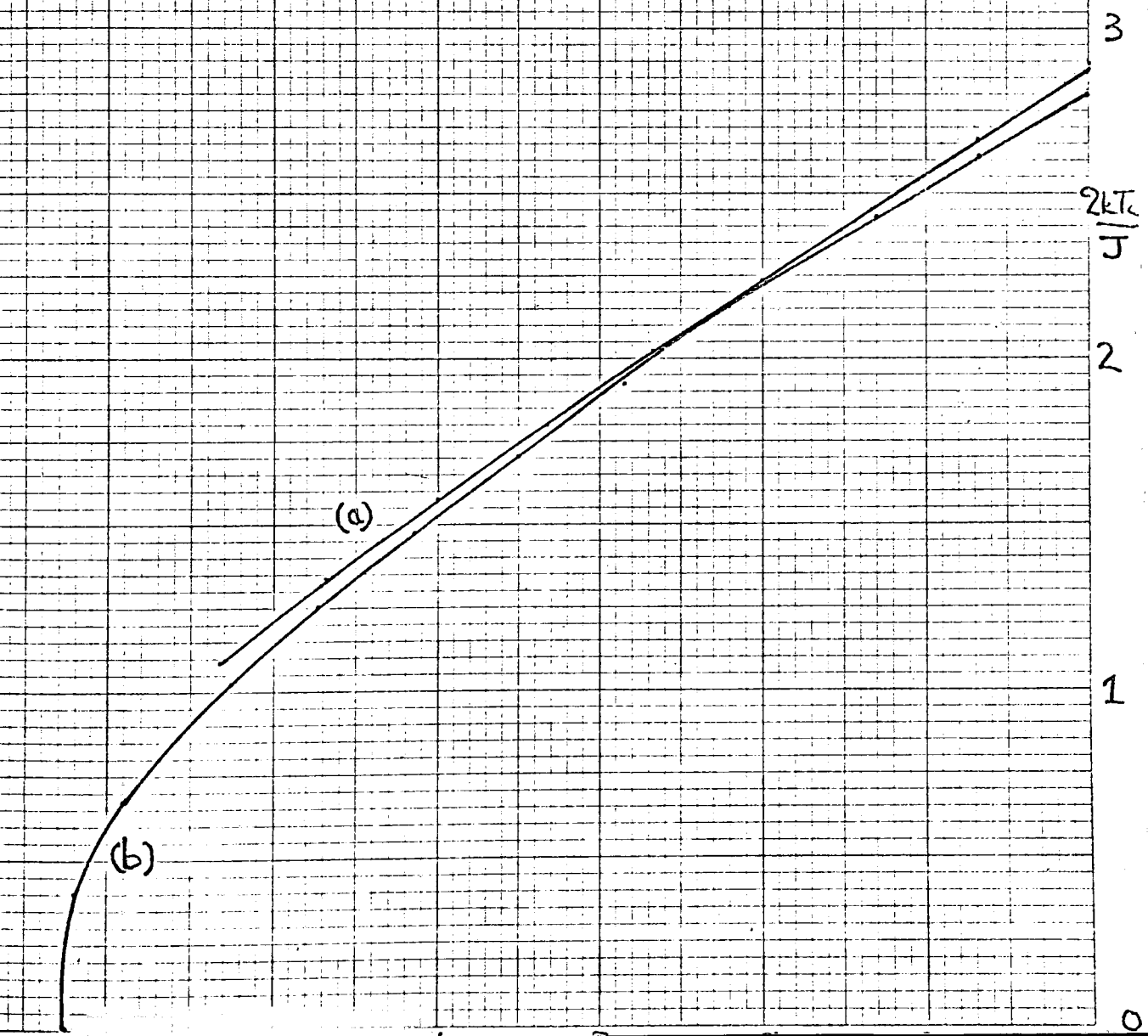
The results from the seven term series differ from those from the six term series by less than 3%, for corresponding

Figure B

Phase Boundary for TZ lattice by method 4.

(a) 6 term series in $(\frac{1}{2}\beta J)$
(b) 6 term series in p

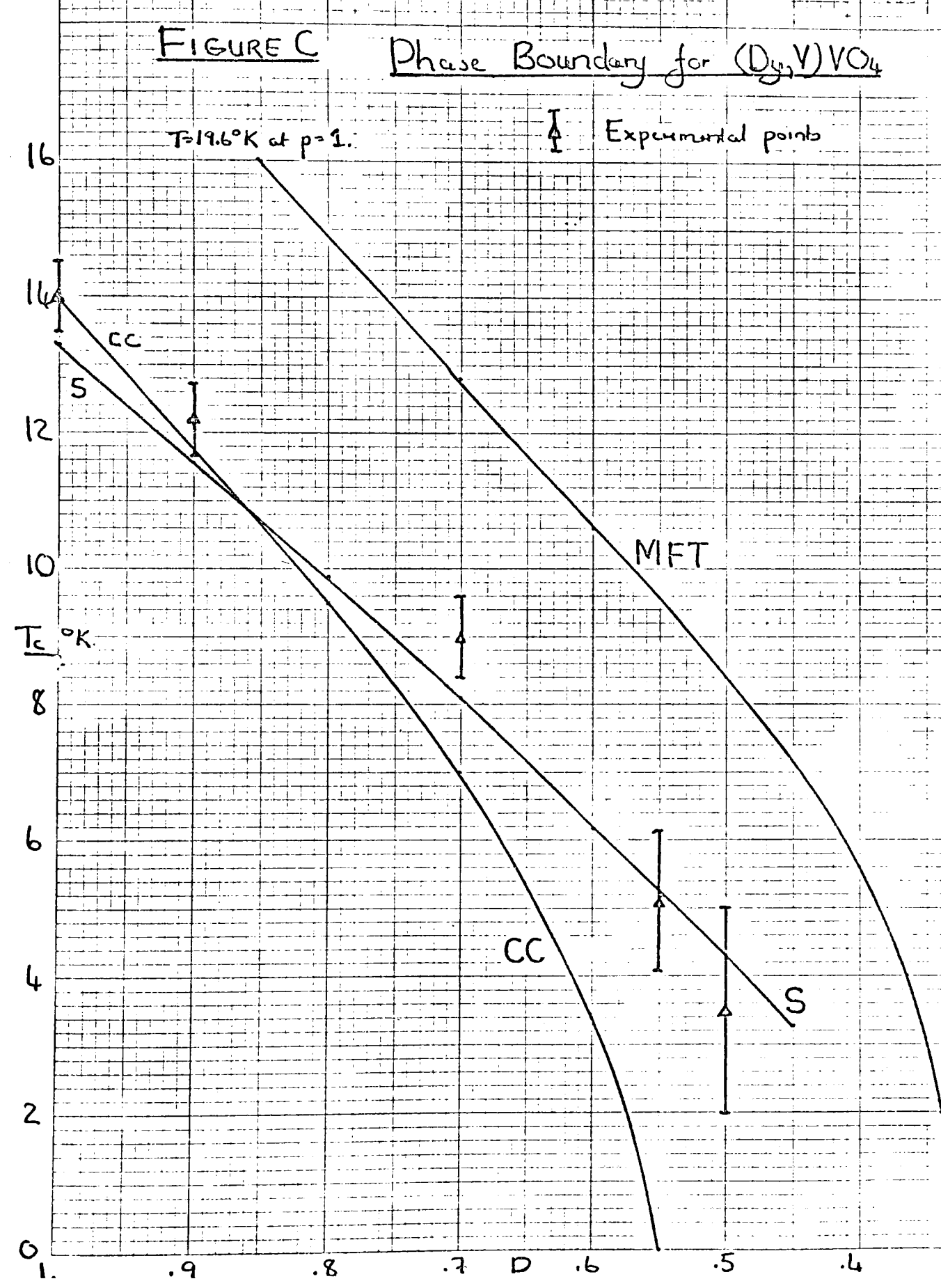
} Zero transverse field



methods. The phase boundary may be drawn with some confidence, therefore, at least down to p=.6. Below that, the six term series provides reasonable values down to p=.45, though, of course, the estimates become increasingly unrealiable as the temperature and concentration fall.

In Fig. B, an attempt is made to see how reliable the low temperature estimates are by comparing the results of method 4 for zero transverse field case on the previously derived series in $(\frac{1}{2}\beta J)$ and p, both of six terms. The p-series is thought to be more reliable at low temperature, and the figure indicates that the $(\frac{1}{2}\beta J)$ series progressively overestimates the critical temperature as p decreases below about p=.6. The results much below this concentration are therefore treated with some caution in the transverse field series, particularly as the spread between the results of methods 4 and 6 becomes more pronounced as p, and therefore $T_c(p)$, decreases. Method 4 is rather arbitrarily chosen to compare with experiment and other theories, since it seems to get the p=1 critical temperature most nearly right when compared with experiment. The results of experiment, method 4, molecular field theory (S.R.P. Smith, private communication) and constant coupling theory (A.P. Young, private communication) are compared in Fig. C.

Molecular field theory (MFT) is seen to give far too high a critical temperature at all p: furthermore it


FIGURE C
Phase Boundary for (Dy,Y)VO4
T=19.6°K at p=1.
Experimental points
16
14
12
10
8
6
4
2
0
CC
S
MFT
CC
S
Tc °K
1.
.9
.8
.7
D
.6
.5
.4

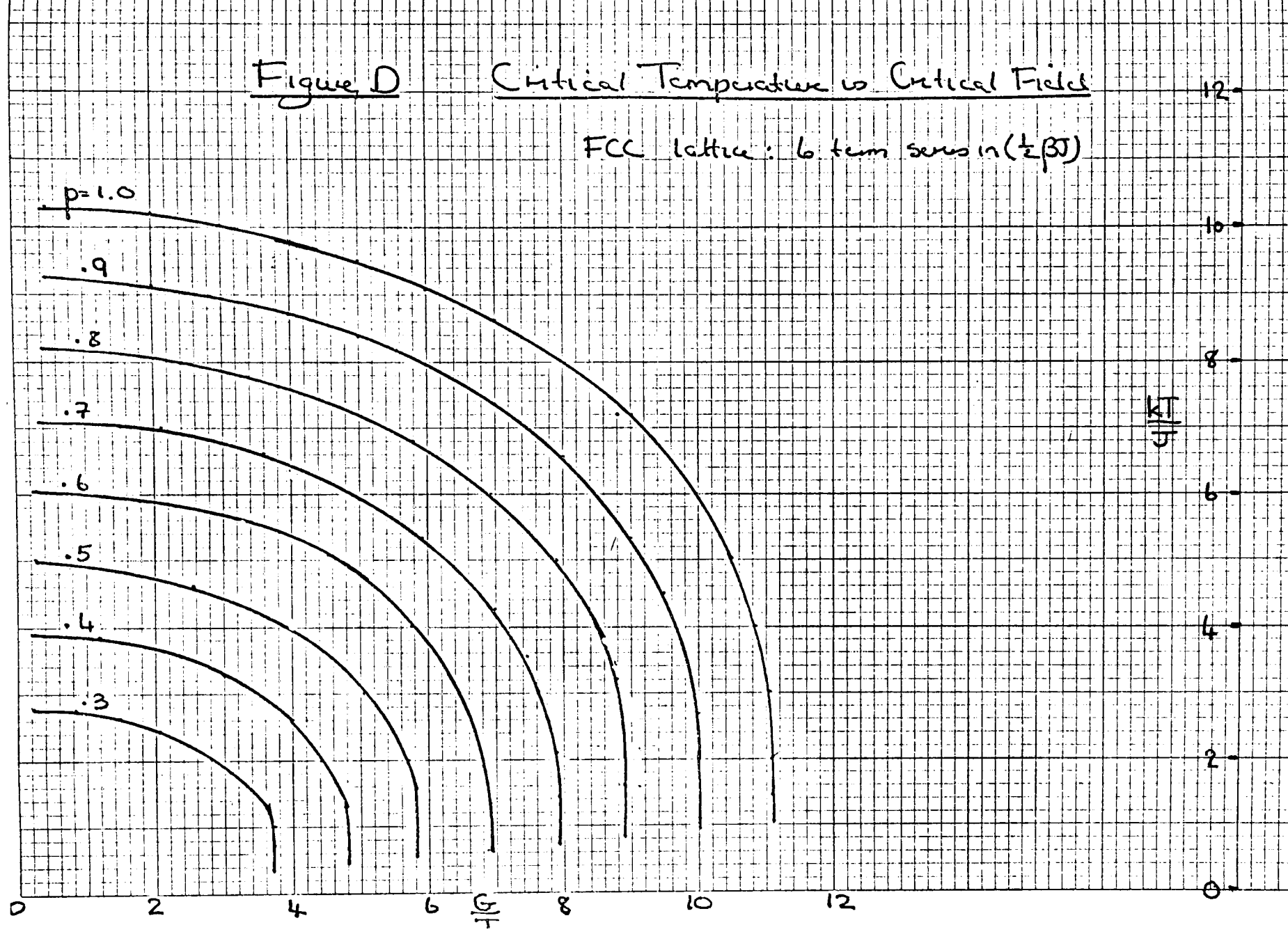
predicts a vanishing T_c at p=.33, which is well below the estimate for p_c^s made in §3 for this lattice. This is hardly surprising, as MFT is successful for long range interactions, and the main interaction is thought to be between next neighbours in $DyVO_4$. The constant coupling theory (CC), due to Young, treats the interaction, and also allows for a long range interaction acting as a molecular field: the results of this are consistently lower than experiment, but constant coupling is known to be generally unsatisfactory at low temperatures (e.g. Sandercock et al., 1972).

The results of method 4 applied to the series (S) are in quite good agreement with experiment, but again tend to underestimate at high p. At lower p, the agreement seems more satisfactory, but then high temperature series are thought to overestimate $T_c(p)$ for the model below p=.6 (e.g. Fig. B) so that it is probably true to say that the Ising model results are consistently rather lower than experiment. However, the fair level of agreement, bearing in mind that the long range interaction has been neglected, indicates that the critical behaviour of $DyVO_4$ is reasonably well described by the first neighbour transverse Ising model.

The six term series derived for the FCC lattice is thought to sample the lattice structure more thoroughly than the six term series for the TZ lattice, and is now

Figure D Critical Temperature vs Critical Field

FCC lattice: 6 term series in $(\frac{1}{2}\beta J)$



analysed in slightly more detail, in an attempt to find the shape of the critical surface and the behaviour of the critical index, γ. At high temperatures, methods 4 and 6 give consistent results, but at lower temperatures estimates become increasingly unreliable and there are substantial discrepancies between estimates by different methods. However, the analysis is pursued to quite low temperatures, by method 4, with the intention of gaining a qualitative rather than a quantitative description of the effects of a transverse field with dilution on the transition.

Fig. D shows the results for critical temperature against field at different values of p, where method 4 has been used to extrapolate down to about $\frac{1}{10}$ of the critical temperature for zero field, for each value of p. MFT would give a sequence of quadrants from $kT_c(p)=12pJ$ to $G=12pJ$: the series method results appear to share the property of being initially normal to each axis, but do not stay equidistant from the axis for intermediate values of G/J and kT_c/J: in particular, G/J at $T=0$ is about 1 bigger than T_c/J at $G=0$ for all p.

In Fig. E, curves of $T_c(p)$ against p are presented for a number of different values of G/J. Extrapolation to quite low temperatures has again been carried out, and the results indicate that the critical concentration rises with field (as predicted by molecular field theory) and

FIGURE E

Temperature vs. Concentration at constant Field

FCC lattice: 6 term series in $(\frac{1}{2}\beta J)$

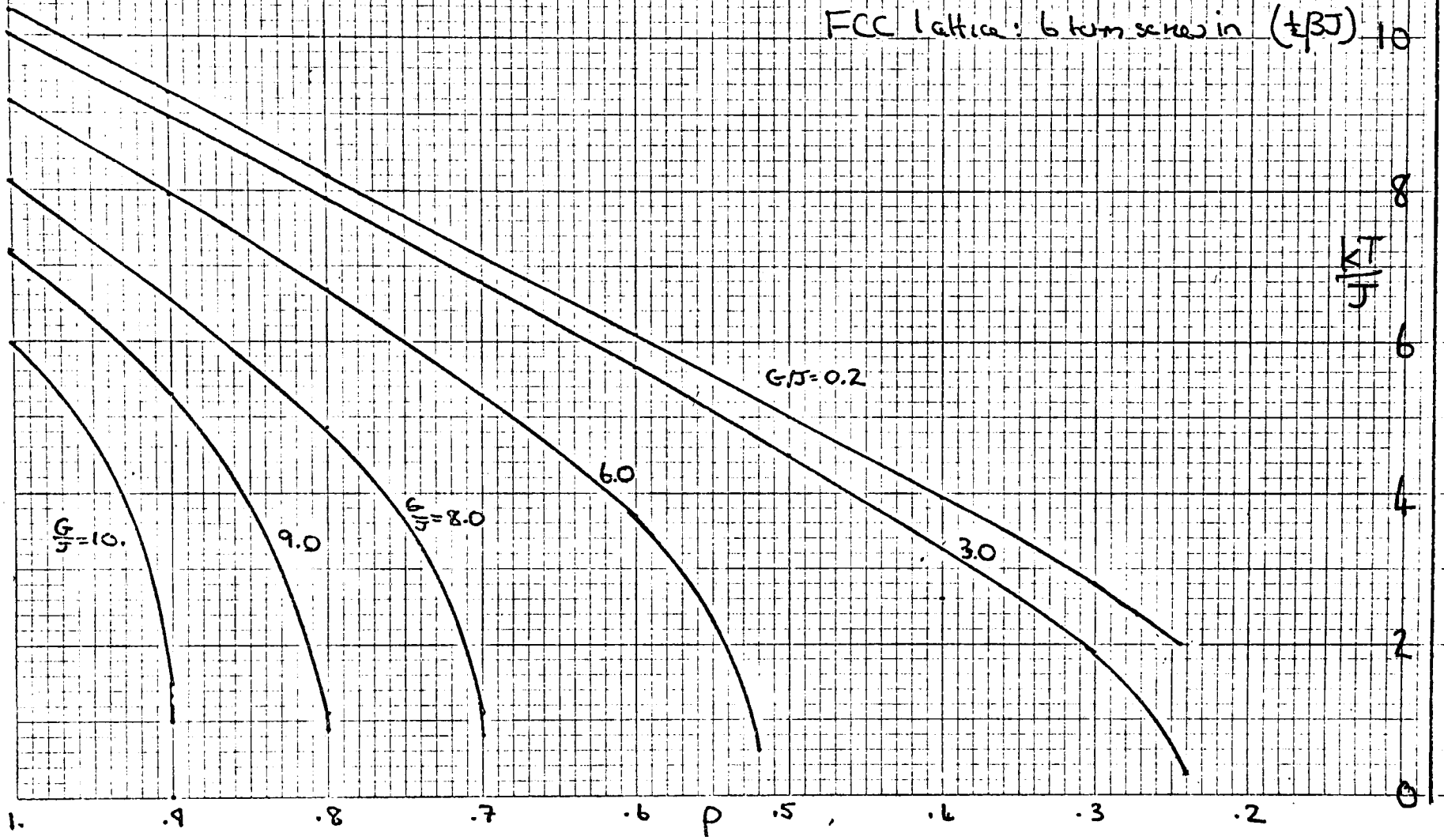
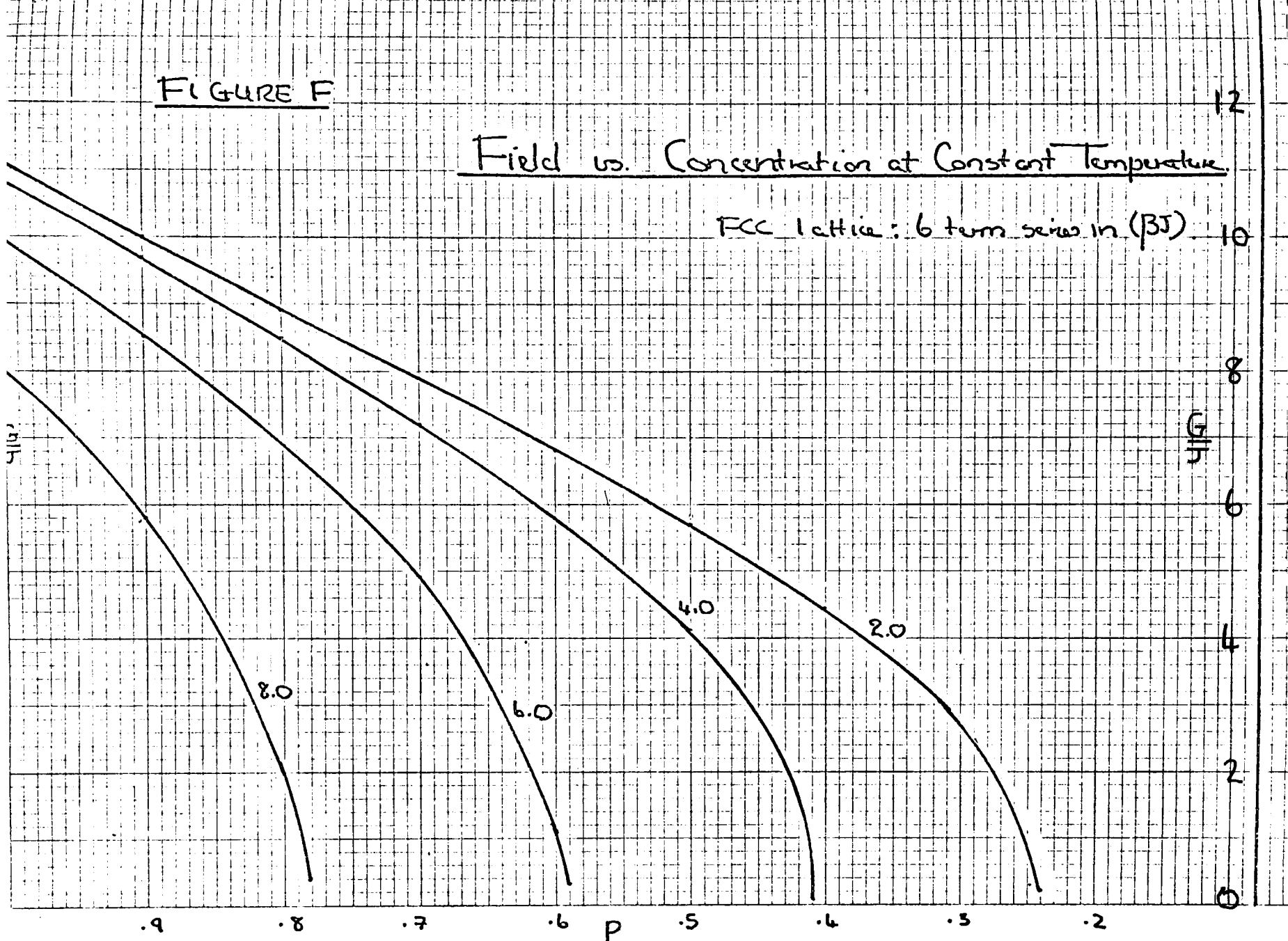


FIGURE F

Field vs. Concentration at Constant Temperature

FCC lattice: 6 term series in (βJ)



that this critical concentration is approached vertically at all values of G/J. This latter indication is particularly strong when it is remembered that this type of series overestimates $T_c(p)$ at low temperatures.

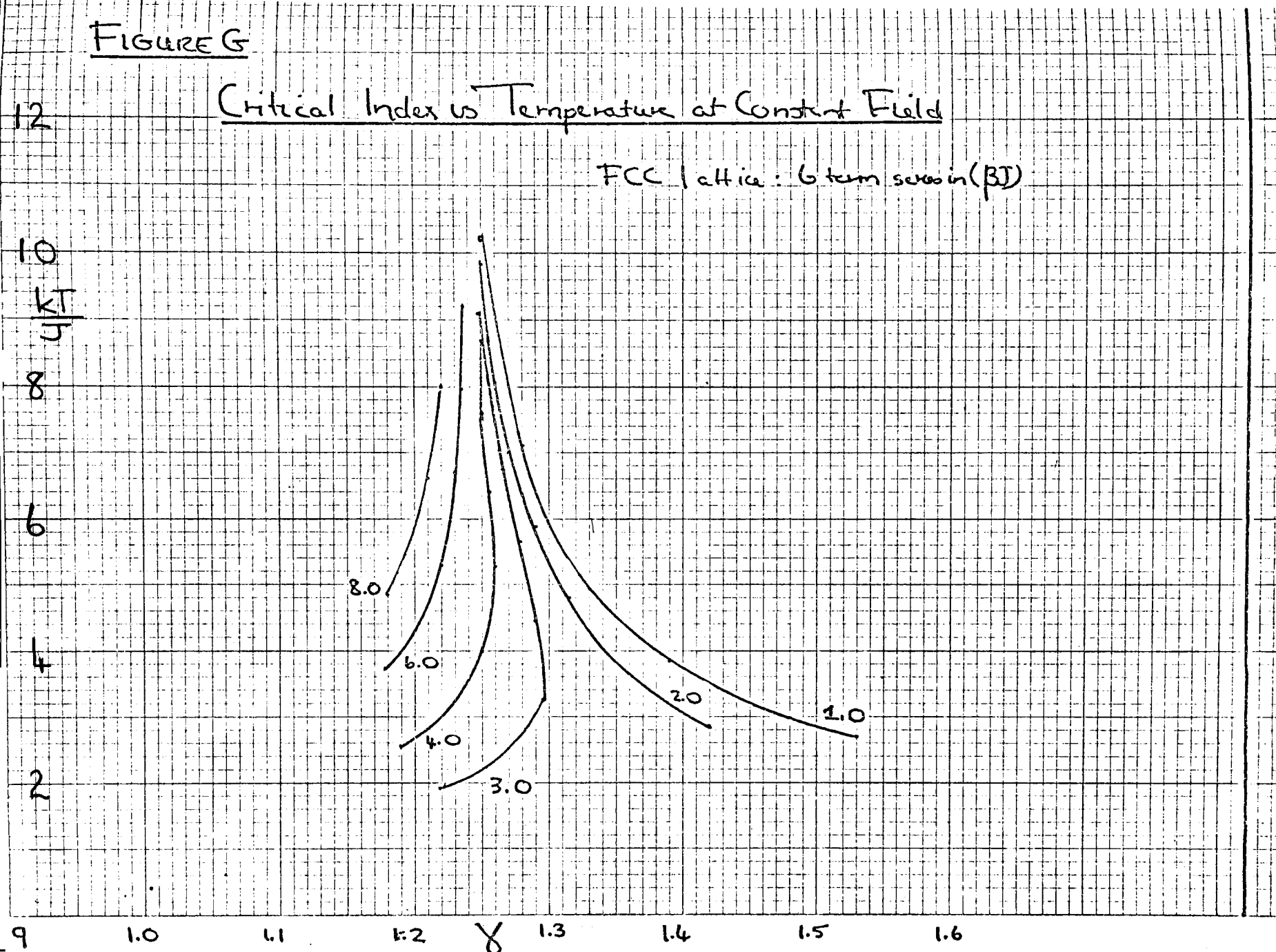
Curves of G/J against p for different fixed temperatures may also be drawn (Fig. F). Again, the results indicate that the concentration p^G below which order does not exist even when G=0 rises steadily with kT/J, as one expects. Furthermore, again p^G appears to be approached vertically at all temperatures as G/J is decreased to zero. This result, which would also appear likely to be true at zero temperature, is borne out by an argument due to Brooks Harris (private communication) which goes as follows. The linear Ising chain is ordered at T=0 until a sufficiently large field ($G_c/J=.25$) is applied: there is then no order. Since the infinite cluster is expected to be at least as connected as the linear chain, and there can be no order in the 3D Ising model till this occurs, at the percolation concentration, p_c^s, the ferromagnetic phase should continue at p_c^s and T=0 until a field at least as big as G_c/J is applied. However, this argument hinges on whether the infinite cluster is at least as connected as a linear chain: it certainly is on average, since $p_c^s > \frac{2}{z}$ for all structures, but the effect of loose ends may be important.

It is also worth noting that Figs. E and F have a

FIGURE G

Critical Index vs Temperature at Constant Field

FCC lattice : 6 term series in (βJ)



marked qualitative resemblance: G/J and kT/J appear in some sense symmetrical.

Ratio methods also yield values for the critical index, γ, which was defined in §3. These values are obtained by varying $G\beta$, that is by the variation of χ along a line through the origin in the T-G plane: however, the same γ should be obtained whatever the way in which the phase boundary is approached, as long as it is not tangentially. Fig. D indicates that this is never so. In Fig. G, the critical exponent is drawn against temperature for a range of values of field, G/J. At low values of G/J the critical index has the value of about 1.25 for temperatures corresponding to p=1, and at higher values of G/J this is slightly reduced for p=1. As the temperature is lowered (and p, therefore, is lowered) the critical index increases smoothly for G/J=1 till it reaches 1.53 at p=.3. This is the typical zero transverse field behaviour of an exponent estimated by ratio methods from a high temperature series: the index in the pure substance has been estimated with great accuracy as $\frac{5}{4}$, and at the percolation concentration and T=0 as $\frac{27}{16}$ in three dimensional systems. The estimates for γ appear to try to reach the percolation value of $\frac{27}{16}$ as the concentration is reduced, but some serious breakdown is encountered well above p_c^s (e.g. Chapter 3).

However, at higher values of G/J, the index no longer

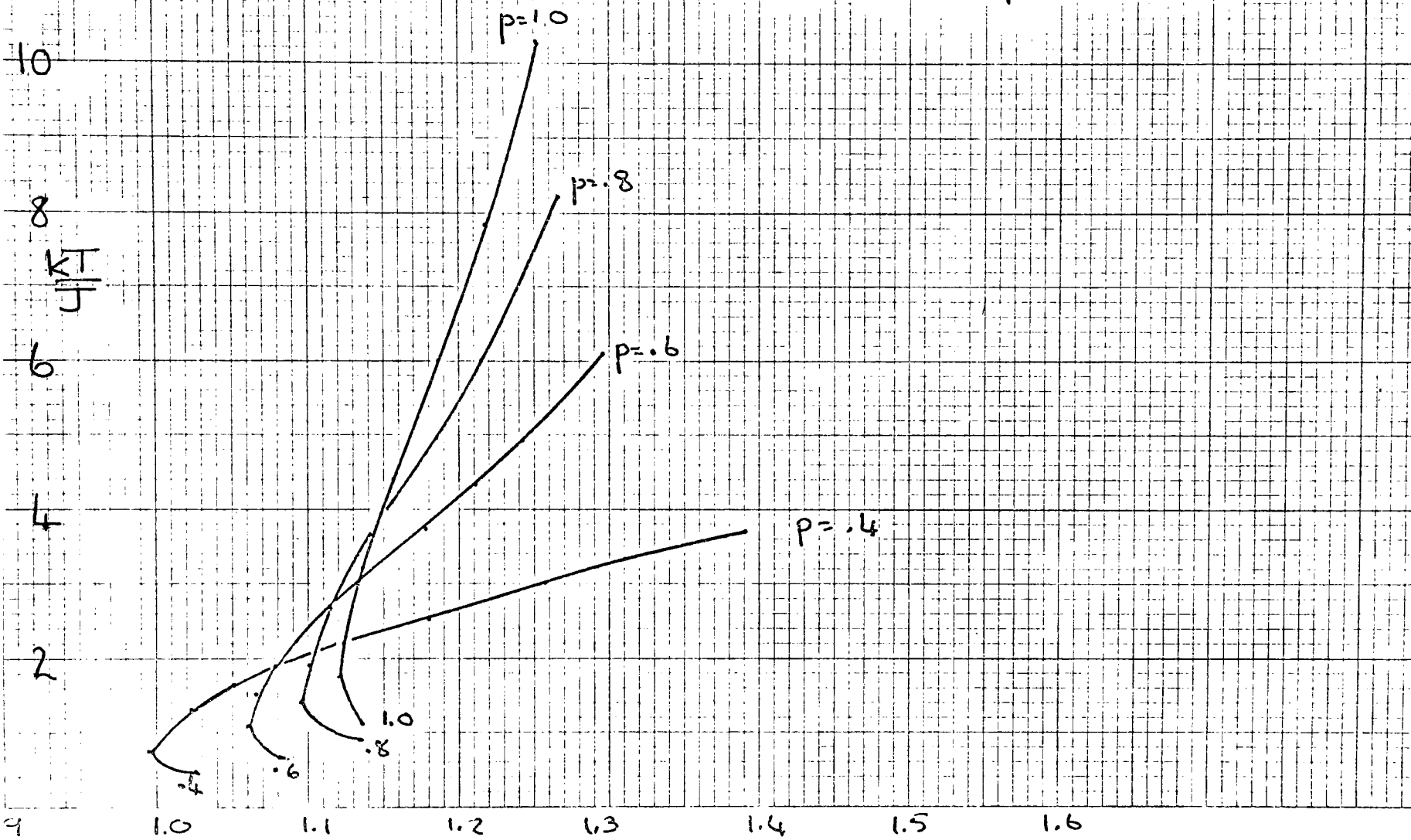
has this behaviour: at G/J=3.0, only a slight bend to higher values is observed as p is decreased, followed by a decrease, and at higher G/J, γ decreases monotonically with p. The reason for this may be simply that at higher G/J, the critical concentration, below which there is no order even at T=0, is some way above p_c^s (see Fig. E) so that the low temperature behaviour of γ is not determined by the percolation properties of the lattice. These conclusions about the behaviour of γ cannot, however, be other than tentative, as not only has work discussed in previous sections thrown rather a shadow over the estimation of γ from high temperature series altogether, but also the results for γ, being biassed in that they depend on the estimate of kT_c/J, are rather unreliable, particularly at low temperature.

Curves of critical index against temperature for fixed concentration may also be drawn (Fig. H). When p=1, γ decreases rather slowly from 1.25 to about 1.12 at $kT_c/J=2$: it then appears to increase again as G/J is increased and T falls. Similar behaviour, but with a progressively faster decrease of γ, is found at lower p. The behaviour of γ for p=1 has been noted before (Elliott and Wood, 1971), and has been thought to be due to the shortness of the series used there for the SC lattice: these authors conjecture that γ is constant except at T=0, when it changes discontinuously to be the value for a

FIGURE H

Critical Index vs Temperature at fixed Concentration

6 term series in $(\frac{1}{2}\beta J)$: FCC lattice



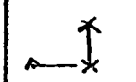
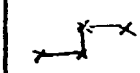
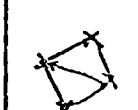
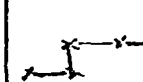
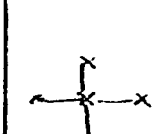
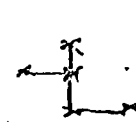
4-dimensional lattice, of 1.07 (see also Pfeuty and Elliott, 1971). Furthermore, γ is calculated as 1.11 by Pfeuty and Elliott using a perturbation technique at T=0. The results shown in Fig. H also seem to suggest $\gamma \sim 1.10$ at T=0 for a variety of values of p, so that perhaps the correspondence invoked by Pfeuty and Elliott between a transverse, T=0, Ising model of d dimensions and an Ising model with zero transverse field and of (d+1) dimensions holds at finite p as well as for the pure lattice. It must be remembered that γ will change with decreasing p in the 4d Ising model. This rise will probably be fairly gradual at first, as it is in the 2d and 3d Ising models studied in Chapter 3: however, when p is small, perhaps of the order of p=.4, γ in 4d will be quite different from its p=1 value. It is hard to see from Fig. H whether the results allow for this behaviour if the correspondence is assumed correct: nor does the author know of any mean cluster size expansions for hypercubic lattices which might give an indication of what $\gamma(T=0)$ is in 4d, or at what percolation concentration this value is found. Confirmation of this must await the extension of the perturbation expansion to the dilute lattice. However, the rapid decline of γ at lower p to about the 4-dimensional zero transverse field Ising value of 1.07 seems difficult to explain as due to the shortness of the series, as there is no region where $\gamma(T)$ is constant against T. The results suggest that

$\gamma(T)$ does change smoothly with G at fixed p. However, Fisher (1967) has conjectured plausibly that γ should only depend on the dimensionality of the system, and the evidence of such a short series is not conclusive.

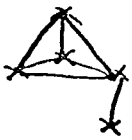
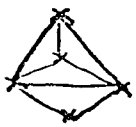
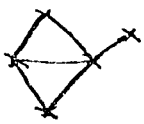
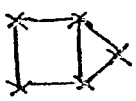
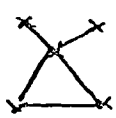
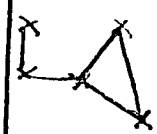
In conclusion, then, it may be said that the transverse Ising spin $\frac{1}{2}$ model may be studied with some success by analysis of series in $(\frac{1}{2}\beta J)$, even in the dilute case. Reasonable agreement with experiments on a system believed to be described well by an Ising $(\frac{1}{2})$ Hamiltonian with a transverse field is found, and some general ideas about the shape of the critical surface in the T-G, G-p and T-p planes are verified. The behaviour of the critical index appears to justify the hypothesis that the dramatic increase in γ as the dilution is increased in an ordinary Ising system is due to an attempt to represent the index "belonging" to the infinite cluster, and also leads one to suppose that the correspondence between the 3d transverse T=0 Ising model and the 4d Ising model suggested by Pfeuty and Elliott may also hold in the dilute case, at least for small dilutions. However, it must be remembered that high temperature expansions are subject to all the caveats expressed in §3, in a dilute system - although reasonably consistent results are obtained for a six term series, at least for $p \geq .6$ (TZ) or $p \geq .3$ (FCC), by different methods or use of series of a different length, it should be remembered that addition of several more terms to the FCC series

without a transverse field leads to inconsistent estimates. Short high temperature series of the length used here appear to give more realistic results for the phase boundary, and compare well with p-series at reasonable temperatures, but the validity of their estimates for the critical index is open to some doubt. Estimation of the significance of the results and conjectures reported here will have to await a resolution of the difficulties implied in the zero field high temperature series.

Cluster Susceptibilities

	1	$1/4$	all
	2	$\frac{1}{1+x}$	all
	3a	$\frac{9+2x+x^2}{4(1+x)^2}$	all
	3b	$\frac{9+3x^2}{4(1+3x^2)}$	FCC
	4a	$\frac{4+2x+2x^2}{(1+x)^3}$	all
	4b	$\frac{4+3x+x^3}{(1+x)^3}$	all
	4c	$\frac{4+4x^2}{1+6x^2+x^4}$	FCC, SC, ⊙
	4d.	$\frac{4+4x^3}{1+4x^3+3x^4}$	FCC
	4e	$\frac{4+2x^2+2x^3}{1+2x^2+4x^3+x^4}$	FCC
	4j	$\frac{4+x+2x^2+x^3}{1+x+3x^2+3x^3}$	FCC
	5a	$\frac{25+20x+30x^2+4x^3+x^4}{4(1+x)^4}$	all
	5b	$\frac{25+9x+30x^2+16x^3+x^4+x^5}{4(1+x)(1+6x^2+x^4)}$	FCC, SC, C
	5c	$\frac{25+36x+6x^2+4x^3+9x^4}{4(1+x)^4}$	All
	5d.	$\frac{25+28x+16x^2+12x^3+x^4}{4(1+x)^4}$	all

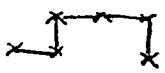
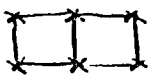
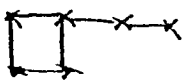
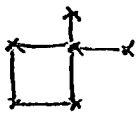
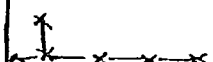
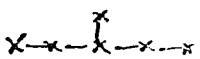
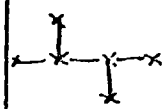
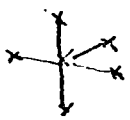
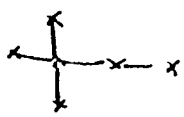
Cluster Susceptibilities continued,

	EO	$\frac{25 + 36x^3 + 13x^4 + 4x^5 + 2x^6}{4(1 + 4x^3 + 5x^4 + 4x^5 + 2x^6)}$
	EP	$\frac{25 + 9x + 28x^3 + 15x^4 + 3x^5}{4(1 + x + 4x^3 + 7x^4 + 3x^5)}$
	EQ	$\frac{25 + 9x^2 + 18x^3 + 21x^4 + 6x^5 + x^6}{4(1 + x^2 + 2x^3 + 5x^4 + 6x^5 + x^6)}$
	ER	$\frac{25 + 18x^2 + 20x^3 + 13x^4 + 4x^5}{4(1 + 2x^2 + 4x^3 + 5x^4 + 4x^5)}$
	ES	$\frac{25 + 9x + 18x^2 + 14x^3 + 13x^4 + x^5}{4(1 + x + 2x^2 + 6x^3 + 5x^4 + x^5)}$
	ET	$\frac{25 + 9x + 10x^2 + 30x^3 + 5x^4 + x^5}{4(1 + x + 2x^2 + 6x^3 + 5x^4 + x^5)}$
	EU	$\frac{25 + 28x^2 + 22x^3 + 3x^4 + 2x^5}{4(1 + 4x^2 + 6x^3 + 3x^4 + 2x^5)}$
	EV	$\frac{25 + 38x^2 + 17x^4}{4(1 + 6x^2 + 9x^4)}$
	EX	$\frac{25 + 18x + 12x^2 + 22x^3 + 3x^4}{4(1 + 2x + 4x^2 + 6x^3 + 3x^4)}$
	EY	$\frac{25 + 18x + 20x^2 + 6x^3 + 11x^4}{4(1 + 2x + 4x^2 + 6x^3 + 3x^4)}$
	EZ	$\frac{25 + 10x + 28x^2 + 14x^3 + 3x^4}{4(1 + 2x + 4x^2 + 6x^3 + 3x^4)}$

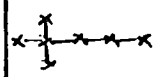
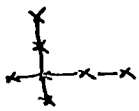
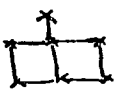
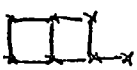
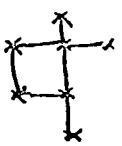
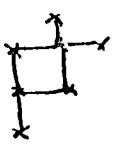
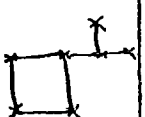
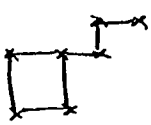
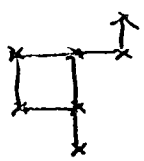
Lattice

FCC

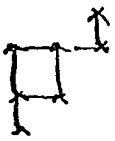
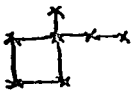
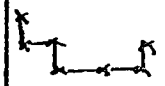
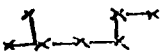
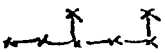
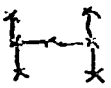
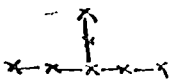
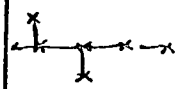
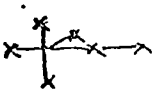
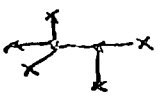
Cluster Susceptibilities cont.

			Lattice
	6o	$\frac{9+10x+20x^2+6x^3+3x^4}{(1+x)^5}$	SC, Q, TZ
	6b	$\frac{9+18x^2+12x^3+5x^4+6x^5}{1+12x^2+18x^3+18x^4+12x^5+x^7}$	SC, Q
	6c	$\frac{9+5x+18x^2+10x^3+5x^4+x^5}{(1+x)^2(1+6x^2+x^4)}$	SC, Q
	6d	$\frac{9+8x+15x^2+8x^3+7x^4+x^6}{(1+x)^2(1+6x^2+x^4)}$	SC, Q
	6e	$\frac{9+8x+12x^2+14x^3+3x^4+2x^5}{(1+x)^2(1+6x^2+x^4)}$	SC, Q
	6j	$\frac{9+8x+11x^2+16x^3+3x^4+x^6}{(1+x)^2(1+6x^2+x^4)}$	SC, Q
	6g	$\frac{9+13x+11x^2+10x^3+x^4+x^5}{(1+x)^5}$	SC, Q, TZ
	6h	$\frac{9+14x+12x^2+10x^3+3x^4}{(1+x)^5}$	SC, Q, TZ
	6i	$\frac{9+16x+10x^2+8x^3+5x^4}{(1+x)^5}$	SC, Q, TZ
	6k	$\frac{9+20x+10x^2+5x^4+6x^5}{(1+x)^5}$	SC
	6o	$\frac{9+30x^2+9x^4}{1+15x^2+15x^4+x^6}$	SC, TZ
	6j	$\frac{9+17x+10x^2+6x^3+5x^4+x^5}{(1+x)^5}$	SC, Q, TZ

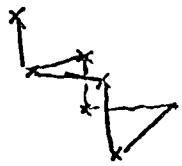
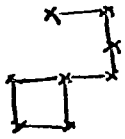
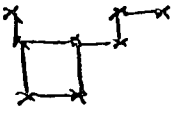
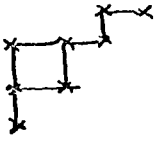
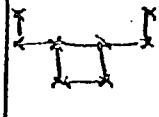
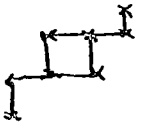
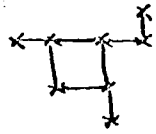
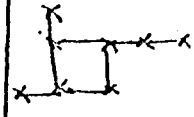
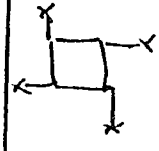
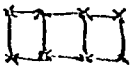
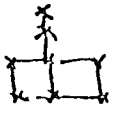
Cluster Susceptibilities continued

	7a	$\frac{49+188x^2+182x^4+28x^6+x^8}{4(1+12x^2+38x^4+12x^6+x^8)}$	SC, Q
	7b	$\frac{49+110x+119x^2+100x^3+62x^4+14x^5+9x^6}{4(1+x)^6}$	SC, Q; TT
	7c	$\frac{49+118x+111x^2+84x^3+63x^4+22x^5+x^6}{4(1+x)^6}$	SC, Q, T
	7d	$\frac{49+75x+81x^2+131x^3+83x^4+17x^5+11x^6+x^7}{4(1+x)^3(1+6x^2+x^4)}$	SC, Q
	7e	$\frac{49+25x+118x^2+95x^3+98x^4+39x^5+22x^6+x^7+x^8}{4(1+x+6x^2+15x^3+18x^4+15x^5+6x^6+x^7+x^8)}$	SC, Q
	7f	$\frac{49+25x+96x^2+143x^3+66x^4+55x^5+11x^6+x^7+x^8}{4(1+x+6x^2+15x^3+18x^4+15x^5+6x^6+x^7+x^8)}$	SC, Q
	7g	$\frac{49+75x+97x^2+115x^3+67x^4+33x^5+11x^6+x^7}{4(1+x)^3(1+6x^2+x^4)}$	SC, Q
	7h	$\frac{49+75x+89x^2+123x^3+83x^4+17x^5+3x^6+9x^7}{4(1+x)^3(1+6x^2+x^4)}$	SC, Q
	7i	$\frac{49+51x+121x^2+131x^3+51x^4+46x^5+3x^6+x^7}{4(1+x)^3(1+6x^2+x^4)}$	SC, Q
	7j	$\frac{49+35x+153x^2+99x^3+83x^4+25x^5+3x^6+x^7}{4(1+x)^3(1+6x^2+x^4)}$	SC, Q
	7k	$\frac{49+59x+105x^2+131x^3+67x^4+33x^5+3x^6+x^7}{4(1+x)^3(1+6x^2+x^4)}$	SC, Q

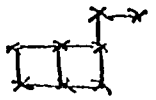
Cluster Susceptibilities continued

	7l	$\frac{49+59x+97x^2+167x^3+67x^4+17x^5+11x^6+x^7}{4(1+x)^3(1+6x^2+x^4)}$	SC, Q
	7m	$\frac{49+59x+129x^2+83x^3+99x^4+17x^5+11x^6+x^7}{4(1+x)^3(1+6x^2+x^4)}$	x_2 Q
	7n	$\frac{49+70x+175x^2+86x^3+63x^4+6x^5+x^6}{4(1+x)^6}$	SC, Q
	7o	$\frac{49+86x+143x^2+116x^3+31x^4+22x^5+x^6}{4(1+x)^6}$	SC, Q
	7p	$\frac{49+96x+127x^2+116x^3+47x^4+14x^5+x^6}{4(1+x)^6}$	SC, Q
	7q	$\frac{49+102x+119x^2+116x^3+47x^4+6x^5+9x^6}{4(1+x)^6}$	SC, Q
	7r	$\frac{49+102x+111x^2+116x^3+63x^4+6x^5+x^6}{4(1+x)^6}$	SC, Q
	7s	$\frac{49+110x+111x^2+100x^3+63x^4+16x^5+x^6}{4(1+x)^6}$	SC, Q
	7t	$\frac{49+150x+135x^2+20x^3+15x^4+54x^5+25x^6}{4(1+x)^6}$	SC
	7u	$\frac{49+134x+119x^2+52x^3+47x^4+38x^5+9x^6}{4(1+x)^6}$	SC
	7v	$\frac{49+75x+121x^2+91x^3+51x^4+49x^5+3x^6+9x^7}{4(1+x)^5(1+6x^2+x^4)}$	SC
	7w	$\frac{49+126x+116x^2+68x^3+63x^4+30x^5+x^6}{4(1+x)^6}$	SC,
	7x	$\frac{49+75x^2+157x^3+63x^4+63x^5+32x^6+3x^7+x^9}{4(1+3x^2+13x^3+15x^4+15x^5+13x^6+3x^7+x^9)}$	SC

Cluster Susceptibilities continued

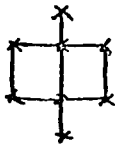
	7y	$\frac{1-49x+175x^2+95x^3+63x^4+39x^5+x^6+x^7}{4(1+x)(1+15x^2+15x^4+x^6)}$	SC, TZ
		8pt clusters.	
	NA	$\frac{16+116x+72x^2+56x^3+48x^4+26x^5+8x^6+2x^7}{(1+x)^4(1+6x^2+x^4)}$	
	MB	$\frac{16+23x+56x^2+69x^3+52x^4+33x^5+6x^6+3x^7}{(1+x)^4(1+6x^2+x^4)}$	
	MC	$\frac{16+23x+51x^2+75x^3+51x^4+29x^5+9x^6+x^7+x^8}{(1+x)^4(1+6x^2+x^4)}$	
	MD	$\frac{16+26x+68x^2+70x^3+56x^4+30x^5+8x^6+2x^7}{(1+x)^4(1+6x^2+x^4)}$	
	ME	$\frac{16+26x+46x^2+78x^3+56x^4+22x^5+12x^6+2x^7}{(1+x)^4(1+6x^2+x^4)}$	
	MF	$\frac{16+31x+43x^2+67x^3+59x^4+29x^5+9x^6+x^7+x^8}{(1+x)^4(1+6x^2+x^4)}$	
	MG	$\frac{16+31x+42x^2+69x^3+60x^4+25x^5+10x^6+3x^7}{(1+x)^4(1+6x^2+x^4)}$	
	MH	$\frac{16+36x+40x^2+60x^3+64x^4+28x^5+8x^6+4x^7}{(1+x)^4(1+6x^2+x^4)}$	
	MI	$\frac{16+64x^2+56x^3+48x^4+64x^5+20x^6+8x^7+4x^8}{1+7x^2+12x^3+26x^4+60x^5+28x^6+12x^7+7x^8+x^{10}}$	
	MJ	$\frac{16+13x+53x^2+63x^3+71x^4+35x^5+19x^6+5x^7+x^8}{(1+x)^2(1+6x^2+9x^3+9x^4+6x^5+x^7)}$	

Cluster Susceptibilities continued



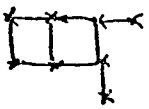
MK

$$\frac{16+13x+66x^2+67x^3+55x^4+63x^5+15x^6+5x^7+x^8}{(1+x)^4(1+6x^2+9x^3+9x^4+6x^5+x^7)}$$



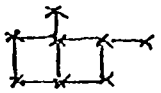
ML

$$\frac{16+18x+68x^2+68x^3+166x^4+26x^5+28x^6+6x^7+2x^8}{(1+x)^2(1+6x^2+9x^3+9x^4+6x^5+x^7)}$$



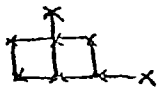
MM

$$\frac{16+18x+34x^2+70x^3+56x^4+38x^5+22x^6+2x^7+2x^8}{(1+x)^2(1+6x^2+4x^3+9x^4+6x^5+x^7)}$$



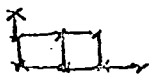
MN

$$\frac{16+18x+60x^2+64x^3+50x^4+62x^5+20x^6+6x^7+2x^8}{(1+x)^2(1+6x^2+9x^3+9x^4+6x^5+x^7)}$$



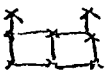
MO

$$\frac{16+18x+60x^2+61x^3+56x^4+61x^5+16x^6+7x^7+x^9}{(1+x)^2(1+6x^2+8x^3+4x^4+6x^5+x^7)}$$



NP

$$\frac{16+18x+32x^2+72x^3+58x^4+34x^5+20x^6+6x^7+2x^8}{(1+x)^2(1+6x^2+9x^3+9x^4+6x^5+x^7)}$$



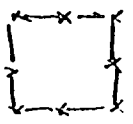
MQ

$$\frac{16+18x+32x^2+73x^3+56x^4+33x^5+26x^6+3x^7+x^9}{(1+x)^2(1+6x^2+4x^3+4x^4+6x^5+x^7)}$$



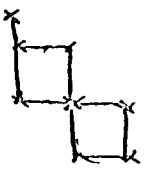
MR

$$\frac{16+53x^2+38x^3+59x^4+52x^5+27x^6+6x^7+5x^8}{1+7x^2+12x^3+26x^4+60x^5+26x^6+12x^7+7x^8+x^{10}}$$



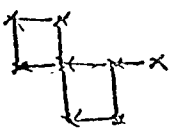
MS

$$\frac{16+112x^2+112x^4+16x^6}{1+28x^2+70x^4+28x^6+x^8}$$



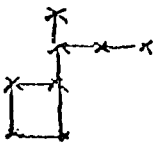
MT

$$\frac{16+9x+60x^2+40x^3+72x^4+38x^5+12x^6+2x^7+x^9}{(1+x)(1+12x^2+38x^4+12x^6+x^8)}$$



ML

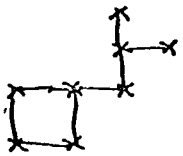
$$\frac{16+9x+63x^2+32x^3+67x^4+43x^5+13x^6+7x^7+x^8}{(1+x)(1+12x^2+38x^4+12x^6+x^8)}$$



NQ

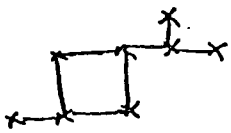
$$\frac{16+22x+56x^2+75x^3+48x^4+34x^5+8x^6+2x^7}{(1+x)^4(1+6x^2+x^4)}$$

Cluster Susceptibilities cont.



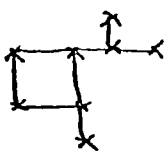
NB

$$\frac{16+19x+59x^2+75x^3+63x^4+33x^5+9x^6+x^7+x^8}{(1+x)^4(1+6x^2+x^4)}$$



NC

$$\frac{16+28x+66x^2+76x^3+56x^4+20x^5+12x^6+6x^7}{(1+x)^4(1+6x^2+x^4)}$$



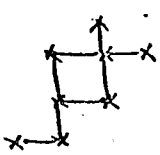
ND

$$\frac{16+28x+67x^2+72x^3+51x^4+28x^5+13x^6+x^8}{(1+x)^4(1+6x^2+x^4)}$$



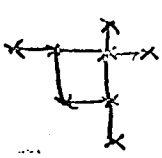
NE

$$\frac{16+36x+67x^2+67x^3+51x^4+29x^5+13x^6+x^7+x^8}{(1+x)^4(1+6x^2+x^4)}$$



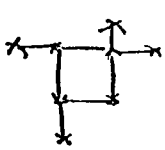
NF

$$\frac{16+36x+63x^2+71x^3+59x^4+28x^5+9x^6+5x^7+x^8}{(1+x)^4(1+6x^2+x^4)}$$



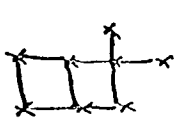
NG

$$\frac{16+36x+66x^2+60x^3+56x^4+28x^5+12x^6+6x^7}{(1+x)^4(1+6x^2+x^4)}$$



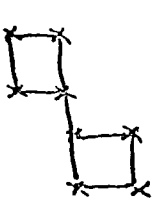
NH

$$\frac{16+36x+63x^2+60x^3+59x^4+28x^5+9x^6+6x^7+x^8}{(1+x)^4(1+6x^2+x^4)}$$



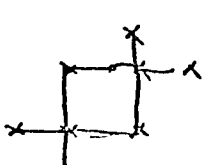
NI

$$\frac{16+18x+36x^2+69x^3+56x^4+33x^5+20x^6+7x^7+x^9}{(1+x)^2(1+6x^2+9x^3+9x^4+6x^5+x^6)}$$



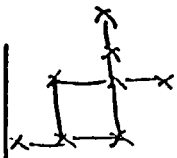
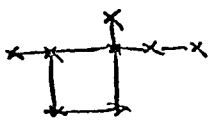
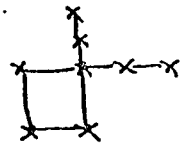
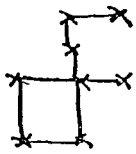
NJ

$$\frac{16+72x^2+60x^3+64x^4+48x^5+8x^6+8x^7}{(1+x)(1+6x^2+x^4)^2}$$

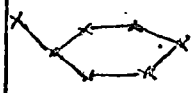
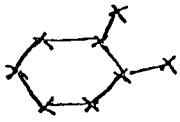
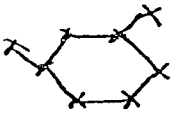
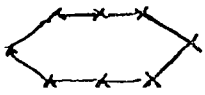


NK

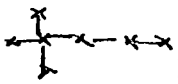
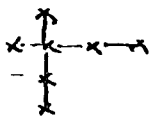
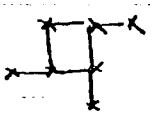
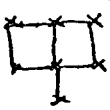
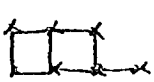
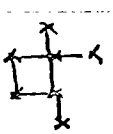
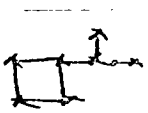
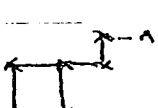
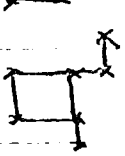
$$\frac{16+36x+66x^2+60x^3+60x^4+28x^5+6x^6+6x^7+6x^8}{(1+x)^4(1+6x^2+x^4)}$$

	NL	$\frac{16+31x+47x^2+63x^3+59x^4+29x^5+5x^6+5x^7+x^8}{(1+x)^4(1+6x^2+x^4)}$
	NM	$\frac{16+31x+56x^2+61x^3+52x^4+33x^5+10x^6+3x^7}{(1+x)^4(1+6x^2+x^4)}$
	NN	$\frac{16+26x+60x^2+66x^3+72x^4+22x^5+12x^6+2x^7}{(1+x)^4(1+6x^2+x^4)}$
	NO	$\frac{16+23x+63x^2+51x^3+67x^4+26x^5+13x^6+x^7+x^8}{(1+x)^4(1+6x^2+x^4)}$

Seven x eight point clusters in t-notation, used in TE series only.

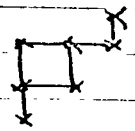
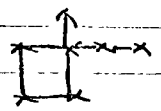
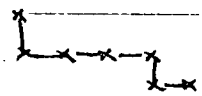
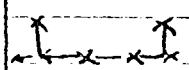
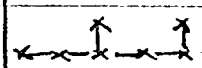
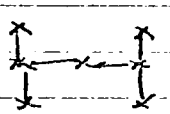
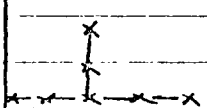
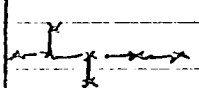
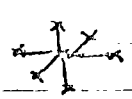
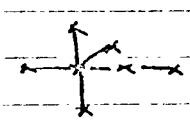
	7y	$\frac{7+16t+16t^2+16t^3+16t^4+16t^5+11t^6+2t^7}{4(1+t^6)}$
	DYA	$\frac{8+16t+20t^2+20t^3+20t^4+24t^5+16t^6+6t^7}{4(1+t^6)}$
	DYB	$\frac{8+16t+20t^2+22t^3+20t^4+20t^5+16t^6+6t^7}{4(1+t^6)}$
	DYC	$\frac{8+16t+20t^2+20t^3+22t^4+20t^5+18t^6+6t^7}{4(1+t^6)}$
	DYD	$\frac{8+16t+22t^2+20t^3+20t^4+20t^5+16t^6+11t^7+2t^8}{4(1+t^6)}$
	DYE	$\frac{8+16t+18t^2+20t^3+20t^4+20t^5+16t^6+8t^7+2t^8}{4(1+t^6)}$
	MS	$\frac{8+16t+16t^2+16t^3+16t^4+16t^5+16t^6+16t^7+8t^8}{4(1+t^8)}$

Occurrences of Seven & Eight Point Clusters.

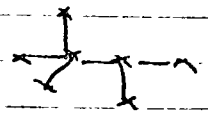
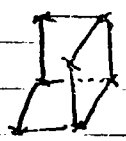
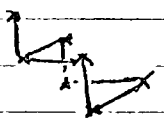
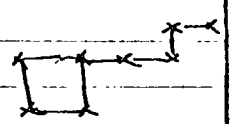
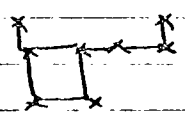
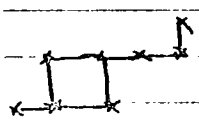
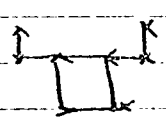
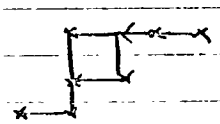
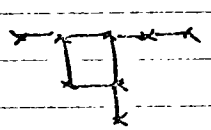
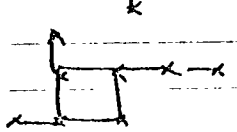
		S.C.	Q.	TZ
	7a	$30p^7$	$2p^7q^{10}$	0
	7b	$684\,p^7$	$(4q^{12}+8q^{11})p^7$	$p^7(24q^{15}+12q^{16})$
	7c	$606p^7$	$6p^7q^{12}$	$p^7(12q^{15}+12q^{16})$
	7d	$504p^7$	$16p^7q^{10}$	0
	7e	$108p^7$	$4p^7q^{10}$	0
	7j	$240p^7$	$16p^7q^{10}$	0
	7g	$360p^7$	$8q^{10}p^7$	0
	7h	$288p^7$	$8p^7q^{10}$	0
	7i	$216p^7$	$8q^{11}p^7$	0
	7j	$720p^7$	$p^7(8q^{13}+24q^{12}+8q^{11})$	0
	7k	$1104p^7$	$p^7(24q^{12}+24q^{11})$	0

Note: $p=(1-q)$. The lowest power of p in the occurrence is given where only this is necessary to produce the series derived.

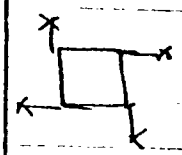
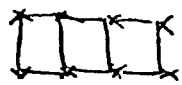
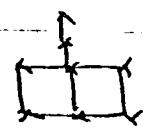
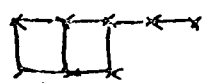
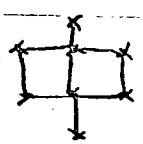
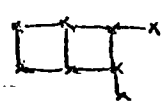
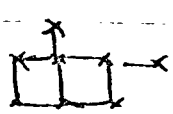
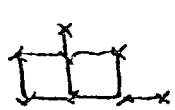
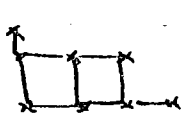
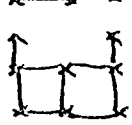
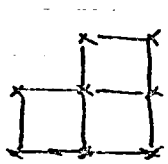
Occurrences continued.

		SC	Q	Tr
	7l	$672p^7$	$16p^7(q^{11}+q^{12})$	0
	7m	$384p^7$	$8p^7q^{11}$	0
	7n	$4623p^7$	$198p^7$	$p^7(24q^{14}+192q^{15}+210q^{16})$
	7o	$3584p^7$	$124p^7$	$p^7(96q^{15}+120q^{16})$
	7p	$5832p^7$	$168p^7$	$p^7(24q^{14}+288q^{15}+288q^{16})$
	7q	$732p^7$	$22p^7$	$p^7(6q^{14}+36q^{15}+12q^{16})$
	7r	$792p^7$	$16p^7$	$p^7(4q^{13}+60q^{15}+44q^{16})$
	7s	$1728p^7$	$24p^7$	$p^7[96q^{15}+120q^{16}]$
	7t	$1p^7$	0	0
	7u	$54p^7$	0	0
	7v	$48p^7$	0	0

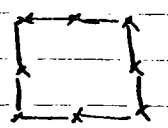
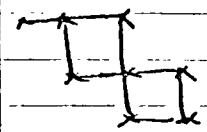
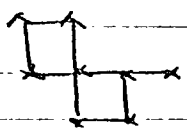
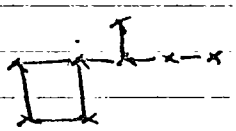
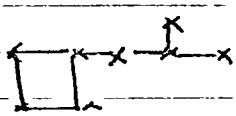
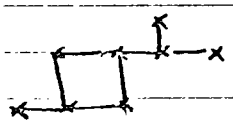
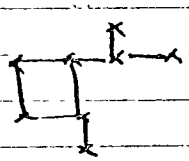
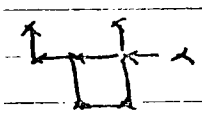
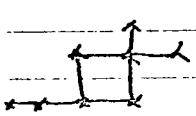
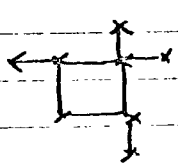
Occurrence continued.

		SC	Q	TZ
	7w	$13p^7$	0	$12p^7q^{16}$
	7x	$8p^7$	0	0
	7y	$72p^7$	0	$24q^{14}$
	MA	—	$96p^8$	0
	MB	—	$120p^8$	0
	MC	—	$80p^8$	0
	MD	—	$48p^8$	0
	ME	—	$32p^8$	0
	MF	—	$32p^8$	0
	MG	—	$64p^8$	0

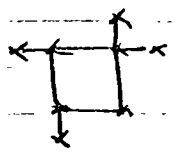
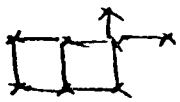
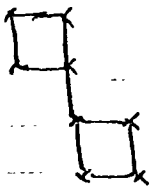
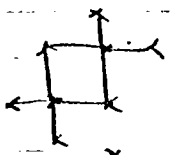
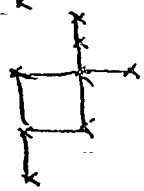
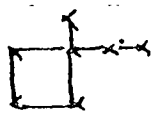
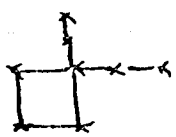
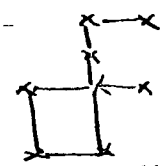
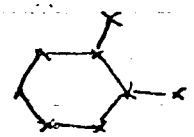
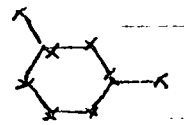
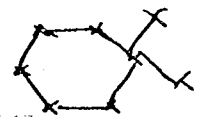
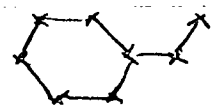
Occurrences continued

		SC	Θ	TZ
	MH	—	$2p^8$	0
	MI	—	$2p^8$	6
	MJ	—	$4p^8$	0
	MK	—	$32p^8$	0
	ML	—	$2p^8$	0
	MM	—	$12p^8$	0
	MN	—	$8p^8$	0
	MO	—	$16p^8$	0
	MP	—	$16p^8$	0
	MQ	—	$16p^8$	0
	MR	—	$4p^8$	0

Occurrences continued

	Q	Tz
 NS	$1p^8$	$3p^8$
 NT	$8p^8$	0
 NU	$8p^8$	0
 NA	$24p^8$	0
 NB	$32p^8$	0
 NC	$16p^8$	0
 ND	$24p^8$	0
 NE	$16p^8$	0
 NF	$16p^8$	0
 NG	$6p^8$	0

Occurrences continued.

	⑦		T2
	NH	$8p^8$	
	NI	$8p^8$	
	NJ	$4p^8$	
	NK	$2p^8$	
	NL	$16p^8$	
	NM	$16p^8$	
	NN	$4p^8$	
	NO	$24p^8$	
	DYA	$24p^8$	
	DYB	$48p^8$	
	DYC	$48p^8$	
	DYD	$12p^8$	
	DYE	$72p^8$	

Simple Cubic Susceptibility p-series

$$\chi^R = \sum_{n=0}^{b} a_{n+1} p^n$$

Mean cluster size series	
1	$a_1 = 1$
6	$a_2 = 3(2) - 6$
30	$a_3 = 15(3a) - 30(2) + 15$
116	$a_4 = 63(4a) + 20(4b) + 3(4c) - 198(3a) + 135(2) - 20$
438	$a_5 = 267(5a) + 48(5b) + 15(5c) + 204(5d) - 48(4c) - 312(4b) - 1038(4a) + 1209(3a) - 360(2) + 15$
1542	$a_6 = 1107(6a) + 18(6b) + 168(6c) + 72(6d) + 156(6e) + 96(6f) + 876(6g) + 696(6h) + 126(6i) + 156(6j) + 6(6k) + 4(6o) - 3864(5d) - 258(5c) - 888(5b) - 5250(5a) + 360(4c) + 2280(4b) + 8043(4a) - 4524(3a) + 630(2) - 6$
5754	$a_7 = 30(7a) + 684(7b) + 606(7c) + 504(7d) + 108(7e) + 240(7f) + 360(7g) + 288(7h) + 216(7i) + 720(7j) + 1104(7k) + 672(7l) + 384(7m) + 4623(7n) + 3564(7o) + 5832(7p) + 732(7q) + 792(7r) + 1728(7s) + 1(7t) + 54(7u) + 68(7v) + 132(7w) + 8(7x) + 72(7y) - 25376(6a) - 372(6b) - 3672(6c) - 1452(6d) - 3288(6e) - 2016(6f) - 19320(6g) - 15432(6h) - 2700(6i) - 3216(6j) - 108(6k) - 80(6o) + 49089(5a) + 7776(5b) + 2091(5c) + 34704(5d) - 38928(4a) - 10360(4b) - 1680(4c) + 11563(3a) - 756(2) + 1$

F.C.C. Susceptibility p-series

$$\chi^R = \sum_{n=0}^{4} a_{n+1} p^n$$

$$a_1 = 1$$

$$a_2 = 6(2) - 12$$

$$a_3 = 42(3a) + 8(3b) - 108(2) + 66$$

$$a_4 = 120(4j) + 24(4c) + 2(4d) + 3(4c) + 44(4b) + 282(4a) - 176(3b) - 996(3a) + 918(2) - 220$$

$$a_5 = 1902(5a) + 48(5b) + 9(5c) + 828(5d) + 6(EO) + 24(EP) + 24(EQ) + 72(ER) + 168(ES) + 240(ET) + 24(EU) + 72(EV) + 576(EX) + 96(EY) + 792(EZ) - 3312(4j) - 624(4c) - 48(4d) - 78(4c) - 1272(4b) - 8316(4a) + 1848(3b) + 11316(3a) - 4896(2) + 495.$$

[Mean cluster expansion!

(Sykes & Essam, PR 133 A P310)

$a_1 = 1$

$a_2 = 12$

$a_3 = 84$

$a_4 = 504$

$a_5 = 3012$

⋮]

Quadratic Susceptibility p-series

Mean cluster size series

1

4

12

24

52

108

224

412

$a_1 = 1$

$a_2 = 2(2) - 4$

$a_3 = 6(3a) - 12(2) + 6$

$a_4 = 14(4a) + 4(4b) + 1(4c) - 44(3a) + 30(2) - 4$

$a_5 = 34(5a) + 8(5b) + 1(5c) + 20(5d) - 8(4c) - 32(4b) - 124(4a) + 140(3a) - 40(2) + 1$

$a_6 = 82(6a) + 2(6b) + 16(6c) + 4(6d) + 12(6e) + 8(6f) + 52(6g) + 32(6h) + 4(6i) + 4(6j) - 192(5d) - 8(5c) - 72(5b) - 352(5a) + 28(4c) + 112(4b) + 490(4a) - 352(3a) + 30(2)$

$a_7 = 2(7a) + 12(7b) + 6(7c) + 16(7d) + 4(7e) + 16(7f) + 8(7g) + 8(7h) + 8(7i) + 40(7j) + 48(7k) + 32(7l) + 8(7m) + 198(7n) + 124(7o) + 168(7p) + 22(7q) + 16(7r) + 24(7s) - 972(6a) - 80(6b) - 168(6c) - 36(6d) - 120(6e) - 80(6f) - 576(6g) - 360(6h) - 40(6i) - 40(6j) + 828(5d) + 28(5c) + 288(5b) + 1656(5a) - 56(4c) - 224(4b) - 1136(4a) + 280(3) - 12(2)$

$a_8 = 2222t^7 + \frac{1}{1+t^4}\left[768t^8 + 216t^9 - 208t^{10} - 888t^{11}\right] + \frac{4}{1+2t^4+t^8}\left[-40t^8 - 32t^9 - 8t^{10} + 32t^{11} - 24t^{12} - 8t^{13} + 8t^{14} + 32t^{15}\right] - \frac{16}{1+t^8}\left[t^9 + t^{10} + t^{11} + t^{12} + t^{13} + t^{14} + t^{15}\right] - \frac{32}{1+2t^4+t^8}\left[2t^8 + 4t^9 + 7t^{10} + 5t^{11} + 2t^{12} + 4t^{13} + 4t^{14} + 3t^{15}\right] - \frac{1}{1+3t^4+2t^6+2t^8}\left[1280t^8 + 1504t^9 + 624t^{10} - 848t^{11} + 384t^{12} - 1120t^{13} - 304t^{14} - 1568t^{15}\right] + \frac{1}{1+2t^4+t^6}\left[736t^8 - 360t^9 - 1424t^{10} - 2624t^{11} - 784t^{12} - 1144t^{15}\right]$

Tetragonal Zircon Susceptibility p-series

$$a_1 = 1$$

$$a_2 = 4t$$

$$a_3 = 12t^2$$

$$a_4 = 36t^3$$

$$a_5 = 108t^4$$

$$a_6 = 324t^5 - \frac{24}{1+t^6}\left[\frac{t^7 - t^{12}}{1-t}\right]$$

$$a_7 = 948t^6 - \frac{96}{1+t^6}\left[\frac{t^8 - t^{13}}{1-t}\right]$$

$$a_8 = 2796t^7 - \frac{384}{1+t^6}\left[\frac{t^9 - t^{14}}{1-t}\right] - \frac{48}{1+t^8}\left[\frac{t^9 - t^{16}}{1-t}\right]$$

tanh series

$$\chi^R = \sum_{n=0} b_{n+1} t^n$$

$$b_1 = 1$$

$$b_2 = 4p$$

$$b_3 = 12p^2$$

$$b_4 = 36p^3$$

$$b_5 = 108p^4$$

$$b_6 = 324p^5$$

$$b_7 = 948p^6$$

$$b_8 = 2796p^7 - 24p^5$$

$\left(\frac{\beta J}{2}\right)$ series

$$\chi^R = \sum_{n=0} c_{n+1} \left(\frac{\beta J}{2}\right)^n$$

$$c_1 = 1$$

$$c_2 = 4p$$

$$c_3 = 12p^2$$

$$c_4 = 36p^3 - \frac{4}{3}p$$

$$c_5 = 108p^4 - 8p^2$$

$$c_6 = 324p^5 - 36p^3 + \frac{8}{15}p$$

$$c_7 = 948p^6 - 144p^4 + \frac{16}{5}p^2$$

APPENDIX II RESULTS FOR FCC, Q AND TZ LATTICES

Face-centred cubic lattice.

A five term series in p for this lattice was derived, one term longer than that derived by Rushbrooke and Morgan (1961). In Fig. 17 the sequence $\{u_n\}$ is plotted vs. $\frac{1}{n}$: it is seen to be rather irregular at higher temperatures. In Fig. 18 the sequence $\{v_n\}$ is plotted, and is seen to be smooth at all temperatures. The sequence $\{w_n\}$ exhibits similar behaviour. Extrapolation by methods 2, 4 and 6 is carried out, and the results of this for the phase boundary and $\gamma_1(T)$ shown in Figs. 19 and 20. The three methods give fairly consistent results for the phase boundary, in reasonable agreement with the accepted values for p_c^s and $kT_c(1)/J$ (see the table below). The results for the critical exponent are less consistent and less satisfactory: methods 4 and 6 indicate a reasonable seeming behaviour, while characteristically (for 3D lattice) overestimating $\gamma_1(T=0)$. Method 2, while again characteristically estimating $\gamma_1(T=0)$ well, indicates the trouble that is to come with longer series with its rightwards bump.

	Method 2	Method 4	Method 6	'Accepted'
p_c^s	.202	.177	.227	.195±.005*
$\gamma_1(T=0)$	1.83	2.24	2.08	$\frac{27}{16}$±.05*
$kT_c(1)/J$	4.886	5.23	4.98	4.897**
$\gamma_1(p=1)$	1.24	1.19	1.15	1.25[1]

* Sykes and Essam (1964

** Taken from Fisher (1967)

1 Domb and Sykes (1961b); Baker (1961)

The series is really too short for P.A.'s to provide useful estimates: however, the [1,3] P.A. provides results in surprisingly good agreement with ratio method estimates throughout the temperature range, as does the [2,2] P.A. for p bigger than above .35. Not surprisingly, perhaps, no complex pairs of poles are found.

The series has been extended by another two terms by Rapaport (1972b), and his results are discussed in Chapter 3. The method of analysis used in this paper is not very suitable for a series which displays oscillatory behaviour, being Method 1, which uses u_n and u_{n-1}. However, the type of phase boundary shown is confirmed, as is the rightward bend shown up by Method 2 in Fig. 20.

Quadratic lattice.

An eight term series for the plane square or quadratic lattice is derived, two more terms than previously known (Heap, 1964). The sequence $\{u_n\}$ vs. $\frac{1}{n}$ is seen to be

highly irregular at all but the lowest temperature (Fig. 21): most of this behaviour is lost in the sequences $\{v_n\}$ and $\{w_n\}$ (Fig. 22). Ratio analysis by methods 2, 4 and 6 is carried out on the series, and the results for the phase boundary are shown in Fig. 23: methods 4 and 6 yield satisfactory curves - in particular method 6 - but method 2 does not, particularly at low temperatures. This is not particularly surprising in such an irregular series. The results for the critical exponent (Fig. 24) are equally inconsistent: methods 4 and 6 yield curves of at least the expected shape, whereas method 2 greatly overestimates $\gamma_1(T=0)$.

	Method 2	Method 4	Method 6	'Accepted'
p_c^s	.803	.528	.618	.59±.01*
$\gamma_1(T=0)$	4.34	2.73	2.25	$\frac{19}{8}$±.05*
$kT_c(1)/J$	1.28	1.27	1.24	1.134 (Exact)
$\gamma_1(p=1)$	.97	1.67	1.11	1.75

* Sykes and Essam (1964)

The P.A.'s are equally inconsistent: [3,4] grossly underestimates p_c^s and $\gamma_1(T=0)$, while [4,3] has a complex pair at T=0. As the temperature is raised, the [3,4] results come into reasonable agreement with methods 4 and 6 at about p=.7, as do the [4,3] results after about p=.8.

The series is so oscillatory that conclusions about the behaviour of the critical index are hard to draw: however, method 6 appears to provide a reasonable estimate of the phase boundary. It is noteworthy that the transient

complex pole behaviour of 3D lattices' P.A.'s to the p-series is not seen here, even with quite a large series, and that no true "right-hand bump" is shown up by ratio methods for the critical index.

Tetragonal Zircon Lattice.

An eight term p-series is derived for this lattice, which has not previously been studied by ratio methods. This is an extremely open lattice, the first looped diagram having six atoms: even with eight terms, little of the lattice structure is sampled. The sequence $\{u_n\}$ is highly irregular, when plotted vs. $\frac{1}{n}$ (Fig. 25), but this behaviour is largely smoothed out in $\{v_n\}$ and $\{w_n\}$ (Fig. 26). Extrapolation by methods 2, 4 and 6 leads to the rather consistent results shown in Fig. 27 for the phase boundary, and to the results of Fig. 28 for the critical index.

	Method 2	Method 4	Method 6	'Accepted'
p_c^s	.468	.404	.471	
$\gamma_1(T=0)$	1.73	2.16	2.10	1.6875
$kT_c(1)/J$	1.36	1.39	1.33	
$\gamma_1(p=1)$	1.24	1.45	1.27	1.25

As usual with 3D lattices, methods 4 and 6 over-estimate the accepted values of $\frac{27}{16}$ for $\gamma_1(T=0)$, whereas method 2 is surprisingly close. The results for the critical index are rather close to what is naively

expected, a steady decrease from $\gamma_1(T=0)$ to $\gamma_1(p=1)$: this is probably because the series is short, in terms of the type of structure it samples.

At T=0, the [3,4] P.A. underestimates p_c^s and $\gamma_1(T=0)$, but is in reasonable agreement with ratio methods when $p \sim .5$: the [4,3] P.A. fails to estimate p_c^s at T=0, not because of complex pairs of poles. After about $p \sim .85$, both P.A.'s give reasonable estimates, right up to p=1. No complex pole pair behaviour is found. This is rather surprising, as other 3D lattice series of this length do have such behaviour, but is probably again due to the shortness of the series, as is the corresponding behaviour of $\gamma_1(T)$ ratio estimates.

Estimates of p_c^s and $kT_c(1)/J$ may be made from the series: methods 2 and 6 work best for the end points of the critical exponent, and agree quite closely for the phase boundary. Accordingly, the crude estimates

$$p_c^s = .47$$

$$kT_c(1)/J = 1.35$$

are made: the corresponding results from a 7 term series would be $p_c^s = .49$ and $kT_c(1)/J = 1.36$, and these perhaps indicate the sorts of uncertainty involved in the estimates, if taken in conjunction with the table.

Figure 17 The sequence {un} vs $\frac{1}{n}$.
for six different temperatures
FCC lattice! first term p-series
$x = T/T_c(0)$

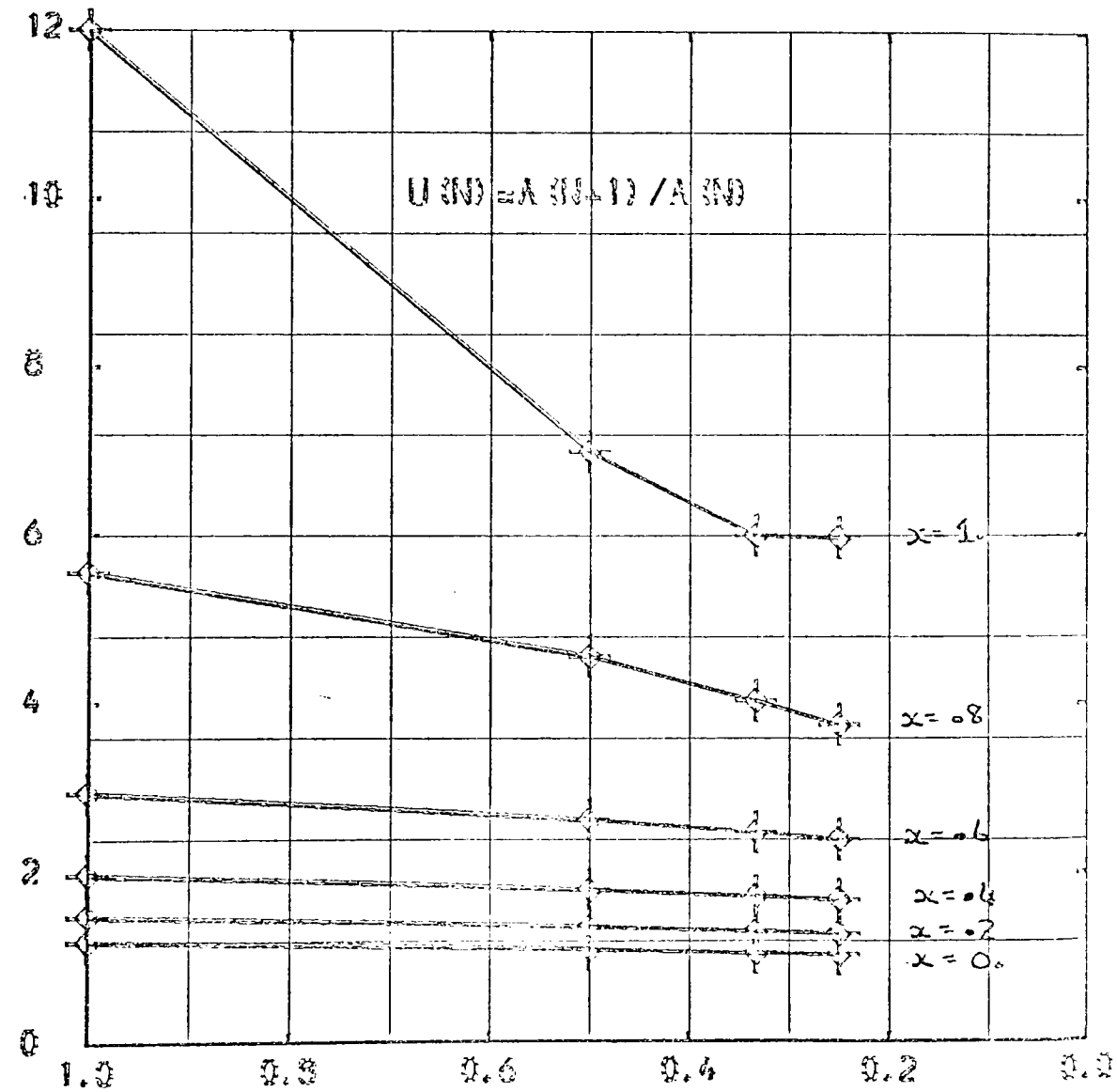


Figure 18 The sequence $\{v_n\}$ to $\frac{1}{n}$.
FCC lattice. 5 term p-series

$x' = T/T_c(1)$

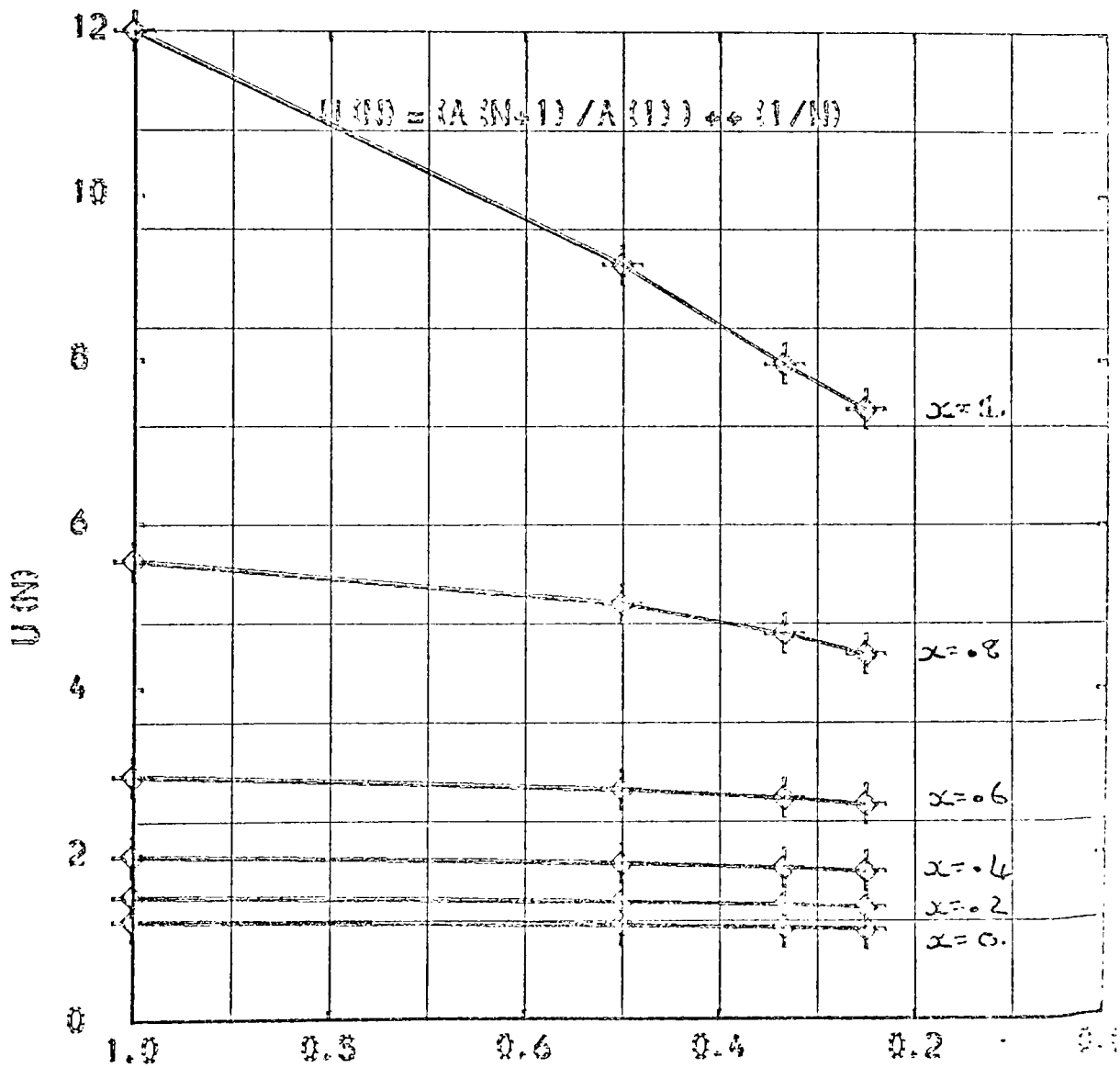


Figure 19 Phase Boundary by Ratio Methods

FCC lattice: 5 term p-series

(I) Method 2

(II) Method 4

(III) Method 6

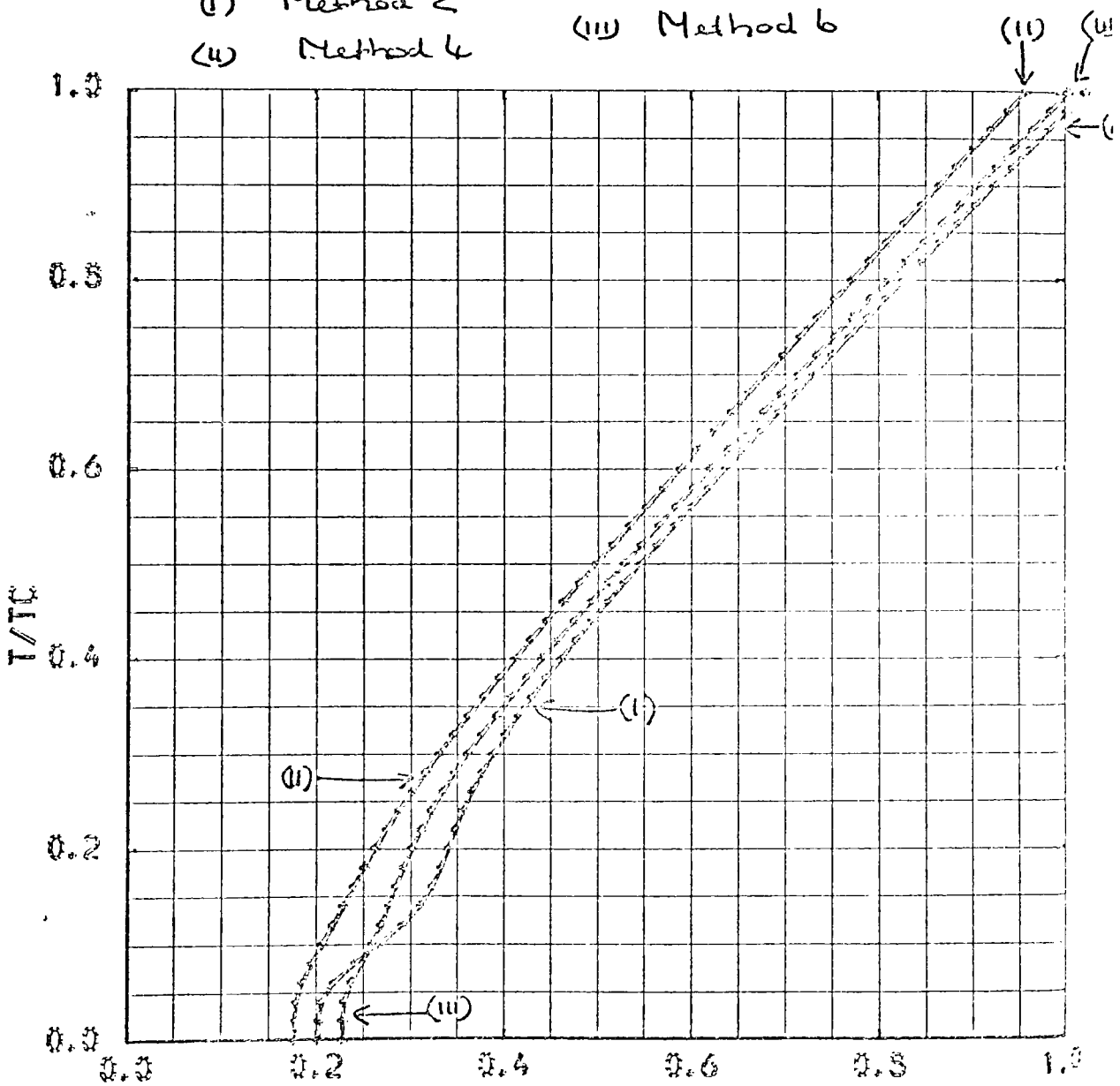


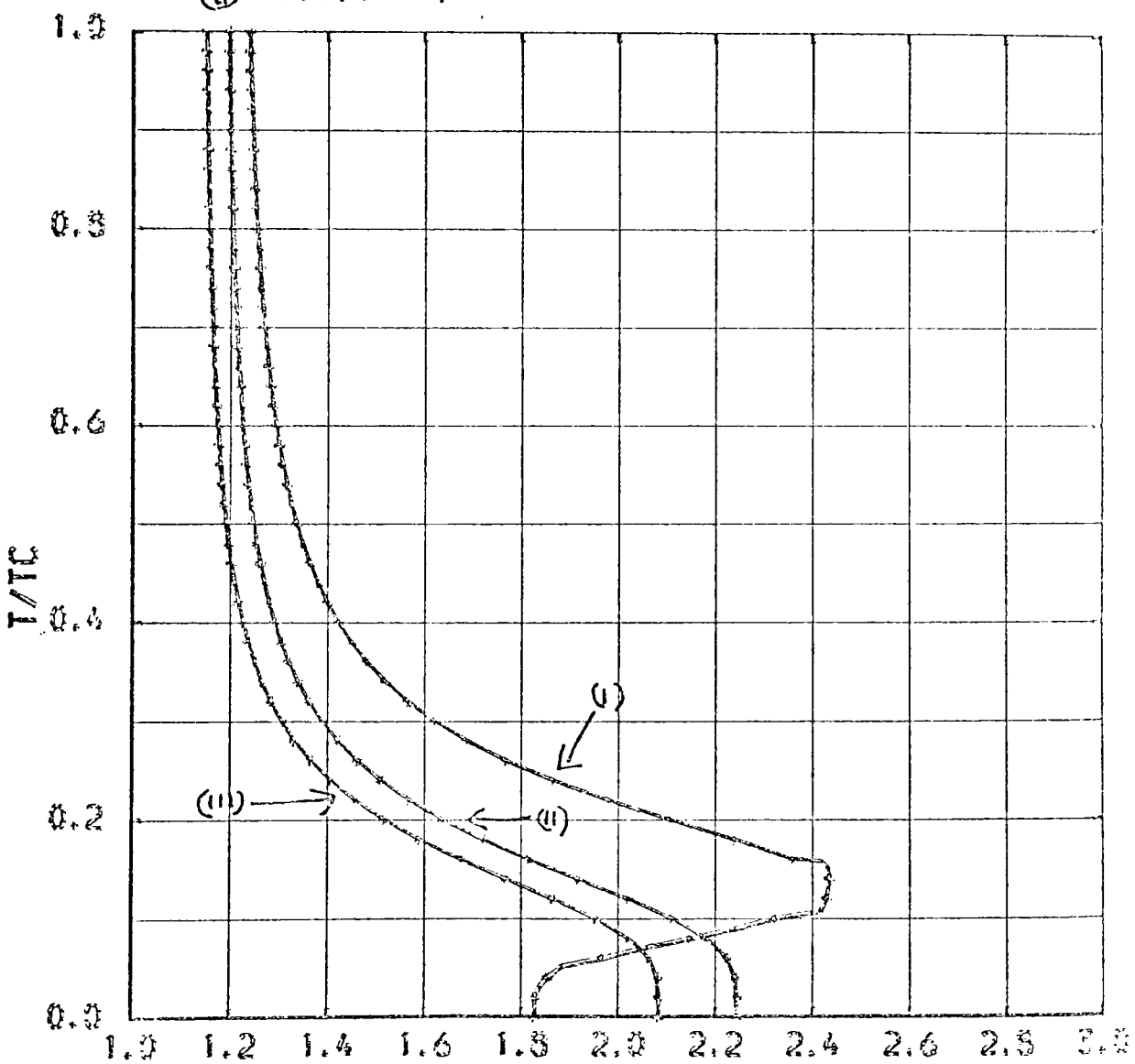
Figure 20 $\gamma(T)$ vs $T/T_c(1)$. by Ratio Method

FCC lattice : 5 term p-series

(I) Method 2

(II) Method 4

(III) Method 6



CRITICAL INDEX

Figure 21 The sequence $\{u_n\}$ vs $\frac{1}{n}$
Q lattice: 8 term p-series
$x = T/(T_c(1))$

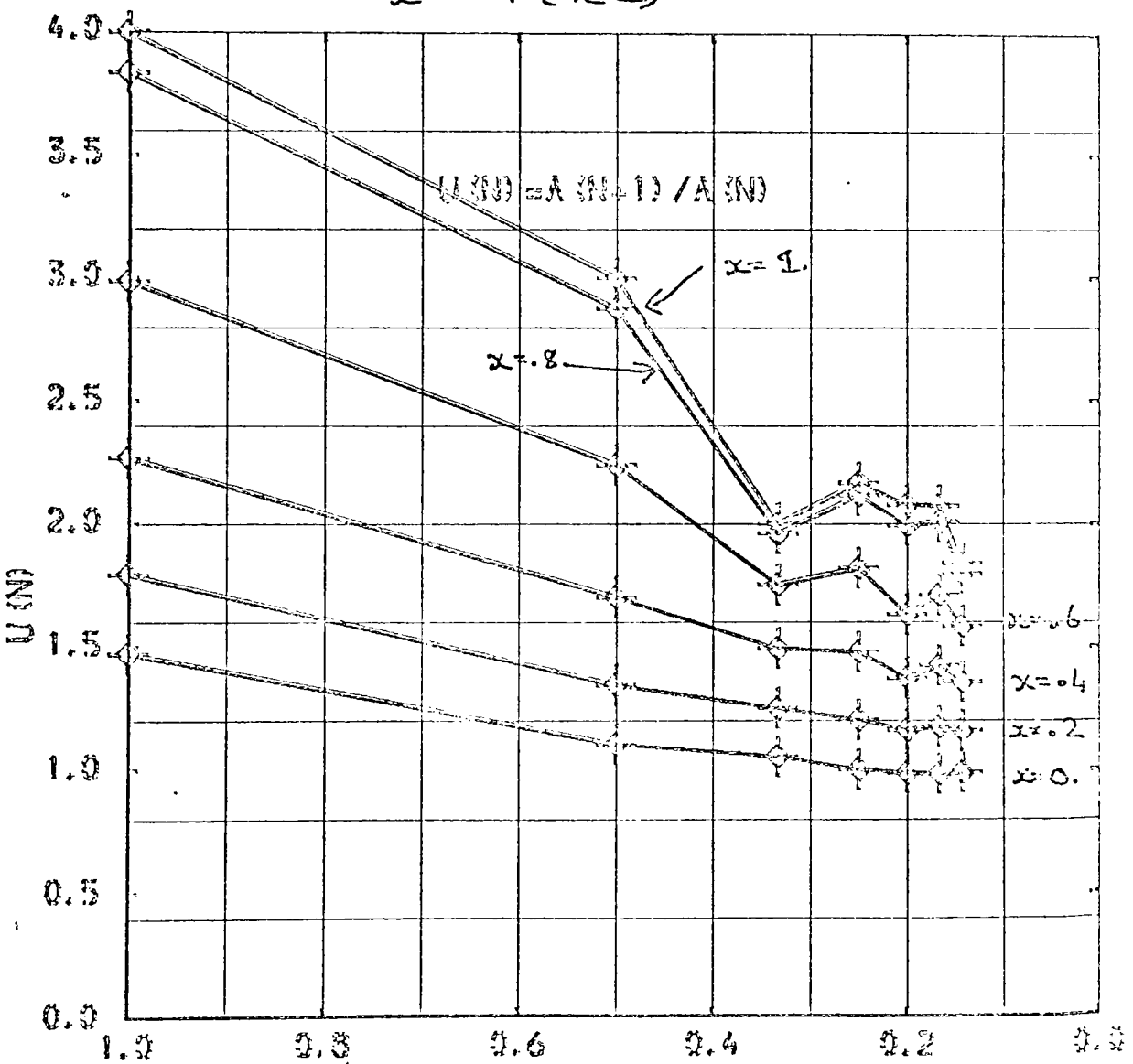


Figure 22 The sequence $\{w_n\}$ of the Gaussian lattice, 8 term p-series
$x = T/T_c(1)$

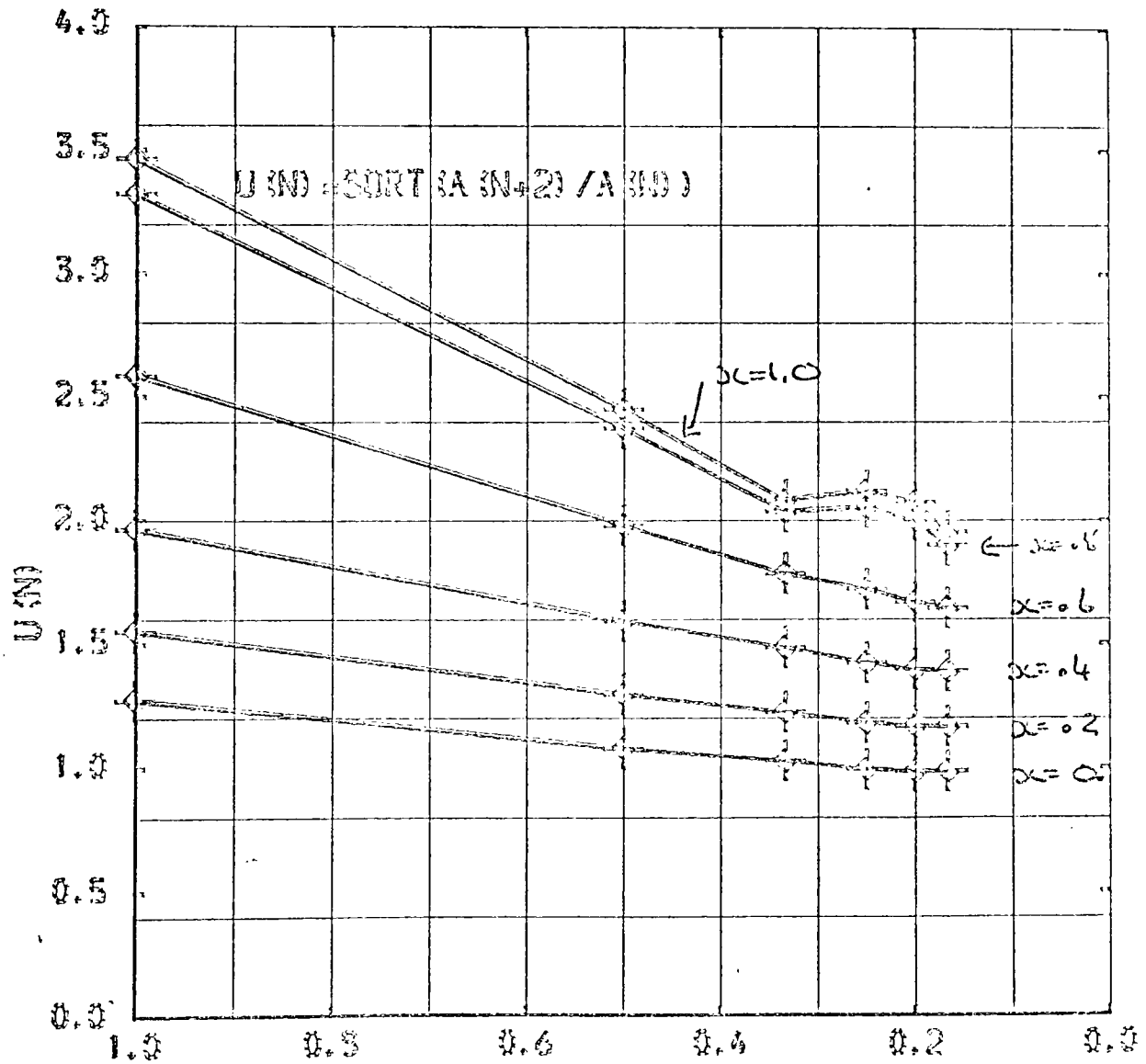


Figure 23 Phase Boundary by Ratio Method.

(a) Lattice: 8 term p-series

(i) Method 3

(ii) Method 4

(iii) Method 6

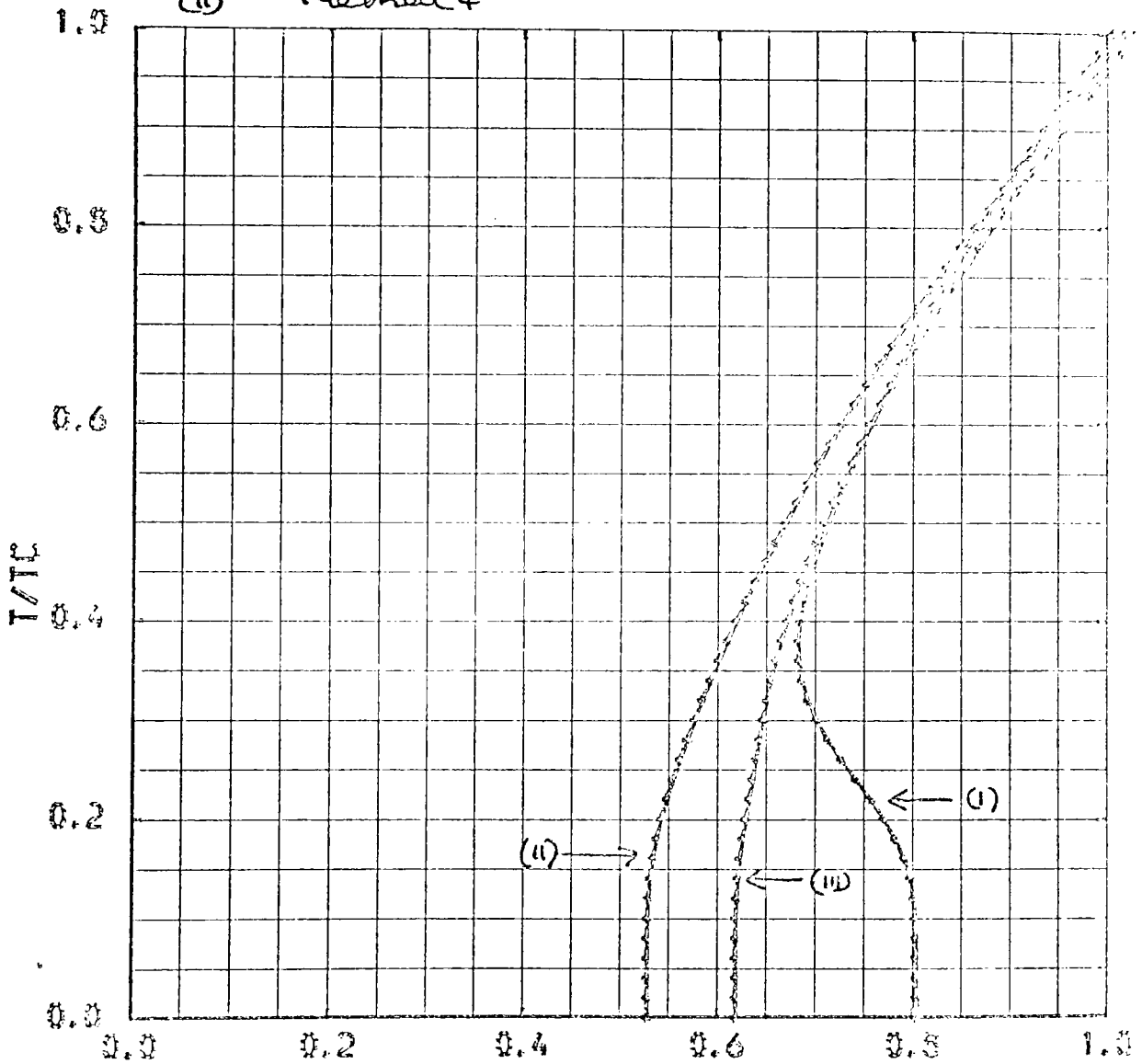
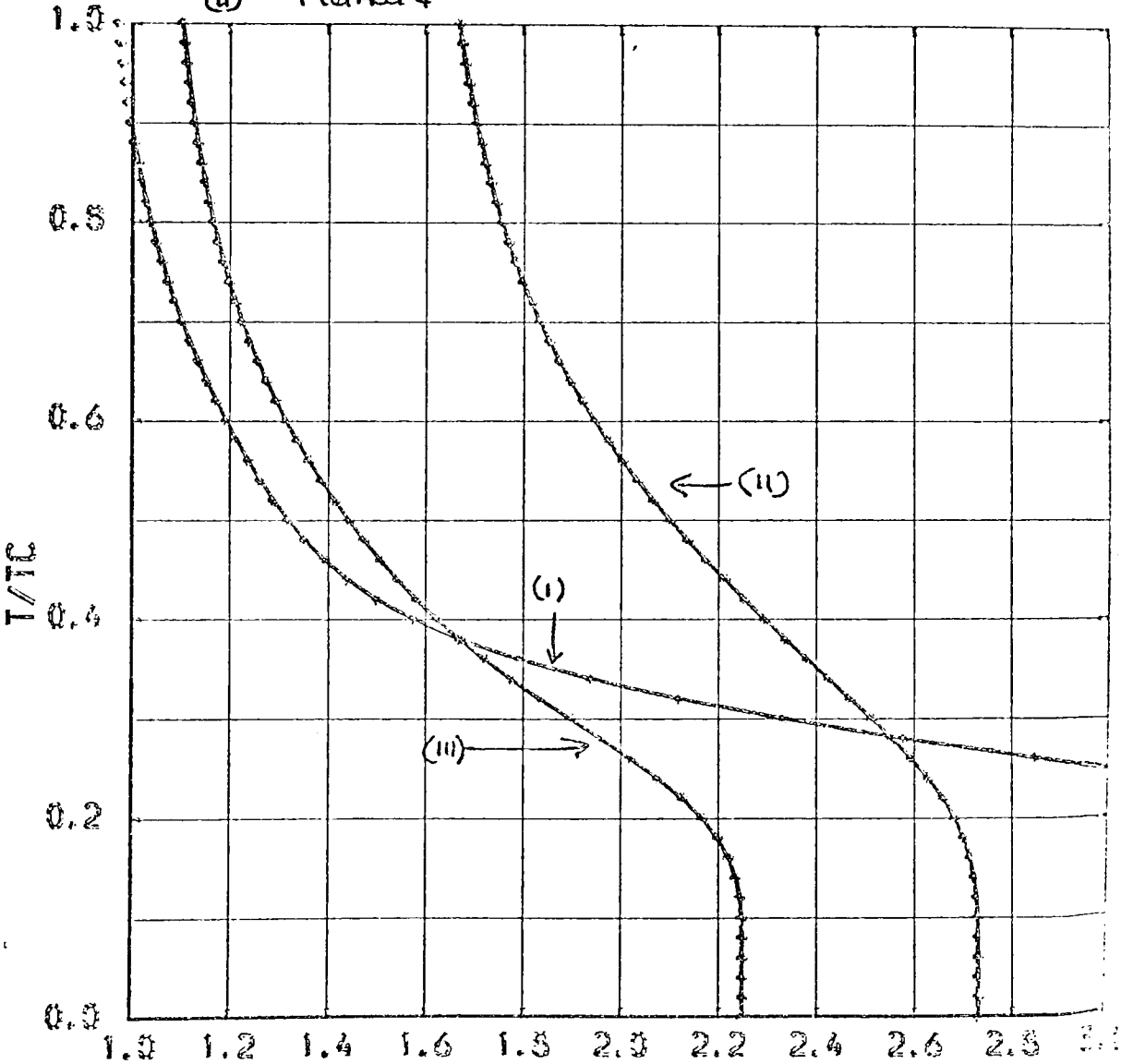


Figure 24 $\gamma(T)$ plotted against $T/T_c(b)$

Q lattice : 8 term p-series

(i) Method 2
(ii) Method 4
(iii) Method 6



CRITICAL INDEX

Figure 25 The sequence $\{u_n\}$ vs. $\frac{1}{n}$.

T-Z lattice: 8 term p-series

$x = T / T_c(1)$

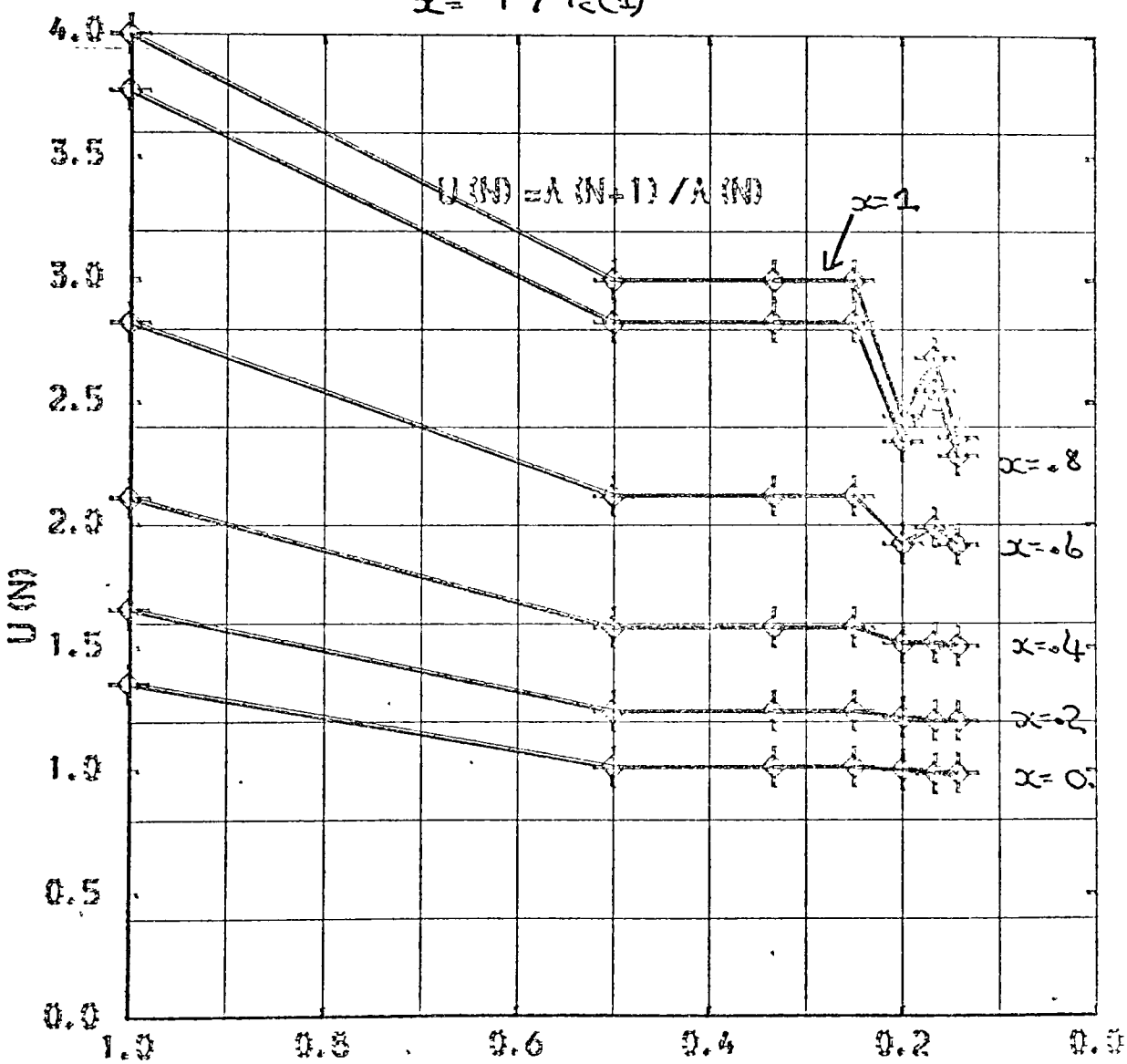


Figure 26. The sequence $\{w_n\}$ to π.

T-Z lattice : 8 term p-series

$x = T/T_c$ (1)

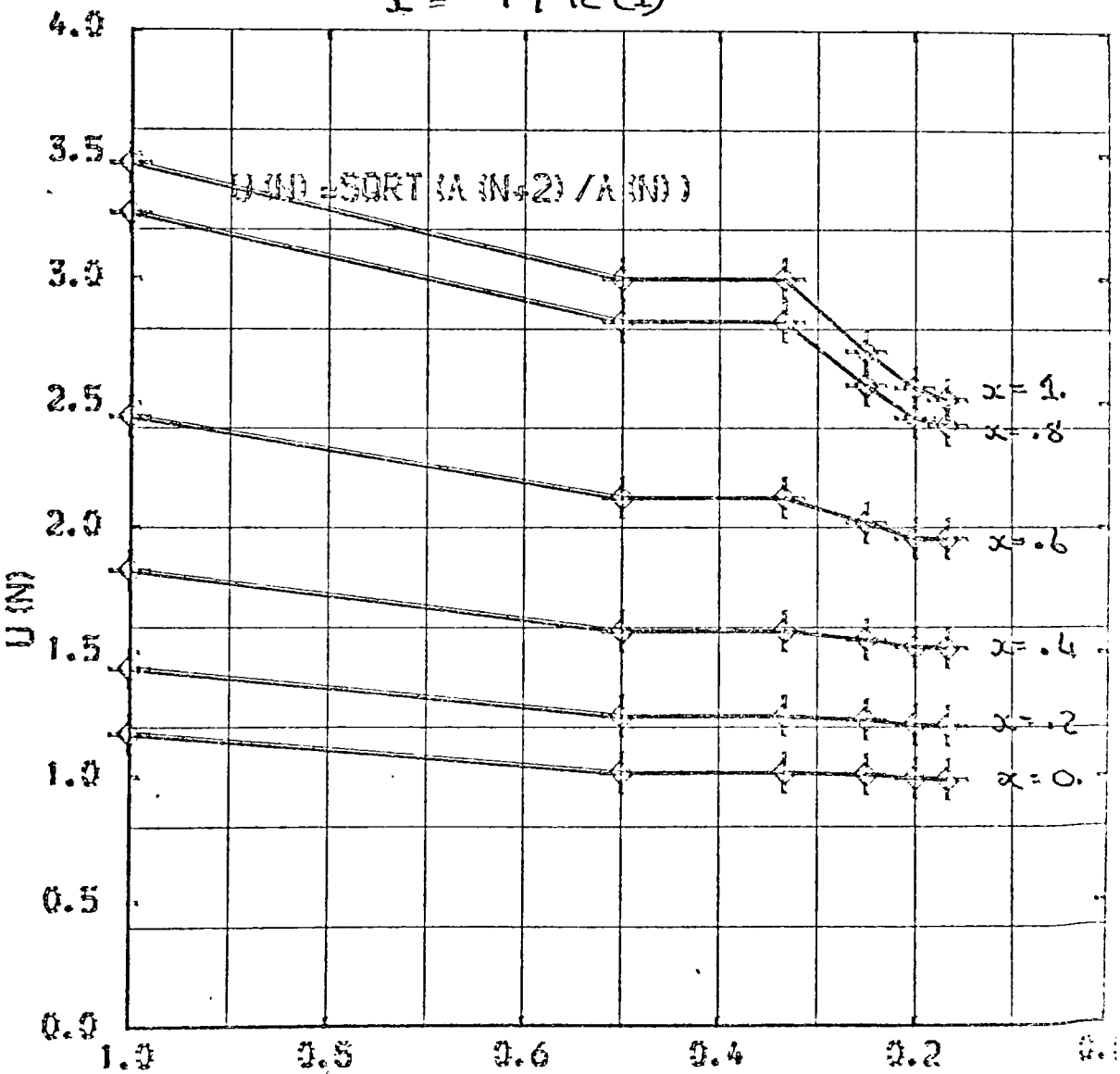


Figure 7 Phase Boundary by Ratio Methods.

TZ lattice : 8 term p-series

(I) Method 2 (II) Method 4 (III) Method 6

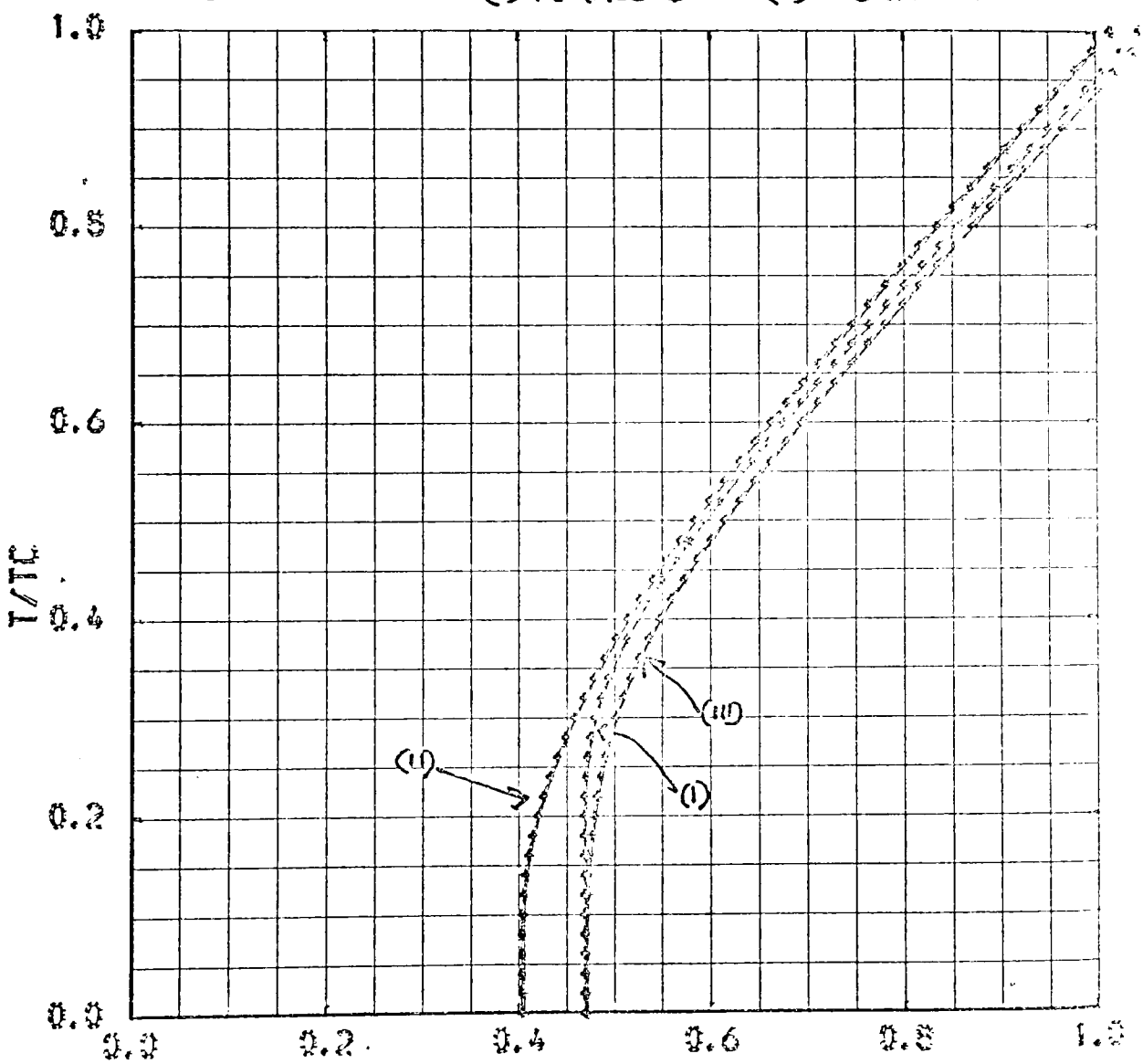
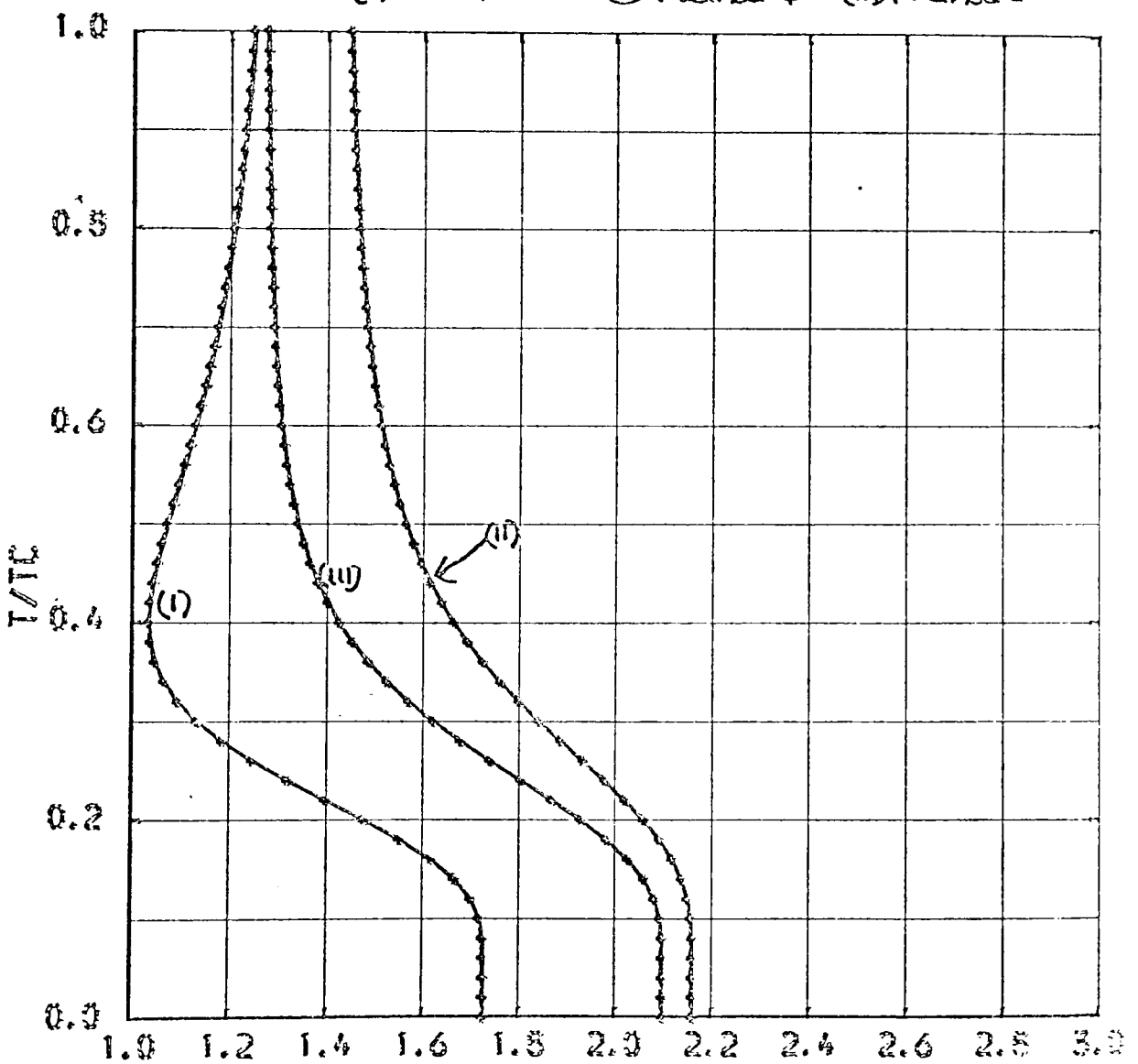


Figure 28 Critical Index vs Temperature

TZ lattice: 8 term p-series

TC = Tc(1). (I) Method 2 (II) Method 4 (III) Method 6



APPENDIX III

Confluent singularity analysis.

The behaviour of the plot $\{u_n\}$ vs. $\frac{1}{n}$ at low p for Rapaport's 11 term t-series for the FCC lattice (Fig. 16) is such that the ratio method, if naively applied, would give higher and higher values of $\gamma(p)$ as later terms in the series were used. One simple possibility for the form of χ that would not yield consistent results to ratio or Padé analysis is the following:

$$\chi = \frac{A_1}{(t_c-t)^{\gamma 1}} + \frac{A_2}{(t_c-t)^{\gamma 2}} + \frac{A_3}{(t_c-t)^{\gamma 3}} \ldots \qquad A.1$$

a series of N confluent singularities. In view of the failure of the simple hypothesis 3.2 it seems worth while analysing the series given by Rapaport by a method recently published by Baker and Hunter (1973), which will find the amplitudes and exponents associated with any number of confluent singularities given the location, $t_c(p)$.

χ is written as a function in $y = \ln(t_c-t)$:

$$\chi(y) = \sum_{i=1}^{N} A_i \, e^{-\gamma_i \ln(t_c-t)}$$

$$= \sum_{i=1}^{N} A_i \, e^{-\gamma_i y}$$

$$= \sum_{i=1}^{N} \sum_{k=0}^{\infty} A_i \frac{\gamma_i^k}{k!} y^k \qquad A.2$$

If the k^{th} term is now multiplied by k!, we obtain

$$F(y) = \sum_{i=1}^{N} \sum_{k=o}^{\infty} A_i \gamma_i^k y^k$$

$$= \sum_{i=1}^{N} \frac{A_i}{(1-y)^{\gamma_i}} \qquad A.3$$

This can be achieved by use of the identity:

$$\int_o^\infty e^{-t} t^n dt = n! \qquad A.4$$

$$F(y) = \int_o^\infty e^{-t} \chi(ty) dt \qquad A.5$$

Suitable Padé approximants to the transformed series $F(y)$ yield the A_i and γ_i if t_c is chosen correctly: if χ has exactly the form A.1, the [N-1,N] PA exactly represents $F(y)$. This procedure also represents functions such as:

$$G(x) = g(x)/(x_c-x)^\gamma$$

$$\text{and} \quad H(x) = \frac{A}{(x_c-x)^\gamma} + h(x)$$

quite accurately if $g(x)$ and $h(x)$ are analytic at $x = x_c$: the result is a series of confluent singularities like A.1, but with $N = \infty$ and each γ_i bigger by 1 than the preceding γ_{i-1}. This corresponds to Taylor series expansions of g and h about $x = x_c$.

Equally, if the procedure is applied to some function $K(x)$ which has no pole at $x = x_c$, the result is just a Taylor series expansion of $K(x)$ about x_c: the smallest γ_i is 1.

This is verified by applying the procedure to the

7-term p-series of Rapaport for the FCC lattice, choosing x_c to be various values near p_c^s. The results from the [2,3], [3,2], [2,4], [4,2] and [3,3] PA's for different values of temperature are tabulated below, for $p_c^s = .199$.

TABLE A1

	t=1.0	t=.9	t=.7	t=.5	t=.3	t=.11
[2,3]	1.207		1.000 1.999	1.001		
[3,2]	1.207		1.000 2.000	1.001		
[2,4]	1.204	1.0003 1.998 3.001	1.013 1.9944	1.000	.966	
[3,3]	1.210		.999 1.994	1.000		
[4,2]			1.013 1.995	1.000		

Where no entries for γ_i appear, the PA has either no poles or poles at points neither consistent with the other PA's nor with the Taylor series behaviour expected. Setting aside the results at t=1.0 for the moment (this is at T=0), it appears that as many as three terms in the Taylor series may be seen at low temperature, dropping to perhaps one at t=.3, near $T_c(1)$. It is rather surprising that the zero temperature result indicates such a low $\gamma(T=0)$, and that no Taylor series terms appear.

A straightforward analysis of $\frac{d}{dp}\ln\chi$ is not very successful for p_c^s or $\gamma(T=0)$, either, at T=0, although quite consistent results are obtained at higher temperature.

	$p_c(T)$	γ
[2,4]	.197	1.61
[3,3]	.194	1.49
[4,2]	.224	2.79
[3,4]	.186	1.32
[4,3]	Double pole	

However, γ is rather insensitive to the choice of x_c (as Baker and Hunter suggest): a 4% variation in x_c only produces 1% change in γ. It seems reasonable, therefore, to apply this procedure to the longer t-series and seek confluent singularities for a given value of p at x_c = some estimate of $t_c(p)$. Although this estimate will necessarily be crude, the results should indicate clearly whether we have one definite exponent γ with, perhaps, Taylor series terms of $(\gamma(p)+1)$, $(\gamma(p)+2)$ etc., or whether there are genuine confluent singularities.

Again, Rapaport's t-series is only tabulated for certain values of p: .3, .5, .7 and .9. Estimates of t_c at these values are made, assuming the sort of phase boundary shown in Appendix II: linear, with a slope of about 8/z, to rather below p=.3.

TABLE A2

$t_c(p)$ estimate	.46	.47	.48	.49	.50
[4,6]	-1.85	-1.87	-1.88	-1.9	-1.9
	-5.22	-4.83	-4.72	-4.7	-4.7
	-6.28	-7.24	-8.02	-8.78	-9.54
[4,7]		-1.87	-1.92	-1.95	-1.98
	-1.87	-5.05	-4.91	-4.89	-4.92
	complex pairs	-6.93	-7.69	-8.36	-8.99
[5,6]			-1.92	-1.95	-1.98
	-1.87	-1.89			
		-5.06	-4.92	-4.89	-4.92
	complex pairs	-6.93	-7.69	-8.36	-8.98
[6,5]	-2.02	-2.04	-2.07	-2.10	-2.14
	complex pairs	complex pair	-5.30	-5.17	-5.16
			-7.30	-8.05	-8.71
[7,4]	-1.99	-2.02			
			-2.05	-2.08	-2.12
		-5.73	-5.24	-5.14	-5.13
	complex pairs	-6.27	-7.36	-8.09	-8.34

The value t=.48 corresponds to $kT_c(p) = 1.92J$, and is estimated from Rapaport's phase boundary curve. The results in Table A2 are less than impressive, but seem to indicate a pole with γ_1 about 1.9, and 2 further poles with γ about 3 bigger each time. These stronger poles are more affected by change in the estimate for x_c than the

first pole, as may be verified by the table, so that their determination is much less certain. However, the first pole γ_1 is bigger than $\gamma(T=0)$, and this is the sort of γ behaviour that has been found from p-series. Also if the stronger poles are not spurious, they certainly are not the result of Taylor-series expansion terms.

The same procedure is applied to the series at p=.5, using an estimate for x_c of t=.246 ($kT_c(p)=3.98J$), and at p=.7 and p=.9. The values for the γ_i given by a few of the PA's are shown in Table A3.

TABLE A3

	p=.5 $t_c(p)=.246$	p=.7 $t_c(p)=.148$	p=.9 $t_c(p)=.111$	
[5,5]	-1.14	-1.24	-1.25	γ_1
	-2.78			
	complex pair (.22±.57i)	complex pair (.43±.16i)	-2.15	
[5,6]	-1.14	-1.30	-1.33	γ_1
	-2.78	complex pair	-1.84	
	complex pair (.24±.19i)	(.31±.17i)	complex pair (1.09±5.05i)	
[6,5]	-1.14	-1.30	-1.34	γ_1
	-2.78	(.31±.17i)	-1.83	
	complex pair (.24±.19i)	complex pair	- .079	

Again, the results are not terribly impressive. However, at high temperatures a value for γ near $\gamma(p=1)$ is obtained, and there are no sets of three evenly spaced

γ_i as were obtained in the p=.3 case. Also it is found that the [3,4] and [4,3] PA's reproduce γ_1 when p=.9, .7, and to a lesser extent, .5 much better than they do when p=.3. This should not be surprising in view of the curvature in u_n apparent at p=.3 (and just visible at p=.5), but gives one some confidence in the method's ability to estimate the leading exponent and to deal with the curvature. It is surprising that the method estimates γ_1 =-1.14 at p=.5 when γ(p=1) is -1.25. The γ_1 estimates are not very sensitive to change in x_c.

In any case, the results at p=.3 are markedly different from those at higher p: a regular sequence of poles differing in strengths by approximately 3 can be seen, which do not seem to result from Taylor series behaviour.

Such a sequence can be produced if the following form for χ is assumed:

$$\chi = \frac{A}{(|t-t_c|^a+\Delta^a)^{\gamma/a}} \qquad t \to t_c(p)$$

Δ is some arbitrary small p-dependent width, and the form is a sort of generalised Lorentzian. If Δ(p) becomes zero as p approaches 1, this form reduces to the hypothesis 3.2. Elsewhere, χ does not have a pole but is peaked about $t=t_c(p)$. If the analysis discussed is applied to such a function at $t_c(p)$, it can be expected to behave as follows:

$$\chi \sim \frac{A}{|t-t_c|^\gamma}\left[1 - \frac{\gamma}{a}\left(\frac{\Delta}{|t-t_c|}\right)^a + \frac{\gamma(\gamma+a)}{a^2}\left(\frac{\Delta}{|t-t_c|}\right)^{2a} \cdots\right.$$

- as a series of confluent singularities with strengths γ_i increasing regularly by a.

In general, a would be a function of p: hence, if such a form were assumed one might deduce

$$a(.37) = 3$$

$$a(.5) = 1.6$$

Estimates of the width Δ would be trebly biassed, in that they would rely on the use of a value γ to analyse the amplitudes of the PA's, which are much more sensitive to the choice of x_c than the poles: the amplitudes do seem to alternate in sign and decrease in modulus in an appropriate way, however.

Little stress should be placed on this tentative explanation: the main point is that the series appears to fit the confluent singularities hypothesis remarkably well, and displays markedly non-Taylor series behaviour. No conclusive interpretation of this behaviour is offered, but it is hoped that these results may encourage other workers to analyse long series more fully, and perhaps help to indicate some better hypothesis for the asymptotic behaviour of the susceptibility.

Appendix 4 Values of the Eight Line Diagrams Required for the TZ Series.

$.05 \leq G\beta \leq 1.25$; in steps of .05

0,000693	0,000692	0,000690	0,000688	0,000686	
0.000684	0,000681	0,000678	0,000675	0,000672	VIIA
0,000668	0,000664	0,000660	0,000643	0,000614	
0,000581	0,000546	0,000508	0,000469	0,000431	
0,000393	0,000357	0,000323	0,000291	0,000262	

0,010376	0,010357	0,010327	0,010290	0,010246	
0,010197	0,010141	0,010080	0,010013	0,009940	VIIB
0,009862	0,009779	0,009690	0,009345	0,008767	
0,008117	0,007425	0,006716	0,006015	0,005341	
0,004706	0,004120	0,003587	0,003109	0,002686	

0,020768	0,020722	0,020663	0,020593	0,020511	
0,020417	0,020312	0,020196	0,020069	0,019931	VII Y
0,019783	0,019625	0,019458	0,018801	0,017703	
0,016463	0,015137	0,013775	0,012422	0,011112	
0,009873	0,008721	0,007668	0,006717	0,005867	

0,001386	0,001383	0,001381	0,001377	0,001373	
0,001368	0,001363	0,001357	0,001351	0,001344	
0,001337	0,001329	0,001321	0,001288	0,001231	VIIZ
0,001167	0,001097	0,001022	0,000947	0,000871	
0,000798	0,000727	0,000660	0.000598	0,000540	

0,124518	0,124178	0,123748	0.123231	0,122627	
0,121939	0,121168	0,120316	0,119386	0,118380	
0,117301	0,116152	0.114936	0,110197	0,102354	VIIXX
0,093648	0,084512	0,075330	0,066419	0,058013	
0,050269	0,043273	0,037055	0,031604	0,026875	

0,010379	0,010359	0,010330	0,010294	0,010252	
0,010204	0,010150	0,010090	0,010025	0,009955	
0,009879	0,009798	0,009712	0,009376	0,008815	VIIC
0,008182	0,007505	0,006811	0,006123	0,005458	
0,004831	0,004249	0,003717	0,003239	0,002813	

0,010413	0,010365	0,010332	0,010295	0,010253	
0,010206	0,010153	0,010094	0,010029	0,009959	
0,009884	0,009804	0,009720	0,009387	0,008831	VIID
0,008203	0,007532	0,006844	0,006160	0,005499	
0,004874	0,004294	0,003763	0,003285	0,002858	

0.027675	0,027619	0,027538	0.027439	0,027323	
0.027192	0,027043	0,026880	0.026701	0,026507	
0,026299	0,026076	0,025841	0.024919	0,023378	VIIF
0,021645	0,019797	0,017907	0.016037	0,014257	
0,012542	0,010977	0,009555	0,008280	0,007148	

0,062273	0,062074	0,061846	0,061575	0,061259	
0,060898	0,060496	0,060050	0,059564	0,059039	
0,058475	0,057875	0,057241	0,054770	0,050690	VIIG
0,046175	0,041454	0,036729	0,032166	0,027884	
0,023964	0,020444	0,017339	0,014636	0,012310	

0,062483	0,062120	0,061874	0,061606	0,061301	
0,060952	0,060563	0,060132	0,059662	0,059154	
0,058609	0,058028	0,057414	0,055019	0,051058	VIIH
0,046664	0,042056	0,037428	0,032940	0,028711	
0,024820	0,021309	0,018193	0,015465	0,013103	

0,082958	0,082742	0,082438	0,082068	0,081636	
0,081144	0,080593	0,079985	0,079321	0,078604	
0,077835	0,077016	0,076150	0,072781	0,067224	VII I
0,061088	0,054688	0,048301	0,042152	0,036402	
0,031157	0,026468	0,022348	0,018777	0,015719	

0.062233	0.062058	0.061829	0,061551	0,061227	
0,060858	0,060445	0,059989	0,059491	0,058953	
0,058376	0,057762	0,057112	0,054585	0,050417	VII J
0,045814	0,041013	0,036222	0,031608	0,027294	
0,023359	0,019841	0,016749	0,014071	0,011777	

0,062300	0,062078	0,061847	0,061574	0,061259	
0,060899	0,060496	0,060050	0,059565	0,059039	
0,058476	0,057876	0,057242	0,054772	0,050692	VII K
0,046179	0,041461	0,036740	0,032181	0,027904	
0,023988	0,020473	0,017372	0,014672	0,012349	

0,248788	0,247939	0,246871	0,245577	0,244072	
0,242357	0,240439	0,238326	0,236020	0,233553	
0,230871	0,228044	0,225058	0,213501	0,194650	VII L
0,174154	0,153159	0,132630	0,113301	0,095659	
0,079966	0,066302	0,054614	0,044760	0,036551	

0,497112	0,495252	0,492779	0,489797	0,486328	
0,482384	0,477978	0,473126	0,467845	0,462156	
0,456078	0,449631	0,442840	0,416684	0,374510	VII M
0,329379	0,284009	0,240581	0,200639	0,165093	
0,134310	0,108252	0,086602	0,068886	0,054568	

0,994610	0,990805	0,986010	0,980244	0,973529	
0,965888	0,957351	0,947947	0,937710	0,926677	
0,914885	0,902375	0,889189	0,838355	0,756201	VII N
0,667996	0,578969	0,493361	0,414209	0,343353	
0,281598	0,228952	0,184881	0,148529	0,118896	

0,124506	0,124156	0,123715	0,123184	0,122564	
0,121858	0,121067	0,120193	0,119239	0,118208	
0,117102	0,115925	0,114678	0,109826	0,101806	VII X
0,092924	0,083626	0,074308	0,065293	0,056820	
0,049043	0,042046	0,035854	0,030449	0,025782	

REFERENCES

Baker, G.A. Jr. 1961 Phys.Rev. 124 P.768

Baker, G.A. Jr. & Hunter D.L. 1973 Phys.Rev. B. 7 P.3377

Behringer R.E. 1957 J.Chem.Phys. 26 P.1506

Block C. & De Dominicis C. 1958 Nucl.Phys. 7 P.449

Brout R. 1959 Phys.Rev. 115 P.824

Domb C. 1960 Adv.Phys. 9 P.149

Domb C. & Sykes M.F. 1961(a) Phys.Rev. 122 P.77

Domb C. & Sykes M.F. 1961(b) J.Math.Phys. 2 P.63

Elliott,R.J., Heap,B.R., Morgan,D.J. & Rushbrooke, G.S. 1960 Phys.Rev.Letters 5 P.366

Elliott,R.J. & Heap, B.R. 1962 Proc.Roy.Soc.A. 265 P.264

Elliott, R.J. 1963 Clarendon Lab. Report 128/63

Elliott, R.J. & Wood, C. 1971 J.Phys.C. 4 P.2359

Elliott,R.J.,Harley,R.T.,Hayes,W., & Smith,S.R.P. 1972 Proc.Roy.Soc.A. 328 P.217

Essam, J.W. & Garelick, H. 1962 Proc.Phys.Soc. 92 P.136

Essam, J.W. 1972 "Phase Transitions & Critical Phenomena" vol.2. Editors G.Domb & M.S.Green (London & New York, Academic Press) P.197

Fisher, M.E. 1967 Rep.Prog.Phys. 30 P.615

De Gennes, P.G. 1963 Sol.State Commun. 1 P.132

Griffiths,R.B. 1969 Phys.Rev.Letters 23 P.17

Heap, B.R. 1963 Proc.Phys.Soc. 82 P.252

Hunter,D.L. & Baker, G.A. Jr. 1973 Phys.Rev.B. 7 P.3346

Kadanoff, L.P. et al. Rev.Mod.Phys. 39 P.395

Kasteleijn, P.W. & van Kranendonk, J. 1956 Physica 22 P.367

van Kranendonk, J. & Kasteleijn, P.W. 1956 Physica 22 P.317

Matsubara, T. 1955 Prog.Theor.Phys. 14 P.351

McCoy, B.M. & Wu, T.T. 1968 Phys.Rev. 176 P.631

McCoy, B.M. 1970 Phys.Rev. B. 2 P.2795

Moore, M.A., Jasnow, D. & Wortis, M. 1969 Phys.Rev.Letters 22 P.940

Morgan, D.J. & Rushbrooke, G.S. 1961 Mol.Phys. 4 P.291

Nagle, J.F. & Temperley,H.N.V. 1968 J.Math.Phys. 9 P.1020

Oguchi, T. 1931 J.Phys.Soc.Japan 6 P.31

Oguchi, T. 1969 J.Phys.Soc.Japan 26 P.580

Pfeuty, P. & Elliott, R.J. 1971 J.Phys.C. 4 P.2370

Rapaport, D.C. 1972(a) J.Phys.C. 5 P.1830

Rapaport, D.C. 1972(b) J.Phys.C. 5 P.2813

Rushbrooke, G.S. & Wood, C. 1955 Proc.Phys.Soc.A. 68 P.1161

Rushbrooke, G.S. & Morgan, D.J. 1961 Mol.Phys. 4 P.1

Rushbrooke, G.S., Muse, R.A., Stephenson, R.L. & Pirnie, K. 1972 J.Phys. C. 5 P.3371

Sandercock, J.R., Palmer, S.B., Elliott, R.J., Hayes, W., Smith, S.R.P. and Young, A.P. J.Phys.C. 5 P.3126

Sayetat F., Boucherle J.X., Belachowsky M., Kalell A., Tcheou F. & Fuess H. 1971 Phys.Lett. 34a P.361

Shante, V.K.S. & Kirkpatrick S. 1971 Adv.Phys. 20 P.325

Stanley H.E. 1971 "Introduction to Phase Transitions and Critical Phenomena" O.U.P.

Sykes M.F. & Essam J.W. 1964 Phys.Rev. 133A P.310

Sykes M.F. 1961 J.Math.Phys. 2 P.52

Syozi I. & Miyazima S. 1966 Prog.Theor.Phys. 36 P.1083

Wojtowicz P.J. 1963 Mol.Phys. 6 P.157

Wood C. 1969 D.Phil. Thesis, Oxford University

PART 2

Moments Calculation for Two-Magnon Raman Scattering in Dilute Heisenberg Antiferromagnets

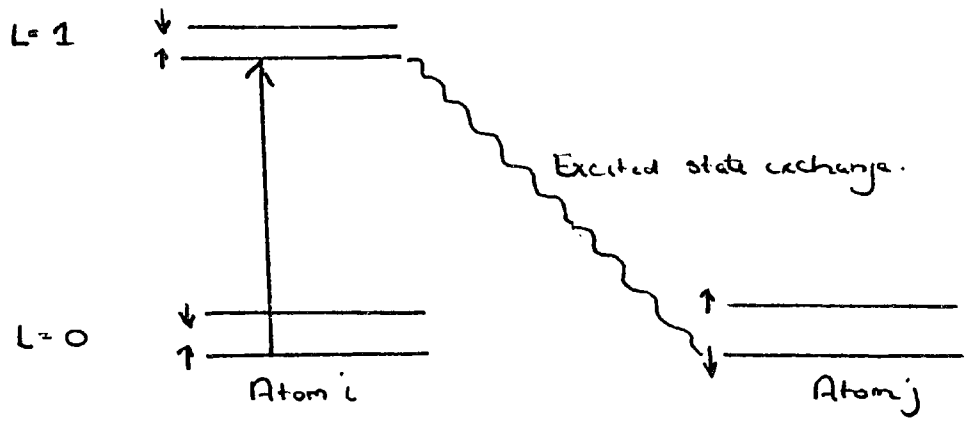
CHAPTER 1

§1.1 Introduction to Two-Magnon Raman Scattering in Antiferromagnets

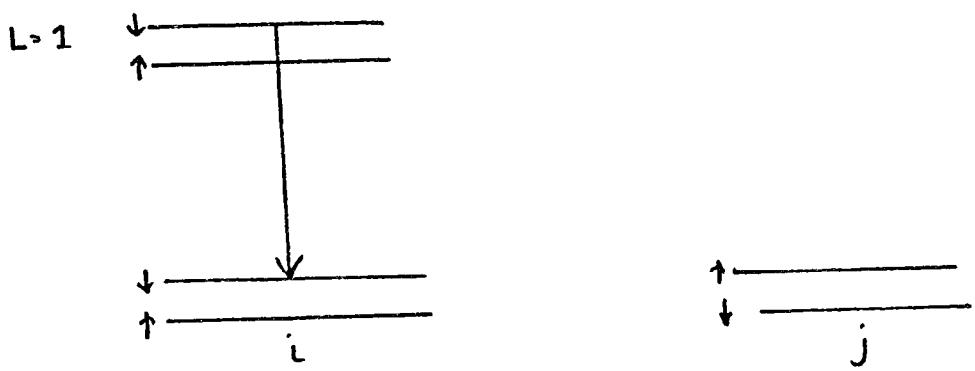
After suggestions by Bass and Kaganov (1960) and Elliott and Loudon (1963) of mechanisms whereby light could be scattered by spinwaves, experiments by Fleury and various collaborators established that Raman scattering by magnons in antiferromagnets did indeed take place (Fleury et al,1966, 1967, 1968; Fleury, 1969). In particular, they discovered, in addition to the scattering by single magnons due to the spin-orbit coupling mechanism of Elliott and Loudon, a relatively strong two-magnon scattering in two sublattice antiferromagnets such as MnF_2 and FeF_2. At low temperatures the scattering profile contained a well-defined peak at about twice the zero-boundary magnon energy: as the temperature was raised, the peak widened and dropped in energy. In some systems a broad peak centred at zero energy shift is seen well above the Néel temperature, T_N, (e.g. Fleury, 1969; Brya et al, 1972).

Some two-magnon scattering is allowed by the one magnon mechanism mentioned: Fleury and Loudon (1968) pointed out that such a second order process occurs with a weight several orders of magnitude smaller than that of the one-magnon scattering, and suggested an excited state exchange mechanism which is different in kind from the spin-orbit mechanism, and so need not occur more weakly. The nature of this mechanism may be naively indicated as follows: consider

two spin $\frac{1}{2}$ magnetic atoms i and j, coupled by some exchange constant, and allow a photon to be absorbed by atom i in its ground state,



so that the transition from $|L=0, s=\frac{1}{2}>$ to $|L=1, s=\frac{1}{2}>$ takes place. Excited state exchange flips the spins on sites i and j.



Now, the decay from $|L=1, s=-\frac{1}{2}>$ to $|L=0, s=\frac{-1}{2}>$ takes place, leaving the spins on sites i and j flipped, and a photon is emitted. Fleury and Loudon conclude that this mechanism is only strong for antiferromagnets, and determine the interaction Hamiltonian from considerations of crystal symmetry as:

$$H' = \sum_{<ij>} [A(E_1^x E_2^x + E_1^y E_2^y) + B(E_1^z E_2^z) + C(E_1^x E_2^y + E_1^y E_2^x)\delta_{ij}^x \delta_{ij}^y$$

$$+ D[(E_1^y E_2^z + E_1^z E_2^y)\delta_{ij}^y \delta_{ij}^z + (E_1^x E_2^z + E_1^z E_2^x)\delta_{ij}^x \delta_{ij}^z]$$

$$+ F[(E_1^y E_2^z - E_1^z E_2^y)\delta_{ij}^y \delta_{ij}^z - (E_1^z E_2^x - E_1^x E_2^z)\delta_{ij}^x \delta_{ij}^z]]$$

$$(\underline{S}_i \cdot \underline{S}_j + (\gamma - 1) S_i^z S_j^z) \qquad - 1.1$$

for rutile structure antiferromagnets, where the sum is over the pairs <ij> coupled by antiferromagnetic exchange, and the constants A, B, C, D, and F are undetermined coupling constants deriving from the ground state-excited state exchange. The factors δ_{ij}^x are phase factors, defined such that δ_{ij}^x is unity with the sign of the x component of the vector joining atoms i and j. The γ factor permits anisotropy allowed by the symmetry of the lattice, since the z direction is taken to coincide with the c-axis of the unit cell, and the incident and outgoing light has electric vectors $\underline{E}_1$ and $\underline{E}_2$.

The tetragonal antiferromagnet of particular interest in this work is MnF_2, for which the asymmetric term F is found experimentally to be negligible. In MnF_2, the exchange constant between a unit-cell centre atom and the eight atoms at the corners of the unit cell is antiferromagnetic, and about five times bigger than the ferromagnetic interaction between nearest neighbours. In addition, the anisotropy factor γ is set equal to unity, for computational

convenience, as the anisotropy is thought to be small. Accordingly, if the scattering geometry (xy) is considered, the interaction Hamiltonian

$$H_I = \sum_{<ij>} C E_1^x E_2^y \, \underline{S}_i \underline{S}_j \, \delta_{ij}^x \delta_{ij}^y \qquad - 1.2$$

is obtained in this limit, and is rewritten as

$$H_I = B' \sum_{\underline{R},\underline{\delta}} \underline{S}_R \cdot \underline{S}_{\underline{R}+\underline{\delta}} \, \delta_{\underline{\delta}}^x \delta_{\underline{\delta}}^y \qquad - 1.3$$

where $\underline{\delta}$ is any vector joining the atom at $\underline{R}$ to its eight next nearest neighbours.

Another system considered in this work is the cubic antiferromagnet $RbMnF_3$: from similar considerations of crystal symmetry Elliott and Thorpe (1969) have determined the interaction Hamiltonian for two magnon Raman scattering, assuming that only the term in $\underline{S}_R \cdot \underline{S}_{\underline{R}+\underline{\delta}}$ is larger.

$$H_I = \sum_{\underline{R},\underline{\delta}} \{B_3(\underline{E}_1 \cdot \hat{\underline{\delta}})(\underline{E}_2 \cdot \hat{\underline{\delta}}) + (B_1 - 1/3 B_3)(\underline{E}_1 \cdot \underline{E}_2)\} \underline{S}_R \cdot \underline{S}_{\underline{R}+\underline{\delta}} \qquad - 1.4$$

Hence B_3 and B_1 are the coupling constants correponding to polarisation combinations transforming like Γ_1^+ and Γ_3^+ respectively. Calculations by Elliott and Thorpe indicate that the Γ_1^+ type scattering should not be appreciable, and this is confirmed in experiments by Fleury (1968). For (xx) scattering geometry, then, 1.4 reduces to

$$H_I = B' \{ \sum_{\substack{\underline{R} \\ \underline{\delta}', = \pm x}} \underline{S}_R \cdot \underline{S}_{\underline{R}+\underline{\delta}} - 1/3 \sum_{\underline{R},\underline{\delta}'} \underline{S}_R \cdot \underline{S}_{\underline{R}+\underline{\delta}} \} \qquad - 1.5$$

where in the first sum only the magnetic atom at $\underline{R}$ and its

two neighbours in the x direction are considered.

The Hamiltonian H_o describing the spin state of the system MnF_2 is thought to be, to a good approximation, the Heisenberg interaction between Mn ions with S = 5/2. There is a small anisotropic dipole-dipole type interaction, and negligible single ion anisotropy: these are neglected in this work. The antiferromagnetic exchange between an ion and its eight neighbours (a, a, L) is the largest: five times as great as the ferromagnetic exchange with the neighbours (O, O, L) (Nicotin et al, 1969).

$RbMnF_3$ is also thought to be well explained by such a Hamiltonian, now with six nearest neighbours. In NiF_2, the eight neighbour Heisenberg Hamiltonian with spin 1 should provide an adequate explanation, although single ion anisotropy is no longer negligible, and some spin canting must be disregarded as well as the dipole-dipole interaction.

The interaction Hamiltonians used create two magnons simultaneously on neighbouring sites: since the interaction has transitional invariance, these magnons must be of equal and opposite wavevector $\underline{k}$ and $-\underline{k}$. This is a reasonable model, as the photon scattered has very small wavevector, and so can give little net momentum to the pair created. The energy of the magnon pairs is $2E(\underline{k})$, and the scattering intensity at some frequency will depend on the density of states of such pairs (similar to the one

magnon density of states, but with a doubled frequency scale), and the coupling constants A, B, C etc., which Loudon has shown are in general smooth in frequency (Loudon, 1968). Accordingly, features in the Raman scattering spectrum must come from critical points in the density of states, or from resonances in the density of states due to magnon interactions: the former cannot explain the well defined peak at about twice the zone boundary magnon energy seen in experiments.

If the Ising model is considered, with an exact Néel grand state, and next neighbour interactions, so that:

$$H = 2I \sum_{<ij>} S_i^z . S_j^z \qquad - 1.6$$

then pairs of magnons created on neighbouring sites have energy 4SzI-2I, where z is the coordination number: pairs of magnons not on neighbouring sites have an energy higher by 2I. The bound pair state is that most strongly created by the scattering. If isotropic exchange is now considered, the two magnon spectrum is expected to broaden into a band: if this band covers the bound pair state, a broadened and shifted resonance is expected at about the bound pair energy, and this explains the experimental results well qualitatively.

§1.2 Theoretical Approaches

The Raman scattering intensity at frequency shift

ω is proportional to

$$I(\omega) = \int_{-\infty}^{+\infty} e^{-i\omega t} \langle H_I(t) H_I(0) \rangle dt \qquad - 1.7$$

where $H_I(t) = e^{iH_o t/h} H_I e^{-iH_o t/h}$,

H_o being the system Hamiltonian, and the triangular brackets indicating a thermal average.

Accordingly a scattering profile may be calculated in terms of time-dependent four spin Green functions: such a calculation was carried out at zero temperature by Elliott and Thorpe (Elliott et al, 1968; Elliott and Thorpe, 1969), allowance for magnon-magnon interactions being made, and good agreement with experimental results was obtained. Various attempts have been made to extend this Green function approach to higher temperature by various techniques, without a great deal of success (for example, Solyom, 1971; Cottam, 1972; Davies, 1972). An alternative approach is that of Buchanan et al (1972), who calculate line shapes for the magnon-scattering in a dilute Ising antiferromagnet at zero temperature by considering the response of a pair of magnetic atoms for each possible set of magnetic and non-magnetic neighbours: the agreement with experiment on $(Mn,Zn)F_2$ reported in this paper is quite good.

However, the calculation of frequency moments of the scattering presents a simple framework in which to work where only static correlations are needed. If the

integrated intensity I is considered,

$$I = \int_o^\infty I(\omega)d\omega$$

$$= \langle H_I(t)H_I(o)\rangle_{t=o}$$

$$= \langle H_I H_I\rangle \qquad - 1.8$$

and higher moments $\langle\omega^n\rangle$ may be found from

$$\langle\omega^n\rangle = \int\omega^n\, I(\omega)d\omega.$$

On integrating by parts n times,

$$\langle\omega^n\rangle = (-i)^n \left\langle \left(\frac{d^n}{dt^n} H_I(t)\right)H_I(o)\right\rangle_{t=o} \qquad - 1.9$$

Expressions 1.8 and 1.9 are now static correlation functions, and are more tractable to analysis. The time derivatives 1.9 may be rewritten as commutators, or expressions for the $\langle\omega^n\rangle$ obtained from consideration of the formula:

$$\langle(\hbar\omega)^n\rangle = \sum_{i,j} (E_i - E_j)^n \qquad - 1.10$$

where $E_i = \langle i|H_o|i\rangle$, the energy of the crystal in state i, and $|i\rangle$, $|j\rangle$ are states of the crystal which are connected by H_I.

The righthand side of 1.10 may be expanded as a sum of products of expectation values and matrix elements of H_o and H_I, using the identity $\sum_i |i\rangle\langle i| = 1$. For example, when n=2,

$$\langle(\hbar\omega)^2\rangle = \sum_{ij} (E_i^2 - E_iE_j - E_jE_i + E_j^2)$$

$$= \sum_{i,j} (\langle i|H_o|i\rangle\langle i|H_o|i\rangle\langle i|H_I|j\rangle\langle j|H_I|i\rangle$$

$$+ \langle i|H_I|j\rangle\langle j|H_o|j\rangle\langle j|H_o|j\rangle\langle j|H_I|i\rangle$$

$$- \langle i|H_o|i\rangle\langle i|H_I|j\rangle\langle j|H_o|j\rangle\langle j|H_I|i\rangle$$

$$- \langle i|H_I|j\rangle\langle j|H_o|j\rangle\langle j|H_I|i\rangle\langle i|H_o|i\rangle)$$

$$= \sum_i \langle i|H_IH_oH_oH_I + H_oH_IH_IH_o - H_oH_IH_oH_I - H_IH_oH_IH_o|i\rangle$$

$$= -\langle [H_o,H_I][H_o,H_I]\rangle \qquad - 1.11$$

Similarly it is found that:

$$\langle \hbar\omega\rangle = \langle [H_o,H_I]\ H_I\rangle \qquad - 1.12$$

and $$(\hbar\omega)^3\rangle = \langle [H_o,[H_o,H_I]][H_o,H_I]\rangle \qquad - 1.13$$

All these moments allow for Stokes and anti-Stokes components of scattered light.

It is now possible to evalue the thermal averages appearing in 1.8, 1.11, 1.12 and 1.13 in the limits of zero and infinite temperature, and to do so in the case where the crystals considered are magnetically dilute: a magnetic atom site has probability p of being occupied by a magnetic atom, (1-p) of being occupied by a non-magnetic impurity atom. Chapter 2 is devoted to the discussion of these limits.

In Chapter 3 the case of finite temperature is considered: the constant coupling model of Kasteleijn and van Kranendonk is chosen as being able to yield a description of the temperature dependence of spin

quantities throughout the whole temperature and dilution range, and some crude decouplings made to allow the calculation of zeroth, first and second moments for the case of spin 1 and body-centred cubic structure. This might be expected to be a reasonable description of NiF_2, which is a rutile structure antiferromagnet with spin 1, and should give an indication of how the moments of the scattering profile in dilute MnF_2 behave despite the Mn ion having spin 5/2. It was hoped that experiments on mixed crystals of MnF_2 might yield sufficiently sharp profiles at a range of temperatures for moments to be calculated, and this so far vain hope prompted much of this work. Sharp profiles for pure NiF_2 have been measured (Brya and Richards; Fleury, 1972), and comparison with this work is made. Recently moment calculations for the pure crystal have been published by Brya and Richards (1973): a rather different approach has been adopted, and discussion of their results is to be found in Chapter 3.

§ 2. Calculation of Moments in the Zero and Infinite Temperature Limits

§ 2.1 Calculation of Commutators

The Hamiltonian

$$H_o = J \sum_{\underline{R},\underline{p}} \underline{S}_{\underline{R}} \cdot \underline{S}_{\underline{R}+\underline{p}} \qquad - 2.1$$

is used to describe the spin interaction, and the interaction Hamiltonian for rutile structure materials is

$$H_I = B' \sum_{\underline{R},\underline{\delta}} \underline{S}_{\underline{R}} \cdot \underline{S}_{\underline{R}+\underline{\delta}} \; \sigma_{\underline{\delta}}^{x} \sigma_{\underline{\delta}}^{y} \qquad - 2.2$$

The first commutator $[H_o, H_I]$ is then found to be

$$[H_o, H_I] = \sum_{\underline{R},\underline{p},\underline{\delta}} 4i \; \underline{S}_{\underline{R}} \cdot (\underline{S}_{\underline{R}+\underline{p}} \times \underline{S}_{\underline{R}+\underline{\delta}}) \; \sigma_{\underline{\delta}}^{x} \sigma_{\underline{\delta}}^{y} JB' \qquad - 2.3$$

A somewhat longer and more tedious calculation gives for the second commutator:

$$\begin{aligned}[H_o, [H_o, H_I]] = -8J^2B' \sum_{\underline{R},\underline{p},\underline{x},\underline{\delta}} \{ & (\underline{S}_{\underline{R}} \times \underline{S}_{\underline{R}+\underline{x}}) \cdot (\underline{S}_{\underline{R}+\underline{p}} \times \underline{S}_{\underline{R}+\underline{\delta}}) \\ & + (\underline{S}_{\underline{R}} \times \underline{S}_{\underline{R}+\underline{x}}) \cdot (\underline{S}_{\underline{R}+\underline{\delta}} \times \underline{S}_{\underline{R}+\underline{\delta}+\underline{p}}) - (\underline{S}_{\underline{R}} \times \underline{S}_{\underline{R}+\underline{x}}) \cdot (\underline{S}_{\underline{R}+\underline{p}} \times \underline{S}_{\underline{R}+\underline{p}+\underline{\delta}}) \\ & + (\underline{S}_{\underline{R}} \times \underline{S}_{\underline{R}+\underline{x}}) \cdot (\underline{S}_{\underline{R}+\underline{x}} \times \underline{S}_{\underline{R}+\underline{\delta}}) - (\underline{S}_{\underline{R}} \times \underline{S}_{\underline{R}+\underline{\delta}}) \cdot (\underline{S}_{\underline{R}+\underline{p}} \times \underline{S}_{\underline{R}+\underline{x}}) \} \end{aligned} \qquad - 2.4$$

The sums in 2.3 and 2.4 are over all sites $\underline{R}$ and all their nearest antiferromagnetic neighbours, but restricted so that spins not explicitly on the same site never become so in the course of the sum. Similar expressions are obtained from the cubic material interaction Hamiltonian. In what follows, the rutile material is discussed first in each section.

§2.2 Zero Temperature Intensity

The total intensity, I, is given by

$$I = \langle H_I H_I \rangle$$
$$= \langle O | B'^2 \sum_{\underline{R},\underline{\delta}} \sum_{\underline{R}',\underline{\delta}'} \underline{S}_{\underline{R}} \cdot \underline{S}_{\underline{R}+\underline{\delta}} \underline{S}_{\underline{R}'} \cdot \underline{S}_{\underline{R}'+\underline{\delta}'} \sigma_{\underline{\delta}}^{x} \sigma_{\underline{\delta}}^{y} \sigma_{\underline{\delta}'}^{x} \sigma_{\underline{\delta}'}^{y} | O \rangle \quad - 2.5$$

where the thermal average is replaced by the expectation value in the ground state. The ground state of an antiferromagnet is not precisely known, and the Néel state, where

$$\langle O | S_{\underline{R}}^{z} | O \rangle = \pm S \quad \text{(depending on the sublattice)} \quad - 2.6$$
$$\langle O | S_{\underline{R}}^{x2} | O \rangle = \langle O | S_{\underline{R}}^{y2} | O \rangle = \tfrac{1}{2} S \quad - 2.7$$
$$\langle O | S_{\underline{R}}^{z2} | O \rangle = S^2 \quad - 2.8$$

is used as an approximation. All correlations between spins on neighbouring sites are also ignored. The spin product expectation value in 2.5 may be written

$$\langle O | \underline{S}_{\underline{R}} \cdot \underline{S}_{\underline{R}+\underline{\delta}} \underline{S}_{\underline{R}'} \cdot \underline{S}_{\underline{R}'+\underline{\delta}'} | O \rangle = S_{\underline{R}}^{z} S_{\underline{R}'}^{z} S_{\underline{R}+\underline{\delta}}^{z} S_{\underline{R}'+\underline{\delta}'}^{z} +$$
$$+ S_{\underline{R}}^{x} S_{\underline{R}'}^{x} S_{\underline{R}+\underline{\delta}}^{x} S_{\underline{R}'+\underline{\delta}'}^{x} + S_{\underline{R}}^{y} S_{\underline{R}'}^{y} S_{\underline{R}+\underline{\delta}}^{y} S_{\underline{R}'+\underline{\delta}'}^{y}$$
$$+ S_{\underline{R}}^{x} S_{\underline{R}'}^{y} S_{\underline{R}+\underline{\delta}}^{x} S_{\underline{R}'+\underline{\delta}'}^{y} + S_{\underline{R}}^{y} S_{\underline{R}'}^{x} S_{\underline{R}+\underline{\delta}}^{y} S_{\underline{R}'+\underline{\delta}'}^{x} \quad - 2.9$$

where the first term contains all the z components, and the other four terms contain products of x and y components, which do contribute to the zero temperature intensity. When the atom pairs $(\underline{R},\underline{R}+\underline{\delta})$ and $(\underline{R}',\underline{R}'+\underline{\delta}')$ coincide, as they may in two ways, the last four terms may be written as

$$S_{\underline{R}}^{x2} S_{\underline{R}+\underline{\delta}}^{x2} + S_{\underline{R}}^{y2} S_{\underline{R}+\underline{\delta}}^{y2} - \tfrac{1}{2} S_{\underline{R}}^{z} S_{\underline{R}+\underline{\delta}}^{z} \quad - 2.10$$

using the replacements

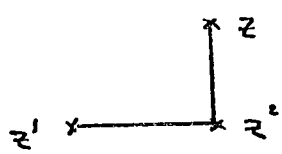
$$S_{\underline{R}}^{x} S_{\underline{R}}^{y} = \frac{i}{2} S_{\underline{R}}^{z} \; : \; S_{\underline{R}}^{y} S_{\underline{R}}^{x} = -\frac{i}{2} S_{\underline{R}}^{z} \quad - 2.11$$

which are valid for any spin in the Néel state, and for spin $\frac{1}{2}$ always, and in the Néel ground state 2.10 contributes

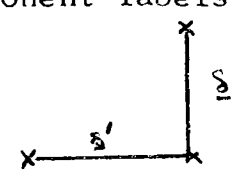
$$(\tfrac{1}{2}S)^2 + (\tfrac{1}{2}S)^2 + \tfrac{1}{2}S^2 = S^2.$$

On summing over $\underline{R}$,$\underline{R}'$,$\underline{\delta}$ and $\underline{\delta}'$ only such coincident pairs contribute, and the result is $16Np^2S^2B'^2$, since each site may be filled by a magnetic atom with probability p.

The first term in 2.9 does not contribute in the limit that p=1, since the sums over $\underline{\delta}$ and $\underline{\delta}'$ are unrestricted, and $\sum_{\underline{\delta}} \sigma_{\underline{\delta}}^{x} \sigma_{\underline{\delta}}^{y} = 0$. However, at smaller p, a contribution is found, from terms where two or no sites coincide. For example, if two sites only coincide in the term (this may happen in four ways), the expectation value in the Néel state is still S^4, but the occurrence when the sum over sites is made is $-8Np^3$ for each such coincidence: a total contribution of $-32Np^3S^4B'^2$. Such a spin expectation value is represented diagrammatically by:



Vector labels attached to the bonds of this diagram, with the spin component labels left off:



are used to describe its occurrence in Appendix I.

The result obtained is that:

$$I = [16NS^2p^2 + 16NS^4(p^2-2p^3+p^4)]B'^2 \qquad - 2.12$$

where the first term comes entirely from the "transverse" part of 2.2, and the second term entirely from the "longitudinal" part. The Hamiltonian 2.2 is rewritten to demonstrate this:

$$H_I = \tfrac{1}{2}B' \sum_{\underline{R},\underline{\delta}} [S_{\underline{R}}^{+} S_{\underline{R}+\underline{\delta}}^{-} + S_{\underline{R}}^{-} S_{\underline{R}+\underline{\delta}}^{+} + 2S_{\underline{R}}^{z} S_{\underline{R}+\underline{\delta}}^{z}] \sigma_{\underline{\delta}}^{x} \sigma_{\underline{\delta}}^{y} \quad - 2.13$$

The x and y components of spin in 2.2 have been re-expressed in terms of spin deviation creation and destruction operators, $S_{\underline{R}}^{\pm} = S_{\underline{R}}^{x} \pm iS_{\underline{R}}^{y}$. This transverse term explicitly creates two spin deviations on neighbouring sites, and may be expected to be mainly responsible for the inelastic scattering. The longitudinal term $S_{\underline{R}}^{z} S_{\underline{R}+\underline{\delta}}^{z}$ allows mainly elastic scattering.

These assignments are confirmed by transformation into spin wave operators, when $S_1^{z} S_2^{z}$, for example, is found to contain a two magnon term, but with a much smaller coefficient than the term responsible for elastic scattering. In the pure substance, there is zero intensity for elastic scattering in the Néel state, but once the translational symmetry is broken by introducing impurities the momentum conservation rule is lost, and scattering may take place at any frequency shift: an intensity is now found.

A similar calculation for the cubic lattice interaction Hamiltonian yields:

$$I_c = [\tfrac{8}{3} Np^2S^2 + \tfrac{8}{3} NS^4[p^2-2p^3+p^4]]B'^2 \quad - 2.14$$

where the terms have similar origins to those in 2.12.

§2.3 Zero Temperature First Moment

The expectation values arising in this are of the type

$$\langle O| \sum_{\underline{R},\underline{\delta}} \underline{S}_{\underline{R}} \cdot \underline{S}_{\underline{R}+\underline{\delta}} \sum_{\underline{R}',\underline{\delta}',\underline{p}'} \underline{S}_{\underline{R}'} \cdot (\underline{S}_{\underline{R}+\underline{p}} \times \underline{S}_{\underline{R}'+\underline{\delta}'}) |O\rangle \qquad - 2.15$$

All eighteen terms appearing in the product 2.15 can be obtained by successive interchange of x,y and z in the three terms considered below. Each term in the first and succeeding moments is denoted by a label of the type 1C, where 1 indicates that the first term in $\underline{S}_o \cdot \underline{S}_1$ has been taken, if $\underline{S}_o \cdot \underline{S}_1$ is written out as $S_o{}^x S_1{}^x + S_o{}^y S_1{}^y + S_o{}^z S_1{}^z$, and C indicates that the third term in $\underline{S}_o \cdot (\underline{S}_1 \times \underline{S}_2)$ has been taken, where $\underline{S}_o \cdot (\underline{S}_1 \times \underline{S}_2) = S_o{}^x S_1{}^y S_2{}^z - S_o{}^x S_1{}^z S_2{}^y - S_o{}^y S_1{}^x S_2{}^z + S_o{}^y S_1{}^z S_2{}^x + S_o{}^z S_1{}^x S_2{}^y - S_o{}^z S_1{}^y S_2{}^x$.

1. 1A $\qquad \langle O| S_{\underline{R}}{}^x S_{\underline{R}+\underline{\delta}}{}^x S_{\underline{R}'}{}^x S_{\underline{R}'+\underline{p}'}{}^y S_{\underline{R}'+\underline{\delta}'}{}^z |O\rangle$

In the Néel state, this only contributes if the pairs $(\underline{R},\underline{R}+\underline{\delta})$ and $(\underline{R}',\underline{R}'+\underline{p}')$ coincide, which they may in two ways: the resulting contraction has expectation value $(\frac{i}{4}S^3)$, and the sum over sites results in an occurrence $(-8Np^3)$ for each coincidence, since the sites $\underline{R}'+\underline{p}'$ and $\underline{R}'+\underline{\delta}'$ are constrained not to coincide: the result then is $(-4iNp^3S^3)$, and the term 2C resulting from interchange of x and y in 1A also contributes this in the Néel state, since x and y components of spin are equivalent. If y and z are interchanged in 1A to give 1B, then

$$- \langle 0|S_{\underline{R}}{}^{x}S_{\underline{R}+\underline{\delta}}{}^{x}\, S_{\underline{R}'}{}^{x}S_{\underline{R}'+\underline{p}'}{}^{z}S_{\underline{R}'+\underline{\delta}'}{}^{y}|0\rangle$$

only contributes if $(\underline{R},\underline{R}+\underline{\delta})$ and $(\underline{R}',\underline{R}'+\underline{\delta}')$ coincide: the expectation value is again $(\frac{i}{4}S^3)$, but now the occurrence comes out to be $(+56Np^3)$ for each coincidence, so that the net result is $(-28iNp^3S^3)$. Interchanging of x and y in 1B (giving 2D) produces another such result.

Any further interchanges in 1A result in terms that do not contribute in the Néel state: so the net contribution from the six terms of type 1A is $(-64iNp^3S^3)$.

2. 1C $\quad -\langle 0|S_{\underline{R}}{}^{x}S_{\underline{R}+\underline{\delta}}{}^{x}S_{\underline{R}'}{}^{y}S_{\underline{R}'+\underline{p}'}{}^{x}S_{\underline{R}'+\underline{\delta}'}{}^{z}|0\rangle$

This term only contributes if $(\underline{R},\underline{R}+\underline{\delta})$ and $(\underline{R}',\underline{R}'+\underline{p}')$ coincide, in which case 1C reduces to

$$-i\langle 0|\tfrac{1}{2}S_{\underline{R}}{}^{z}(S_{\underline{R}+\underline{\delta}}{}^{x})^{2}S_{\underline{R}+\underline{\delta}'}{}^{z}|0\rangle$$

which contributes $+\frac{i}{4}S^3$ in the Néel state. The summation over the sites gives an occurrence of $(-8Np^3)$, and term 2A, resulting from interchange of x and y, gives the same contribution. No other terms of this type contribute in the zero temperature limit, and the net result is $(-8iNp^3S^3)$.

3. 1D $\quad \langle 0|S_{\underline{R}}{}^{x}S_{\underline{R}+\underline{\delta}}{}^{x}S_{\underline{R}'}{}^{y}S_{\underline{R}'+\underline{p}'}{}^{z}S_{\underline{R}'+\underline{\delta}'}{}^{x}|0\rangle$

Now $(\underline{R},\underline{R}+\underline{\delta})$ and $(\underline{R}',\underline{R}'+\underline{\delta}')$ must coincide: the expectation value is $(\frac{i}{4}S^3)$ for each, and the occurrence is $(56Np^3)$. Only 1D and 2B, resulting from interchange of x and y in 1D, contribute of the six terms of 1D type, and the net result is $(-56iNp^3S^3)$.

In this fashion, the first moment is found to be

given by

$$\hbar\langle\omega\rangle = B'^2 J.512\ Np^3S^3 \qquad - 2.16$$

The normalised first moment $\hbar\langle\omega\rangle_N$, given by dividing 2.16 by the total intensity I, is a more useful quantity to consider: when p=1, $\hbar\langle\omega\rangle_N$ is seen to reduce to 4zJS, where z is the coordination number. Calculations that follow show that $\hbar^2\langle\omega^2\rangle_N = \hbar^2\langle\omega\rangle_N^2$, and $\hbar^3\langle\omega^3\rangle_N = \hbar^3\langle\omega\rangle_N^3$, at p=1, in the Néel state, so that a line shape which is just a delta function at twice the zone boundary magnon frequency is predicted for the pure substance at zero temperature. This is a disappointing result, as both naive theory of the type outlined in the introduction and the many experimental results indicate a peak with some width, centred some way below this frequency.

§2.4 Transverse and longitudinal Moments

However, the intensity form derived in §2.3 (equation 2.12) indicates what may be wrong: there are separate contributions from transverse and longitudinal parts of the interaction Hamiltonian to the intensity, so that the first moment $\langle\omega\rangle_N$ (and all moments) also contains longitudinal, elastic components. Accordingly, the zero temperature moments are worked out separately for inelastic and elastic components, with distinguishing suffices T and N. From 2.12

$$I^T = 16NS^2p^2B'^2$$

and $I^L = 16NS^4p^2(1-2p+p^2)B'^2$

may be written down at once. The parts of the commutator 2.3 that belong to the transverse Hamiltonian are B, D, E and F, and those coming from the longitudinal part are A and C, in the notation of §2.3: terms 1 and 2 in $\underline{S}_o.\underline{S}_1$ are transverse, term 3 is longitudinal. Terms in the first moment may now be gathered to give expressions for a longitudinal and transverse first moment.

$$\left.\begin{aligned} \hbar\langle\omega\rangle^T &= 448Np^3S^3B'^2J \\ \hbar\langle\omega\rangle^L &= 0 \end{aligned}\right\} \qquad - 2.17$$

However, a 'mixed' contribution is found, even at zero temperature, to the first moment, coming from terms 1A, 1C, 2A, 2C, 3B, 3D, 3E and 3F, so that

$$\hbar\langle\omega\rangle^M = 64Np^3S^3B'^2J \qquad - 2.18$$

In the Néel state there is no corresponding intensity contribution, but at higher temperatures, one will be found (Chapter 3). In addition, terms which "belong" to the transverse part also arise from the commutator

$$[H_o, H_I^T] = B'J \sum_{\substack{R,\underline{p} \\ R',\underline{\delta}'}} [\underline{S}_R.\underline{S}_{R+\underline{p}}, (S_{R'}^x S_{R'+\underline{\delta}'}^x + S_{R'}^y S_{R'+\underline{\delta}'}^y)]\sigma_{\underline{\delta}'}^x\sigma_{\underline{\delta}'}^x$$

in the case that the two sites in each product coincide, and there is an equal contribution of opposite sign belonging to the longitudinal part. This commutator is of course zero for spin $\frac{1}{2}$, and may be shown to be

$$\sum_{\underline{R},\underline{\delta}} B'J[4(S_{\underline{R}}^{y}S_{\underline{R}+\underline{\delta}}^{x}S_{\underline{R}+\underline{\delta}}^{z}-S_{\underline{R}}^{x}S_{\underline{R}+\underline{\delta}}^{y}S_{\underline{R}+\underline{\delta}}^{z})-2(S_{\underline{R}}^{x}S_{\underline{R}+\underline{\delta}}^{x}+S_{\underline{R}}^{y}S_{\underline{R}+\underline{\delta}}^{y})] \times \sigma_{\underline{\delta}}^{x}\sigma_{\underline{\delta}}^{y} \qquad - 2.19$$

for the transverse part. The last two terms, denoted by P and Q, in 2.19, only contribute to the first moment when multiplied by the transverse part of H_I: a contribution of $-32Np^2B'^2JS^2$ is easily found to $\hbar\langle\omega\rangle^T$, with no contribution to $\hbar\langle\omega\rangle^L$, and an equal and opposite one to $\hbar\langle\omega\rangle^M$. The first two, R and S, give slightly more complicated contributions: consider, for example, 1R.

$$\langle O|S_{\underline{R}}^{x}S_{\underline{R}+\underline{\delta}}^{x}S_{\underline{R}'}^{y}S_{\underline{R}'+\underline{\delta}'}^{x}S_{\underline{R}'+\underline{\delta}'}^{z}|O\rangle$$

Contributions are only found if $(\underline{R},\underline{R}+\underline{\delta})$ and $(\underline{R}',\underline{R}'+\underline{\delta}')$ coincide: in that case $\langle O|S_{\underline{R}}^{x}S_{\underline{R}}^{y}S_{\underline{R}+\underline{\delta}}^{x}S_{\underline{R}+\underline{\delta}}^{x}S_{\underline{R}+\underline{\delta}}^{z}|O\rangle$ is obtained which comes to $(-\frac{i}{4}S^3)$ on performing the contraction.

An additional contribution of $64Np^2B'^2J(S^3)$ to $\hbar\langle\omega\rangle^T$ is found, with an equal and opposite contribution to $\hbar\langle\omega\rangle^M$, and no contribution to $\hbar\langle\omega\rangle^L$. The results obtained are:

$$\hbar\langle\omega\rangle^T=32NB'^2Jp^2S^2[14Sp + 2S-1]$$

$$\hbar\langle\omega\rangle^L=0$$

$$\hbar\langle\omega\rangle^M=32NB'^2Jp^2S^2.$$

The normalised transverse first moment is found to be:

$$\hbar\langle\omega\rangle^T_N = (28Sp + 2(2S-1))J$$

This result is much more satisfactory: an interaction energy $(-2J)$ has been found at $p=1$ as predicted

in the Green's function theory of Elliott and Thorpe (1969). However, a "mixed" first moment has also been found, with no corresponding intensity at T=0 and of no obvious physical significance: it is disregarded for the moment, and will be discussed in §2.8.

The Raman spectrum at T=0 may therefore be imagined as two humps, one at the origin due to the longitudinal term, one at $\hbar\langle\omega\rangle_N^T$ due to the transverse term: experiments take no account of zero frequency shift scattering, since this is lost in the Rayleigh peak, so that those moments directly comparable with experiment may be expected to be the transverse ones, or, possibly, total moments normalised by the transverse intensity only. These latter will be denoted by a suffix P and are identical with total moments normalised by total intensity at p=1.

$$\hbar\langle\omega\rangle^P = 4pzJS$$

The corresponding results for the cubic system are:

$$\begin{aligned}
\hbar\langle\omega\rangle_N^T &= (4(z-1)pS + 2(2S-1))J \\
\hbar\langle\omega\rangle_M^L &= 0 \\
\hbar\langle\omega\rangle^M &= \tfrac{16}{3}NB'^2Jp^2S^2 \qquad - 2.20 \\
\hbar\langle\omega\rangle &= 64Np^3S^3B'^2J \\
\hbar\langle\omega\rangle^P &= 4pzJS.
\end{aligned}$$

Detailed discussion of the significance of moments will be found in §2.8.

§2.5 Second Moment

The second moment involves the expectation value

$$\langle 0|\underline{S}_{\underline{R}}\cdot(\underline{S}_{\underline{R}+\underline{p}}\times\underline{S}_{\underline{R}+\underline{\delta}})\underline{S}_{\underline{R}'}\cdot(\underline{S}_{\underline{R}'+\underline{p}'}\times\underline{S}_{\underline{R}'+\underline{\delta}'})|0\rangle$$

Only terms in the product which have the x and y spin components in the first triple product coincident with the x and y components in the second will contribute in the Néel state: there are twenty such, and these can all be obtained from the consideration of eight products, together with interchange of x and y, and use of AB=BA. Expectation values of the type

$$\langle 0|(S_{\underline{R}}{}^{x})^{2}(S_{\underline{R}+\underline{p}}{}^{y})^{2}S_{\underline{R}+\underline{\delta}}{}^{z}S_{\underline{R}+\underline{\delta}'}{}^{z}|0\rangle$$

and

$$\langle 0|S_{\underline{R}}{}^{z}S_{\underline{R}+\underline{p}}{}^{z}S_{\underline{R}+\underline{\delta}}{}^{z}S_{\underline{R}+\underline{p}+\underline{\delta}'}{}^{z}|0\rangle$$

are found, with different combinations of site labels. The expectation values of these products are $\frac{1}{4}S^4$ and S^4 respectively in the Néel state, and the occurrences of the diagrams required when the sum is performed are again to be found in Appendix I. Further details of the calculation are set out in §3.4. The result for the second moment is:

$$\hbar^2\langle\omega^2\rangle = (2048p^3 + 14336p^4)NS^4J^2B^2$$

and

$$\hbar^2(\langle\omega^2\rangle^P - \langle\omega\rangle^{P^2}) = 16zJ^2S^2p(1-p)$$

so that the normalised second moment about the mean is zero for the pure substance: a δ-function distribution at $\langle\omega\rangle^P$ is predicted.

Calculation of longitudinal, transverse and mixed components is rather tedious. If

$$[H_o, H^T] = 4i[B+D+E+F+R+S] - 2[P+Q]$$

in the previous notation, where the constants and phase factors are left out just now, terms of the following type arise in the calculation of $\hbar\langle\omega\rangle^T$.

1) $\langle O|(B,D,E,F)(B,D,E,F)|O\rangle$

These have been calculated: the contribution is $(896p^3 + 11648p^4)NS^4J^2B'^2$.

2) $\langle O|(P,Q)(P,Q)|O\rangle$

These terms are just like those needed for I^T: the contribution is $-64p^2S^2NB'^2J^2$.

3) $\langle O|(P,Q)(B,D,E,F)|O\rangle + \langle O|(B,D,E,F)(P,Q)|O\rangle$

These two terms cancel exactly in the Néel state.

4) $\langle O|(P,Q)(R,S)|O\rangle + \langle O|(R,S)(P,Q)|O\rangle$

All four terms in the first expectation value may be shown to contribute $+32NB'^2J^2p^2S^3$, as they are similar to 1R evaluated for the first moment. All four terms in the second product are also the same, and may be shown to be $-32NB'^2J^2p^2(S^3-S^2)$. The net contribution is $+128NB'^2J^2p^2S^2$.

5) $\langle O|(R,S)(B,D,E,F)|O\rangle$

Products of R or S with E or F are found not to contribute in the Néel state: the usual methods to deal with multiple spin operators or a site are employed, and a contribution $+1792NB'^2J^2p^3(S^4-S^3)$ obtained.

6) $\langle O|(B,D,E,F)(R,S)|O\rangle$

In a similar fashion, this is found to contribute

$+1792NB'^2J^2p^3S^4$.

7) $\langle O|(R,S)(R,S)|O\rangle$

A typical term here is

$$+\langle O|S_{\underline{R}}{}^{y}S_{\underline{R}+\underline{\delta}}{}^{x}S_{\underline{R}+\underline{\delta}}{}^{z}S_{\underline{R}'}{}^{y}S_{\underline{R}'+\underline{\delta}'}{}^{x}S_{\underline{R}'+\underline{\delta}'}{}^{z}|O\rangle$$

A contribution is only found if $(\underline{R},\underline{R}+\underline{\delta})$ and $(\underline{R}',\underline{R}'+\underline{\delta}')$ coincide: the result is

$$\langle O|S_{\underline{R}}{}^{y2}S_{\underline{R}+\underline{\delta}}{}^{x}S_{\underline{R}+\underline{\delta}}{}^{z}S_{\underline{R}+\underline{\delta}}{}^{x}S_{\underline{R}+\underline{\delta}}{}^{z}|O\rangle$$

or, on commuting,

$$\langle O|S_{\underline{R}}{}^{y2}S_{\underline{R}+\underline{\delta}}{}^{x}[iS_{\underline{R}+\underline{\delta}}{}^{y}+S_{\underline{R}+\underline{\delta}}{}^{x}S_{\underline{R}+\underline{\delta}}{}^{z}]S_{\underline{R}+\underline{\delta}}{}^{z}|O\rangle$$

In the Néel state, the first term is $(-\frac{S^3}{4})$ and the second is $(\frac{S^4}{4})$: the occurrence, on inserting phase factors and summing, is $8Np^2$. All four terms give the same: the result is $+256p^2[S^4-S^3]NB'^2J^2$.

In this way, the result is found that

$$\hbar^2\langle\omega^2\rangle^T = ((11648p^4+4480p^3+256p^2)S^4-(+1792p^3+256p^2)S^3+64p^2S^2)NB'^2J^2.$$

On normalising, the transverse second moment about the mean is:

$$\hbar^2[\langle\omega^2\rangle_N^T-\langle\omega\rangle_N^{T^2}] = 56J^2S^2p(1-p) \qquad - 2.21$$

A width is also found for the longitudinal moment when some more terms are evaluated:

$$\hbar^2\langle\omega^2\rangle^L = 64J^2S^2NB'^2\{(4p^2+6p^3-10p^4)S^2+(4p^3-4p^2)S+p^2\} \qquad - 2.22$$

In the pure substance, the scattering profile due solely to the transverse component is therefore a δ-function at $(4zS-2)J$; as impurities are introduced, the peak moves towards the origin, and becomes wide. Equation 2.21 predicts a maximum width when

$$p = .5 \qquad - 2.23$$

This behaviour is in reasonable agreement with experiment: the scattering profile is quite a sharp peak at low temperature, and moves toward the origin as p is lowered. Further discussion of this is to be found in §2.8.

The corresponding results for the cubic system are:

$$\hbar^2\langle\omega^2\rangle = (256p^3 + 1280p^4)NS^4J^2B'^2$$

$$\hbar^2(\langle\omega^2\rangle^P - (\langle\omega\rangle^P)^2) = 16zpJ^2S^2(1-p)$$

$$\hbar^2(\langle\omega^2\rangle_N^T - (\langle\omega\rangle_N^T)^2) = 8(z-1)S^2p(1-p)J^2 \qquad - 2.24$$

$$\hbar^2\langle\omega^2\rangle^L = 4NB'^2J^2p^2S^2[(4+2p-6p^2)S^2 + (4p-4)S+1]$$

leading to similar predictions.

§2.6 Third Moment

The calculationsleading to the third moment are extremely tedious, involving the consideration of 360 expectation values: not all of these contribute, of course. The expectation values of spin products are trivial to find in the Néel state, and all the occurrences required are again in Appendix I. The result found is:

$$\hbar^3\langle\omega^3\rangle = (512p+9984p^2+22272p^3).16p^2S^5J^3NB'^2$$

$$\hbar^3\langle(\omega-\langle\omega\rangle^P)^3\rangle^P = 64z(1-p)(1-\tfrac{7}{2}p)S^3J^3p \qquad - 2.25$$

for the tetragonal lattice, and

$$\hbar^3\langle\omega^3\rangle = (32p+448p^2+672p^3).32p^2S^5J^3NB'^2$$

$$h^3\langle(\omega-\langle\omega\rangle^P)^3\rangle^P = 64zp(1-p)(1-3p)S^3J^3 \qquad - 2.26$$

for the cubic lattice.

Both of these are zero at p=1, verifying the delta

function result already produced for the zero temperature total moment: it is also of interest that the normalised p-type third moment about the mean has zeroes at $p=\frac{2}{7}$ and $p=\frac{1}{3}$ for the rutile and cubic antiferromagnets respectively. The calculation is not pursued to yield a form for the transverse third moment, as the second commutator required has rather a complicated form.

§2.7 Infinite Temperature Limit

In this limit, the only non-zero spin quantities of interest for the first four moments are:

$$\langle S_R^{x2}\rangle = \langle S_R^{y2}\rangle = \langle S_R^{z2}\rangle = \tfrac{1}{3}S(S+1) \qquad - 2.27$$

The intensity or zeroth moment involves:

$$\langle \underline{S}_R \cdot \underline{S}_{R+\delta}\ \underline{S}_{R'} \cdot \underline{S}_{R'+\delta'}\rangle$$

and this can only contribute when the pair $(\underline{R},\underline{R}+\underline{\delta})$ and $(\underline{R}',\underline{R}'+\underline{\delta}')$ coincide: the result is easily seen to be

$$I(T\to\infty) = \frac{16}{3}Np^2S^2(S+1)^2B'^2 \qquad - 2.28$$

The corresponding result for the cubic system is

$$I(T\to\infty) = \frac{8}{9}Np^2S^2(S+1)^2B'^2 \qquad - 2.29$$

All odd moments are identically zero, since they involve only thermal averages of odd numbers of spins: accordingly, the scattering profile is centred at zero energy shift, and symmetric about its centre. Experiment indicates that the profile approaches this shape as the temperature is raised above T_N (e.g. Fleury, 1969).

The second moment involves

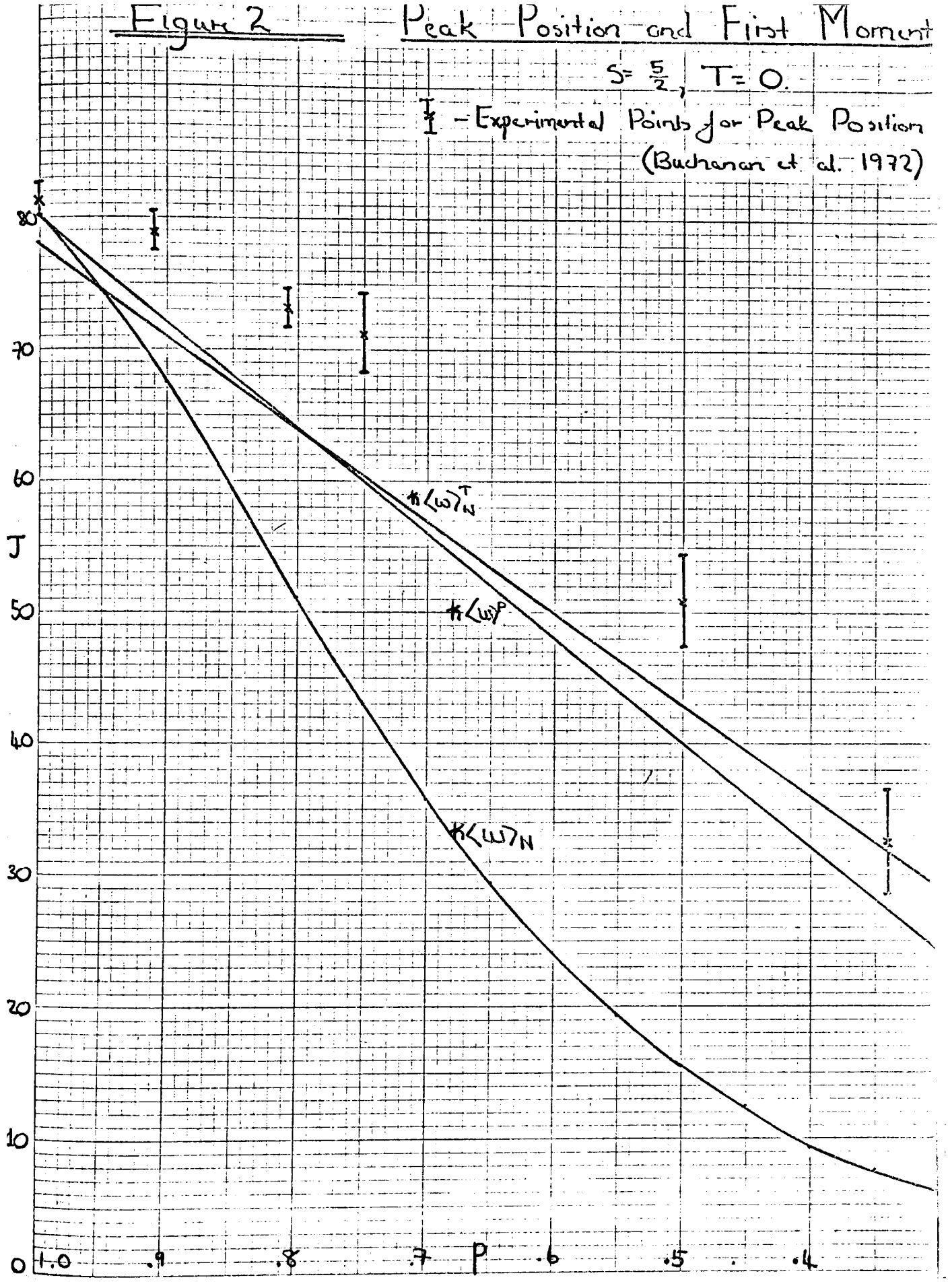
$$\langle \underline{S}_{\underline{R}} \cdot (\underline{S}_{\underline{R}+\underline{p}} \times \underline{S}_{\underline{R}+\underline{\delta}}) \underline{S}_{\underline{R}'} \cdot (\underline{S}_{\underline{R}'+\underline{p}'} \times \underline{S}_{\underline{R}'+\underline{\delta}'}) \rangle$$

and again contributions are found only if the three sites in the first product coincide with the three sites in the second in such a way that only terms of type 2.27 are produced: all twelve such terms may be produced by interchange of x,y and z in AA and AB. The first of these contributes $896p^3N(\frac{1}{3}S(S+1))^3B'^2J^2$: the second, $128p^3N(\frac{1}{3}S(S+1))^3B'^2J^2$. The following result for the infinite temperature limit of the normalised second moment is found:

$$\hbar^2\langle\omega^2\rangle_N = \frac{16}{3}zpS(S+1)J^2 \qquad - 2.30$$

and an identical result for the cubic lattice.

Breaking up moments into components loses its significance above the Néel temperature, since x,y and z components of spin become effectively indistinguishable: the total second moment and intensity 2.28 and 2.30 should correspond best to experiment. Comparison with experiment in this limit is made in the following section.


Figure 2
Peak Position and First Moment
S = 5/2, T = 0.
I - Experimental Points for Peak Position
(Buchanan et al. 1972)
$\hbar\langle\omega\rangle_N^T$
$\hbar\langle\omega\rangle^P$
$\hbar\langle\omega\rangle_N$
J
80
70
60
50
40
30
20
10
0
1.0
.9
.8
.7
P
.6
.5
.4

§2.8 Analysis of Results

There are two classes of experiment which may be compared with the results obtained so far: one is work by Buchanan et al (1972) on crystals of $(Mn,Zn)F_2$ at very low temperature for a range of concentrations of manganese, which yields some information about lineshapes, but none about moments, because of the difficulty of subtracting off the background scattering due to impurity induced phonons and crystal imperfections as well as the usual phonon scattering. Brya and Richards (1973) have done some accurate experiments which provide zeroth and first moment measurements over a range of temperatures for pure $RbMnF_3$, MnF_2, and NiF_2: comparison with their zero and infinite temperature limit results will be made here, but the full temperature dependence will be discussed for NiF_2 in §3.5.

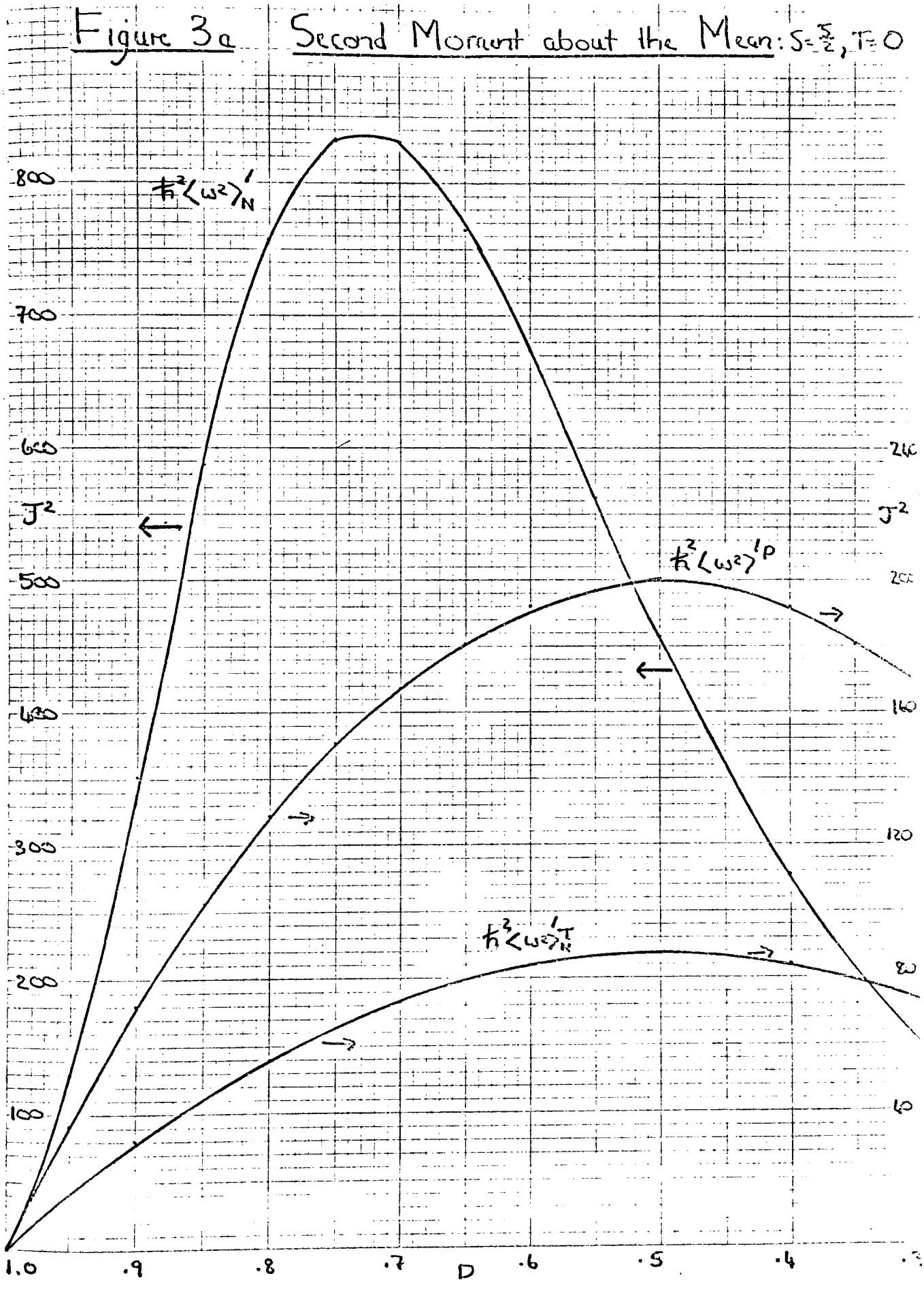
At zero temperature no estimate of the variation of intensity can be made as p is varied in $(Mn,Zn)F_2$, for the reasons stated above. However, the peak position may be measured for a range of values of p, and this is shown in Fig. 2, as are the predictions of

$$\hbar\langle\omega\rangle_N^T = [(4(z-1)p+4)S-2]J$$

$$\hbar\langle\omega\rangle^p = 4zpJS$$

and $$\hbar\langle\omega\rangle_N = 64zp^2JS^2/(16p^2S^2+16S^4(p^2-2p^3+p^4))$$

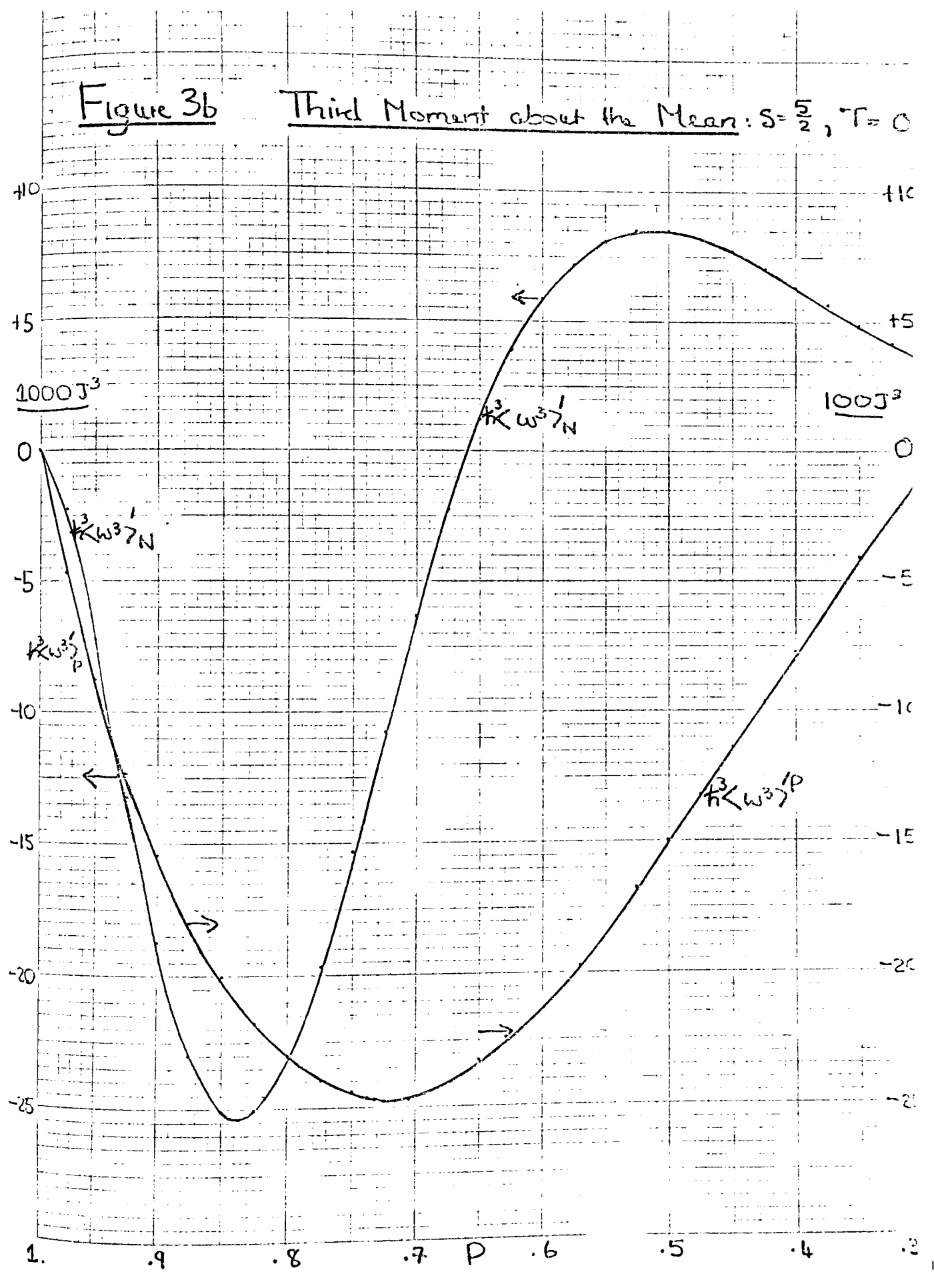
Agreement is good at $p=1$, but for lower p the theoretical lines lie well below the experimental points. This is


Figure 3a
Second Moment about the Mean: S=5/2, T=0
$\hbar^2\langle\omega^2\rangle'_N$
$\hbar^2\langle\omega^2\rangle'_P$
$\hbar^2\langle\omega^2\rangle'_T$
J²
800
700
600
500
400
300
200
100
240
200
160
120
80
60
1.0
.9
.8
.7
D
.6
.5
.4

because the experimental points are for peak position: the good agreement at p=1 indicates that the line shape is a sharp peak there. At lower p, the line shape is skewed towards zero frequency shift: this is indicated both by the experiments of Buchanan et al and by equation 2.25. Accordingly the first moment is less than the peak position.

Fig. 3a shows the prediction of the transverse, P-type, and total second moments about their appropriate means, denoted by $\langle\omega^2\rangle'^{T}_{N}$, $\langle\omega^2\rangle'^{P}$ and $\langle\omega^2\rangle'^{N}$ respectively. Again only values down to p=.3 are shown, as the model has no Néel state even at zero temperature below p=.285. Experiment on $(Mn,Zn)F_2$ has also produced a curve of full width at half height as p is varied down to about p=.5: below that, the uncertainties become very large. The width rises steadily from 7 cm^{-1} at p=1 to 35 cm^{-1} at p=.5, and then appears to level off: this is in qualitative agreement with $\langle\omega^2\rangle'^{T}_{N}$ and $\langle\omega^2\rangle'^{P}$ in Fig. 3a, but not with the total moment prediction. At p=.5, if a Gaussian shape is assumed, $\langle\omega^2\rangle'^{P}$ corresponds to a full width at half height of 44.6 cm^{-1}, $\langle\omega^2\rangle'^{T}_{N}$ to 31 cm^{-1}, and $\langle\omega^2\rangle'_{N}$ to 72 cm^{-1}. However, as the shape certainly is not Gaussian, no more significance can be read into these figures than that the total moment is again not a very good description.

The third moment results for the Néel state are also plotted (Fig. 3b). The total moment about the mean, $\langle\omega^3\rangle'_{N}$, becomes zero at p=.6, and the P-type moment does this at


Figure 3b Third Moment about the Mean: S = 5/2, T = 0
+10
+5
1000J^-3
0
-5
-10
-15
-20
-25
100J^-3
$\hbar^3\langle w^3\rangle'_N$
$\hbar^3\langle w^3\rangle'_P$
1.
.9
.8
.7
P
.6
.5
.4

$p=\frac{2}{7}$: above these concentrations, both predict a line shape skewed towards the zero frequency side of the mean, and below them, the skew is reversed. An Ising cluster theory due to Buyers (Buchanan et al) for the antiferromagnet at zero temperature yields line shapes in fair agreement with experiment, and predicts that the line shape is symmetric about the mean at p=.5: neither of the above predictions agrees well with this Ising theory or experiment. However, the experimental results are extremely uncertain.

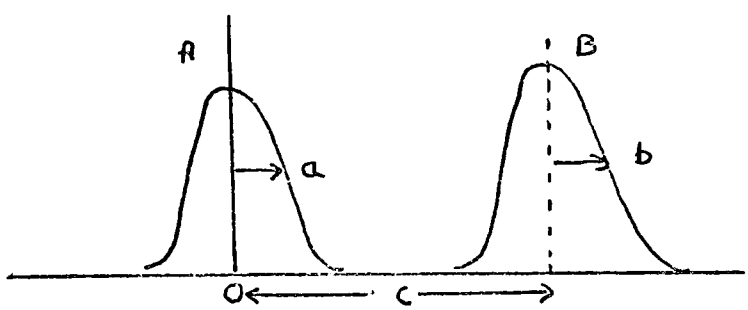
The large discrepancy between the predictions of different sorts of moments even in the Néel state requires that some thought be given to the meaning of these different sorts.

Two difficulties in the naive identification of H_I^L with elastic scattering and H_I^T with two-magnon scattering arise at once: one is, as already discussed, that H_I^L contains two magnon terms as well as elastic terms in its magnon operator representation (H_I^T contains a similar mixture). The admixture is quite small, but may have a significant effect in moments higher than the zeroth. In particular, the scattering due to inelastic terms in H_I^L may be expected to give a large width for the longitudinal peak, and this is apparent in the formulae derived even at p=1, where the elastic response might be expected to be a δ-function at the origin, of zero intensity.

The occurrence of mixed moments also indicates that

splitting up the moments may not be valid: there is no mixed intensity, but fairly large mixed first and second moments do occur. That there is no integrated mixed intensity indicates that the intensity due to mixed components is negative at some frequencies: only $\langle H_I^{T2} \rangle$ and $\langle H_I^{L2} \rangle$ need be positive everywhere, and $\langle H_I^T H_I^L \rangle$ may well be negative. Where in the frequency spectrum such intensity occurs cannot, of course, be estimated, nor can its effects on the elastic and inelastic peaks. In addition, it must be remembered that only an approximate ground state is being used.

However, one may regard the total moments as being a valid description of the complete scattering profile, and try to estimate its shape by assuming that at all p the elastic and inelastic peaks are both Gaussian curves,



so that $I(u) = Ae^{-\omega^2/2a^2} + Be^{-(\omega-c)^2/2b^2}$.

Such a form is perhaps slightly inconsistent: the negative frequency side of curve A must be kept, however, since the elastic peak is expected to be symmetric about zero frequency. The integrated or total intensity I is

$$I = Aa\sqrt{2\pi} + Bb\sqrt{2\pi}$$

It is now assumed that I_T and I_L will get the ratio of inelastic to elastic scattering right, although this is by no means obviously correct, so that

$$\frac{Aa}{Bb} = S^2(1-p)^2$$

The first moment is given by

$$\langle\omega\rangle = cbB\sqrt{2\pi}$$

and, normalised by I, is

$$\langle\omega\rangle_N = \frac{c}{(1-p)^2S^2+1}$$

Comparison with the total moment $\langle\omega\rangle_N$ derived gives $c = 32pSJ/\hbar$. Further integration yields

$$\langle\omega^2\rangle_N = (a^2S^2(1-p)^2 + b^2+c^2)/(1+S^2(1-p)^2)$$

and $$\langle\omega^3\rangle_N = (32cb^2 + b^3)/(1+S^2(1-p)^2)$$

Comparison with the forms derived in the previous section gives $b^2 = \frac{8}{3}S^2(1-p)(2+41p)J^2/\hbar^2$

and $a^2 = \frac{8}{3}\frac{7p-2}{1-p}J^2/\hbar^2$

These expressions for b^2 and a^2 are just the second moments about the mean for each Gaussian, normalised by the intensity of that Gaussian. $\hbar^2b^2$ may be compared with the transverse second moment about the mean,

$$\hbar^2(\langle\omega^2\rangle_N^T - \langle\omega\rangle_N^{T2}) = 56pS^2(1-p)J^2$$

and with $\hbar^2[\langle\omega^2\rangle^P - \langle\omega\rangle^{P2}] = 128pS^2(1-p)$

It is seen to be very nearly equal the latter, and be about twice as large as the former. In addition, c is just

$\langle\omega\rangle^P$ and $\langle\omega^3\rangle'^P$ is much closer to zero at all p than $\langle\omega^3\rangle_N$ (Fig. 3b). It seems, therefore, that p-type moments give a good description of the inelastic peak if this Gaussian assumption is made: since p-type moments are total moments normalised with I_T only, this suggests that the zero frequency intensity mainly due to H_I^L does not give important contributions to higher moments of the inelastic peak.

Since the completion of much of this work, Brya and Richards have measured moments with some consistency in several pure antiferromagnets: they have also repeated some of the calculations reported here for the pure substance, and have evaluated the total first moment in the spin-wave ground state (Richards and Brya, 1973).

The quantity $R = I(T=\infty)/I$ may be measured with some precision if assumptions are made that allow subtraction of the background phonon scattering. For MnF_2, the measurement gives 4.45 at room temperature (essentially infinite, for MnF_2) and 2^oK: the moment calculation gives

$$R = \frac{1}{3}(S+1)^2 = \frac{49}{12}$$

if the anisotropy factor $(\gamma-1)$ in H_I is ignored, as seems reasonable. The agreement is reasonable: but Brya and Richards apply a spin wave ground state correction to R, and reduce it to 3.7. In NiF_2, R is measured as 1.4, whereas the simple prediction in the Néel state is 1.33, and this is reduced by spin-wave corrections to 1.16,

(Brya and Richards: Fleury, 1972), if again $(\gamma-1)$ is ignored. These authors explore several possible reasons for the discrepancy, and conclude that anisotropy and other scattering mechanisms are unlikely to be responsible. The excited state exchange or scattering parameters may be temperature dependent, or the assumption used to subtract off the background unreliable at high temperature.

The first moment at zero temperature is measured for several substances. The results are shown below in tabular form, in cm^{-1}.

	Experiment	$\hbar\langle\omega\rangle_T$	$\hbar\langle\omega\rangle_N$	BαR
$RbMnF_3$	131.4±.5	136.9 ± 12	141.6 ±12	131.8 ±12
MnF_2	97.6 ±.7	95.55 ±.8	98 ± .8	95.5±1.5
NiF_2	201.1±.7	204 ± 6	222 ± 6	196.3±11

The results are for xy polarisation in the tetragonal antiferromagnets, and uncertainties in the moments are due to uncertainties in measurements of the antiferromagnetic exchange.

The numbers in the column headed BαR are obtained by those authors from a calculation of the first moment in the spin wave ground state, with an Oguchi correction, using the total H_I: in the case of MnF_2, allowance is made for dipolar effects and for ferromagnetic exchange with other neighbours. In NiF_2, single ion anisotropy is also included. It seems a general feature that the spin wave result is almost the same as the transverse moment, once the Oguchi

correction is applied, and corrections due to dipolar effects and so on are very small (about 1% for MnF_2). For the purposes of explaining the experimental results simply, the transverse moment in the Néel state seems to work well: however, Richards and Brya succeed in determining the weak ferromagnetic exchange constants in MnF_2 with some accuracy by comparing the first moments for xy and xz scattering, using the spin wave ground state.

The value of $\langle\omega^2\rangle^{\frac{1}{2}}$ at high temperature has also been measured in MnF_2 and NiF_2. For the first, Brya and Richards obtain 25.5 cm^{-1}: the prediction of total moments is 23.4 cm^{-1}. In NiF_2, the corresponding results are 60 cm^{-1} and 62.2 cm^{-1}.

One may conclude, then, that use of the simple interaction and spin Hamiltonian assumed earlier for these systems produces results in fair agreement with experiment. Better agreement may be reached at zero temperature for the pure substance by a spin wave calculation, and some allowance for anisotropy and dipolar effects. However, this simple moment theory may be expected to also give reasonable results at temperatures other than zero, and in dilute crystals, particularly if P_--type moments are compared with experiment.

CHAPTER 3

§3. Finite Temperature Moments

In this section approximate forms for the intensity, first and second moments are found for arbitrary temperature and concentration: the model discussed is that described by Hamiltonian 2.1 and interaction Hamiltonian 2.2 for spin 1, and should indicate the scattering profile expected in dilute rutile structure antiferromagnets. The constant coupling model of Kasteleijn and Von Kranendonk (1956 a,b) is chosen as being able to provide values for $\langle S_1^z \rangle$, $\langle S_1^{x^2} \rangle$, $\langle S_1^{z^2} \rangle$, $\langle S_1^z S_2^z \rangle$ and $\langle S_1^x S_2^x \rangle$ for all temperatures and concentrations, where the atoms on sites 1 and 2 are magnetic next neighbours, and rather crude decouplings of spin thermal averages are made in terms of these quantities.

§3.1 Constant Coupling Model

Various theories which treat the ordering problem in a ferromagnet have been developed in which the interactions within a pair or cluster of magnetic atoms are correctly treated, while the rest of the lattice is represented by some sort of approximate field (Bethe, 1935; Guggenheim, 1935; Peierls 1936): these prove convenient and fairly accurate, in particular the constant coupling model of Van Kranendonk and Kasteleijn (1956), which works well for the Heisenberg model with spin $\frac{1}{2}$. Some of these models have been modified to cover the case of

dilution (Sato, Arrott and Kikuchi, 1959; Smart, 1960), but the constant coupling approximation seems most successful above and below the transition temperature in this case.

No such satisfactory theory exists for the two sublattice antiferromagnet: the constant coupling model predicts not only a Curie temperature, T_c, but an anti-Curie temperature below which there is no magnetic order (Kasteleijn and Van Kranendonk, 1956): accordingly, it only provides a good approximation above T_c. It is thought that an adequate description of an antiferromagnet may be obtained from simple theories by reversing the sign of J in H_o, and the sign of the next neighbour correlation function (e.g. Elliott, 1960). This procedure is carried out and the extension to spin 1 and magnetic dilution made.

The Hamiltonian used is

$$H_o = -2J \sum_{<ij>} \underline{S}_i \cdot \underline{S}_j - 2\mu H \sum_i S_i^z \qquad - 3.1$$

in the usual notation. It is possible to show that the most general effective Hamiltonian of a pair (1,2) is

$$H_e = -2A_1 \underline{S}_1 \cdot \underline{S}_2 - 2A_2 S_1^z S_2^z - 2\mu A_3 (S_1^z + S_2^z) \qquad - 3.2$$

where A_1 and A_2 are effective coupling constants, and A_3 is an effective field. The constant coupling approximation consists in setting $A_1 = J$ and $A_2 = 0$: A_3 is determined by minimising the free energy.

The Hamiltonian 3.1 is written in the form 3.2, giving

$$H' = -2J\ \underline{S}_1.\underline{S}_2 - (2\mu H/z)(S_1^z+S_2^z) \qquad - 3.3$$

H' is diagonal in the representation in which $\underline{S}_1.\underline{S}_2$ and $S_1^z+S_2^z$ are diagonal, as is 3.2, since $[H',H_e] = 0$. Accordingly, the energy of the crystal is

$$E = \tfrac{1}{2}Nz \sum_\nu f_\nu E_\nu \qquad - 3.4$$

where E_ν are the eigenvalues of H', and f_ν are given by

$$f_\nu = \exp(-\beta\varepsilon_\nu)/(\Sigma_\nu \exp(-\beta\varepsilon_\nu)) \qquad - 3.5$$

where ε_ν are the eigenvalues of H_e.

$\underline{S}^o$	$S_1^z+S_2^z$	$\underline{S}_1,\underline{S}_2$	ν	E_ν	ε_ν
0	0	-2	1	4J	4J
1	-1	-1	2	$2J+\frac{2\mu H}{z}$	$2J+2\mu A_3$
	0	-1	3	2J	2J
	+1	-1	4	$2J-(2\mu H/z)$	$2J-2\mu A_3$
2	-2	+1	5	$-2J+4\mu H/z$	$-2J+4\mu A_3$
	-1	+1	6	$-2J+2\mu H/z$	$-2J+2\mu A_3$
	0	+1	7	-2J	-2J
	+1	+1	8	$-2J-2\mu H/z$	$-2J-2\mu A_3$
	+2	+1	9	$-2J-4\mu H/z$	$-2J-4\mu A_3$

The states of the pair are described in terms of the total spin $\underline{S}^o = \underline{S}_1+\underline{S}_2$: the values of $\underline{S}_1.\underline{S}_2$, E_ν and ε_ν quickly follow. Defining $w = \exp(-\beta J)$ and $u = \exp(-2\beta\mu A_3)$, forms for the f_ν may be written down in terms of x and u. In addition, $\sum_\nu f_\nu = 1$. The long range order parameter,

$S = \overline{S_1^z + S_2^z}$, is given by

$$S = f_4 - f_2 + f_8 - f_6 + 2(f_9 - f_5) \qquad - 3.6$$

and $$\tau = 4\overline{\underline{S}_1 \cdot \underline{S}_2} = 4(f_5+f_6+f_7+f_8+f_9-f_2-f_3-f_4-2f_1) \qquad - 3.7$$

Now E may be written as

$$E = -1/4J\tau Nz - N\mu HS \qquad - 3.8$$

and it may be shown that

$$\sum_v f_v \ln f_v = \tfrac{1}{2}\beta J\tau + 2\beta\mu A_3 S - \ln z_e \qquad - 3.9$$

where $z_e = Tr\{\exp(-\beta H_e)\}$

The partition function of the crystal at a given temperature, z, is given by z_{s*} in the limit $N \to \infty$, where

$$z_s = \sum_l \exp(-\beta E_l)$$

the sum being over all eigenstates of 3.1 that belong to a given value of the order parameter, and S* is that value of S for which z_s is biggest.

Van Kranendonk and Kasteleijn show that

$$\ln z_s = -\beta E(\beta,S) - \tfrac{1}{2}Nz\sum_v f_v \ln f_v - z\ln g(S) - \tfrac{1}{2}N\left(\sum_v f_v \ln f_v\right)_{\beta=0} \qquad - 3.10$$

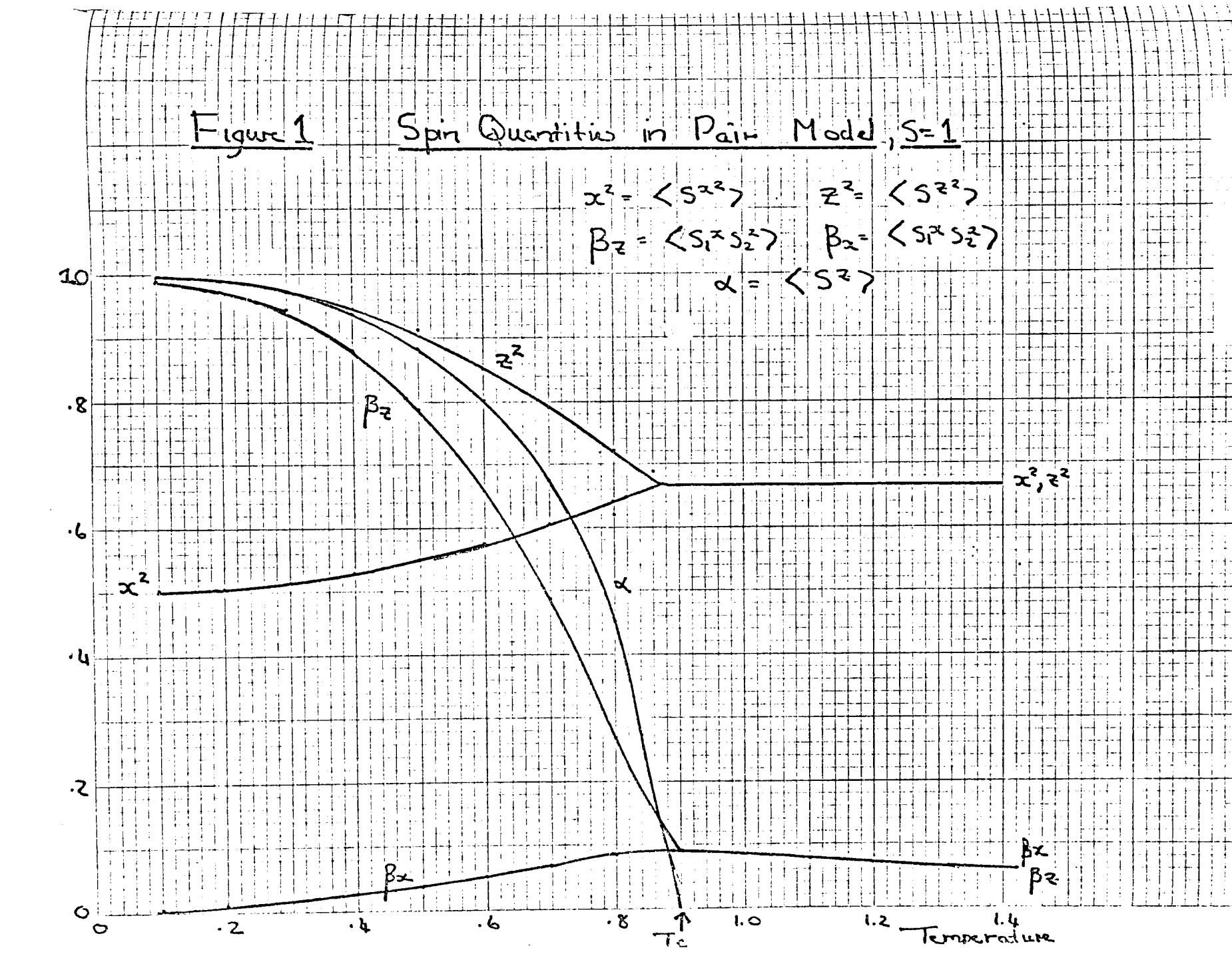
where g(s), the entropy, is

$$g(s) = z_s(\beta=o) = \frac{N!}{(\frac{1}{2}N(1-s/2-\gamma))!N\gamma!(\frac{1}{2}N(1+s/2-\gamma))!} \qquad - 3.11$$

The additional order parameter γ is introduced, such that $N\gamma$ pairs have total spin zero. Equation 3.10 is now maximised with respect to s and γ simultaneously. Differentiation with respect to γ, recalling 3.8 and 3.9, produces the condition

$$0 = \frac{\partial}{\partial\gamma} \ln g(s) \qquad - 3.12$$

and this is solved to yield:


Figure 1 Spin Quantities in Pair Model, S=1
$x^2 = \langle S^{x2} \rangle$ $z^2 = \langle S^{z2} \rangle$
$\beta_z = \langle S_1^x S_2^z \rangle$ $\beta_x = \langle S_1^x S_2^x \rangle$
$\alpha = \langle S^z \rangle$
1.0
.8
.6
.4
.2
0
z^2
β_z
x^2, z^2
x^2
α
β_x
β_x
β_z
0
.2
.4
.6
.8
T_c
1.0
1.2
1.4
Temperature

$$\gamma = 1/6\left(\sqrt{4+12\left(1-\left(\frac{s}{2}\right)^2\right)} - 2\right) \qquad - 3.13$$

Differentiation of 3.10 with respect to γ gives

$$0 = N\mu\beta H - Nz\beta\mu A_3 - z\frac{\partial}{\partial s}\ln g(s) - \tfrac{1}{2}N\frac{\partial}{\partial s}\left[f_\nu \ln f_\nu\right]_{\beta=0} \qquad - 3.14$$

H is chosen to be zero, and it is easily shown that

$$\frac{\partial \ln g(s)}{\partial s} = \frac{N}{4}\ln\left(\frac{1-s/2-\gamma}{1+s/2-\gamma}\right)$$

and $$\frac{\partial}{\partial s}\left[\Sigma f_\nu \ln f_\nu\right]_{\beta=0} = -\tfrac{1}{2}\ln\left(\frac{1-s/2-\gamma}{1+s/2-\gamma}\right)$$

Substitution of these into 3.14 results in:

$$-4z\beta\mu A_3 = (z-1)\ln\left(\frac{1-s/2-\gamma}{1+s/2-\gamma}\right) \qquad - 3.15$$

or $$\ln u^2 = \frac{z-1}{z}\ln\left(\frac{1-s/2-\gamma}{1+s/2-\gamma}\right)$$

Equation 3.6 for S may be rewritten as

$$S = \{(u-u^3)(1+w^4) + 2(1-u^4)\}/Q \qquad - 3.16$$

with $Q = w^6u^2 + w^4(u+u^2+u^3) + 1+u+u^2+u^3+u^4$.

Equations 3.13, 3.15 and 3.16 may now be used iteratively to find solutions for S and u for any choice of x.

The following thermal averages may now be calculated in terms of the f_ν:

$$\langle S^{x^2}\rangle\ ,\ \langle S^{z^2}\rangle, \langle S_1^{\,x} S_2^{\,x}\rangle, \langle S_1^{\,z} S_2^{\,z}\rangle, \langle S^z\rangle.$$

Figure 1 shows their behaviour against temperature for the pure rutile lattice, where $z = 8$. The predicted transition temperatures is $kT_c/J = 9$: the best value from high temperature series is 7.599 (Ritchie and Fisher, 1972).

The results for the pair correlation function by this method may be compared with those recently obtained

for the pure body centred cubic ferromagnet above T_c by Ritchie and Fisher (1972) by high temperature series methods. Approximants for the scattering intensity function $\hat{\chi}(\underline{q},T)$ are obtained for all $\underline{q}$ and all $T > T_c$: since the correlation function is the inverse Fourier transform of $\hat{\chi}(\underline{q},T)$, values for it may be obtained by integration throughout the Brillouin zone. Such calculations have been performed by Brya and Richards (1973). This becomes unreliable near T_c and values for the critical next neighbour correlation are estimated by extrapolation of series for the correlation function. Estimates for the normalised critical correlation $\langle \underline{S}_1 \cdot \underline{S}_2 \rangle / S(S+1)$ for various spins by these two methods are tabulated below, together with the results of constant coupling.

Spin	Integration of $\chi(\underline{q},T)$	Series extrapolation	Constant coupling
∞	.259	.273	-
5/2	.250	.263	-
3/2	.242	.254	-
1	.229	.240	.143
1/2	.190	.199	.143

The constant coupling result is $\frac{1}{z-1}$ for the normalized critical correlation, for any spin: this value is seen to be about 50% below those of more sophisticated theories for spin 1. However, the critical correlations for spin 5/2

and spin 1 are not very different so that the results for NiF_2 and MnF_2 scattering profiles may be similar. Obviously the constant coupling method does not provide a very good description of the critical correlation: however, it is the only method available which describes the correlations consistently at all temperatures and concentrations.

Extension to the dilute case is naively made by replacing z by pz in 3.10: this takes some account of an average dilute neighbourhood for the pair, but does not seem appropriate when a pair which must itself consist of two magnetic atoms is considered. Such an approximation gives a critical concentration of $\frac{2s+1}{sz}$ = .375 for the BCC lattice and spin 1: percolation theory predicts .243 ± .01 (Sykes and Essam, 1964). A more reasonable procedure, perhaps is to replace (z-1) by p(z-1) in 3.10: the average coordination number round each atom of a pair fixed to be magnetic (e.g. Elliott, 1960). The result $p_c = \frac{s+1}{s(z-1)}$ = .286 is obtained for this model at zero temperature, and this compares better with the mean cluster size series result. Accordingly, this is the method used.

Recently a calculation has been performed by Brya and Richards (1973) for the intensity and first moment in several pure antiferromagnets which uses the values of Ritchie and Fisher above and at T_N, with the approp-

riate sign change. Below T_N, empirical approximations are made, invoking molecular field theory at low temperatures and symmetry of I and <w> about T_N. The results of this work are discussed more fully in the following sections.

§3.2 Temperature Dependent Form of the Intensity

The equation used is 2.5,

$$I = \langle B'^2 \sum_{\underline{R},\underline{\delta}} \sum_{\underline{R}',\underline{\delta}'} \underline{S}_{\underline{R}} \cdot \underline{S}_{\underline{R}+\underline{\delta}} \; \underline{S}_{\underline{R}'} \cdot \underline{S}_{\underline{R}'+\underline{\delta}'} \sigma_{\underline{\varepsilon}}^{x} \sigma_{\underline{\varepsilon}}^{y} \sigma_{\underline{\varepsilon}'}^{x} \sigma_{\underline{\varepsilon}'}^{y} \rangle$$

and this will be rewritten as a product of thermal averages denoted by the following:

$$\beta_x = \langle S_{\underline{R}}^{x} S_{\underline{R}+\underline{p}}^{x} \rangle$$

$$\beta_y = \langle S_{\underline{R}}^{y} S_{\underline{R}+\underline{p}}^{y} \rangle$$

$$\beta_z = \langle S_{\underline{R}}^{z} S_{\underline{R}+\underline{p}}^{z} \rangle$$

$$x^2 = \langle S_{\underline{R}}^{X2} \rangle : \; y^2 = \langle S_{\underline{R}}^{y2} \rangle : \; z^2 = \langle S_{\underline{R}}^{z2} \rangle$$

$$\alpha = \langle S_{\underline{R}}^{z} \rangle \quad : \quad \alpha_x = \langle S_{\underline{R}}^{x} \rangle$$

The simplest contribution arises with an occurrence $8Np^2$ when the sites in each product coincide. The trace

$$\langle (S_1^{x} S_2^{x} + S_1^{y} S_2^{y} + S_1^{z} S_2^{z})^2 \rangle = \beta^* \qquad - 3.17$$

must be evaluated.
This term may be easily calculated as a whole in the pair theory in terms of the f_v: however, such a procedure introduces the wrong sign before correlation-like terms such as

$$\langle S_1^x S_2^x S_1^y S_2^y \rangle$$

which is found to be $-1/4\beta_z$ with a small correction. This is because results for the antiferromagnet are obtained from the pair theory results by reversing the sign of J and correlations obtained from that theory. Such sign reversal is carried out without further comment henceforth in the calculations, except for β_x, β_y and β_z, which are understood to be negative quantities. Accordingly, 3.17 is split up into the following terms, which are evaluated by replacing S^x and S^y:

$$S^x = \tfrac{1}{2}(S^+ + S^-)$$
$$S^y = \frac{1}{2i}(S^+ - S^-)$$

by spin creation and annihilation operators. For example,

$$\langle S_1^{x2} S_2^{x2} \rangle = \frac{1}{16}\langle (S_1^+ + S_1^-)(S_1^+ + S_1^-)(S_1^+ + S_2^-)(S_2^+ + S_1^-) \rangle$$
$$= \frac{1}{16}\langle S_1^+ S_1^+ S_2^- S_2^- + S_1^- S_1^- S_2^+ S_2^+ \rangle$$
$$+ \frac{1}{16}\langle (S_1^+ S_1^- + S_1^- S_1^+)(S_2^+ S_2^- + S_2^- S_2^+) \rangle$$

retaining the terms that have non-zero matrix elements for the spin 1 pair. In terms of the eigenfunctions f_v, the following results are obtained.

$$\langle S_1^+ S_1^- S_2^+ S_2^- \rangle = (\tfrac{4}{3}w^6 v^2 + 4w^4 u^3 + \tfrac{8}{3}u^2 + 4u^3 + 4u^4)/Q$$

$$\langle S_1^+ S_1^+ S_2^- S_2^- \rangle = \langle S_1^- S_1^- S_2^+ S_2^+ \rangle$$
$$= (\tfrac{4}{3}w^4 u^2 - 2w^4 u^3 + 3u^2)/Q \quad .$$

$$\langle S_1^- S_1^+ S_2^- S_2^+ \rangle = (\tfrac{4}{3}w^6u^2 + 4w^4u + \tfrac{8}{3}u^2 + 4 + 4u)/Q$$

$$\langle S_1^+ S_1^- S_2^- S_2^+ \rangle = \langle S_1^- S_1^+ S_2^+ S_2^- \rangle = (\tfrac{8}{3}w^6u^2 + 2w^4u + 2w^4u^2 + 2w^4u^3 + 2u + 2u^3 + \tfrac{10}{3}u^2)/Q$$

so that an expression for $\langle S_1^{x2} S_2^{x2} \rangle$ is obtained,

$$\langle S_1^{x2} S_2^{x2} \rangle = \langle S_1^{y2} S_2^{y2} \rangle = \tfrac{1}{16}[\tfrac{32}{3}w^6u^2 + 8w^4 \quad (u+u^3) + 4+8u + \tfrac{40}{3}u^2 + 8u^3 + 4u^4]/Q$$

Similarly, expressions for the following are obtained:

$$\langle S_1^{z2} S_2^{z2} \rangle = (\tfrac{2}{3}w^6u^2 + w^4u^2 + 1 + \tfrac{1}{3}u^2 + u^4)/Q$$

$$\langle S_1^x S_1^y S_2^x S_2^y \rangle = \langle S_1^y S_1^x S_2^y S_2^x \rangle = \tfrac{1}{16}(\tfrac{8}{3}w^6u^2 - 4w^4u^2 + \tfrac{4}{3}u^2)/Q - \tfrac{1}{4}\beta_z.$$

$$\langle S_1^x S_1^z S_2^x S_2^z \rangle = \langle S_1^z S_1^x S_2^z S_2^x \rangle = \langle S_1^z S_1^y S_2^z S_2^y \rangle$$

$$= \langle S_1^y S_1^z S_2^y S_2^z \rangle = \tfrac{1}{4}[+\tfrac{4}{3}w^6u^2 - \tfrac{4}{3}u^2]/Q$$

Accordingly,

$$\beta^* = [\tfrac{11}{3}w^6u^2 + w^4(u+\tfrac{1}{2}u^2+u^3) + \tfrac{3}{2}+u+u^3 + \tfrac{3}{2}u^4+\tfrac{5}{6}u^2] - \tfrac{1}{2}\beta_z.$$

For the longitudinal and transverse intensities, the following traces are required:

$$\beta^L = \langle S_1^z S_2^z S_1^z S_2^z \rangle = (\tfrac{2}{3}w^6u^2 + w^4u^2 + 1 + \tfrac{1}{3}u^2 + u^4)/Q$$

$$\beta^T = \langle (S_1^x S_1^x + S_1^y S_1^y)(S_2^x S_2^x + S_2^y S_2^y) \rangle \qquad - 3.18$$

$$= (\tfrac{5}{3}w^6u^2 + w^4(u-\tfrac{1}{2}u^2+u^3) + \tfrac{1}{2} + u + \tfrac{11}{6}u^2+u^3+\tfrac{1}{2}u^4)/Q - \tfrac{1}{2}\beta_z.$$

A contribution with occurrence $(-8Np^3)$ is found when one of the sites in the first scalar product coincides

with one in the second: the trace required is

$$\langle \underline{S}_{\underline{R}} \cdot \underline{S}_{\underline{R}+\underline{\delta}} \; \underline{S}_{\underline{R}} \cdot \underline{S}_{\underline{R}+\underline{\delta}'} \rangle$$

and this is decoupled as $\langle \underline{S}_{\underline{R}} \cdot \underline{S}_{\underline{R}+\underline{\delta}} \rangle^2$ which is exact at zero temperature. The usual high temperature decoupling of this term is:

$$\langle \underline{S}_{\underline{R}} \cdot \underline{S}_{\underline{R}+\underline{\delta}} \; \underline{S}_{\underline{R}} \cdot \underline{S}_{\underline{R}+\underline{\delta}'} \rangle = \frac{1}{3} S(S+1) \langle \underline{S}_{\underline{R}+\underline{\delta}} \cdot \underline{S}_{\underline{R}+\underline{\delta}'} \rangle + \frac{2}{3}\left[1 - \frac{3}{4s(s+1)}\right] \langle \underline{S}_{\underline{R}} \cdot \underline{S}_{\underline{R}+\underline{\delta}} \rangle \langle \underline{S}_{\underline{R}} \cdot \underline{S}_{\underline{R}+\underline{\delta}'} \rangle \qquad - 3.19$$

which is exact for spin ½, and correct to first non-vanishing order in $\frac{1}{T}$ in a high temperature expansion (Tahir-Kheli and ter Haar, 1962). Possibly the most important difference between the decoupling used and 3.19 is that only 3.19 takes account of the number of common magnetic next-neighbours that sites $(\underline{R}+\underline{\delta})$ and $(\underline{R}+\underline{\delta}')$ may have: when this number is 2, and for spin 1, 3.19 has a coefficient of $(\beta J)^2$ which is bigger by only 8%: when the number is 4, it is bigger by 70%, and when it is 1, smaller by 25%. For the rutile structure, then, at very high temperatures the decoupling used will underestimate by an average of 30%, if a weighted average over the possible configurations $(\underline{R}, \underline{R}+\underline{\delta}, \underline{R}+\underline{\delta}')$ is taken.

However, the rationale behind this work is that a model and decoupling is sought to provide estimates of the moments at all temperatures and concentrations: in addition, the term in p^3 is much smaller at high temperatures than the p^2 term. Throughout this work the trace

of many site diagrams will be required in a two site formalism: the approach taken will be to disregard correlations between different spin compounds on neighbouring sites whenever this will enable the trace to be broken up into one and two site averages: sometimes grosser approximations will be necessary to accomplish this. However, in all cases the decouplings and approximations are correct in the zero and infinite temperature limits.

A contribution in p^4 also arises, when none of the four sites coincides: the zero temperature decoupling

$$\langle \underline{S}_{\underline{R}} \cdot \underline{S}_{\underline{R}+\underline{\delta}} \cdot \underline{S}_{\underline{R}'} \cdot \underline{S}_{\underline{R}'+\underline{\delta}'} \rangle = \langle \underline{S}_{\underline{R}} \cdot \underline{S}_{\underline{R}+\underline{\delta}} \rangle^2$$

is used: this also agrees with the high temperature decoupling, correct to the first order in $\frac{1}{T}$, if the four sites do not form a next neighbour ring. If they do, it underestimates by 25%.

The following expression for the intensity is found:

$$I = NB'^2[16p^2\ \beta^* - (32p^3 - 16p^4)(\beta x + \beta y + \beta z)^2] \qquad - 3.20$$

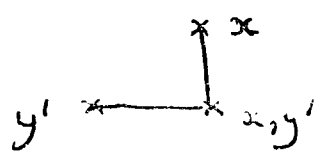
or, in terms of transverse, longitudinal and mixed components,

$$I^T = 16NB'^2[p^2\beta^T - (2p^3 - p^4)(\beta x + \beta y)^2]$$

$$I^L = 16NB'^2[p^2\beta^L - (2p^3 - p^4)(\beta z)^2]$$

$$I^M = 16NB'^2[p^2[\beta^* - \beta^T - \beta^L] - 2(2p^3 - p^4)\beta z(\beta x + \beta y)]$$

Terms like



have been decoupled as $\beta x \beta y$, in the spirit of the preceding work.

All the above intensity results agree with those previously derived in the limits of zero and infinite temperature. Further discussion follows in §3.5.

§3.3 Temperature Dependent First Moment

The thermal average to be considered is

$$\langle \underline{S}_{\underline{R}} \cdot \underline{S}_{\underline{R}+\underline{\delta}} \; \underline{S}_{\underline{R}'} \cdot (\underline{S}_{\underline{R}'+\underline{p}'} \times \underline{S}_{\underline{R}'+\underline{\delta}'}) \rangle \qquad - 3.21$$

As correlations between different components of spins on neighbouring sites are ignored, contributions arise when one or both the sites in the scalar product coincides with sites in the triple product. Equation 3.21 contains eighteen terms, which may be generated by interchange of x,y and z in the following three.

1A $\quad \langle S_{\underline{R}}^{x} S_{\underline{R}+\underline{\delta}}^{x} S_{\underline{R}'}^{x} S_{\underline{R}'+\underline{p}'}^{y} S_{\underline{R}'+\underline{\delta}'}^{z} \rangle$

If the pairs $(\underline{R},\underline{R}+\underline{\delta})$ and $(\underline{R}',\underline{R}'+\underline{p}')$ coincide, terms of the type $\langle S_{\underline{R}}^{x2} S_{\underline{R}+\underline{\delta}}^{x} S_{\underline{R}+\underline{\delta}}^{y} S_{\underline{R}+\underline{\delta}}^{z} \rangle$ are obtained: this can only be handled on a pair theory by decoupling to

$$\langle S_{\underline{R}+\underline{\delta}'}^{z} \rangle \langle S_{\underline{R}}^{x2} \; S_{\underline{R}+\underline{\delta}}^{x} \; S_{\underline{R}+\underline{\delta}}^{y} \rangle \qquad - 3.22a$$

or

$$\langle S_{\underline{R}+\underline{\delta}}^{x} S_{\underline{R}+\underline{\delta}}^{y} \rangle \langle S_{\underline{R}}^{x2} S_{\underline{R}+\underline{\delta}'}^{z} \rangle \qquad - 3.22b$$

However, if the latter term in 3.22a is rewritten in terms of S^+ and S^-, the only terms with matrix elements in the states of the spin 1 pair are

$$- \frac{i}{16}\langle S_1^- S_1^- S_2^+ S_2^+ - S_1^+ S_1^+ S_2^- S_2^- \rangle$$

and $$+ \frac{4i}{16}\langle (S_1^+ S_1^+ + S_1^- S_1^-) S_2^z \rangle$$

The former of these is zero, since sites 1 and 2 are equivalent: the latter may be evaluated as $\frac{i}{4}G$, where

$$G = [1 + u - u^3 - u^4 + w^4(u-u^3)]/Q \qquad - 3.23$$

and is just $\frac{i}{2}\langle S_1^{x2} S_2^z \rangle$, so that 3.22a is

$$\tfrac{i}{2}\langle S_{\underline{R}+\underline{\delta}'}^z \rangle \langle S_{\underline{R}}^{x2} S_{\underline{R}+\underline{\delta}}^z \rangle$$

However, the first term in 3.22b is just $\frac{i}{2}\langle S_{\underline{R}+\underline{\delta}'}^z \rangle$ in the pair theory, since correlations with $S_{\underline{R}}^{x2}$ have already been ignored: both decouplings give the same result ($\frac{1}{4}\langle G$), which is correct at zero and infinite temperature. If x and y are interchanged in 3.22 another such term is obtained: any other interchanges lead to terms like

$$\langle S_{\underline{R}}^{x2} S_{\underline{R}+\underline{\delta}}^x S_{\underline{R}+\underline{\delta}}^z S_{\underline{R}+\underline{\delta}'}^y \rangle \qquad - 3.24$$

When this is decoupled, the two alternatives are

$$\langle S_{\underline{R}+\underline{\delta}'}^y \rangle \langle S_{\underline{R}}^{x2} S_{\underline{R}+\underline{\delta}}^x S_{\underline{R}+\underline{\delta}}^z \rangle$$

in which the first term is zero at once

and $$\langle S_{\underline{R}+\underline{\delta}}^x S_{\underline{R}+\underline{\delta}}^z \rangle \langle S_{\underline{R}}^{x2} S_{\underline{R}+\underline{\delta}'}^y \rangle$$

in which the first term, on a pair theory, is just $-\frac{i}{2}\langle S_{R+\delta}^y \rangle$, again zero.

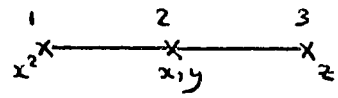
The occurrence of this class of term is $(-8Np^3)$ when phase factors are inserted, and similar terms result from the pairs $(\underline{R},\underline{R}+\underline{\delta})$ and $(\underline{R}',\underline{R}'+\underline{\delta}')$ coinciding, but with occurrences ($56Np^3$), so that the total contribution is $256B'^2JNp^3 \alpha G$.

There are no contributions of order p^4 from such

terms, since correlations between similar spin components not on the same or neighbouring sites are ignored. However, some are found in the terms that follow.

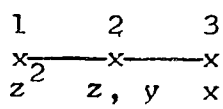
1C $\quad -\langle S_{\underline{R}}{}^{x} S_{\underline{R}+\underline{\delta}}{}^{x} S_{\underline{R}'}{}^{y} S_{\underline{R}'+\underline{\rho}'}{}^{x} S_{\underline{R}'+\underline{\delta}'}{}^{z} \rangle$

When the pairs $(\underline{R},\underline{R}+\underline{\delta})$ and $(\underline{R}',\underline{R}'+\underline{\rho}')$ coincide, a term similar to 3.22 is obtained, which may be represented diagrammatically as



In this term, if correlations between the operators on sites 2 and 3 are neglected, a contribution $(-\frac{i}{4}\alpha G)$ is obtained, the sign acknowledging that the S^z components are on different sublattices. The alternative decoupling is to evaluate $\langle S_1{}^{x2}\rangle\langle S_2{}^{x} S_2{}^{y} S_3{}^{z}\rangle$, but this neglects correlations between $S_1{}^{x2}$ and $S_2{}^{x} S_2{}^{y}$, which are probably just as large as the correlations allowed for between $S_2{}^{x} S_2{}^{y}$ and $S_3{}^{z}$. Obviously an arbitrary choice between these schemes must be made, and the latter is chosen, to be consistent with the only decoupling that yields a contribution when x and z are interchanged. The contribution resulting from this is easily shown to be $(\frac{1}{2}x^2\beta z)$ in the pair model, and the corresponding occurrence factor is $(+56Np^3)$.

When x and z are interchanged, to give



- then, since $S_1{}^{z2}$ is diagonal in the pair representation of (1,2), this may be reasonably approximated to give

$$\langle S_1^{z2}\rangle\langle S_2^{z} S_2^{y} S_3^{x}\rangle$$

where now the latter trace is to be considered in the pair formalism. Again replacing S^y and S^x by creation and annihilation operators, the product $\frac{1}{4i}\langle S_2^{z}(S_2^{+}-S_2^{-})(S_3^{+}+S_3^{-})\rangle$ is obtained. The non-zero parts of this are

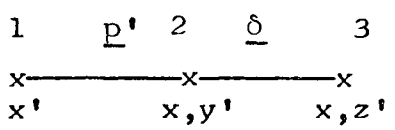
$$\frac{1}{4i}\langle S_2^{z}(S_2^{+}S_3^{-} - S_2^{-}S_3^{+})\rangle \qquad - 3.25$$

which may be evaluated exactly in terms of the pair eigenfunctions, f_v: when this is done, the result is seen to be

$$\langle S_2^{z}(S_2^{+}S_3^{-} - S_2^{-}S_3^{+})\rangle = +2(\beta x+\beta y)$$

so that 3.25 is $(-\frac{1}{2}i\beta x)$. Terms of this type therefore contribute $(-\frac{1}{2}i\beta x z^2)$, and have occurrence $(56p^3N)$. Similar terms occur with the interchange of y and z in 1C: these are decoupled as $(\frac{1}{5}y^2\beta x)$ on the same basis.

If the pairs $(\underline{R},\underline{R}+\underline{\delta})$ and $(\underline{R}',\underline{R}'+\underline{\delta}')$ coincide, terms of the type:



are obtained. These can not be handled in a pair theory, since none of these sites carries only diagonal spin operators: however, if x and z are interchanged, the result may be approximated by:

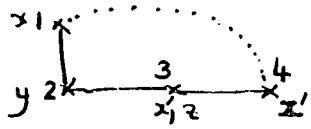
$$\langle S_1^{z}\rangle\langle S_2^{z} S_2^{y} S_3^{z} S_3^{x}\rangle$$

The latter trace may be written as

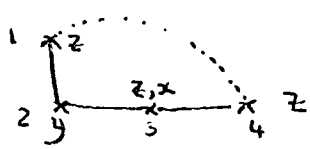
$$\frac{1}{4i}\langle S_2^{z} S_3^{z}(S_2^{+}-S_2^{-})(S_3^{+}+S_3^{-})\rangle$$

for the pair, and the only possible contributing terms of this are $\frac{1}{4i}\langle S_2^{z} S_3^{z}(S_2^{+}S_3^{-} - S_2^{-}S_3^{+})\rangle$ - 3.26

In fact, 3.26 contributes zero for the spin 1 pair, since all contributing states have either S_2^z or S_3^z zero. With this as a guide, all the terms of this type with x,y and z interchanged are put equal to zero. Terms in p^4 also occur in 1C: a typical one may be represented diagrammatically as :



The dotted line indicates that sites 1 and 4 may be neighbours. Since neither of the spin operators on sites 2 or 4 are diagonal, an obvious decoupling leaving a part to be considered as before cannot be performed. The result for 3.25, however, encourages us just to replace S^xS^z by $-\frac{1}{2}S^y$ on site 3: this is unlikely to be very wrong, and in any case this term is small. The only contribution then is when 1 and 4 are neighbours (with occurrence $-32Np^4$), and the appropriate trace is taken to be $(-\frac{1}{2}\beta x\beta y)$. If x and y or y and z are interchanged, the term resulting is represented by



This is decoupled to

$$\langle S_1^z\rangle\langle S_4^z\rangle\langle S_2^y S_3^z S_3^x\rangle$$

or $$\beta z\ \langle S_2^y S_3^z S_3^x\rangle$$

if 1 and 4 are neighbouring sites. The trace is just that

which led to 3.25, but with x and y interchanged: it may therefore be replaced by $(\frac{i}{2}\beta y)$.

In this way, the contribution of the six terms of type 1C is found to be

$$B'^2JN[-32p^3(\beta x(y^2+z^2) + \beta y(x^2+z^2) + \beta z(x^2+y^2) + 256p^4(\beta x\beta y+\beta x\beta z+\beta y\beta z) - 288p^4\alpha^2(\beta x+\beta y)] \qquad - 3.27$$

1D $\quad <S_{\underline{R}}{}^{x}S_{\underline{R}+\underline{\delta}}{}^{x}S_{\underline{R}'}{}^{y}S_{\underline{R}'+\underline{p}'}{}^{z}S_{\underline{R}'+\underline{\delta}'}{}^{x}>$

The traces appearing in this term are just the same as those in 1C, but with different occurrences: the result is:

$$B'^2J\,N[-224p^3(\beta x(y^2+z^2)+\beta y(x^2+z^2)+\beta z(x^2+y^2) + 256p^4(\beta x\beta y+\beta x\beta z+\beta y\beta z)+ 288p^4\alpha^2(\beta x+\beta y)]$$

so that

$$\hbar<\omega> = B'^2JN[256p^3\alpha G-256p^3(\beta x(y^2+z^2)+\beta y(x^2+z^2) + \beta z(x^2+y^2)) + 512p^4(\beta x\beta y+\beta x\beta z+\beta y\beta z)] \qquad - 3.28$$

Again, the first moment is split into transverse, longitudinal and mixed components: of the terms already studied, 1B, 1D, 1E, 1F, 2B, 2D, 2E and 2F are transverse, and 3A and 3C are longitudinal.

In addition, terms due to P, Q, R and S of equation 2.189 must be considered.

$$P+Q = -2B'J \sum_{R,\delta} \sigma_{\underline{\delta}}{}^{x}\sigma_{\underline{\delta}}{}^{y}(S_{\underline{R}}{}^{x}S_{\underline{R}+\underline{\delta}}{}^{x} + S_{\underline{R}}{}^{y}S_{\underline{R}+\underline{\delta}}{}^{y})$$

These are simply shown to contribute $(-32B'^2JNp^2\beta^T)$ to the transverse first moment, and $(+16B'^2JNp^2(\beta^*-\beta^T-\beta^L))$ to $\hbar<\omega>^L$ in order p^2.

Now consider

$$R+S = 4iB'J \sum_{\underline{R},\underline{\delta}} \sigma_{\underline{\delta}}{}^{x}\sigma_{\underline{\delta}}{}^{y} \quad (S_{\underline{R}}{}^{y}S_{\underline{R}+\underline{\delta}}{}^{x}S_{\underline{R}+\underline{\delta}}{}^{z} - S_{\underline{R}}{}^{x}S_{\underline{R}+\underline{\delta}}{}^{y}S_{\underline{R}+\underline{\delta}}{}^{z})$$

1R $\quad <S_{\underline{R}}{}^{x}S_{\underline{R}+\underline{\delta}}{}^{x}S_{\underline{R}'}{}^{y}S_{\underline{R}'+\underline{\delta}'}{}^{x}S_{\underline{R}'+\underline{\delta}'}{}^{z}>$

When the pairs of sites coincide, and the usual replacements are made, only the terms

$$X = <(S_1{}^{-}S_1{}^{-}S_2{}^{+}S_2{}^{+}-S_1{}^{+}S_1{}^{+}S_2{}^{-}S_2{}^{-})S_2{}^{z}> \qquad - 3.29$$

and $$Y = -2<S_1{}^{z}(S_1{}^{+}S_1{}^{-}+S_1{}^{-}S_1{}^{+})S_2{}^{z}> \qquad - 3.30$$

are found to contribute. An equal contribution is found from 2S.

1S $\quad - <S_{\underline{R}}{}^{x}S_{\underline{R}+\underline{\delta}}{}^{x}S_{\underline{R}'}{}^{x}S_{\underline{R}'+\underline{\delta}'}{}^{y}S_{\underline{R}'+\underline{\delta}'}{}^{z}>$

Again, when the pairs of sites coincide, contributions are only found from a term like 3.29 and also from

$$Z = -2<(S_1{}^{+}S_1{}^{-} + S_1{}^{-}S_1{}^{+})S_2{}^{z}S_2{}^{z}> \qquad - 3.31$$

These three terms are evaluated in terms of pair functions as follows,

$$X = (-\tfrac{8}{3}w^6u^2 + 4w^4u^2 - \tfrac{4}{3}u^2)/Q$$

$$Y = (\tfrac{8}{3}w^6u^2 + 4w^4u^2 - 4 + \tfrac{4}{3}u^2 - 4u^4)/Q$$

$$Z = -2(\tfrac{4}{3}w^6u^2+2w^4(u+u^2+u^3)+2+2u+\tfrac{2}{3}u^2+2u^3+2u^4)/Q$$

Remembering that these have been evaluated for a ferromagnetic pair, so that the sign of Y should be reversed, the following contribution is obtained:

$$TT = +8Np^2B'^2J[+8+4u+\tfrac{8}{3}u^2+4u^3+8u^4+w^4(4u-8u^2+4u^3) + \tfrac{16}{3}w^6u^2]/Q$$

to the transverse moment.

Terms in the transverse moment also come in order p^3 and p^4 from P, Q, R and S: if the site carrying two operators in R or S does not coincide with a site in 1

or 2, they may be contracted to S^y or S^x to a reasonable approximation, and then each term in R will cancel with a corresponding term involving Q, and similarly for P and S. The remaining terms in p^3 cannot be approximated consistently in this work, and are small in comparison to the p^2 terms: they are therefore discarded. The approximate result for $<\omega>^T$ is:

$$\hbar<\omega>^T = B'^2JN[224p^3\alpha G - 256p^3(x^2\beta y + y^2\beta x) - 224p^3(x^2+y^2)\beta z + 256p^4(\beta x\beta y + \beta x\beta z + \beta y\beta z) - 32p^2\beta^T] + TT.$$

The terms introduced by R and S into $<\omega>^L$ are

$$\underline{3R} \qquad 4i<S_{\underline{R}}{}^z S_{\underline{R}+\underline{\delta}}{}^z S_{\underline{R}'}{}^y S_{\underline{R}'+\underline{\delta}}{}^x S_{\underline{R}'+\underline{\delta}'}{}^z>$$

The trace on the pair $(\underline{R},\underline{R}+\underline{\delta})$ is

$$<S_1{}^z(S_1{}^+ - S_1{}^-)S_2{}^z(S_2{}^+ + S_2{}^-)S_2{}^z>$$

in terms of creation and annihilation operators. This has zero trace for the spin 1 pair, since $<S_2{}^z>$ is zero for one of any pair of states linked by $S_2{}^+$ or $S_2{}^-$. 3S is also found to give zero. Again neglecting terms in p^3, the result is found that

$$\hbar<\omega>^L = B'^2JN[-224p^3z^2(\beta x+\beta y) + 128p^4\beta_z(\beta x+\beta y) - 288p^4\alpha^2(\beta x+\beta y) + 16p^2(\beta^x - \beta^T - \beta^L)]$$

$$\hbar<\omega>^M = h<\omega> - h<\omega>^T - h<\omega>^L.$$

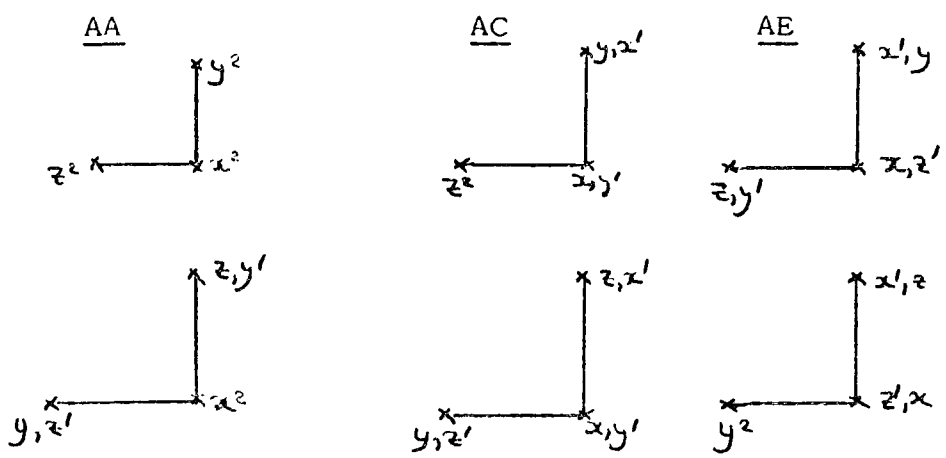
§3.4 Temperature Dependent Second Moment

The thermal average to be approximated is

$$\langle \underline{S}_{\underline{R}} \cdot (\underline{S}_{\underline{R}+\underline{p}} \times \underline{S}_{\underline{R}+\underline{\delta}}) \underline{S}_{\underline{R}'} \cdot (\underline{S}_{\underline{R}'+\underline{p}'} \times \underline{S}_{\underline{R}'+\underline{\delta}'}) \rangle \qquad - 3.31$$

The calculation here is considerably more complicated, as terms in p^3, p^4, p^5 and p^6 may occur and be non-zero in the approximation used. All thirty six terms in 3.31 may be obtained by interchange of x,y and z in the six terms AA, AB, AC, AD, AE and AF, so long as terms involving αx or αy are retained when interchange will lead to the replacement of all the αx or αy by α. A short description follows of the type of term encountered at each order of p. Use is made of the fact that diagrams representing terms in AA, AC and AE also represent terms in AB, AD and AF respectively with $\underline{p}'$ and $\underline{\delta}'$ interchanged.

Terms in p^3



The table indicates the terms that arise in each case, it being understood that all interchanges of spin coordinates in the above diagrams also occur. In the first term in

AA, the arbitrary decoupling to $\langle S^{z2}\rangle\langle S_1{}^{x2}S_2{}^{y2}\rangle$ might be made, and $\langle S_1{}^{x2}S_2{}^{y2}\rangle$ evaluated in the pair model: however, when x and z were interchanged, another arbitrary decoupling would be required. Correlations between different spin components or neighbouring sites are therefore ignored, and the decoupling to $(x^2y^2z^2)$ made.

The second term presents more difficulty: in the previous section, it was found that in the pair theory S^{x2} is effectively diagonal, so that an operator combination on a neighbouring site could be contracted to a reasonable approximation by use of $S^xS^y = \frac{i}{2}S^z$ and so on. Here there are two neighbouring sites to the one with S^{x2}, so that the position is not clear: however, the procedure adopted is to carry out a contraction on both sites, and decouple the resulting trace as $(\frac{1}{4}\beta x^2)$.

The first term in AC may be decoupled as

$$\langle S_1{}^{z2}\rangle\langle S_2{}^{x}S_2{}^{y}S_3{}^{y}S_3{}^{x}\rangle$$

and the spin components in the latter trace replaced by creation and annihilation operators to give:

$$-\frac{1}{16}\langle(S_2{}^{+}+S_2{}^{-})(S_2{}^{+}-S_2{}^{-})(S_3{}^{+}-S_3{}^{-})(S_3{}^{+}+S_3{}^{-})\rangle$$

The terms that contribute in the pair theory are:

$$+\frac{1}{16}\langle S_2{}^{+}S_2{}^{+}S_3{}^{-}S_3{}^{-} + S_2{}^{-}S_2{}^{-}S_3{}^{+}S_3{}^{+}\rangle \qquad - 3.32$$

and $$-\frac{1}{16}\langle(S_2{}^{-}S_2{}^{+} - S_2{}^{+}S_2{}^{-})(S_3{}^{+}S_3{}^{-} - S_3{}^{-}S_3{}^{+})\rangle$$

$$= \frac{1}{4}\langle S_2{}^{z}S_3{}^{z}\rangle \qquad - 3.33$$

Equation 3.32 may be evaluated as

$$F_1 = \frac{1}{4}(\frac{2}{3}w^6u^2 - w^4u^2 + \frac{1}{3}u^2)/Q$$

in the notation of §3.1, and AC is decoupled as $(z^2(F_1+\frac{1}{4}\beta z))$. The same result is found with x and y interchanged. If z and x are interchanged, the result is decoupled as

$$\langle S_1^{x2}\rangle\langle S_2^z S_2^y S_3^y S_3^z\rangle$$

since S^{x2} is effectively diagonal: the second trace can be easily shown to be

$$F_2 = -\frac{1}{4}((u^3+u)(w^4-1))/Q$$

There is also the same term with y and z interchanged to consider, contributing

$$\langle S_1^{x2}\rangle\langle S_2^y S_2^z S_3^z S_3^y\rangle$$

Commutation in the second trace yields

$$\langle(iS_2^x+S_2^zS_2^y)(-iS_3^x+S_3^yS_3^z)\rangle$$
$$= \langle S_2^xS_3^x\rangle + i\langle S_2^xS_3^yS_3^z - S_3^xS_2^zS_2^y\rangle + F_2.$$

It has been previously shown that $\langle S_2^xS_3^yS_3^z\rangle = \frac{i}{2}\beta x$ on the pair model: this term therefore also contributes F_2. In fact F_2 differs from $(\frac{1}{4}\beta x)$ only by

$$F_2 = \frac{1}{4}\beta x - (\frac{4}{3}u^2 - \frac{4}{3}w^6u^2)/Q$$

Again, the choice of a decoupling to a pair term and a single site term is rather arbitrary, but does at least allow a consistent treatment of both the above terms: it is, furthermore, correct at low and infinite temperatures.

The second term in AC is more difficult to deal with: however, it contains terms of the type considered in 1C and set to zero. These terms are again set to zero. In

any case, any contribution would be small.

The traces in AE are the same as for AC, and the same approximations are made. The following contribution is obtained:

$$16NB'^2J^2p^3[384(x^2y^2z^2) - 256(z^2(\tfrac{1}{4}\beta z+F_1) + (x^2+y^2)F_2) - 32(\beta x^2+\beta y^2+\beta z^2)] \qquad - 3.34$$

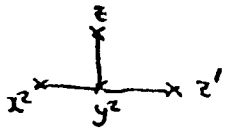
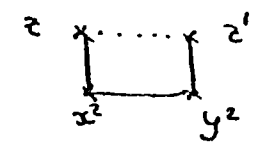
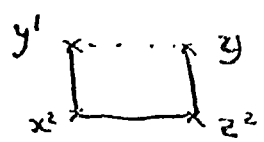
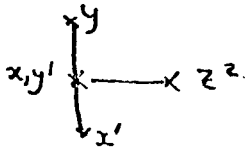
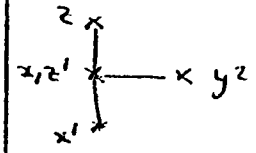
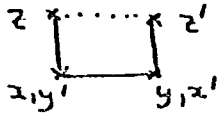
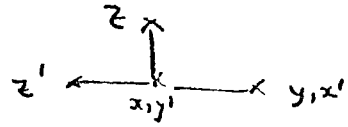
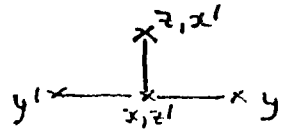
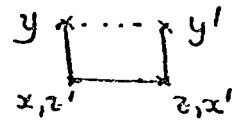
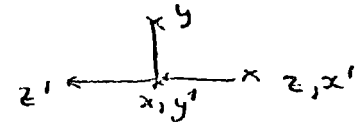
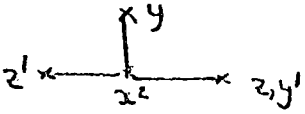
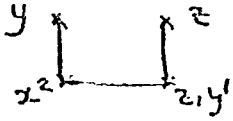
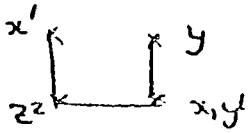
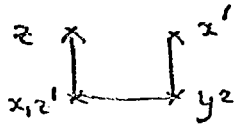
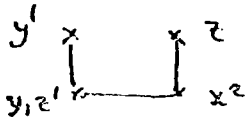
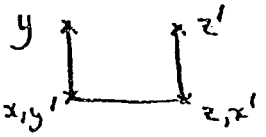
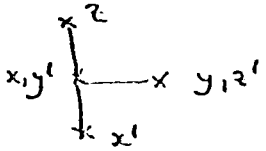
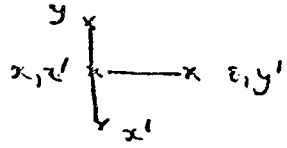
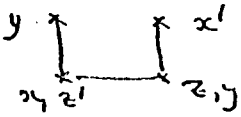
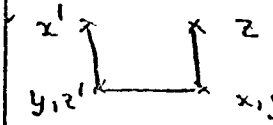
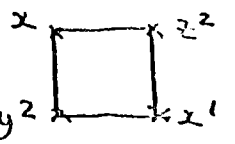
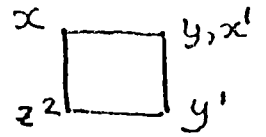
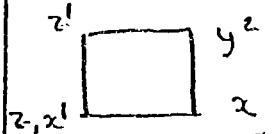
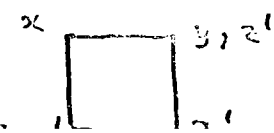
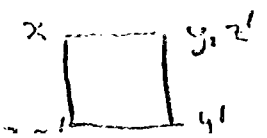
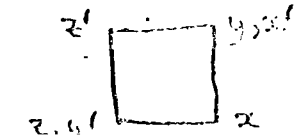
Terms in p^4

Table 1 shows the ten traces of four sites which result from each term AA. The first and second are decoupled as $(x^2y^2\alpha^2)$ and $(x^2z^2\alpha y^2)$: the third is decoupled as $\beta z(\frac{1}{4}\beta z+F_1)$.

If z and x or z and y are interchanged, a diagram of type 4 is obtained (and vice versa): the correlation between S^y and S^xS^z on neighbouring sites is arbitrarily ignored, and the $\langle S_1^xS_1^zS_2^zS_2^x\rangle$ term resulting is F_2, so that if the sites joined by a dotted line are neighbours, a contribution βyF_2 is obtained. The fifth and sixth terms do not contribute: the seventh and eighth are decoupled as $\beta x\beta y\beta z$, on the same principle as led to $S_1^xS_2^xS_2^yS_3^y$ being decoupled as $\beta x\beta y$ in the intensity. The ninth is just $(z^2y^2\alpha x^2)$, and the tenth is arbitrarily decoupled as $\langle S_1^xS_2^yS_2^z\rangle\langle S_3^xS_4^zS_4^y\rangle$, which is $\frac{1}{4}\beta x^2$ by the result used for term 1C. Some of these decouplings involve approximation to an extent that is hard to estimate in a pair model. It is not obvious, however, how they could be improved.

Spin Diagrams of Four Sites

Table 1

	AA	AC	AE
1			
2			
3			
4			
5			
6			
7			
8			
9			
10			

AC and AE have a common set of spin diagrams and decouplings, with different occurrence factors. Term 1 is decoupled as $(-x^2y^2\alpha^2)$ or $x^2y^2\beta z$: term 2 as $z^2\beta x\beta y$, in line with previous practice. Term 3 is decoupled as $\alpha^2\langle S_1^x S_1^y S_2^y S_2^x\rangle$, or $\alpha^2(\frac{1}{4}\beta z + F_1)$, as before. If z and x or z and y are interchanged in 3, terms in $\alpha y^2 F_2$ would be obtained, which are of course zero. In terms 4 and 7, a rather complicated mixture of operators appears, which cannot be estimated in a pair theory: the rather arbitrary approximation is made of replacing these by $\alpha^2\beta x\beta y$, where correlation between different components of spin on the same site is ignored. On the same principle, terms 5 and 6 are approximated by $\alpha y^2x^2\beta^z$ and $\alpha x^2y^2\beta^z$ respectively. In terms 8 and 10, the product is arbitrarily decoupled as $\langle S_1^y S_2^x S_2^z\rangle\langle S_3^x S_4^z S_4^y\rangle$, which is, by previous results, $\frac{1}{4}\beta x\beta y$. Term 9 is decoupled as $z^2\beta x\beta y$.

Occurrences may now be inserted, in rather a lengthy calculation, to give the result:

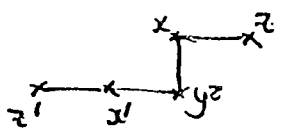
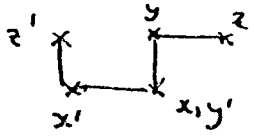
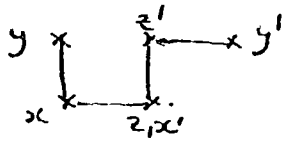
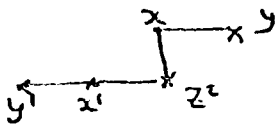
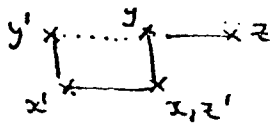
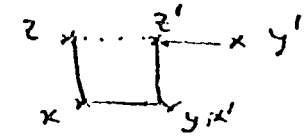
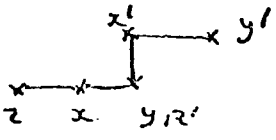
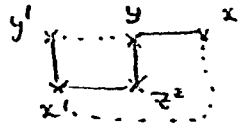
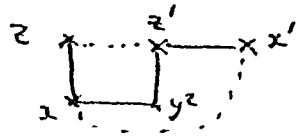
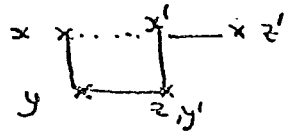
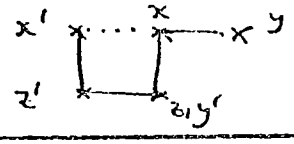
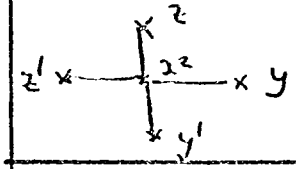
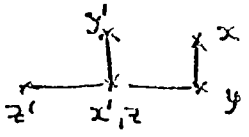
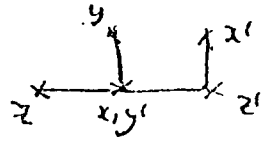
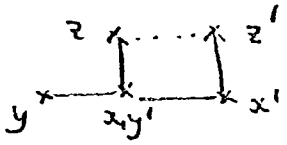
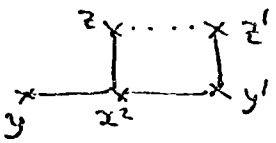
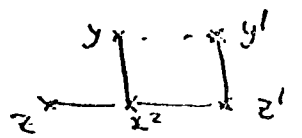
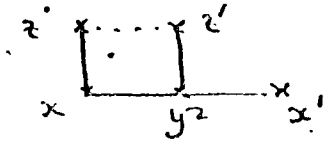
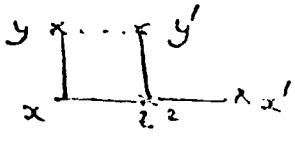
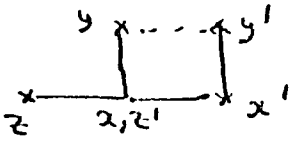
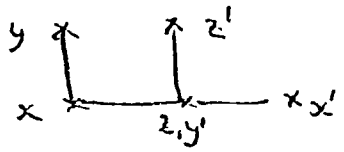
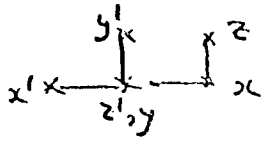
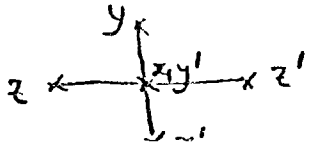
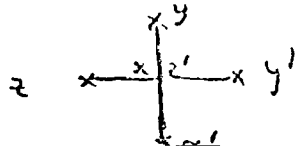
$$16NB'^2J^2p^4\,[1280x^2y^2\alpha^2-384(x^2y^2\beta z+y^2z^2\beta x+x^2z^2\beta y)$$
$$+1024(\beta z(\tfrac{1}{4}\beta z+F_1)+(\beta x+\beta y)F_2)-768\alpha^2(\tfrac{1}{4}\beta z+F_2)$$
$$+32(\beta x^2+\beta y^2+\beta z^2)+320(\beta z\beta y+\beta x\beta z+\beta y\beta z)$$
$$-512(z^2\beta x\beta y+x^2\beta y\beta z+y^2\beta x\beta z)-3072\beta x\beta y\beta z+1536\ \alpha^2(\beta x\beta y)$$
$$+1024\ \alpha^2(x^2\beta y+y^2\beta x)].$$

Terms in p^5

Again, the spin diagrams required are tabulated, in Table 2. The decouplings are now much easier to perform,

Spin Diagrams of Five Sites

Table 2

	AA	AC	AE
1.			
2			
3			
4	No 3		
5			
6			
7	No 6		
8			
9	No 8		

but the occurrences are harder to calculate.

Terms 1, 2, 3, 4 and 5 of AA may not be decoupled as other than zero: terms 6 and 8 are simply decoupled as $\beta x\beta y\beta z$ if the sites joined by dotted lines are nearest neighbours, and $(-\beta x\beta y\alpha^2)$ and $(-\beta x\beta z\alpha y^2)$ respectively otherwise, with no new procedures being invoked.

AC and AE contribute the same spin diagrams again, but with different occurrences. Terms 1, 2 and 4 are decoupled as terms like $(\beta x\beta y\alpha^2)$, if sites joined by dotted lines are next neighbours. This is rather arbitrary, for terms 2 and 4, but is in line with the approximation made previously. Term 3 is decoupled as $z^2\beta x\beta y$, if both dotted lines take effect, and as terms like $(-z^2\beta x\alpha y^2)$ if only one does. Terms 5 and 8 give no contribution: terms 6 and 7 are decoupled as terms like $(x^2\alpha y^2\beta z)$, if the dotted line takes effect. Term 9 is decoupled as $(\alpha^2\beta x\beta y)$, on the principle earlier adopted. Again, no new procedures are invoked.

The occurrences may now be inserted, and interchange of x,y and z performed: the resulting contribution is:

$$16NB'^2J^2p^5[3840\beta x\beta y\beta z + 512\alpha^2\beta x\beta y + 128[z^2\beta x\beta y+x^2\beta y\beta x+y^2\beta x\beta z]-1280\alpha^2[x^2\beta y+y^2\beta x]] \qquad - 3.35$$

Terms in p^6

Such terms are produced when none of the sites coincide, but both the x and y spin components in the

triple products lie on neighbouring sites. Obvious decouplings are made to produce terms in $(\beta x\beta y\beta z)$ and $(\alpha^2\beta x\beta y)$: the result is

$$16NB'^2J^2p^6[384\beta x\beta y\beta z + 256\alpha^2\beta x\beta y] \qquad - 3.36$$

The required occurrences are again in Appendix 1.

The following result is obtained for $\hbar^2\langle\omega^2\rangle$.

$$\begin{aligned}\hbar^2\langle\omega^2\rangle = 16NB'^2J^2[&384p^3x^2y^2z^2-32p^3(\beta x^2+\beta y^2+\beta z^2)\\
&-256p^3[z^2(\tfrac{1}{4}\beta z+F_2)+(x^2+y^2)F_2]+ 1280p^4x^2y^2\alpha^2\\
&-384p^4(x^2y^2\beta z+y^2z^2\beta x+x^2z^2\beta y) + 1024p^4(\beta_z(\tfrac{1}{4}\beta z+F_2)\\
&+(\beta x+\beta y)(F_2)) + 32p^4(\beta x^2+\beta y^2+\beta z^2) - 768p^4\alpha^2(\tfrac{1}{4}\beta z+F_1)\\
&+320p^4(\beta x\beta y+\beta x\beta z+\beta y\beta z) - 512p^4(z^2\beta x\beta y+x^2\beta y\beta z+y^2\beta x\beta z)\\
&-3072p^4\beta x\beta y\beta z+1536p^4\alpha^2\beta x\beta y+1024p^4\alpha^2(x^2\beta y+y^2\beta x)\\
&+128p^5(x^2\beta y\beta z+y^2\beta x\beta z+z^2\beta x\beta y) - 1280p^5\alpha^2(x^2\beta y+y^2\beta x)\\
&+3840p^5\beta x\beta y\beta z+512p^5\alpha^2\beta x\beta y+384p^6\beta x\beta y\beta z+256p^6\alpha^2\beta x\beta y].\end{aligned}$$

When the separation into components is made, fresh terms have to be considered. Those arising from P and Q are just

$$-64B'^2J^2N[p^2\beta^T - (2p^3-p^4)(\beta x+\beta y)^2]$$

for the transverse second moment, and an equal contribution for the longitudinal second moment. For each term of the type PA or PR there is an equal and opposite term AP or RP: the only other terms to be considered are those arising from R and S with A to F, or R and S or P and Q. Some of these are large: those arising from R and S with B and D give a contribution $(3584S^4-1792S^3)NB'^2J^2p^3$ in the Néel state, for example. However, they are

extremely difficult to calculate and so the same procedure as for the first moment is adopted: only terms which have a Néel state contribution are calculated. The results for the various types of term follow for $\langle\omega^2\rangle^T$ only, and are correct in the zero and infinite temperature limits.

1) $\langle(P,Q),(R,S)\rangle + \langle(R,S),(P,Q)\rangle$

$\langle(P,Q),(R,S)\rangle$ are essentially the same terms as $\langle(1,2),(R,S)\rangle$ evaluated for the first moment. It will be recalled that PR produced terms like:

$$\frac{1}{16i}\langle(S_1^+ S_1^+ S_2^- S_2^- - S_1^- S_1^- S_2^+ S_2^+)S_2^z\rangle$$

and $$\frac{1}{16i}\langle(-2S_1^z)(S_2^+ S_2^- + S_2^- S_2^+)S_2^z\rangle$$

RP is found to produce the same terms, but with the sign of the second reversed, and in addition a term $\langle S_1^y S_1^x S_2^x S_2^y\rangle$, which was previously found to be $(\frac{1}{4}\beta z + F_1)$. Similarly, when PS and SP are added together, another term like the above is found, as well as a new term $\langle S_1^{y2} S_2^{x2}\rangle$. This term has been decoupled just as (x^2y^2) in the past, when in association with other operators: now that there is just a pair, it is evaluated and found to be

$$F_3 = \frac{1}{16}[\frac{16}{3}w^6u^2 + 8w^4(u+u^3) + 8w^4u^2 + 4 + 8u^2 + \frac{32}{3}u^2 + 8u^3 + 4u^4]/Q$$

On adding together all eight terms of this type, the result to order p^2 is found to be

$$-B'^2J^2Np^2[256(\tfrac{1}{4}\beta z + F_2) - 256F_3 + 64X]$$

2) $\langle(R,S),(R,S)\rangle$

New terms are introduced here: consider RR.

$$-16\langle S_{\underline{R}}^{y} S_{\underline{R}+\underline{\delta}}^{x} S_{\underline{R}+\underline{\delta}}^{z} S_{\underline{R}'}^{y} S_{\underline{R}'+\underline{\delta}'}^{x} S_{\underline{R}'+\underline{\delta}'}^{z}\rangle$$

If $\underline{R}$ and $\underline{R}'$ coincide, and $\underline{\delta}$ and $\underline{\delta}'$, the term

$$\langle S_1^{y2} S_2^{x} [iS_2^{y} + S_2^{x} S_2^{z}] S_2^{z}\rangle$$

is obtained on performing the commutation. The first term is similar to those obtained in the previous class of terms: the latter, $\langle S_1^{y2} S_2^{x2} S_2^{z2}\rangle$, is new. Different terms are obtained if $\underline{R} = \underline{R}' + \underline{\delta}'$ and $\underline{R}' = \underline{R} + \underline{\delta}$. The following contribution is found when all four terms are added:

$$-16p^2 [32\langle S_1^{y2} S_2^{x2} S_1^{z} S_2^{z})\rangle + 32\langle S_1^{y} S_1^{x} S_2^{x} S_2^{y} S_2^{z2}\rangle$$

$$+ 4\langle S_1^{z2}(S_2^{+}S_2^{-} + S_2^{-}S_2^{+})\rangle - 4\langle S_1^{z} S_2^{z}(S_1^{+}S_2^{-} + S_1^{-}S_1^{+})\rangle]$$

These terms are evaluated in the pair model: it should be remembered that in this model sign changes are needed in all but the third term. In terms of the pair eigenfunctions the contribution is

$$-16p^2 B^2 J^2 N[8w^4(u+4u^2+u^3) + 8u + 8u^3]/Q.$$

3) $\langle(R,S),(B,D)\rangle + \langle(B,D),(R,S)\rangle$

These are the only terms that have a contribution in the Néel state. On performing the same sort of calculation as before, regarding the S^z on site $(\underline{R}+\underline{p})$ as decoupled from the other terms, the following contribution in p^3 is obtained.

$$3584\alpha Np^3B'^2J^2[i[\langle S_1^y S_1^x S_2^{x2}\rangle - \langle S_1^x S_1^y S_2^{y2}\rangle]$$

$$-[\langle S_1^{x2} S_2^{y2} S_2^z\rangle + \langle S_1^{y2} S_2^{x2} S_2^z\rangle]-[\langle S_1^y S_1^x S_2^x S_2^y (S_1^z+S_2^z)\rangle]$$

When the traces are evaluated in terms of w and u, the following results:

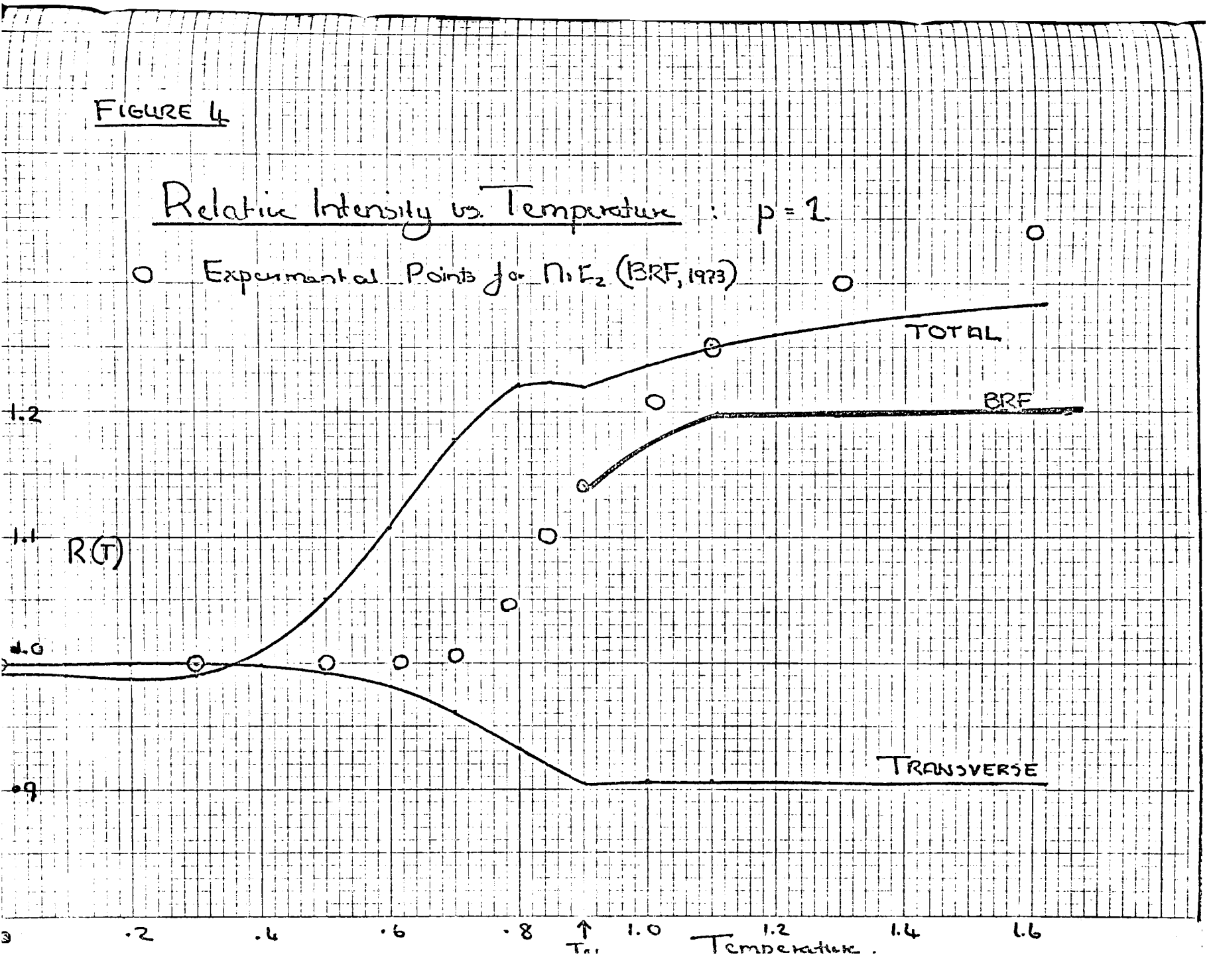
$$3584\alpha Np^3B'^2J^2[\tfrac{1}{2}-\tfrac{1}{2}u+\tfrac{1}{2}u^3-\tfrac{1}{2}u^4]$$

In detailed work of this sort, it is rather hard to guard against mistakes: however, all the expressions used have been checked that they reduce to the correct limit at zero and infinite temperature, as have the results of each addition. The result obtained is the following:

$$\begin{aligned}\hbar^2\langle\omega^2\rangle^T = {} & 16NB'^2J^2[240p^3x^2y^2z^2-32p^3\beta z^2-2p^3(\beta x^2+\beta y^2)\\
&-112p^3z^2(\tfrac{1}{4}\beta z+F_1)-128p^3(x^2+y^2)F_2+1136p^4x^2y^2\alpha^2-192p^4x^2y^2\beta z\\
&-128p^4(x^2z^2\beta y+y^2z^2\beta x)+32p^4\beta z^2+784p^4\beta^2(\tfrac{1}{4}\beta z+F_1)\\
&+520p^4(\beta x+\beta y)F_2+8p^4(\beta x^2+\beta y^2)+20p^4\beta x\beta y+256p^4\beta z(\beta x+\beta y)\\
&+160p^4z^2\beta x\beta y-640p^4(x^2\beta y\beta z+y^2\beta x\beta z)-1284\beta x\beta y\beta zp^4\\
&+1536p^4\alpha^2\beta x\beta y+896p^4\alpha^2(x^2\beta y+y^2\beta x)-672\alpha^2(\tfrac{1}{4}\beta z+F_1)p^4\\
&+128p^5(y^2\beta x\beta z+x^2\beta y\beta z)-32p^5z^2\beta x\beta y-1408p^5\alpha^2(x^2\beta y+y^2\beta x)\\
&+1792p^5\beta x\beta y\beta z+1520p^5\alpha^2\beta x\beta y+320p^6\beta x\beta y\beta z+320p^6\alpha^2\beta x\beta y)\\
&-64B'^2J^2N[p^2\beta^T-(2p^3-p^4)(\beta x+\beta y)^2]-B'^2J^2Np^2[256(\tfrac{1}{4}\beta z+F_2)\\
&-256F_3+64X]-16B'^2J^2Np^2[8w^4(u+4u^2+u^3)+8u+8u^3]/Q\\
&+3584\alpha Np^3B'^2J^2[\tfrac{1}{2}-\tfrac{1}{2}u+\tfrac{1}{2}u^3-\tfrac{1}{2}u^4]/Q \qquad - 3.37\end{aligned}$$

This result reduces to that of Chapter 2 in the zero temperature limit, and is also correct in the infinite temperature limit, as are all the decouplings used. This is simply verified, since at $T=0$, $u=w=0$ and at $T\to\infty$, $u=w=1$.

FIGURE 4


Relative Intensity vs. Temperature : p = 2
Experimental Points for Nb_3Sn (BRF, 1973)
TOTAL
BRF
TRANSVERSE
R(T)
1.2
1.1
1.0
.9
.2
.4
.6
.8
T_c
1.0
1.2
1.4
1.6
Temperature.

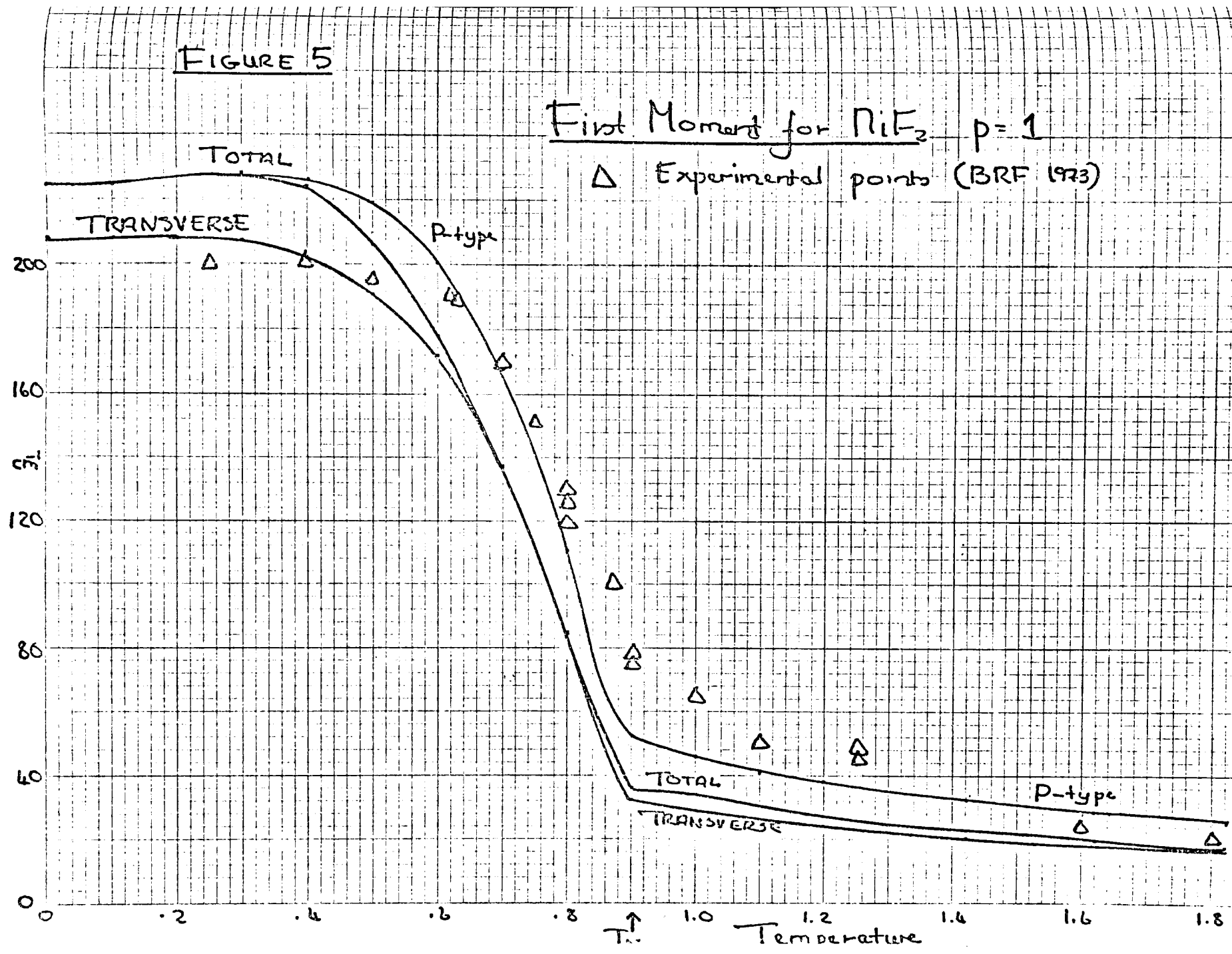
§3.5 Results for the Finite Temperature Moments

In this section comparison is made between the predictions of the moment formulae derived previously and recent experimental work on pure NiF_2 by Brya and Richards, and Fleury (1973) - henceforward referred to as BRF. The zeroth, first and second moments are also plotted for a number of different concentrations and a range of temperatures, although there are as yet no experimental results on two magnon Raman scattering in diluted antiferromagnets.

The simplest quantity to discuss is the intensity ratio R(T) defined as the intensity at some temperature T divided by zero temperature intensity. Such a procedure avoids the great experimental difficulty of measuring an absolute intensity, and obviates the need to calculate the constant B' in the interaction Hamiltonian. As discussed in §2, BRF subtract off the background due to phonon scattering, and, for NiF_2, the rather strong optical absorption, to obtain consistent estimates of the magnetic scattering profile, which allows calculation of relative intensities and the first moment. Fig. 4 shows the results of this for the intensity in the (xy) scattering geometry, together with the predictions of §3.2 for p=1. The 'total' intensity I is seen to have similar behaviour to that found experimentally: initially constant as T is

raised from zero, then climbing sharply below T_N, and rather more slowly after T_N is reached. However, the calculated intensity starts to rise at a lower temperature (about .45 T_N instead of .8 T_N), and rises more slowly after T_N. Furthermore, the zero temperature intensity is calculated using the Néel state: Richards and Brya (1973) have shown that spin wave corrections increase this by ~15%, so that the discrepancy in Fig. 4 between experiment and theory is even larger than it appears. Much of this discrepancy is probably due to the shortcomings of the constant coupling model. The variation of the transverse intensity is also shown in Fig. 4: it is interesting that while the total intensity increases as T rises from O to T_N, the transverse intensity, mainly due to two-magnon scattering and containing most of the two-magnon scattering, falls. It appears therefore that the increase in total intensity is due mainly to increased elastic scattering as one might expect.

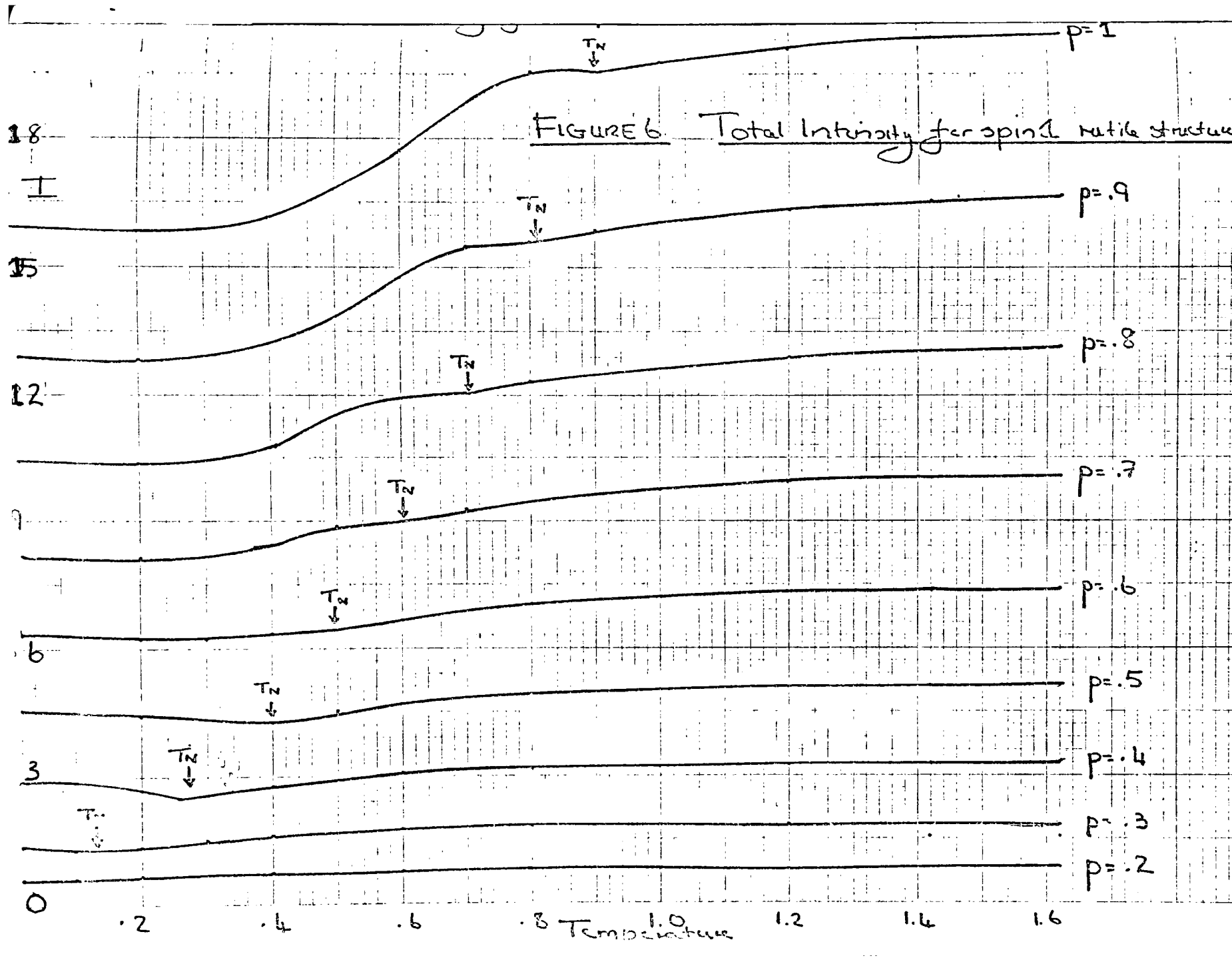
Brya and Richards (1973) also calculate the total intensity above T_N, using high temperature decouplings and the results of Ritchie and Fisher (1972) for critical and high temperature correlations: their curve is roughly reproduced and marked BRF on Fig. 4. They find good agreement at T_N, but fail to reproduce the steady increase in observed intensity above T_N, which may well be due to other scatterings, or temperature effects on scattering


FIGURE 5
First Moment for NiF2 p = 1
Δ Experimental points (BRF 1973)
TOTAL
TRANSVERSE
P-type
200
160
120
80
40
0
0
.2
.4
.6
.8
1.0
1.2
1.4
1.6
1.8
Tc
Temperature
TOTAL
P-type
TRANSVERSE

parameters or exchange constants.

In Fig. 5 the first moment found by BRF is plotted against temperature, as are the predictions of the total, transverse and P-type first moment. While all moments seem to reproduce the behaviour of NiF_2 quite well, the P-type moment does significantly better after about $\frac{2}{3}T_N$. The constant coupling theory underestimates correlations, and this may be why the experimental points are higher than the theory around T_N. This result for the P-type moment is encouraging, in the light of the suggestion made in Chapter 2 that this might agree best with experiment. It is also interesting that the experimental points suggest a discontinuity in gradient at T_N, as do all three moments. It should be noticed, however, that the zero temperature experimental result is very close to the prediction $(4zS-2)J$ of the transverse moment, which includes the interaction energy $(-2J)$, not allowed for in the P-type moment. This again indicates the difficulties inherent in comparing these moment calculations with experimental profiles. BRF also calculate the total first moment above T_N using only the dominant exchange for NiF_2, and obtain excellent agreement with experiment. Their curve is not reproduced here, but agrees with experiment within the experimental error from T_N up to about $4T_N$.

No further comparison with experiment is possible at


FIGURE 6 Total Intensity for spin 1 cubic structure
I
18
15
12
9
6
3
0
T_N
p= 1
p= .9
p= .8
p= .7
p= .6
p= .5
p= .4
p= .3
p= .2
.2
.4
.6
.8
1.0
1.2
1.4
1.6
Temperature

the moment, as curves of second moment against temperature have not been published, and the dilute crystal has not been much studied. It is appropriate to mention that Brya and Richards have also measured and calculated the relative intensity and the first moment in MnF_2, using Ritchie and Fisher's correlation results. Again excellent agreement is obtained above T_N for the first moment, and R(T) is accurate at T_N but underestimates for higher temperatures. Estimates below T_N are also made using molecular field theory, with empirical corrections to allow for fluctuations. The behaviour of the intensity and first moment are qualitatively similar to those of NiF_2.

It is also of some interest to examine the predictions of the calculations made here for concentrations other than unity. Fig. 6 shows the curves expected for the total intensity at different p for spin 1. At all values of p which allow order (i.e. $p \geq .3$), the intensity falls slowly at low temperatures, and then increases more rapidly till T_N is reached: the rate of increase becomes zero or negative at T_N, and then becomes positive again after T_N. The intensity rises as T is increased from 0 to high temperatures for all p, even below $p=.3$. It is rather hard to tell which of these features, apart from the steady rise, is real and which is due to defects in the estimation of spin quantities on the constant coupling

model. Experiment at p=1 did not detect any initial fall in the intensity at low temperatures, or any local maximum just below T_N, so one is inclined to ascribe these to vagaries of the model.

In Fig. 7 the transverse and P-type first moments are shown for NiF_2 at p=.9, .6 and .4. Below p=.5, the P-type moment should be lower at T=0: the constant coupling gives the P-moment higher than the transverse moment even at p=.4 at low temperatures, but this is another defect of the estimates of correlations in this model. A more regular feature is that at all p, the P-type moment changes only slowly with temperature at first, and is substantially higher at $T_N(p)$ than the transverse moment. These properties should make it possible to determine from experiments on dilute crystals whether the P-type moment gives the better description of the profile measured. Above $T_N(p)$ variation of p seems to have very little effect on the first moment: when p drops from 1.0 to .3, $\hbar\langle\omega\rangle^P$ at $T_N(p)$ drops only by about 6%, and $\hbar\langle\omega\rangle^T_N$ by even less. When p is sufficiently small that there is no order even when T=0, the first moment drops steadily and slowly as T increases, as might be expected.

Estimates of second moment are also made as T varies: however, the P-type second moment about the mean, zero at T=0, becomes large and negative as T rises until $T\sim.8T_N(p)$, because $\hbar\langle\omega\rangle^P$ falls only slowly as T is raised, whereas

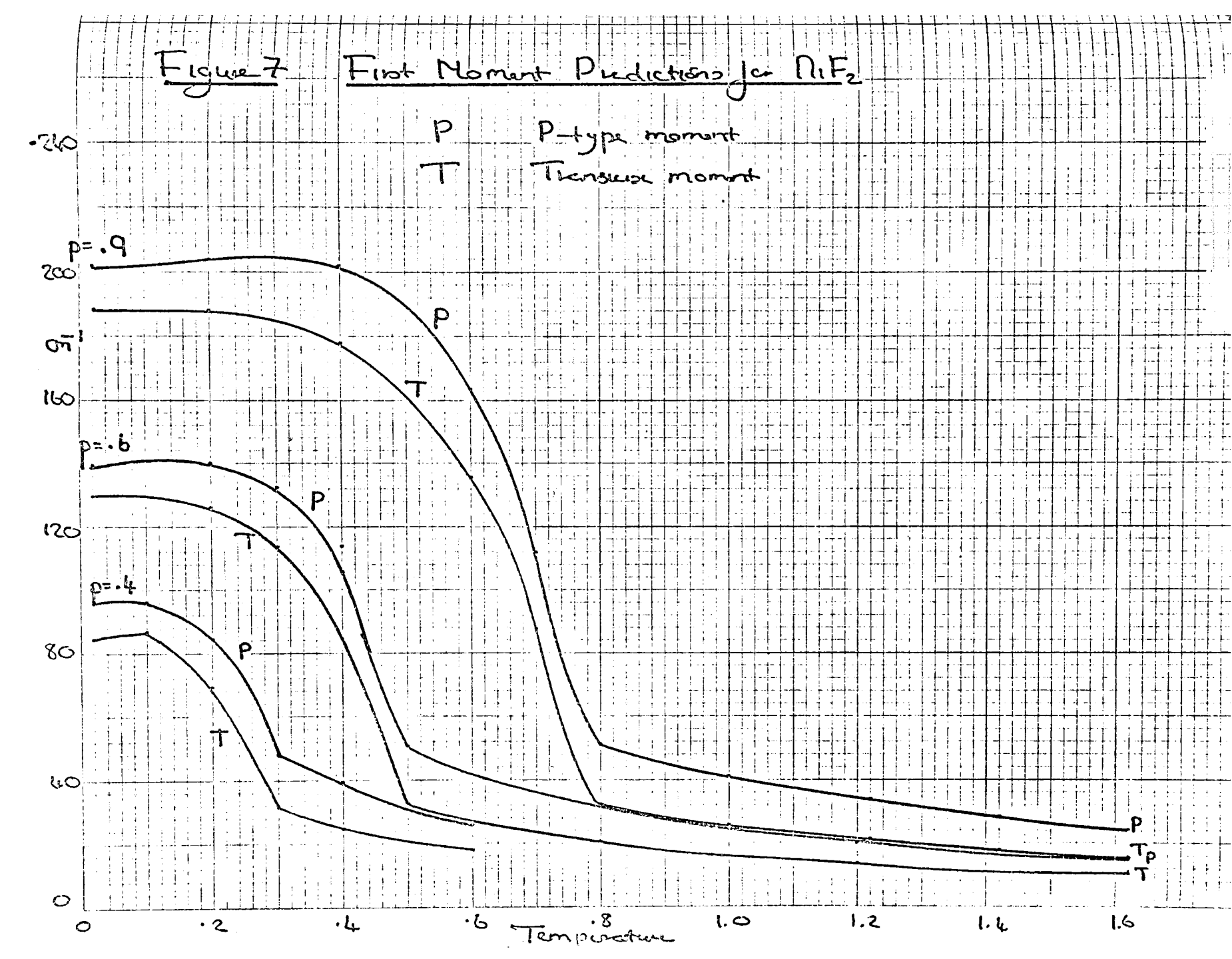
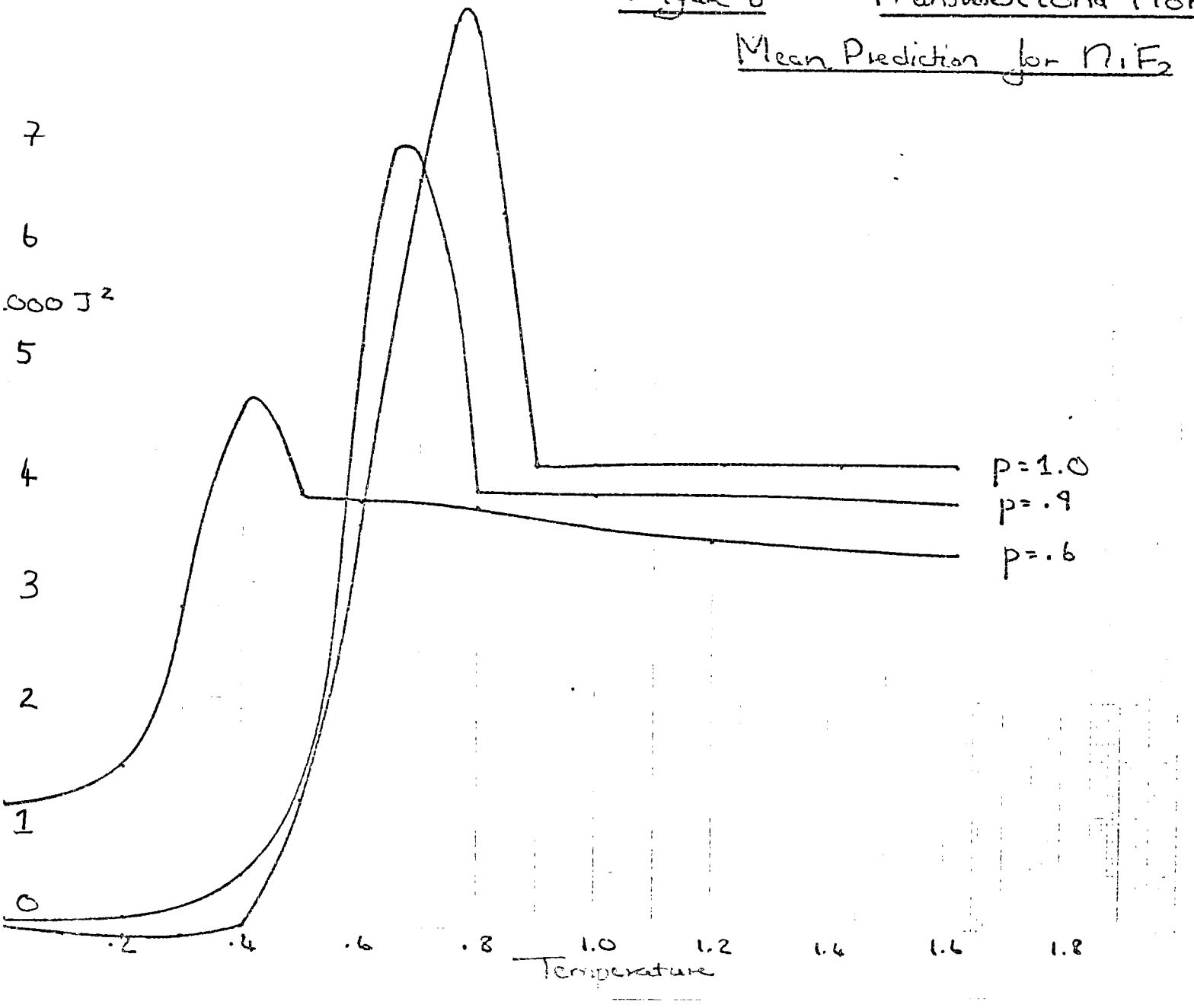

Figure 7 First Moment Predictions for NiF_2
P P-type moment
T Transverse moment
p=.9
p=.6
p=.4
P
T
T_P
0
.2
.4
.6
.8
1.0
1.2
1.4
1.6
Temperature
0
60
80
120
160
200
240

Figure 8 Transverse Second Moment about the Mean Prediction for $\Pi_1 F_2$



$\hbar^2\langle\omega^2\rangle^p$ falls quite quickly. Accordingly, only curves of $\hbar^2\langle\omega^2\rangle'^T_N$, the second transverse moment about $\hbar\langle\omega\rangle^T_N$, are presented. This quantity is also negative for low T, because the constant coupling model gives crude values of spin quantities there, and $\hbar^2\langle\omega^2\rangle'^T_N$ is the difference of two large quantities, $\hbar^2\langle\omega^2\rangle^T_N$ and $(\hbar\langle\omega\rangle^T_N)^2$: compared with $\hbar^2\langle\omega^2\rangle^T_N$, it only becomes negative by about .5%.

Fig. 8 presents the results for $\hbar^2\langle\omega^2\rangle'^T_N$: for p=1, the transverse second moment about the mean is about zero for some time as the temperature is raised, and then rises rapidly to a peak just below T_N: it then falls rapidly till T_N, and falls more slowly above T_N. Rather similar behaviour, but to a less marked extent, is found at lower values of p. The second moment is no longer small at low temperatures, but becomes increasingly large as p diminishes. When p=.4, the moment increases right up to T_N as T increases, and then falls slowly. When p=.2, there is no order even at zero temperature and the significance of the transverse moment is lost: the total second moment falls slowly as T rises. Unfortunately, no experimental measurements of second moment except at very high temperature have been made. In particular it would be interesting to know if the strong maximum just below $T_N(p)$ is a real feature of the system. However, great care must be taken in associating the transverse moments with any particular part of the spectrum, for the reasons given in §2.8. Firstly,

not all the two magnon scattering is given by H_I^T, nor is H_I^T solely made up of two magnon scattering terms. Secondly, the existence of a "mixed" intensity, quite possibly large and negative at some frequencies and large and positive at others, makes any identification extremely dubious. The total moments of the profile are unambiguous, but are probably not comparable with those measured. (The total $\hbar^2\omega^2>_N'$ about the mean behaves rather like $\hbar^2\omega^2>'^T_N$, but with a less pronounced peak below T_N).

An attempt was made to produce a moment that would be identified with experiment at the end of the previous chapter, and the P-type moments were found to fit a two peak assumption reasonably well at T=0 for all p. The first moment measurements of BRF in pure NiF_2 have also been seen to be reasonably well explained by $<\omega>^p$. However, the complete failure of $<\omega^2>'^p$ to provide a reasonable behaviour for the experimental width against temperature leaves the position of moment calculations rather unclear. The very great amount of labour necessary to produce higher moments renders it improbable that sufficient data to allow a fit of total moments (the only unambiguous ones) to a more complicated set of peaks than two Gaussians will ever be accumulated, and until some clearer explanation of what moments correspond to experiment can be found, accurate comparison with experiment will be difficult to rationalise.

However, the aim in this work has been to produce a

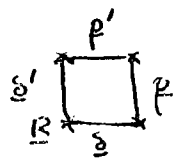
simple moment calculation that would describe the scattering profile consistently at all temperatures and impurity concentrations. A fair measure of qualitative agreement with experiment has been found in the rather limited areas where experiments have so far been successful. Above T_N, and in the pure substance, the recent calculations by Brya and Richards using explicitly high temperature decouplings and high temperature correlation function calculations have proved superior, as might be expected. However, below T_N, or in a dilute substance, sophisticated values for the correlations have not yet been calculated even for a ferromagnet, let alone an antiferromagnet, and so the type of moment calculation presented here may be expected to give qualitative predictions. Experimental results for dilute substances and for higher moments in the pure substance would be of great assistance in the determination of what moments correspond best to observation.

APPENDIX I OCCURRENCE OF LATTICE DIAGRAMS.

a) Body-centred cubic lattice.

Here the weak embeddings of the diagram of interest are counted, the phase factors σ^x and σ^y on each of the bonds $\underline{\delta}$ and $\underline{\delta}'$ being taken into account. When the bonds $\underline{\delta}$ and $\underline{\delta}'$ coincide, the phase factors are always unity: however, the vast majority of diagrams do not possess this simplifying feature. The procedure adopted is the following, entirely arithmetical, one.

Consider, for example, the next-neighbour loop:



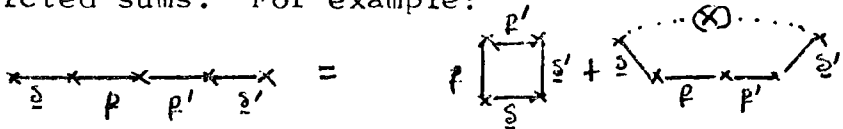
The bond $\underline{\delta}'$ is chosen to lie in the positive phase factor direction, and this is denoted by a +1: the other bonds are now added, and their phase factors indicated similarly, whether or not these are actually included in the sum.

δ	$\underline{\delta}'$	$\underline{p}'$	$\underline{p}$	
+1	+1	+1	+1	×1
	+1	+1	+1	×1
	+1	-1	-1	×2
	-1	+1	-1	×2
	-1	+1	-1	×2
		-1	+1	×2
		-1	+1	×2

The factors 2 and 1 indicate how many loops of a

given configuration there are: all twelve loops that may be based on $\underline{R}$ and $(\underline{R}+\underline{\delta})$ are included. The factors ± 1 are the values of $\sigma^x\sigma^y$ for the bond they belong to: so the occurrence of the loop is found by multiplying the factors belonging to $\underline{\delta}$ and $\underline{\delta}'$ and the number of loops together in each row, adding up the results, and multiplying by 8 since $\underline{\delta}'$ was arbitrarily fixed in the beginning. The result in this case is -32, which is multiplied by Np^4 since there are four sites in the diagram.

Once the occurrences are obtained, and the process is very tedious for large diagrams, checks may be made on them in the usual way, by allowing restricted and unrestricted sums. For example:



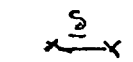
where the first chain is unrestricted, and the second is restricted not to form a loop, as indicated by the dotted line and cross. The occurrences of all three are separately worked out, and the check made. In this way, the following table of occurrences is found. Diagrams are grouped under the temperature-dependent moment for which they are first required. The site label $\underline{R}$ is left out: when only one of $\underline{\delta}$, $\underline{\delta}'$ appears, $\underline{\delta}$ and $\underline{\delta}'$ are understood to coincide on that bond. The sum is over $\underline{R}$ and all vector labels specified.

The cubic lattice diagrams involve three sets of

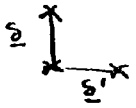
occurrences like the following, one each for the cases: $\underline{\delta}$ and $\underline{\delta}'$ are both restricted to the x-direction: one of $\underline{\delta}$, $\underline{\delta}'$ is restricted to the x-direction: neither $\underline{\delta}$ nor $\underline{\delta}'$ is restricted. However, each set of occurrences is much easier to find. They are not given here, due to limitations of space.

Occurrences of Lattice Diagrams.

I

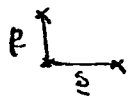


$8Np^2$

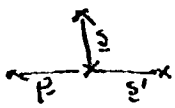


$-8Np^3$

⟨W⟩



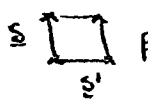
$56Np^3$



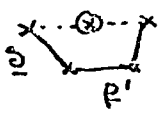
$-48Np^4$



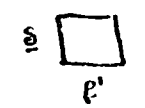
$-24Np^4$



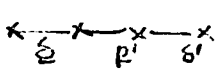
$-32Np^4$



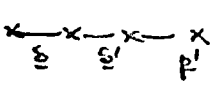
$-24Np^4$



$+32Np^4$

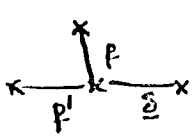


$8Np^4$

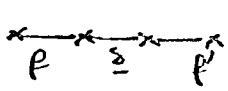


$-56Np^4$

⟨W²⟩



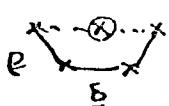
$336Np^4$



$392Np^4$

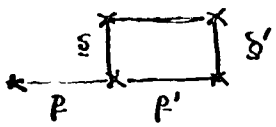


$96Np^4$

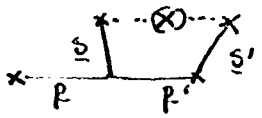


$296Np^4$

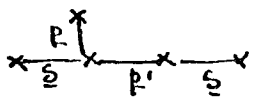
$\langle W^2 \rangle$ continued.



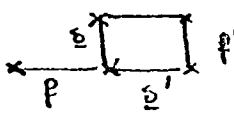
$192p^5N$



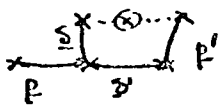
$-144Np^5$



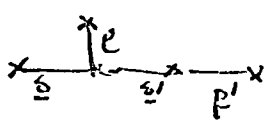
$+48p^5N$



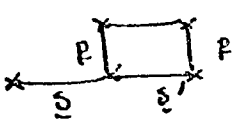
$-192Np^5$



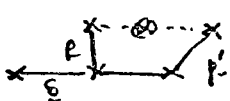
$-144Np^5$



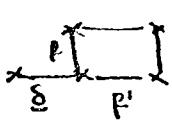
$-336Np^5$



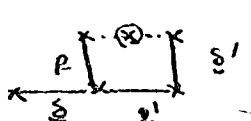
$-64Np^5$



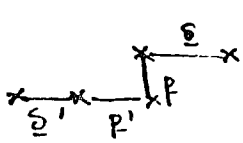
$-272Np^5$



$0Np^5$



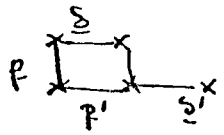
$48Np^5$



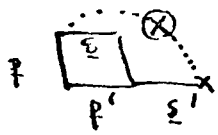
$24Np^5$

(NB: the ends must not share a site)

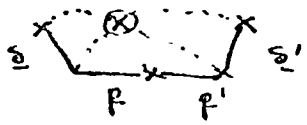
$\langle W^2 \rangle$ continued



$0 N p^5$



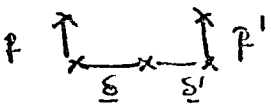
$-16 N p^5$



$40 N p^5$

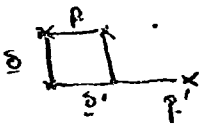


$+16 N p^5$

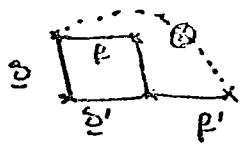


$-360 N p^5$

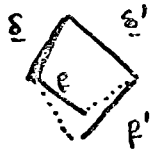
(NB the ends must not share a site)



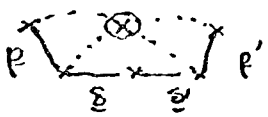
$-192 N p^5$



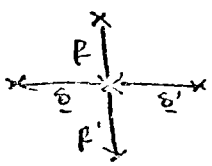
$-144 N p^5$



$-48 N p^5$

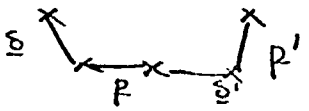


$-24 N p^5$



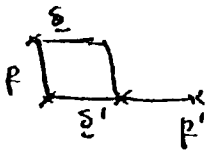
$-240 N p^5$

$\langle W^2 \rangle$ continued

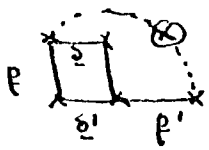


$24Np^5$

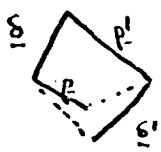
[NB : the ends must not share a site]



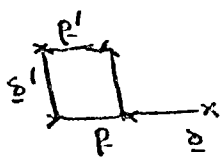
$192Np^5$



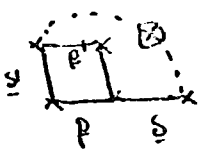
$176Np^5$



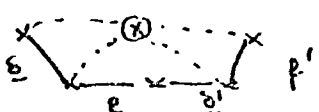
$16Np^5$



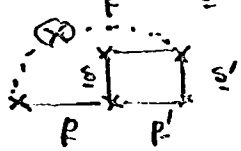
$0Np^5$



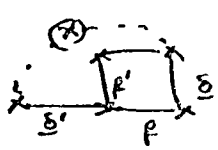
$-16Np^5$



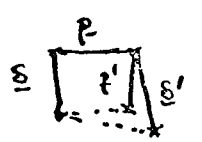
$-152Np^5$



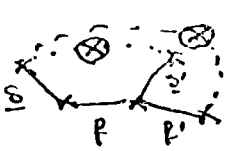
$160p^5N$



$-32p^5N$

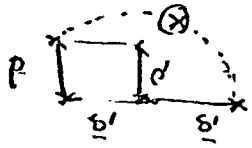


$+32p^5N$

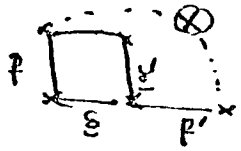


$-112p^5N$

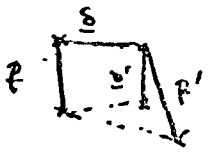
$\langle W^2 \rangle$ continued



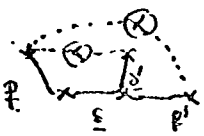
$-16Np^5$



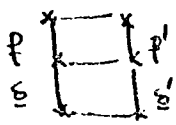
$-144Np^5$



$-48Np^5$



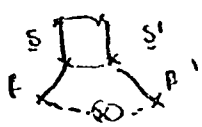
$-128Np^5$



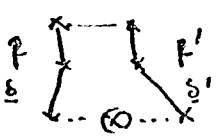
$96Np^6$



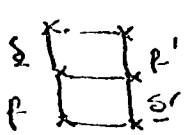
$-32Np^6$



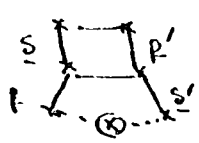
$1056Np^6$



$-32Np^6$

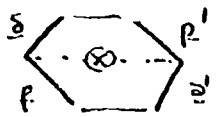


$+32Np^6$

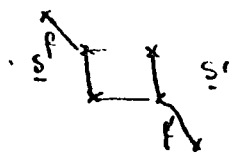


$-32Np^6$

$\langle W^2 \rangle$ continued



$+32 N p^6$



$1152 N p^6$

REFERENCES

Bass F.G. & Kaganov M.I. 1960 Soviet Phys. JET 10 P.986

Belhe H.A. 1935 Proc.Roy.Soc. A 150 P.552

Brya W.J., Richards B.M. & Bartkowski

Brya W.J. & Richards P.N.: Fleury P.A. 1972 A.I.P. Conference Proceedings 10 P.729

Brya W.J. & Richards 1973 Phys.Rev.: to be published

Buchanan M, Buyers W.J.L., Elliott R.J., Harley R.T., Hayes W., Perry A.M. and Saville I.D. 1972 J.Phys. C 5 P.2011

Cottam M.G. 1972 Sol.Stat.Commun. 11 P.889

Davies R.W. 1972 Phys.Rev. B 5 P.4598

Elliott R.J. 1960 J.Phys.Chem.Solids 16 P.165

Elliott R.J., Thorpe M.F., Imbusch G.F., Loudon R., & Parkinson J.B. 1968 Phys.Rev.Letters 24 P.147

Elliott R.J. & Loudon R. 1963 Phys.Letters 3 P.189

Elliott R.J. & Thorpe M.F. 1969 J.Phys. C 2 P.1630

Fleury P.A., Porto S.P.S., Cheesman L.E. & Guggenheim H.J., 1966 Phys.Rev.Letters 17 P.84

Fleury P.A., Porto S.P.S. & Loudon R. 1967 Phys.Rev. Letters 18 P.658

Fleury P.A. 1968 Phys.Rev.Letters 21 P.151

Fleury P.A. & Loudon R. 1968 Phys.Rev. 166 P.514

Fleury P.A. 1969 Phys.Rev. 180 P.591

Guggenheim E.A. 1935 Proc.Roy.Soc. A 148 P.304

Kasteleijn P.W. & van Kranendonk J. 1956 Physica 22 P.367

van Kranendonk J. & Kasteleijn P.W. 1956 Physica 22 P.317

Loudon R. 1968 Adv.Phys. 17 P.243

Nicotin O., Lindgard P.A. & Dietrich O.W. 1969 J.Phys. C 2 P.243

Peierls R.E. 1936 Proc.Camb.Phil.Soc. 32 P.447

Richards P.M. & Brya W.J. 1973 Phys.Rev.: to be published

Ritchie D.S. & Fisher M.E. 1972 Phys.Rev. 135 P.2668

Sato H., Arrott A. & Kikuchi R. 1959 J.Phys.Chem.Solids 10 P.19

Smart J.S. 1960 J.Phys.Chem.Solids 16 P.169

Sólyom J. 1971 Z.Physik. 243 P.382

Sykes M.F. & Essam J.W. 1964 Phys.Rev. 133A P.310

Tahir-Kheli R.A. & ter Haar D. 1962 Phys.Rev. 127 P.88

PART 3

More Random Systems

PART 3

CHAPTER 1

§1.1 Introduction to the Spin Glass

This section is concerned with the development of an approximation that will allow a more random model of a magnet than those considered previously to be studied: one such model is the "spin-glass" extensively studied by Handrich and various collaborators (Handrich, 1972; Handrich, Hemmerling and Abdullah, 1973) where the spins are fixed on regular lattice sites, but the interactions between them have some distribution of values. It is thought that this model might bear some resemblance to materials where the moment carrying atoms are not fixed on lattice sites: truly random systems. For example, the alloy $Ni_{85}P_{15}$ has both a crystalline and an amorphous state at a range of temperatures which allows the study of the magnetisation right up to the critical temperature, T_c, and the interactions between spins are thought to have a distribution which allows positive and negative values, (Simpson and Brambley, 1972; Tsuei, Longworth and Lin, 1968).

Much work on models which have such distributions has been done by Handrich, who has developed a constant coupling approximation which permits estimation of the critical temperature, magnetisation and susceptibility in both Ising and Heisenberg models. Earlier work allowed

the estimation of the magnetisation Curie and temperature by essentially molecular field methods (Handrich, 1969): such methods did not take account of local fluctuations, and so gave a value of T_c independent of structure fluctuations, where the constant coupling method gives T_c dependent on fluctuations: this will be discussed later. Other theoretical work on this problem has been done by Montgomery, Krugler and Stubbs (1970), who obtain magnetisation curves by Green's function techniques.

An approximation is developed which replaces the disordered lattice by an average lattice using a CPA-type self energy equation: the Curie temperature is estimated for several random models.

§1.2

The Ising Hamiltonian

$$H = -\sum_{<i,j>} J_{ij} S_i S_j \qquad - 1.1$$

is used, where $S_i = \pm 1$ only, and the sum counts each pair of atoms once only. An equation for the Fourier transform of the spin correlation function will be developed following Brout (1965). Suppose that spin 1 is up: then $<S_1 S_2> = <S_2>$ in this ensemble. The field on spin 2 due to its neighbouring spins is

$$H^I = J_{12} + \sum_{j \neq 1} J_{2j} S_j \qquad - 1.2$$

H^I is now averaged over the ensemble with $S_1 = 1$, and the

correlation of the S_j with spin 2 is ignored, so that molecular field theory may be used to give

$$\langle S_2 \rangle = \tanh[\beta \langle H_2 \rangle] \qquad - 1.3$$

The right hand side of 1.3 is now expanded and only terms linear in βJ_{ij} kept: this is valid round the critical region, where $\beta J_{ij} \sim \frac{1}{z}$. The following equation for the correlation between S_1 and S_2 is obtained:

$$\langle S_1 S_2 \rangle = \beta J_{12} + \sum_{j \neq 1} \beta J_{2j} \langle S_i S_j \rangle \qquad - 1.4$$

Since, by translational symmetry, $\langle S_i S_j \rangle$ is a function only of $(\underline{R}_i - \underline{R}_j)$, the convolution in 1.4 may be handled by Fourier transformation, defined as follows.

$$g(\underline{R}_i - \underline{R}_j) = \langle S_i S_j \rangle$$

$$g(\underline{q}) = \sum_{\underline{R}_i \neq \underline{R}_j} g(\underline{R}_i - \underline{R}_j) \exp(i\underline{q}.(\underline{R}_i - \underline{R}_j))$$

$$g(\underline{R}) = \frac{1}{N} \sum_{\underline{q}} g(\underline{q}) \exp(i\underline{q}.\underline{R})$$

N is the number of sites in the lattice, and $\underline{q}$ is summed over all allowed values in the first Brillouin zone. Equation 1.4 becomes:

$$g(\underline{R}_1 - \underline{R}_2) = \beta J(\underline{R}_1 - \underline{R}_2) + \beta \sum_{j \neq 1} J(\underline{R}_2 - \underline{R}_j) g(\underline{R}_j - \underline{R}_1) \qquad - 1.5$$

However, the restriction on the sum may be lifted in 1.5 since if j=1, the term $\beta J(\underline{R}_2 - \underline{R}_1) G(\underline{O})$ is created, and G(O) is the self correlation $\langle S_i S_i \rangle$, which is unity. Accordingly,

$$g(\underline{R}_1-\underline{R}_2) = \beta\sum_j J(\underline{R}_2-\underline{R}_j)g(\underline{R}_j-\underline{R}_1) \qquad - 1.6$$

for $\underline{R}_1 \neq \underline{R}_2$, and also

$$g(\underline{R}=0) = 1$$

Fourier transformation yields

$$g(\underline{q}) = 1 + \sum_{\substack{\underline{R}_j \\ \underline{R}_2 \neq \underline{R}_1}} \beta J(\underline{R}_2-\underline{R}_j)g(\underline{R}_j-\underline{R}_1)\exp(i\underline{q}.(\underline{R}_2-\underline{R}_1)) \qquad - 1.7$$

where the latter term would be just $\beta J(\underline{q})g(\underline{q})$ if the restriction $\underline{R}_2 \neq \underline{R}_1$ were lifted.

The term introduced by $\underline{R}_2 = \underline{R}_1$ is

$$\sum_{\underline{R}_j, \underline{R}_1} \beta J(\underline{R}_1-\underline{R}_j)g(\underline{R}_1-\underline{R}_j) \qquad - 1.8$$

which is just $\sum_{\underline{q}} J(\underline{q})g(\underline{q})$: accordingly,

$$g(\underline{q}) = 1 + \beta J(\underline{q})g(\underline{q}) - \beta\sum_{\underline{q}} J(\underline{q})g(\underline{q}) \qquad - 1.9$$

$$\text{or } g(\underline{q}) = \frac{X}{1-\beta J(\underline{q})} \qquad - 1.10$$

$$\text{where } X = 1 - \beta\sum_{\underline{q}} J(\underline{q})g(\underline{q}) \qquad - 1.11$$

In what follows, the constant X is treated as arbitrary, to be defined by the requirement that $g(\underline{r}=o) = 1$.

The simple cubic lattice with first neighbour interactions only will be studied in this work, so that

$$\begin{aligned} J(\underline{q}) &= \sum_{\underline{R}} J(\underline{R}) e^{i\underline{q}.\underline{R}} \\ &= J\sum_{\underline{\delta}} e^{i\underline{q}.\underline{\delta}} \\ &= J\gamma(\underline{q}), \end{aligned} \qquad - 1.12$$

where $\underline{\delta}$ is $\pm a$ in the x,y or z direction.

$g(\underline{q})$ may now be related to the susceptibility as follows: the partition function Z in the presence of a field A in the z direction in 1.1 is

$$Z = \mathrm{Tr}\{\exp-\beta[-J \sum_{<ij>} S_i S_j - A\Sigma S_i]\}$$

where now the sum is over all next-neighbour pairs i,j. Differentiation with respect to A gives:

$$\begin{aligned}\chi &= \frac{1}{\beta}\frac{\partial^2}{\partial A^2}[\ln z]\Big|_{A=0} \\ &= \beta\langle(\Sigma S_i)^2\rangle - \beta\langle\Sigma S_i\rangle^2 \\ &= \beta\langle\Sigma S_i S_j\rangle \qquad \text{- 1.13}\end{aligned}$$

Comparison with 1.10 gives

$$\chi = \beta \lim_{\underline{q}\to 0} \frac{X(T)}{1-\beta J\gamma(\underline{q})} = \frac{\beta X(T)}{1-z\beta J} \qquad \text{- 1.14}$$

which is just the molecular field result if X=1. A better result for the critical temperature T_c than that predicted by 1.13, $kT_c=zJ$, may be obtained by series expansions for $\chi(T)$. In particular, the expansion

$$\chi \propto 1 + \sum_{n=1}^{\infty} z(z-1)^{n-1} t^n \qquad \text{- 1.15}$$

where $t = \tanh(\beta J)$, which is exact for a Cayley tree, gives an 'improved' value of $kT_c = 4.97J$ for z=6, which compares quite well with the normal series expansion value of 4.51J. Equation 1.15 may be summed as

$$\chi \propto \frac{1}{1-z\frac{t}{1+t}} \qquad - 1.16$$

Accordingly, βJ is arbitrarily replaced by $K = \frac{t}{1+t}$ in equation 1.10, to give

$$g(\underline{q}) = \frac{\chi(T)}{1-K\gamma(\underline{q})} \qquad - 1.17$$

Only the system with βJ will be discussed explicitly in what follows, as the replacement is easily made.

This theory, which gives a good value for kT_c/J in a perfect Ising lattice, must now be modified to take account of J being allowed to vary from bond to bond. The molecular field approximation is just to replace J by the average J, $\bar{J}$, in 1.9 or 1.15: this takes no account of fluctuations due to the variation of J, and will give the same transition temperature for all distributions of J constrained to have the same $\bar{J}$. The CPA is invoked to replace $g(\underline{q})$ by some average $G(\underline{q})$, and $J(\underline{q})$ by $\bar{J}(\underline{q})+\Sigma(\underline{q})$ where $\Sigma(\underline{q})$ is a self energy calculated self consistently, so as to replace the random system by an average, effective system. The self energy is determined by the usual equation

$$\underline{\underline{\Sigma}} = \int f(x)\,\underline{\underline{\Delta}}\,(\underline{\underline{1}}-(\underline{\underline{\Delta}}-\underline{\underline{\Sigma}})\underline{\underline{G}})^{-1}dx \qquad - 1.18$$

where $\underline{\underline{\Delta}}$ measures the deviation from $\bar{J}$ on a given bond, occurring with probability $f(x)$.

$$\underline{\underline{\Sigma}} = \begin{pmatrix} \Sigma_o & \Sigma_1 \\ \Sigma_1 & \Sigma_o \end{pmatrix}$$

$$\underline{\underline{\Delta}} = \begin{pmatrix} 0 & (x-1)\beta\bar{J} \\ (x-1)\beta\bar{J} & 0 \end{pmatrix}$$

$$\underline{\underline{G}} = \begin{pmatrix} G_o & G_1 \\ G_1 & G_o \end{pmatrix}$$

G_o is the self correlation and G_1 the next neighbour correlation. The replacement of $J(\underline{q})$ by $\bar{J}(\underline{q})+\Sigma(\underline{q})$ in 1.9 leads to

$$G(\underline{q}) = \frac{X}{(1-z\Sigma_o)-(\bar{J}+\Sigma_1)\gamma(\underline{q})} \qquad - 1.19$$

By inverse Fourier transformation of 1.19,

$$G(\underline{r}=0) = \frac{X}{\beta\bar{J}+\Sigma_1}\frac{1}{N}\sum_{\underline{q}}\frac{1}{Y-\gamma(\underline{q})} \qquad - 1.20$$

where $$Y = \frac{1-6\Sigma_o}{\beta\bar{J}+\Sigma_1}$$

and since G_o is always 1, X is determined by

$$\frac{1}{N}\sum_{\underline{q}}\frac{1}{Y-\gamma(\underline{q})} = \frac{\beta\bar{J}+\Sigma_1}{X} \qquad - 1.21$$

Now the next neighbour correlation function G_1 may be found.

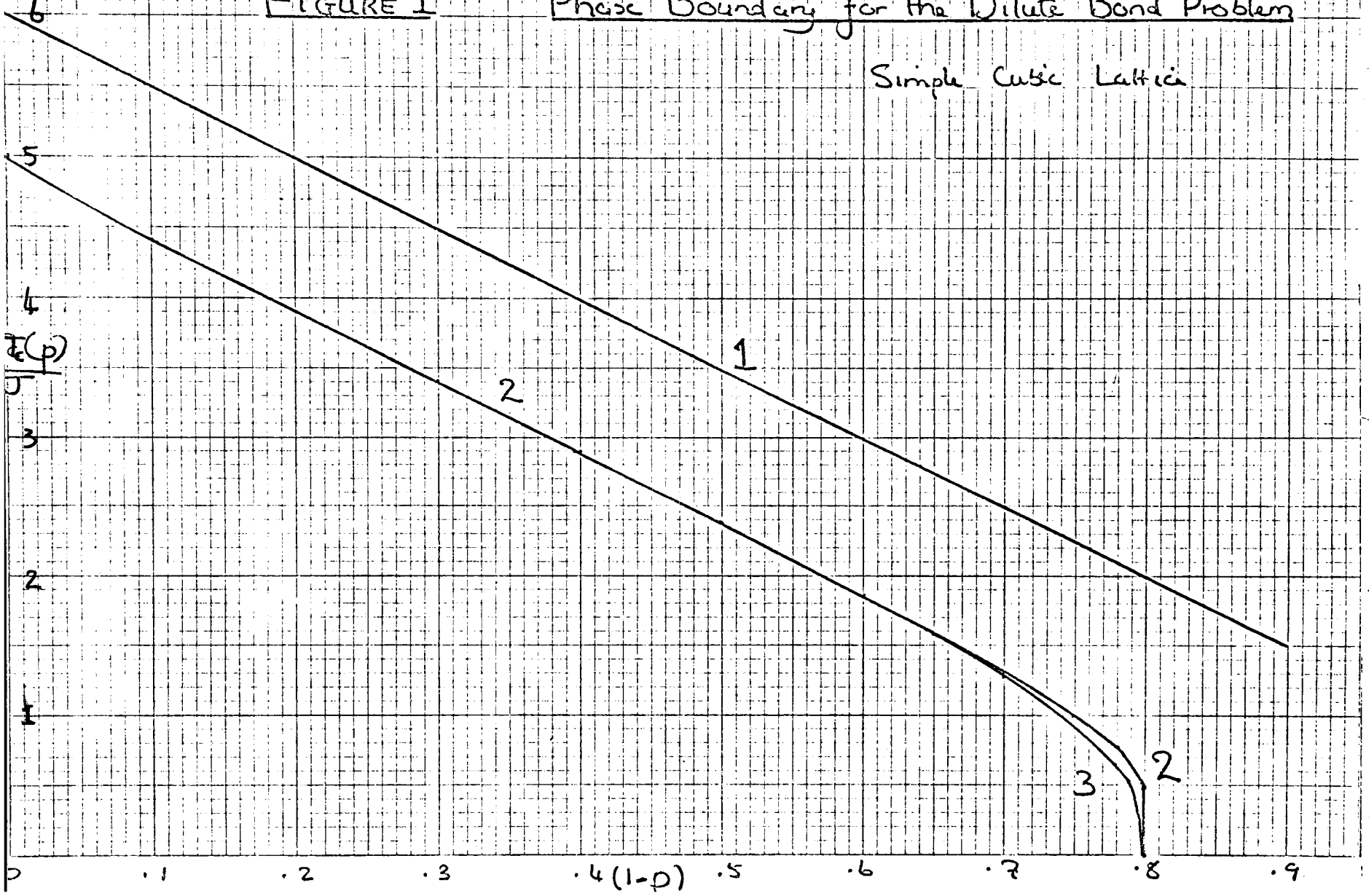
$$\begin{aligned} G_1 &= \frac{1}{6N}\sum_{\underline{q}} G(\underline{q})\gamma(\underline{q}) \\ &= \frac{1}{6N}\sum_{\underline{q}}\frac{-X}{\beta\bar{J}+\Sigma_1}\left[1 - \frac{Y}{Y-\gamma(\underline{q})}\right] \\ &= \frac{1}{6}Y - \frac{X}{6(\beta\bar{J}+\Sigma_1)} \end{aligned} \qquad - 1.22$$

The critical temperature, T_c, is determined by the divergence of

$$\begin{aligned} \chi &= \beta \lim_{t\to o} G(\underline{q}) \\ &= \beta\,\frac{X(T)}{(1-6\Sigma_o)-6(\beta\bar{J}+\Sigma_1)} \end{aligned}$$

so that $\beta_c J = \frac{1}{6} - \Sigma_o - \Sigma_1$ - 1.23

FIGURE 1 Phase Boundary for the Dilute Bond Problem



At the critical point, Y=6, and the Watson integral corresponding to 1.20 has the value $\frac{1}{4}$: equation 1.21 now gives $G_1 = \frac{1}{3}$. Accordingly, the critical temperature may be estimated by solving the self energy equation 1.18 for Σ_o and Σ_1 self consistently with 1.23, setting $G_o = 1$ and $G_1 = \frac{1}{3}$. The matrix inversion 1.18 may be performed, and the following two equations result at T_c:

$$\Sigma_o = \int f(x)dx\left[(1-x)\beta\bar{J}\left[\tfrac{1}{3}\Sigma_o+\Sigma_1+(1-x)\beta\bar{J}\right]\right]/Q \qquad - 1.24$$

$$\Sigma_1 = \int f(x)dx\left[(x-1)\beta\bar{J}\left[1+\Sigma_o+\tfrac{1}{3}(\Sigma_1+(1-x)\beta\bar{J})\right]\right]/Q \qquad - 1.25$$

with $$Q = 1+2\Sigma_o+\tfrac{8}{9}(\Sigma_o^2-\left[(1-x)\beta\bar{J}+\Sigma_1\right]^2)+\tfrac{2}{3}(\Sigma_1+(1-x)\beta\bar{J}) \qquad - 1.26$$

In the following sections this model is applied firstly to the dilute bond problem familiar in the literature to gauge whether the replacement of $\beta\bar{J}$ by $\bar{K}$ is more successful in dealing with a well studied problem, and then that method is applied to more complicated random systems.

§ 1.3 The Dilute Bond Problem

This random system is obtained by setting

$$f(x) = p\delta(x=1)+(1-p)\delta(x=0):$$

there is a probability $(1-p)$ of there being no interaction between two neighbouring atoms. Equations 1.24, 1.25 and 1.23 are now solved by iteration for given values of p to obtain Σ_o, Σ_1 and βJ. The results of this procedure for $kT_c(p)/J$ are shown in Fig. 1. At p=1, the molecular field result of 6 is obtained, and the transition temperature

falls steadily but never reaches zero as p is increased. This result is unsatisfactory, as susceptibility expansions in t have been carried out for this problem (e.g. Rapaport, 1972) and a p_c^s found at which $T_c(p)$ is zero: equally, percolation theories at T=0 have estimated the p_c^s below which no infinite connected cluster of ferromagnetic bonds of the type necessary for ferromagnetism can exist (Sykes and Essam, 1964): a naive estimate of this may be made by considering that each bond in the infinite cluster has two bonds attached to it on average; since there are 2(z-1) neighbours available for the two bonds, so $p_c^s = \frac{1}{z-1}$. This is an exact result on a Cayley tree.

Fig. 1 displays the results transformed by $\beta\bar{J} \to \bar{K} = (\frac{t}{1+t})$ (curve 2), and the Cayley tree result is seen to be recovered for p_c^s. This is in fact quite a reasonable phase boundary for the cubic lattice bond problem, as the $T_c(1)$ estimate has already been seen to be about 10% from the best value, and the estimate for p_c^s is within .05 of the percolation theory result, .247.

The results obtained by replacement of $\bar{J}$ by $\bar{K}$ are much more satisfactory, and this indicates that $\bar{K}$ is the more appropriate variable to find the effective one-bond value of by the self energy equations 1.24 and 1.25, even although this is harder to understand intuitively than use of $\bar{J}$.

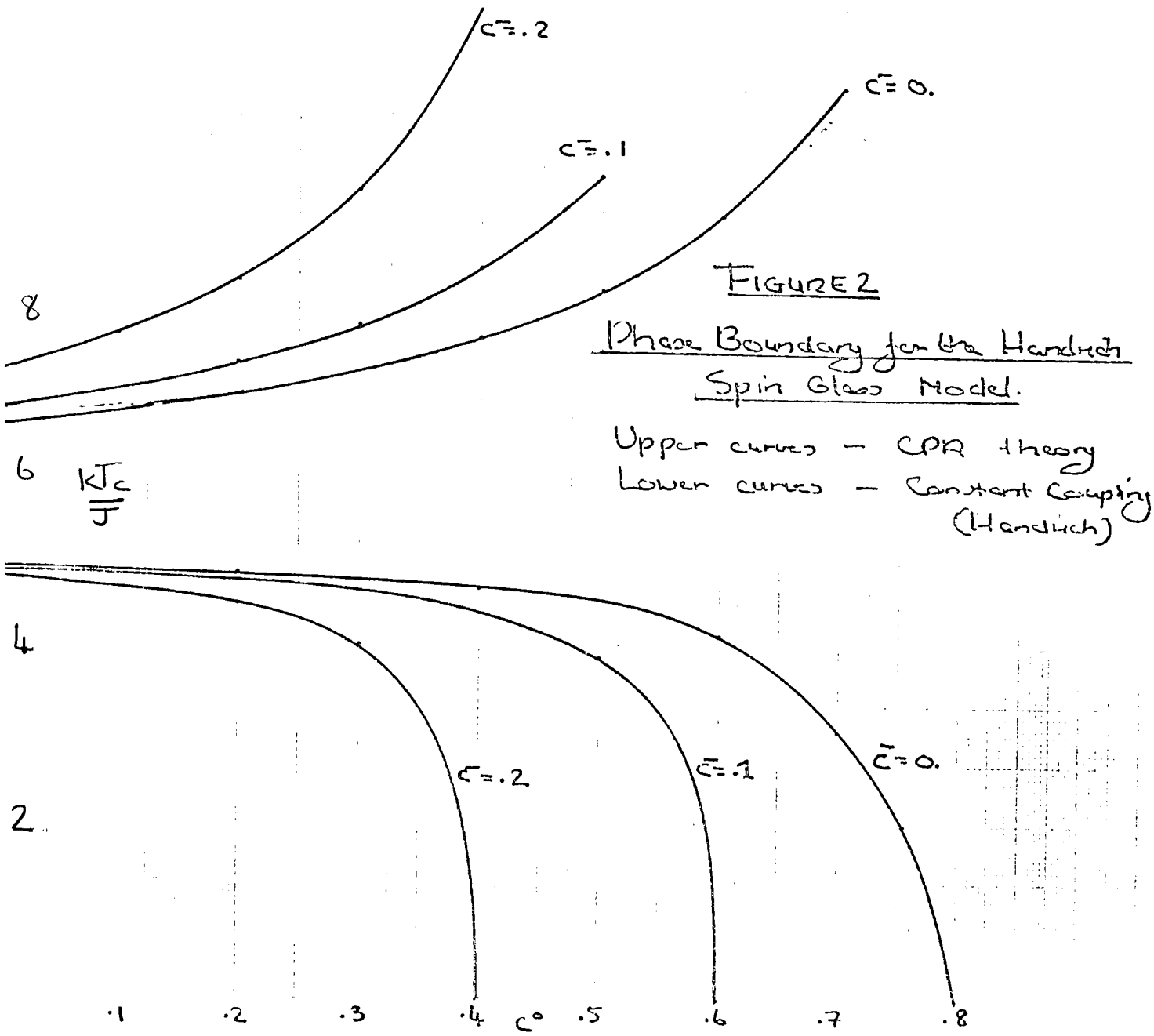


FIGURE 2

Phase Boundary for the Handrich Spin Glass Model.

Upper curves — CPR theory
Lower curves — Constant coupling (Handrich)

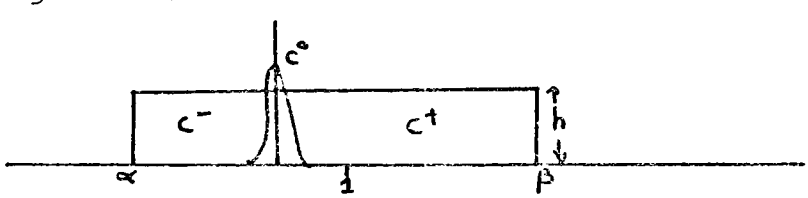
The constant coupling model of Handrich (q.v.) produces the compact result

$$\frac{z}{2(z-1)} = \int f(x) \frac{1}{1+e^{-\beta_c(1-x)J}} dx$$

when $\beta_c = \frac{1}{kT_c}$, and this is found to give a phase boundary very close to curve 2 in Fig. 1, but approaching $p_c^s = .8$ less steeply, and labelled 3 at low temperature. Simple arguments indicate that p_c^s should be approached vertically by a phase boundary curve (Elliott, 1963), so that perhaps the self energy method leading to curve 2 gives the better result.

§1.4 More Random Models

Of more current interest are models where the interactions between neighbouring spins belong to more general distributions. Such a model has been recently proposed by Handrich and curves for the transition temperature obtained by a modified constant coupling theory (Handrich). On a cubic lattice with next neighbour interactions, f(x) is chosen to have the form of a square distribution of weight c^o at the origin, so that J varies, and so does the number of next neighbours.



c^- is the concentration of negative interactions, and the following results hold:

$$c + c^o + c^- = 1.$$

$$h\int_{\alpha}^{\beta} f(x)dx = c^{+}+c^{-}$$
$$h\int_{\alpha}^{\beta} xf(x)dx = 1.$$

Such a distribution always introduces the same interaction J on each bond, but the width of the distribution changes as c^{o} is increased for constant c^{-}. An increased value of c^{-} for constant c^{o} also means a wider distribution of J. The theory outlined may be applied to this model, and the results shown in Fig. 2 as the upper set of curves, for $\beta\bar{J}$. The replacement of $\beta\bar{J}$ by $\bar{K}$ has not been carried out, as it will only shift the positions of the curves in this case and not affect the trend, since $\beta\bar{J}$ is never small. The lower set are those resulting from Handrich's constant coupling formula, given in 1.2 and predict the vanishing of the Curie temperature at values of c^{o} given by

$$c^{o} = \frac{z-2}{z-1} - 2c^{-}. \qquad \text{(Handrich, 1972)}$$

It is rather unsatisfactory that this contradiction should exist: the Handrich theory and this work appear to introduce fluctuations in J with opposite signs into the transition temperature, as constant coupling predicts a falling transition temperature, and this work a rising transition temperature, as bigger fluctuations are introduced. Furthermore, no very simple arguments can tell one how fluctuations affect T_c: spatial fluctuations in $\mathbf{J}$ are usually considered by writing a high temperature expansion for χ.

$$\chi \propto 1 + \beta\sum_j J_{ij} + \beta^2 \sum_{j,k}\left[J_{ij}J_{ik} - \sum_k (J_{ik})^2\right] \ldots.$$

where J_{ij} is the interaction between next neighbours only, i and j. Now, if J_{ij} are random

$$\chi \propto 1 + \beta z\bar{J} + \beta^2\left[\bar{J}^2 z^2 - z\overline{J^2}\right] \ldots.$$

and the fluctuation term $(-z\beta^2\overline{J^2})$, of topological origin, indicates how molecular field theory should be modified to take account of spatial fluctuations. The fluctuations are not of a spatial nature in the problem considered here.

Equation 1.18 may be examined for small $\underline{\underline{\Delta}}$ and $\underline{\underline{\Sigma}}$ by expanding the denominator:

$$\underline{\underline{\Sigma}} \sim \int f(x)\underline{\underline{\Delta}}(1 + (\underline{\underline{\Delta}} - \underline{\underline{\Sigma}})\underline{\underline{G}})dx$$

Now $\int f(x)\underline{\underline{\Delta}}dx = 0$, since the distribution does not change the average value of J, and

$$\underline{\underline{\Sigma}} \sim \int f(x)\underline{\underline{\Delta}}\underline{\underline{G}}(\underline{\underline{\Delta}} - \underline{\underline{\Sigma}})dx$$

$$\sim \int f(x)\underline{\underline{\Delta}}\underline{\underline{G}}\underline{\underline{\Delta}}dx$$

or $$\Sigma_0 \sim \int f(x)(1-x)^2(\beta\bar{J})^2 dx \qquad - 1.27$$

and $$\Sigma_1 \sim \int \tfrac{1}{3} f(x)(1-x)^2(\beta\bar{J})^2 dx \qquad - 1.28$$

using the definitions made earlier. The left hand side of 1.27 directly measures the fluctuation $\beta^2(\overline{J^2} - \bar{J}^2)$, which is positive always in the model considered here. So, to a crude approximation,

$$\beta\bar{J} = \frac{1}{6} - \frac{4}{3}\beta^2(\overline{J^2} - \bar{J}^2) \qquad - 1.29$$

The transition temperature is raised by the immediate effect of fluctuations: it would be surprising if the CPA, even in this naive theory, gave the wrong answer for the

effect of fluctuations on the transition temperature.

It also appears surprising at first sight that the CPA method gives an adequate phase boundary for the bond problem as well as Handrich's approximation, if they take opposite account of fluctuations in J. However, the mean field theory result for the bond problem is a straight line from kT = 6J at p=0 to T=0 at p=1: the CPA results using $\bar{J}$ as a variable always lie above this, due to account being taken of fluctuations. The transformation in $\bar{J} \rightarrow \bar{K}$ has no real effect on the slope of the transition curve till kT(p) = 2J is reached, which corresponds to T=0 in $\bar{K}$. So the CPA always gives a raised transition temperature with increased fluctuations. Handrich's constant coupling appears to do so initially at least in the bond problem, but not for the more complicated model of this section.

Calculations have also been carried out for a 'Gaussian' spin glass, where the interactions have a Gaussian distribution about $\bar{J}$. Again, the CPA indicates that T_c rises monotonically as the Gaussian gets wider while its peak position is held fixed.

One possible source of error in this work is that a factor $X = 1 - \sum_{\underline{q}} J(\underline{q})G(\underline{q})$ has been introduced via equation 1.11 where the CPA usually has unity: X is a constant for fixed temperature, but presumably has some dependence on the self energies as well, which it has not proved possible

to estimate yet.

The situation, then, is rather unclear: some experiments on amorphous alloys indicate a lowered transition temperature (e.g. Simpson and Brambley, 1972), but it is by no means certain that such systems are described by the model discussed here. There appear to be no simple arguments that indicate the behaviour of T_c as fluctuations in J increase, and the two theories available give contradictory answers. The field of amorphous substances is one of growing interest, and it is to be hoped that this contradiction will be resolved in the near future.

REFERENCES

Elliott R.J. 1963 Clarendon Lab. Report 128/63

Handrich K. 1969 Phys.stat.solidi.(b) 32 P.K55

Handrich K. 1971 Phys.stat.solidi(b) 44 P.K17

Handrich K. 1972 Phys.stat.solidi(b) 53 P.K17

Handrich K., Hemmerling J. & Abdullah N. 1973 Phys.stat. solidi(b) 56 K1

Montgomery C.G., Krugler J.I. & Stubbs R.N. 1970 P.R. Letters 25 P.669

Rapaport D.C. 1972 J.Phys. C. 5 P.1830

Sykes J.W. & Essam M.F. 1964 Phys.Rev. 133A P.310

C.C. Tsuei, G. Longworth & Lin S.H. 1968 Phys. Rev. 170 P 603

Simpson R.W. & Brambley D.R. 1972 Phys. stat. solidi (b) 49 P 685